

Epitokous metamorphosis, reproductive swimming, and early development of the estuarine polychaete, *Neanthes glandicincta* Southern, 1921 (Annelida, Nereididae) on the east coast of the Malay Peninsula

Siti Syazwani Azmi¹, Yusof Shuaib Ibrahim², Saowapa Angsupanich³,
Pornsan Sumpuntarat³, Masanori Sato⁴

1 Institute of Oceanography and Environment, Universiti Malaysia Terengganu, 21030, Kuala Nerus, Terengganu, Malaysia **2** Faculty of Science and Marine Environment, Universiti Malaysia Terengganu, 21030, Kuala Nerus, Terengganu, Malaysia **3** Marine and Coastal Resources Institute, Prince of Songkla University, Hat Yai, Songkhla 90112, Thailand **4** Research Field in Science, Science and Engineering Area, Kagoshima University, 1-21-35 Korimoto, Kagoshima 890-0065, Japan

Corresponding author: Yusof Shuaib Ibrahim (yusofshuaib@umt.edu.my)

Academic editor: C. Glasby | Received 18 October 2020 | Accepted 13 December 2020 | Published 18 January 2021

<http://zoobank.org/4DE3A0C4-F8D4-43CF-938B-9B99C78B1857>

Citation: Azmi SS, Ibrahim YS, Angsupanich S, Sumpuntarat P, Sato M (2021) Epitokous metamorphosis, reproductive swimming, and early development of the estuarine polychaete, *Neanthes glandicincta* Southern, 1921 (Annelida, Nereididae) on the east coast of the Malay Peninsula. ZooKeys 1011: 1–24. <https://doi.org/10.3897/zookeys.1011.59780>

Abstract

The reproductive and developmental characteristics of the nereidid polychaete, *Neanthes glandicincta* Southern, 1921, commonly recorded in tropical estuaries in the Indo-West Pacific, were examined from Malaysia (the mangrove area of Kuala Ibai, Terengganu) and Thailand (the Lower Songkhla Lagoon) on the east coast of the Malay Peninsula. Epitokous metamorphosis of fully mature males and females and their reproductive swimming behaviour were recorded based on ten Malaysian epitokous specimens, which were collected at night during spring tides in a period of January 2018 to March 2019. Six Thailand epitokes were obtained in February and March 2006 by the laboratory rearing of immature worms. Epitokous metamorphosis is characterised by the enlargement of eyes in both sexes, division of the body into three parts and modification of parapodia with additional lobes in the mid-body of males, and replacement of atokous chaetae in the mid-body by epitokous natatory chaetae, completely in males and incompletely in females. The diameter of coelomic unfertilised eggs in females was 100–140 µm. After fertilisation, each egg formed a jelly layer, inside which embryonic development progressed. Trochophores

hatched out of the jelly layer, entering a short free-swimming larval phase followed by demersal life at the early stage of 3-chaetiger nectochaeta one day after fertilisation. Then, the larvae entered benthic life as juveniles, crawling on the bottom, at the late stage of 3-chaetiger nectochaeta two days after fertilisation. The results indicate that *N. glandicineta* has an annual life cycle, which is usually completed within an estuary with limited larval dispersal ability.

Keywords

Kuala Ibai, natatory chaetae, pelagic larvae, Songkhla Lagoon, South China Sea, trochophore

Introduction

The nereidid polychaete, *Neanthes glandicineta* Southern, 1921 (type locality near Calcutta, India) is commonly reported from Asian tropical estuaries in Indo-Western Pacific Oceans (Fauvel 1932, 1939, 1953; Wu 1967; Wu et al. 1985; Lee and Glasby 2015; Ibrahim et al. 2019). Lee and Glasby (2015) synonymised *Ceratonereis burmensis* Monro, 1937 (type locality: Maungmagan, Burma, and off Bombay, India) with *N. glandicineta*, and also described *N. wilsonchani* Lee & Glasby, 2015 from Singapore, which is similar to *N. glandicineta* but distinguishable by the number of paragnaths. Ibrahim et al. (2019) established the *Neanthes glandicineta* species complex, which included these two species. Hsueh (2019) described *N. kaomeiensis* from Taiwan, which is similar to both *N. glandicineta* and *N. wilsonchani* but differs from them in the absence of a notopodial prechaetal lobe in posterior chaetigers, and thus it is regarded as the third species of the *Neanthes glandicineta* species complex. Lee and Glasby (2015), Sato (2017), and Ibrahim et al. (2019) suggested that several more cryptic species belonging to this species complex may be distributed in the South China Sea and East China Sea coasts.

Reproductive and developmental modes of nereidids are conspicuously variable even among morphologically similar congeneric species (Sato 1999, 2017), although all nereidids are semelparous (breeding only once in a lifetime) (Olive 1983). Many nereidids show swarming behaviour (mass-swimming of sexually mature adults) to shed gametes freely into the water, accompanied by a common set of drastic morphological changes (known as epitokous metamorphosis) into epitokes of the 'heteronereis form' in both males and females or males only. These changes include marked enlargement of the eyes, division of the body into two or three parts, enlargement and/or modification of the parapodial ligules and cirri with the addition of some lappets (most marked in the middle or posterior body), and replacement of atokous chaetae by paddle-like natatory chaetae (Clark 1961; Schroeder and Hermans 1975). However, some species spawn without any epitokous metamorphosis and swarming (Sato 2017). These previous findings indicate that reproductive and developmental characteristics may be useful to distinguish morphologically similar but distinct species.

Fauvel (1932) found 'subepitokous' males of *N. glandicineta*, which were collected from Vizagapatam, India from May to June 1926; they were on the way to epitokous

metamorphosis, with the dorsal cirri crenate, and with atokous chaetae mixed with the paddle-like natatory chaetae. Later, Fauvel (1939) described epitokous males, which had the body divided into three parts, with epitokous modification in the middle part (beginning at chaetiger XX), based on specimens collected in Singapore (plankton sample) probably during their reproductive swimming. Monro (1937) reported typical epitokous metamorphosis in several males of this species based on part of the *C. burmensis* type material collected from off Bombay, describing the eyes as markedly enlarged, the body divided into three parts, the epitokous modification of parapodia occurring in the middle half of the body (beginning at chaetiger XXI), with the anterior and posterior parts remaining unmodified. It should be noted that both Fauvel (1939) and Monro (1937) reported the epitokous metamorphosis of only males, not referring to that of females.

On the other hand, Wu et al. (1985) described the epitokous metamorphosis of this species (as *C. burmensis*) as follows: eyes were enlarged, the body was divided into two parts, and the epitokous modification of parapodia occurred in the posterior body (beginning at chaetiger XIV) in a male (benthic sample), whereas eyes were enlarged, the body was divided into three parts, the inconspicuous epitokous modification of parapodia occurred in the middle body (chaetigers XVI–XXXIII), and a cleft was present on the anterior margin of the prostomium in a female (plankton sample).

Lee and Glasby (2015) described the epitokous morphology of both *N. glandicincta* and *N. wilsonchani* based on the epitokes obtained from the sediment samples collected from the mudflats in Singapore in a period of December to April, even though some of their materials seemed not fully matured. They concluded that there were no significant differences in the epitokous metamorphosis between the two species or between the sexes of each species, judging that the observed differences between them appeared to be related to the degree of maturity of the specimen. There is no previous report on the early development of any species from the *Neanthes glandicincta* species complex.

It is important, therefore, to clarify the epitokous metamorphosis of both sexes of *N. glandicincta* and their reproductive and developmental characteristics based on the fully mature adults, in order to reveal unknown cryptic species that have been confused with *N. glandicincta*.

In the present study, we obtained fully mature swimming adults of *N. glandicincta* from two localities in Malaysia and Thailand along the east coast of the Malay Peninsula during one-year monthly night sampling in the field and from laboratory culture, respectively. Using this material of *N. glandicincta*, we describe the epitokous metamorphosis of fully mature males and females, their reproductive swimming behaviour, and early development.

Materials and methods

At Aowsai in the Lower Songkhla Lagoon (Outer Songkhla Lake) (old name, Thale Sap Songkhla) in Thailand (Fig. 1A), immature worms of *N. glandicincta* were collected

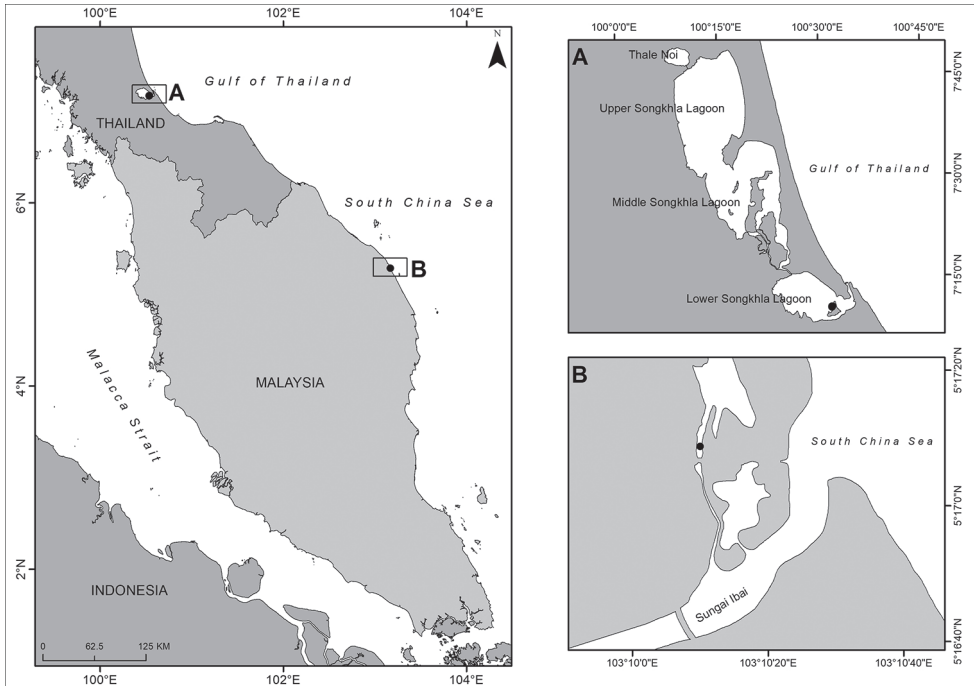


Figure 1. Map showing the collection sites (closed circles) in two estuaries on the east coast of the Malay Peninsula **A** lower Songkhla Lagoon, Thailand **B** mangrove area in Kuala Ibai branched from Sungai Ibai in Terengganu, Malaysia.

from the sediment samples dug out from intertidal or shallow subtidal bottoms using shovels in 2005 and 2008. For atokous morphology observation, some of them were fixed in 10% formalin and later transferred to 80% ethanol for preservation. The other worms were reared in indoor cement ponds (length 270 cm, width 176 cm, height 70 cm) containing coarse sand (10 cm thick) and seawater diluted to a salinity of 15 psu to obtain sexually mature adults. The ponds were maintained with aeration and fed on commercial dry food for shrimps.

Spawning occurred at midnight on 28 February and 2 March 2008 in the ponds. After the spawning of mature adults, all spent worms were fixed in 10% formalin and later transferred to 80% ethanol for preservation. The successfully fertilised eggs, which were obtained independently from three pairs of male and female epitokes in the ponds, were transferred to plastic bottles (diameter 8 cm, height 30 cm; wrapped in black plastic sheets) containing fresh diluted seawater of 15 psu salinity with aeration for embryonic development observation. Swimming trochophore larvae were transferred to glass jars (diameter 22 cm, height 35 cm; wrapped with black plastic sheets at the lower part) containing fresh diluted seawater for larval development observation. A few of developing embryos and larvae were periodically taken out from the plastic bottles and glass jars using a pipette to a glass slide for microscopy. All the development observations were carried out at room temperature (25–30 °C).

Monthly night samplings were carried out in the mangrove area in the estuary of Kuala Ibai, Terengganu, Malaysia, with 365 kilometres distance from the Thailand site (Fig. 1B). The survey was conducted 2–8 h after sunset, around the new or full moon in the period of January 2018 to March 2019. An underwater lamp was used as an artificial light to attract swimming worms. In total, ten epitokes of *N. glandicincta* (9 males, 1 female) were collected with a scoop net as they were swimming in the water surface. In-situ parameters, including salinity and temperature, were measured using Hydrolab Multiparameter. Live specimens were brought to the laboratory for sex determination by examining the coelomic contents (oocytes or sperm) and were fixed in 80% ethanol for preservation.

The maximum body width (BW), excluding the parapodia within chaetigers X–XXX was measured for each specimen. The body length (BL) of the complete specimens was measured from the base of the antenna to the end of the body, excluding anal cirri, and the total number of chaetigers were also counted. The paragnaths on the proboscis were counted in each area. The first and last natatory chaetigers in the middle body of epitokous males were determined by the appearance/disappearance of lamellae at the upper and lower portions on the base of the ventral cirri.

Photographs were taken with digital cameras (Nikon D3400, Nikon FDX-35, Touptek Photonics Toupcam E32SPM) on stereomicroscopes (Olympus SZX7, Olympus SZX16) and compound microscopes (Leica DM300, Nikon Eclipse E600). In some cases, several photographs were stacked to improve the depth of field using a software of Touptek Photonics Toupcam E32SPM. Drawings were prepared with a camera Lucida attached to the microscopes. The ArcGIS 10.3 software was used to prepare the map.

The usage of the nereidid morphology terminology is according to Villalobos-Guerrero and Bakken (2018).

The rainfall and air temperature dataset were obtained from the Malaysian Meteorological Department of the Environment and Water Ministry Malaysia.

Specimens were deposited at the South China Sea Repository and Reference Centre of Universiti Malaysia Terengganu, Malaysia (UMT), and the Phuket Marine Biological Centre, Phuket, Thailand (PMBC).

Results

Taxonomic account

Neanthes glandicincta (Southern, 1921)

Figs 2–7

Nereis (Nereis) glandicincta Southern, 1921: 589–593, text fig. 5a–e, pl. 23, fig. 9A–L.
Nereis glandicincta: Fauvel 1932: 92–93; Fauvel 1939: 314–315, Fauvel 1953: 181–182, fig. 91f–h.

Neanthes glandicincta: Lee and Glasby 2015: 80–85, figs 7–9; Misra 1999: 161–162; Ibrahim et al. 2019: 86–89, figs 3, 4.

Ceratonereis burmensis Monro, 1937: 532–536, fig. 1a–f; Misra 1999: 149; Ng et al. 2011: 426.

Nereis (Ceratonereis) burmensis: Fauvel 1953: 196–197, fig. 97d–f.

Ceratonereis (Composetia) burmensis: Hartmann-Schröder 1985: 49 (list); Chan 2009: 165–167, fig. 5a–r, in part.

Not *Neanthes glandicincta*: Wu et al. 1985: 150–151, fig. 84; Wu et al. 1985: 174–177, figs 98, 99 (described as *Ceratonereis burmensis*).

Type locality. Brackish lakes or pools at four localities in Barantolla, Dhappa, and Garia near Calcutta in India (Southern 1921).

Material examined. Sexually fully mature specimens (epitokes). Epitokes collected during reproductive swimming in the mangrove area of Kuala Ibai (5°17'7.6"N, 103°10'10.3"E), Terengganu, Malaysia: 2 males (BW, 1.6–1.9 mm; UMTAnn 445–446), coll. YS Ibrahim, 31 January 2018; 2 males and one female (2.1–2.4 mm; UMTAnn 447–449), coll. YS Ibrahim, 28 February 2018; 3 males (2.2–3.2 mm; UMTAnn 450–452), coll. SS Azmi, 6 January 2019, 2 males (2.1–2.6 mm; UMTAnn 453–454), coll. SS Azmi, 21 January 2019.

Epitokes obtained by rearing immature atokes collected from Aowsai in the lower reaches of Songkhla Lagoon (7°10'37.4"N, 100°32'26.2"E), Thailand (PMBC 20732): 3 males (BW, 1.2–2.1 mm) and 3 females (BW, 1.5–1.7 mm), coll. P Sumpuntarat, 2 March 2006.

Atokous specimens collected from the same locality as the epitokes. Immature atokes collected from Aowsai in the lower reaches of Songkhla Lagoon, Thailand (as above): 5 specimens (BW, 1.6–2.5 mm; PMBC 21209), coll. P. Sumpuntarat, during the period from September to December 2005; 4 specimens (BW, 1.2–1.3 mm; PMBC 21211), coll. S Angsupanich et al., 1 March 2008; 1 specimen (BW, 1.5 mm; PMBC 21212), coll. S Angsupanich, 19 November 2008.

Description of atokes. Ten atokes, including six complete specimens, 27–85 mm BL (Mean \pm SD: 60.8 \pm 19.7, n = 6), 1. 2–2.5 mm BW (1.7 \pm 0.5, n = 10), with 86–122 chaetigers (108.3 \pm 15.8, n = 4) (Table 1). Colour in preserved specimens whitish cream (Fig. 2A).

Two pairs of eyes arranged trapezoidally (anterior pair with space wider than that of posterior pair); anterior pair reniform; posterior pair round; two pairs of eyes almost same in size (Figs 2A, 3E). Approximately ten transverse grooves conspicuous in each of massive palpophores. Apodous segment (peristomium) with four pairs of tentacular cirri of unequal length; posterodorsal tentacular cirri longest, reaching back to chaetigers V–VII.

Proboscis with pair of semi-transparent amber jaws, each with ca. ten teeth. Typical conical paragnaths present on maxillary ring (Fig. 2C–F); number of paragnaths and their arrangement on each area of everted proboscis as follows (Table 1): area I: 4–11, scattered and unequal (Fig. 2C); area II: 12–17, in two arched rows, markedly large paragnaths with sharply tapering and curved tip present in anterior and middle

Table 1. Variation in number of paragnaths of epitokes of *Neanthes glandicineta* collected from two estuaries in the coast of Peninsular Malaysia in the present study, in comparison with data of atokes in the present and previous studies.

Locality (no. of specimens examined)	Body width (mm)	Body length (mm) ¹	No. of total chaetigers ¹	Number of paragnaths ²							Total ⁴	References
				I	II ³	III	IV ³	V	VI ³	VII–VIII		
Epitokes												
Songkhla Lagoon, Thailand (6)	1.2–2.1	17–34	68–117	8.0±2.8 (3–10)	14.2± 4.3 (8–19)	41.0± 7.9 (32–50)	11.2±3.5 (6–16)	0 (0–0)	0 (0–0)	0 (0–0)	98.4±27.9 (58–124)	Present study
Kuala Ibai, Malaysia (10)	1.6–3.2	33–43	62–123	5.3±1.8 (3–8)	14.8±3.0 (8–19)	41.5±6.2 (32–50)	11.2±1.6 (9–13)	0 (0–0)	0 (0–0)	0.3±0.7 (0–2)	95.8±11.3 (74–113)	Present study
Atokes												
Songkhla Lagoon, Thailand (10)	1.2–2.5	27–85	86–122	7.0±2.4 (4–11)	15.2±1.6 (12–17)	48.3±5.0 (38–55)	12.1±1.3 (10–14)	0 (0–0)	0.1±0.3 (0–1)	0.1±0.3 (0–1)	107.3±9.2 (94–119)	Present study
Eastern coast of Peninsular Malaysia (23) ⁵	0.7–2.0	15–70	114–132	8.8±3.0 (3–13)	16.7±1.8 (13–20)	50.1±5.8 (39–58)	13.5±1.8 (11–17)	0 (0–0)	0.2±0.4 (0–1)	0.04±0.2 (0–1)	117.7±11.4 (94–137)	Ibrahim et al. (2019)
Nine sites in Singapore (54) ⁶				9.0±3.4 (0–17)	17.3±2.5 (11–23)	49.2±7.2 (35–63)	14.1±2.5 (10–22)	0 (0–0)	0.1±0.3 (0–1)	1.2±2.1 (0–8)	120.1±13.9 (93–148)	Lee and Glasby (2015)
Maungmagan in Myanmar (8) ^{6,7}				5.8±3.9 (2–14)	13.1±2.0 (11–17)	41.3±9.7 (30–60)	14.0±2.9 (11–20)	0 (0–0)	0 (0–0)	0 (0–0)	101.3±19.9 (80–138)	Lee and Glasby (2015)
Calcutta in India (1)				10	12	38	7	0	1	2	90	Lee and Glasby (2015)
Near Calcutta in India (26) ⁸		88	123	10	(10–13)	50	(10–12)	0	(0–1)	Up to 7		Southern (1921)

¹ Data from complete specimens. ² Mean±SD (range). ³ Larger value at a left or right side. ⁴ All total with numbers from both sides of areas II, IV and VI. ⁵ Pooled data from 3 sites, including two atokes collected from Kuala Ibai where epitokes were obtained in the present study. ⁶ Calculated based on the individual data shown in table 3 in Lee & Glasby (2015). ⁷ A part of syntypes of *Ceratonereis burmensis* Monro, 1937. ⁸ Original description of *Nereis (Nereis) glandicineta* Southern, 1921.

positions (Fig. 2D); area III: 38–55, in three or four rows of transversely elongated bands, each paragnath with papilla-like base (Fig. 2E); area IV: 10–14, in triangular patch with markedly large paragnaths present in middle and posterior positions (Fig. 2F). Oral ring with no or few minute paragnaths; number of paragnaths on each area are as follows (Table 1): area V: none; area VI: none or single minute paragnath present, seated on tip of each papilla (usually pair of small nipple-like round papillae visible in right and left of area VI; Fig. 2B); area VII–VIII: none or single minute paragnath present. Total number of paragnaths 94–119.

Uniramous parapodia of first two chaetigers without notoacacula. In following biramous parapodia, notopodia consisting of dorsal cirrus and three ligules/lobe (dorsal ligule, prechaetal lobe and median ligule) throughout. Neuropodia consisting of four ligules/lobes (superior lobe, inferior lobe, postchaetal lobe, ventral ligule) and ventral cirrus in anterior and middle body; superior lobe absent in posterior body (from chaetiger L).

Notochaetae consisting of homogomph spinigers throughout. Upper neurochaetae including homogomph spinigers with long blades and heterogomph spinigers with short blades throughout; some or most of heterogomph spinigers replaced by heterogomph falcigers in middle body. Lower neurochaetae include heterogomph spinigers

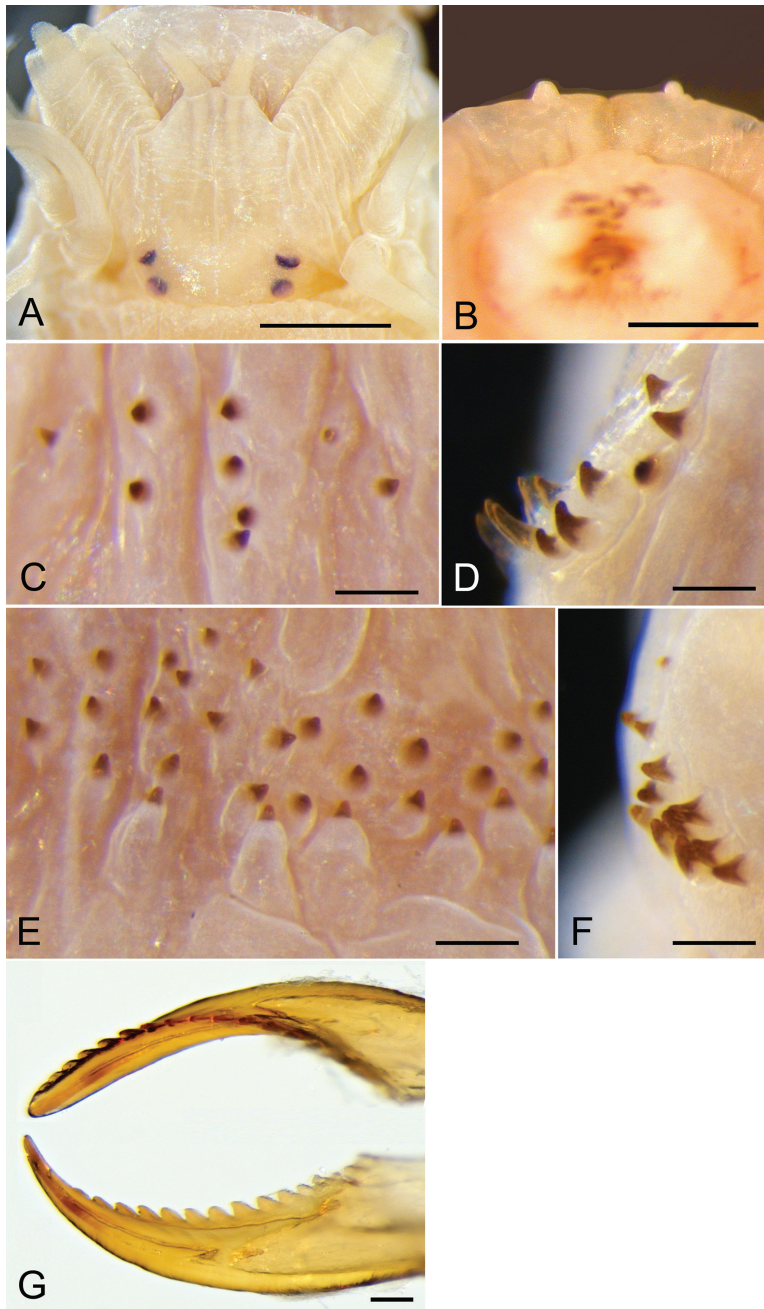


Figure 2. Atokes (**A–F**) and an epitoke (**G**) of *Neanthes glandicineta* (Southern, 1921) collected from the Lower Songkhla Lagoon, Thailand **A** prostomium of an atoke (ind. no. 10 with BW of 1.7 mm, PMBC 21209) **B** anterior view of an everted proboscis, showing a pair of small nipple-like round papillae on area VI in an atoke (ind. no. SL-2 with BW of 1.5 mm, PMBC 21212) **C–F** paragnaths in areas I (**C**), II (anterior and middle parts of left side, **D**), III (central part, **E**), and IV (right side, **F**) of an atoke (ind. no. 1 with BW of 2.3 mm, PMBC 21209) **G** dorsal (upper) and ventral (lower) views of the right jaw of a male epitoke (ind. no. 3M with BW of 1.2 mm, PMBC 20732).

with long blade (at upper position) and heterogomph spinigers with short blade (at lower position) throughout; some or most of heterogomph spinigers with short blades replaced by heterogomph falcigers in anterior-mid body (from chaetigers XI–XIX usually). Heterogomph falcigers with finely serrated slender blades; few heterogomph falcigers rarely (two of ten specimens) present in lower neurochaetae of chaetiger 1. Conspicuous glandular patches present in dorsal ligules.

Coelom of three individuals filled with many oocytes with maximum diameter of ca. 100 μm .

Description of epitokes. Twelve males, including eight complete specimens, 17–43 mm BL (Mean \pm SD: 32.4 ± 8.3 , $n = 8$), 1.2–3.2 mm BW (2.2 ± 0.5 , $n = 12$), with 62–123 chaetigers (100.9 ± 19.4 , $n = 8$). Four females, including three complete specimens, 25–34 mm BL (28.7 ± 4.7 , $n = 3$), 1.5–2.4 mm BW (1.8 ± 0.4 , $n = 4$), with 84–116 chaetigers (102.0 ± 16.4 , $n = 3$). There was no significant difference in BL, BW, and the number of chaetigers between males and females (Wilcoxon-Mann-Whitney test, $P > 0.2$). Live spent worms after spawning semi-transparent; live females with greenish eggs.

Two pairs of eyes enlarged in both males (Figs 3C, 4A, B) and females (Figs 3B, D, 5A–C) in comparison with those in atokes (Fig. 3E); enlargement of eyes more remarkable in males than females; two pairs of eyes almost same in size, shape (round or ovoid) and space between right and left eyes. Apodous segment with four pairs of tentacular cirri of unequal length; posterodorsal tentacular cirri longest, reaching back to chaetigers VII–X.

Proboscis with pair of semi-transparent amber jaws, each with ca. ten teeth (up to ca. 15 teeth in dissected jaw, Fig. 2G). Dark pigmentation present on surface of proboscis (in particular, ventral surface) of four males of Malaysian specimens (Fig. 4B, C). Conical paragnaths present on maxillary ring (Fig. 4B, C); number of paragnaths and their arrangement on each area of everted proboscis as follows (Table 1): area I: 3–10, scattered and unequal; area II: 8–19, in two arched rows, markedly large paragnaths with sharply tapering and curved tip present in anterior and middle positions; area III: 32–50, in three or four rows of transversely elongated bands; area IV: 6–16, in triangular patch with markedly large paragnaths present in middle and posterior positions. Oral ring with no or few minute paragnaths; number of paragnaths on each area are as follows (Table 1): area V: none; area VI: none; area VII–VIII: 0–2, in transverse row. Total number of paragnaths 58–124. Pair of small nipple-like round papillae usually visible in right and left of area VI, as those in atokes (Fig. 2B).

Male bodies divided into three regions (Fig. 3A): anterior (pre-natatory), middle (natatory), and posterior (post-natatory) regions; parapodia of pre-natatory and post-natatory regions similar to those of atokes (Fig. 6A, D).

Male pre-natatory region with 18–25 chaetigers, with dorsal cirri of first seven or eight chaetigers thickened mainly at base, and with ventral cirri of first 5–7 chaetigers thickened throughout (Fig. 7A). Neuropodial heterogomph falcigers (Fig. 6G) present in few chaetigers of pre-natatory region, appearing from chaetigers XV–XXI, or completely absent.

Male natatory region constituting of 30–56 chaetigers, with parapodia markedly modified (Figs 6B, 7B); round lobes newly present on upper and lower base of ventral cirri,

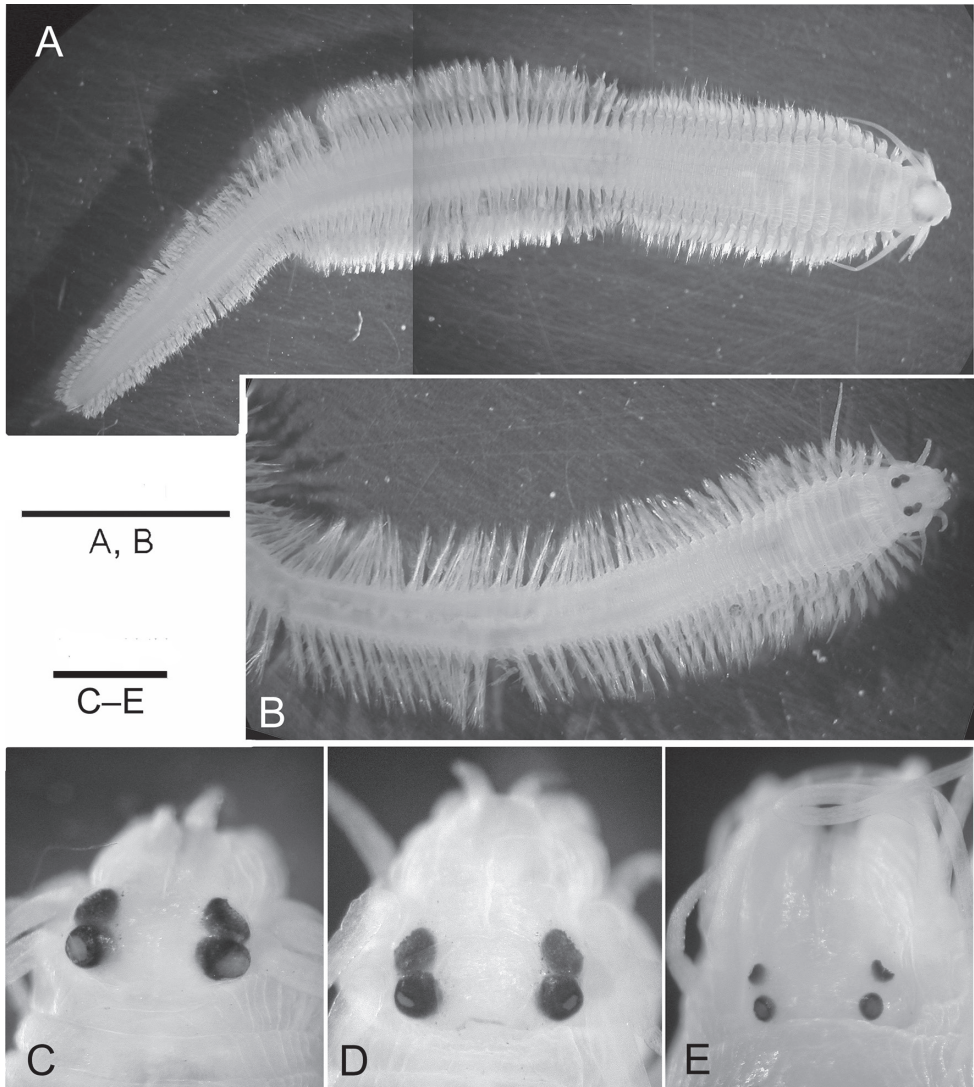


Figure 3. Epitokous males (**A, C**) and females (**B, D**) of *Neanthes glandicineta* (Southern, 1921) collected from the Lower Songkhla Lagoon, Thailand (PMBC 20732) in comparison with an atoke from the same locality (**E**) (PMBC 21209) **A** dorsal view of the whole body of a male **B** dorsal view of the anterior body of a female **C–E** enlargement of anterior dorsal end of a male epitoke (**C**), a female epitoke (**D**), and an atoke (**E**). Scale bars: 5 mm (**A, B**); 0.5 mm (**C–E**).

appearing from chaetigers XIX–XXVI to chaetigers LII–LXXIII. Neuropodial postchaetal lobe developing into large round flat lamella with or without small triangular protrusion on lateral edge in almost same range of chaetigers; dorsal cirri frequently serrated on lower edge, slightly elongated; ovoid lobe newly present on upper base of dorsal cirri; all parapodial ligules and lobes enlarged as thin lamellae (Figs 6B, 7B). Epitokous paddle-like natatory chaetae (Figs 6H, 7E) appearing from chaetigers XXII–XXVIII to chaetigers LIV–LXXVIII, substituting atokous chaetae (Fig. 6E–G) completely in most of middle

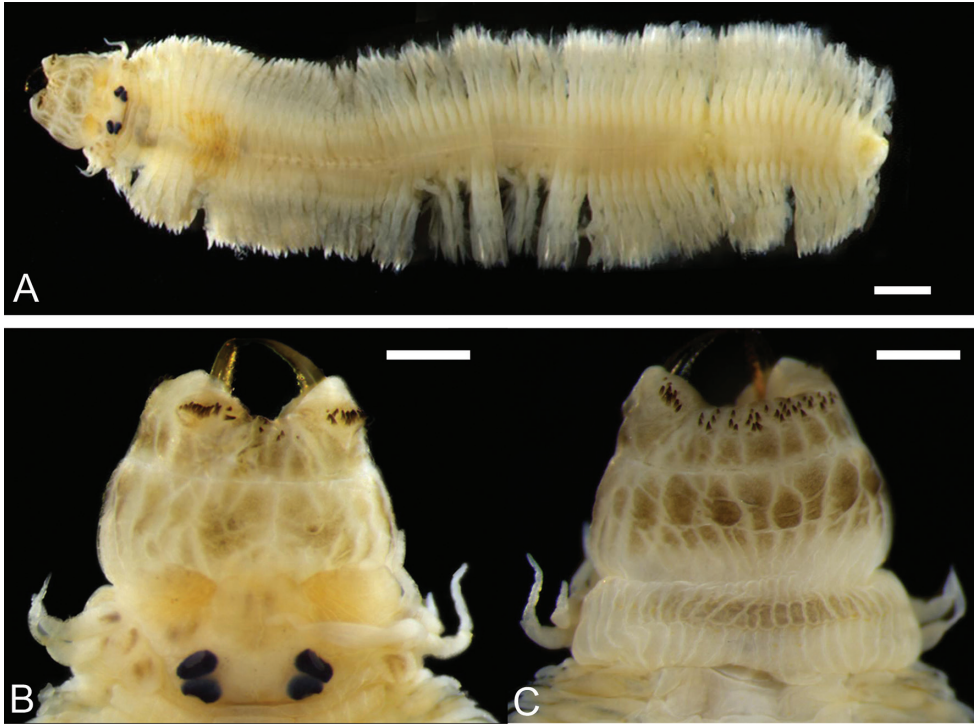


Figure 4. Male epitoke of *Neanthes glandicincta* (Southern, 1921) collected from Kuala Ibai, Malaysia (UMTAnn 453) **A** dorsal view of the whole body (incomplete, with the pre-natatory and natatory regions) **B** dorsal view of the proboscis with pigmentation **C** ventral view of the proboscis with pigmentation. Scale bars: 1 mm (**A**); 0.5 mm (**B, C**).

natatory region, and incompletely in few anteriormost and posteriormost chaetigers of this region (with atokous chaetae remaining there); blade of epitokous paddle chaetae semi-transparent, flat and wide, with minutely serrated edge on one side, and tapering tip.

Male post-natatory region constituting 13–64 chaetigers, with unmodified parapodia (Figs 3A, 6D); neuropodial heterogomph falcigers absent. Pygidium with pygidial rosette.

Females with unmodified parapodia throughout, except for with dorsal cirri of first 4–8 chaetigers thickened mainly at base, and with ventral cirri of first 4–8 chaetigers slightly thickened throughout (Figs 3B, 5A, 6C, 7C, D). Epitokous paddle chaetae present together with atokous chaetae in both notochaetae and neurochaetae in middle body from chaetigers XXVI–XXXV to chaetigers XLVI–LII. Neuropodial heterogomph falcigers usually appearing from chaetigers XV–XVIII to chaetigers LIV–LXXII. Pygidium without pygidial rosette. Few eggs (full-grown oocytes) remained in coelom of females; eggs spherical, 100–140 μm in diameter in fixed specimens.

In both sexes, body wall of epitokes thin. Small slits on body wall of ventral surface at base of parapodia present in middle and posterior chaetigers of females (Fig. 5D).

Variation. Paragnath numbers in epitokes from Thailand and Malaysia and atokes from Thailand are summarised together with the atokes from the previous studies in Table 1.

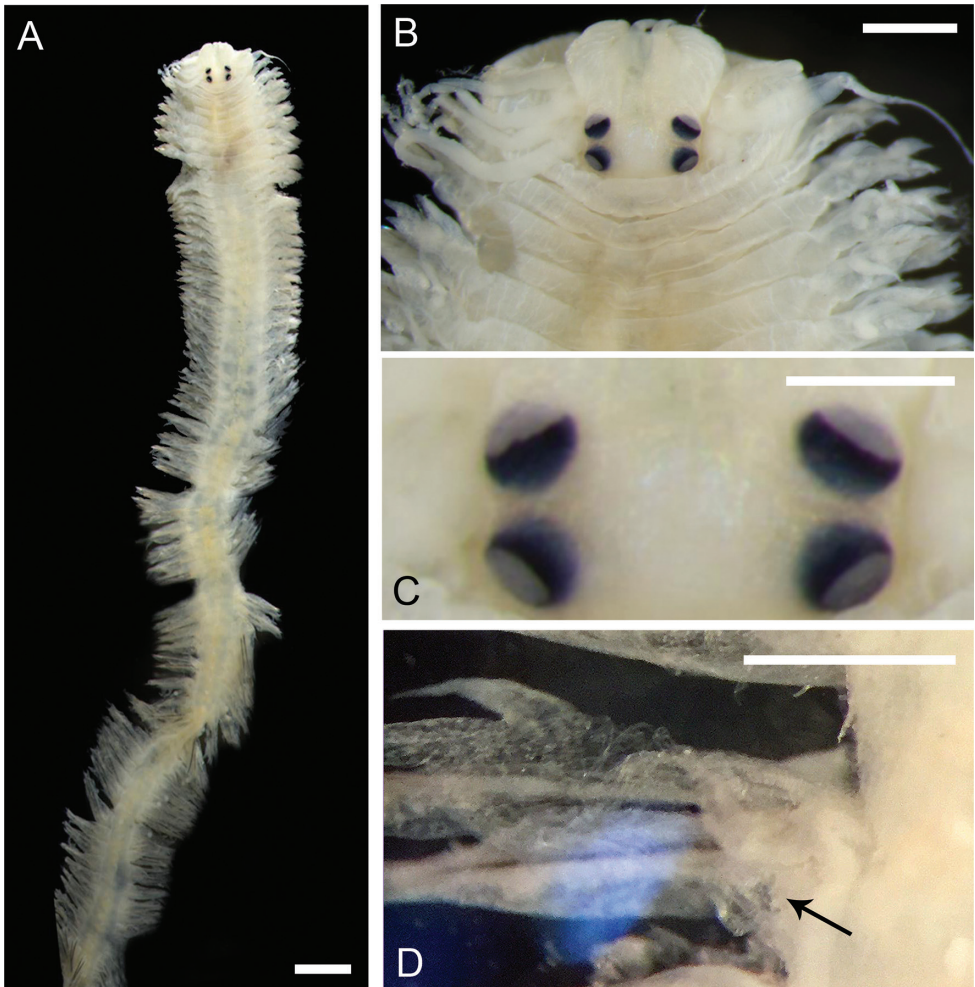


Figure 5. Female epitoke of *Neanthes glandicineta* (Southern, 1921) collected from Kuala Ibai, Malaysia (UMTAnn 449) **A** dorsal view of the whole-body **B** enlargement of anterior end **C** enlargement of eyes **D** rupture of body wall at the ventral surface in the posterior body (arrow). Scale bars: 1 mm (**A**); 0.5 mm (**B–D**).

In three specimens, an epitokous female (PMBC 20732) and two atokes (PMBC 21211, 21212), a few heterogomph falcigers were present in the lower neurochaetae of chaetiger 1, whereas falcigers were usually absent in the anterior chaetigers (at least first 10 chaetigers) in the present study, as reported in the previous studies on *N. glandicineta* (Southern 1921; Lee and Glasby 2015; Ibrahim et al. 2019).

The papilla-like base of paragnaths in area III was not conspicuous in the ethanol-fixed epitokous materials.

Habitat. Intertidal and shallow subtidal bottoms of sandy or muddy sediment in the estuaries, where the salinity of ambient water widely ranges from 18 to 32 psu at Kuala

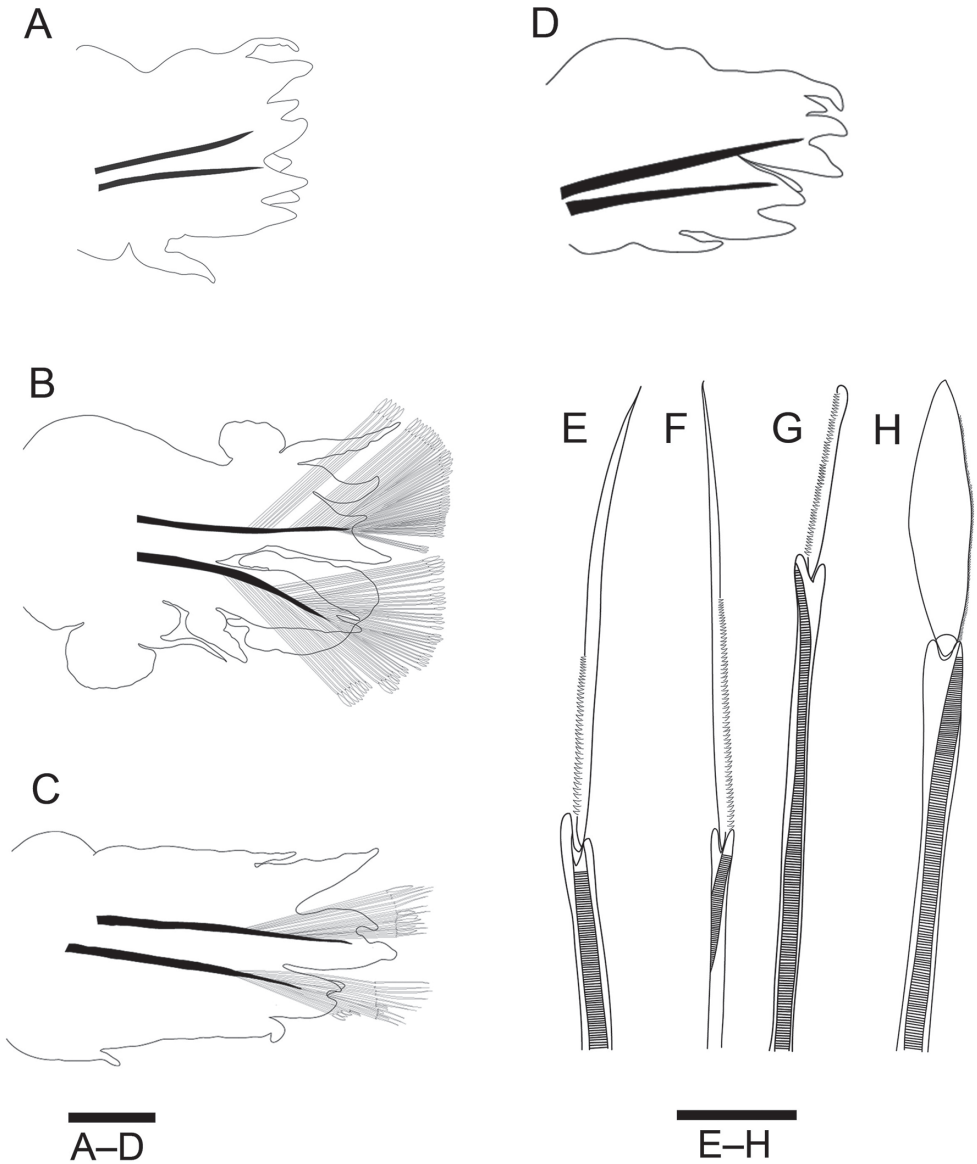


Figure 6. Drawings of epitokes of *Neanthes glandicincta* (Southern, 1921) collected from Kuala Ibai, Malaysia **A** posterior view of the right parapodium 8 in the pre-natatory region of a male (UMTAnn 453) **B** posterior view of the right parapodium 35 in the natatory region of a male (UMTAnn 445) **C** anterior view of the left parapodium 35 of a female (UMTAnn 449) **D** posterior view of the right parapodium 66 in the post-natatory region of a male (UMTAnn 446) **E** heterogomph spiniger from the lower neurochaetae in chaetiger 8 of a male (UMTAnn 453) **F** homogomph spiniger from the upper neurochaetae in chaetiger 8 of a male (UMTAnn 453) **G** heterogomph falciger from the lower neurochaetae in chaetiger 36 of a female (UMTAnn 449) **H** epitokous natatory chaeta from the neuropodium of chaetiger 36 of a male (UMTAnn 453). Scale bars: 1 mm (**A–D**); 0.05 mm (**E–H**).

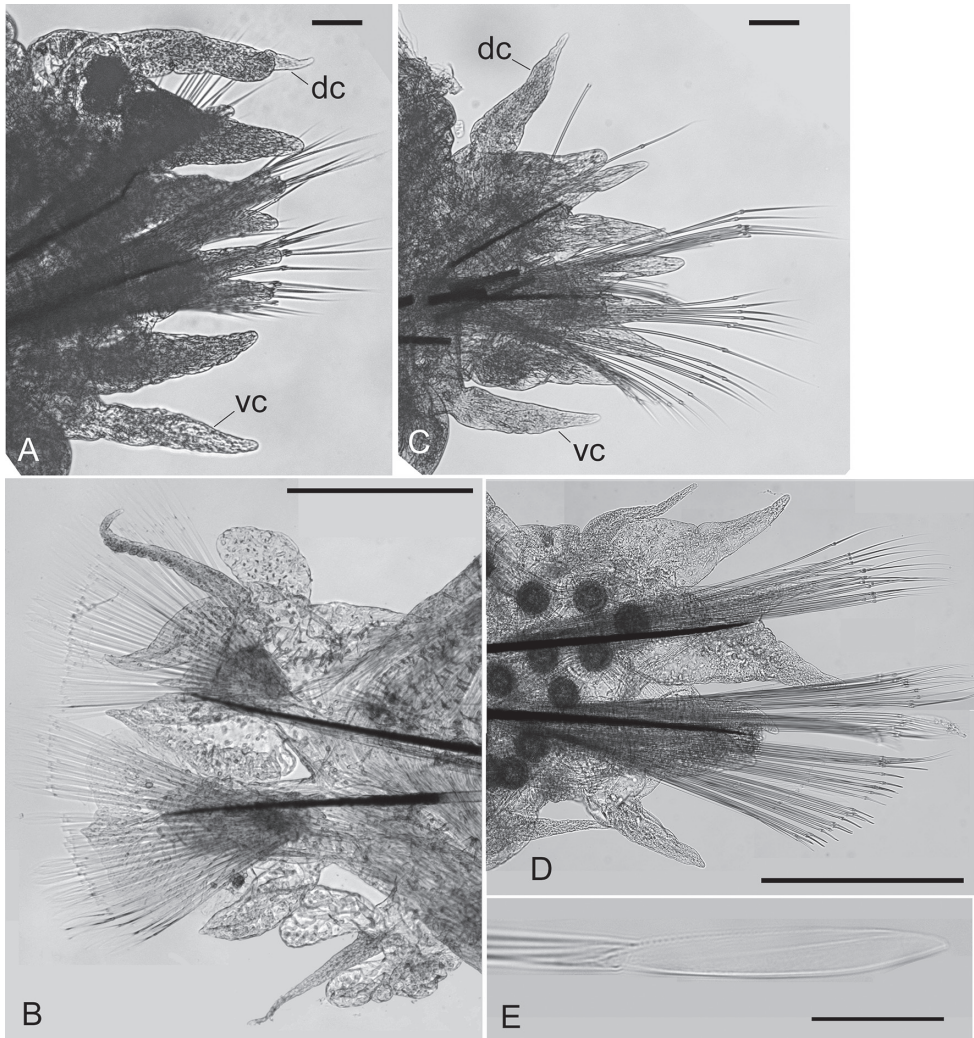


Figure 7. Epitokous males (**A, B, E**) and a female (**C, D**) of *Neanthes glandicincta* (Southern, 1921) collected from the Lower Songkhla Lagoon, Thailand (PMBC 20732) **A** anterior view of left parapodium of chaetiger 5 in the pre-natatory region of a male epitoke **B** anterior view of right modified parapodium of chaetiger 34 in the natatory region of the same male as (**A**) **C** posterior view of right parapodium of chaetiger 3 of a female epitoke **D** posterior view of right parapodium of chaetiger 37 of the same female as (**C**) **E** enlargement of an epitokous paddle chaeta of another male epitoke. Abbreviations: dc, dorsal cirrus; vc, ventral cirrus. Scale bars: 0.1 mm (**A, C**); 0.5 mm (**B, D**); 0.05 mm (**E**).

Ibai in Malaysia (see below), and from 1 to 33 psu in the coast of the lower reaches of Songkhla Lagoon (Angsupanich and Rakkheaw 1997; S Angsupanich, unpublished data).

Geographic distribution. India, Myanmar, Singapore, the east coast of Malay Peninsula (Malaysia and Thailand). Based on Southern (1921), Fauvel (1932, 1939, 1953), Misra (1999), Lee and Glasby (2015), Ibrahim et al. (2019), and the present study.

Remarks. The morphological characteristics of present Thailand and Malaysian specimens of swimming epitokes agreed well with the atokes collected from Thailand in the present study and also the atokes previously described from India (Southern 1921; Lee and Glasby 2015), Myanmar (Monro 1937; Lee and Glasby 2015), Singapore (Lee and Glasby 2015), and Malaysia (Ibrahim et al. 2019), except for their epitokous modification of parapodia and chaetae in the middle body, and enlarged eyes. However, we found that a few falcigers were exceptionally present in the lower neurochaetae of chaetiger 1 in three Thailand specimens, unlike the previous descriptions of this species and also the diagnosis of *Neanthes glandicincta* species complex (Ibrahim et al. 2019). Therefore, the diagnosis of this species and the *Neanthes glandicincta* species complex should be amended here from Ibrahim et al. (2019) to allow for the occasional presence of falcigers in chaetiger 1.

The Indian specimens described as *N. glandicincta* by Misra (1999) seem to belong correctly to this species if Misra's description "Notosetae homogomph spinigers and homogomph falcigers" is a mistake. The Chinese specimens described as *N. glandicincta* by Wu et al. (1985) seem to belong to an undescribed species of another member of the *Neanthes glandicincta* species complex because they differ from all other members of this species group in the absence of notopodial prechaetal lobe. Both atokous and epitokous specimens collected from southern China and identified as *Ceratonereis burmensis* by Wu et al. (1985) do not seem to belong to *N. glandicincta*; atokes with a lesser number of paragnaths seem to belong to *N. wilsonchani*, according to Lee and Glasby (2015) and the key of Ibrahim et al. (2019), whereas an epitoke with an indented anterior margin of the prostomium seemed to belong to *Ceratonereis*.

Reproductive period and swimming behaviour of epitokes in Kuala Ibai in Malaysia

A total of ten swimming epitokes of *Neanthes glandicincta* was collected during high tide at night (mostly within one hour before or after high tide, 20:45–23:49) around new moon or full moon in January and February during our 15-month sampling period from January 2018 to March 2019 in Kuala Ibai, Malaysia (Table 2). During this period, the water temperature (and salinity) varied in the range of 28–32 °C (18–32 psu) at the sampling site (Fig. 8A); salinity (24–32 psu) was relatively high, and the temperature was relatively low (28–30 °C) in January and February. The lowest and highest monthly amount of rainfall was recorded in February (11 mm) and December (877 mm) in 2018, respectively, with the general tendency that the average air temperature is relatively high in the dry season from March to August (28.0–28.6 °C), and relatively low in the rainy season from October to January (26.7–27.4 °C) at Kuala Ibai, according to the weather data of the Malaysian Meteorological Department (2019) (Fig. 8B).

On the other hand, based on the daily tidal records in Kuala Terengganu (Worldwide Tides and Currents Predictor 2018), the monthly maximum height of the sea level at high tide was highest in June–July and December–January (2.26–2.28 m), and lowest in April and October (1.90–1.92 m) (Fig. 8C).

Table 2. Occurrence of reproductive swimming of *Neanthes glandicincta* in Kuala Ibai, Terengganu.

Date	Age of moon	Time of night high tide (Height of sea level) ¹	Sunset	Duration of observation	Catch time of epitokes (no. of inds. and sex ²)
2018					
31-Jan [2] ³	14.0 (○) ⁴	21:29 (2.20 m)	19:17	19:30–22:00	20:45 (1M), 21:35 (1M)
28-Feb [3]	12.3 (○)	20:23 (2.01 m)	19:20	19:20–22:00	20:50 (1M) 21:05 (1M) 21:15 (1F)
02-Mar	14.3 (○)	21:36 (1.99 m)	19:20	19:30–22:00	19:20
31-Mar	13.6 (○)	20:53 (1.69 m)	19:16	19:23–22:30	19:16
30-Apr	14.0 (○)	20:27 (1.26 m)	19:13	19:10–22:30	19:13
15-May	29.0 (●)	19:30 (1.14 m)	19:14	19:31–02:00	19:14
29-May	13.6 (○)	19:09 (1.03 m)	19:16	19:10–22:30	19:16
28-Jun	14.3 (○)	09:40 (2.04 m)	19:23	19:25–04:00	19:23
13-Jul	0.0 (●)	09:27 (2.19 m)	19:25	19:25–23:00	19:25
28-Jul	15.0 (○)	09:24 (2.05 m)	19:24	19:25–22:30	19:24
11-Aug	29.0 (●)	18:55 (0.89 m)	19:21	18:55–01:30	19:21
26-Aug	14.7 (○)	19:40 (0.97 m)	19:16	19:30–22:30	19:16
25-Sep	15.4 (○)	20:55 (1.28 m)	19:02	19:10–22:00	19:02
09-Oct	29.4 (●)	21:01 (1.38 m)	18:55	18:56–22:00	18:55
25-Oct	16.0 (○)	21:41 (1.69 m)	18:50	19:00–23:00	18:50
08-Nov	30.0 (●)	21:44 (1.80 m)	18:48	18:58–22:30	18:48
23-Nov	15.4 (○)	21:37 (1.94 m)	18:49	19:15–23:00	18:49
23-Dec	15.8 (○)	22:05 (2.20 m)	19:00	19:10–23:00	19:00
2019					
06-Jan [3]	29.9 (●)	22:02 (2.13 m)	19:07	19:20–23:00	21:30 (3M) around 10 s interval
07-Jan	1.0 (●)	22:35 (2.15 m)	19:08	19:30–23:00	
21-Jan [2]	15.0 (○)	21:49 (2.25 m)	19:14	19:18–00:00	22:39 (1M), 23:49 (1M)
28-Jan	22.0 (☾)	01:10 (1.64 m)	19:16	19:18–23:30	
05-Feb	0.3 (●)	22:14 (2.04 m)	19:18	19:20–23:00	
19-Feb [1] ⁵	14.3 (○)	21:22 (2.14 m)	19:20	19:35–23:35	22:10
21-Mar	14.5 (○)	21:18 (1.83 m)	19:18	19:20–01:00	

¹ Based on data of Worldwide Tides and Currents Predictor (2018). ² M: male, F: female. ³ Number of epitokes found. ⁴ ○: within three days before or after full moon; ●: within three days before or after new moon; ☾: last quarter. ⁵ Specimen is not available, due to failure of catching it.

Male epitokes swam fast with a circular motion around artificial light. On 28 February 2018, two swimming males first appeared around half an hour after the high tide, followed by the occurrence of a swimming female ca. one hour after the high tide (Table 2). On 6 January 2019, three swimming males were collected at approximately 21:30 with an interval of ca. 10 seconds for each collection, but not followed by any swimming female. On 19 February 2019, an actively swimming adult was found just after the high tide at night but could not be collected.

Mating behaviour and early development under laboratory culture in Thailand

In the cement ponds where the Thailand atokous specimens had been reared for several months, a pair of male and female epitokes were found swimming simultaneously out of the sediments and spawned in the water at 0:15 am on 28 February, and two more pairs of epitokes spawned at 1:55 am on 2 March 2006. In all three pairings, the male swam for a longer duration (ca. 30 min) than the female (ca. five min) and started swimming earlier than the female. At spawning, the male swam around the female. After spawning, the spent worms of both sexes sank to the bottom.

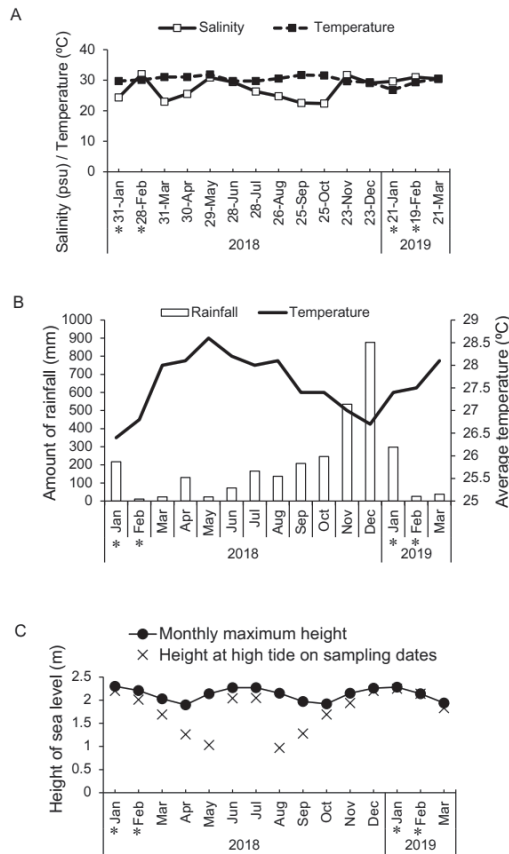


Figure 8. Seasonal changes of environmental parameters in Kuala Ibai, Malaysia during the sampling period **A** monthly changes in the salinity and temperature of the surface water at the sampling site (represented by our data at the end of each month) **B** monthly changes in the amount of rainfall and average air temperature at Kuala Ibai based on the data of Malaysian Meteorological Department **C** monthly changes of the maximum height of sea level at high tide (closed circles), with the height of sea level at high tide on each sampling date (x marks), based on the data of Worldwide Tides and Currents Predictor (2018). The asterisks indicate the x months when the swimming epitokes of *Neanthes glandicinca* appeared.

The eggs (fully-grown oocytes) just after fertilisation were relatively transparent and contained ca. 20 lipid drops surrounding the nucleus (germinal vesicle) (Fig. 9A). Successfully fertilised eggs formed a transparent cortex of 8–15 μm thickness beneath the egg surface, and a jelly layer ca. 50 μm thickness outside the egg surface (Fig. 9A). The embryonic development through 2-cell and 4-cell stages (Fig. 9B) up to the trochophore stage (Fig. 9C) progressed within the jelly layer. Trochophores hatched out of the jelly layer 8–9 h after the fertilisation, entering a free-swimming larval life (Fig. 9D). Approximately one day (20–23 h) after fertilisation, the larvae became early metatrochophores (Fig. 9E) and 2-chaetiger late metatrochophores (Fig. 9F), which were slightly elongated, posteriorly with two pairs of chaetal tufts. The larvae became early 3-chaetiger nectochaetes 22–27 h after fertilisation and began to enter a demersal life around the bottom layer, with a slow swimming behaviour (Fig. 9G). Approximately

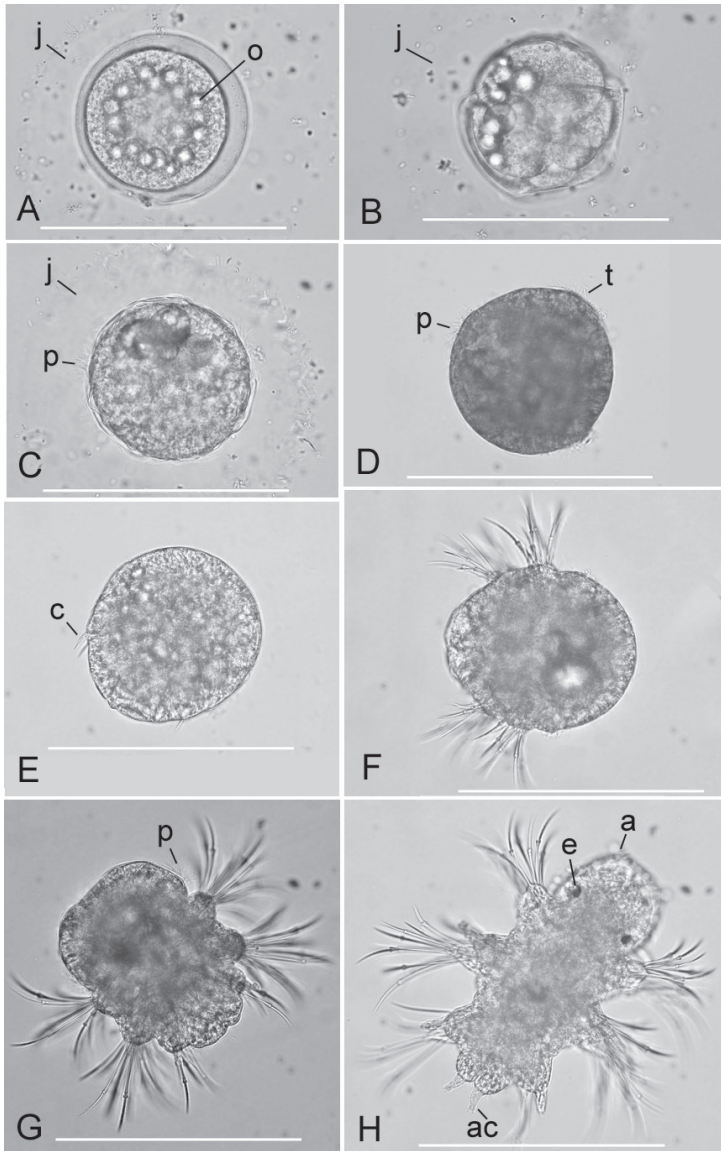


Figure 9. Early development of *Neanthes glandicineta* (Southern, 1921) after fertilisation in the laboratory. The material from the Lower Songkhla Lagoon, Thailand **A** fertilised egg surrounded by a jelly layer (j), 10 min after fertilisation; many sperm were trapped in the jelly layer; lipid (oil) drops (o) surrounded the germinal vesicle **B** 4-cell stage, 1 h and 10 min after fertilisation **C** early trochophore stage, 7 h and 30 min after fertilisation; ciliary movement of the prototroch (p) began within the jelly layer **D** free-swimming trochophore larva just after hatching out of the jelly layer, 8 h after fertilisation; ciliary bands of the prototroch and telotroch (t) were present **E** free-swimming early-metatrochophore larva, 20 h after fertilisation; two pairs of chaetal tufts (c) were present **F** free-swimming 2-chaetiger late-metatrochophore larva, 21 h after fertilisation; two pairs of chaetal tufts well developed **G** free-swimming early 3-chaetiger nectochaeta larva, 22 h after fertilisation; three pairs of chaetal tufts were developed; the prototroch and lipid drops remained in the anterior body **H** demersal late 3-chaetiger nectochaeta larva, 48 h after fertilisation; a pair of eyes (e), antennae (a), and anal cirri (ac) appeared. Lipid drops disappeared. Scale bars: 0.2 mm.

two days (48 h) after fertilisation, the larvae became late 3-chaetiger nectochaetes in which a pair of eyes and antennae in the prostomium, and a pair of anal cirri in the pygidium appeared (Fig. 9H); all of them crawled on the bottom surface, entering a benthic life as juveniles. Several large lipid drops, which probably originated from the smaller ones of the unfertilised eggs, were contained within the anterior body during the early larval stages but disappeared before the late 3-chaetiger nectochaeta stage.

Discussion

Epitokous metamorphosis and swimming behaviour of epitokes

In the present study, the reproductive characteristics of *Neanthes glandicineta* were examined using spawning fully mature adults in the field and laboratory culture. The results revealed that the typical epitokous metamorphosis to heteronereid form occurred in only males, including the enlargement of eyes, marked modification of parapodia, and complete substitution of atokous chaetae by natatory paddle-like chaetae in the natatory region. Whereas, only a partial epitokous metamorphosis occurred in mature females, including the enlargement of eyes, and incomplete substitution of atokous chaetae by natatory paddle-like chaetae with no modification of parapodia in the middle body.

Our findings well agreed with the previous reports of Fauvel (1939) who described that the male body divided into three parts with the epitokous modification occurring in the middle part (beginning at chaetiger XX) based on the specimens collected from Singapore. The present findings also agree with Monro (1937), who described that the eyes were markedly enlarged, the body was divided into three parts, and the epitokous modification of parapodia occurred in the middle part (beginning at chaetiger XXI), with the anterior and posterior parts remain unmodified, based on several males (a part of type material of *Ceratonereis burmensis*) collected from off Bombay, India. Lee and Glasby (2015) also described almost the same morphology of epitokous males in which the unmodified anterior part consisted of 20–22 chaetigers, and thereafter parapodia were modified bearing crenulate dorsal cirri in the mid-body.

The epitokous metamorphosis of certainly full-mature females is first described in the present study. In contrast to our result, Lee and Glasby (2015) described that 'epitokous females' had modified parapodia; same as those of males except for the absence of crenulate dorsal cirri based on the two specimens that were probably not fully matured. At present, the reason for the different findings is unknown.

The swimming behaviour of the epitokes of *N. glandicineta* was also first described in the present study, based on the field and laboratory observations. We found that both mature males and females spawn in estuarine waters while swimming at night high tide around the new moon and full moon in January and February in the field and that males swam longer than females before the paired mating behaviour and spawning occurred in laboratory conditions.

The sex ratio was heavily biased towards males (nine males: one female) in the field. The larger male proportion seems to be caused by males commencing swimming

earlier and for a longer duration than females and thus can be collected more easily, as suggested in the reproductive swarming of the estuarine nereidids, *Hediste japonica* and *H. diadroma* (Hanafiah et al. 2006).

The typical epitokous metamorphosis to a heteronereid form in males seems to be significant, serving to increase the swimming ability of male epitokes, which need to swim at high speed to escape from predators and for a longer time to meet a female for successful spawning. On the other hand, the inconspicuous epitoky without parapodial modification in females seems to correspond to the short swimming duration of female epitokes.

As for spawning, Chan (2009) reported that the gametes are shed from the body wall in *N. glandicineta*. This is supported by our finding that ruptures existed in the body wall of the ventral surface of parapodia of spent worms after spawning.

The result of our monthly night sampling for swimming epitokes in Kuala Ibai indicates that the Malaysian population of *N. glandicineta* has a reproductive period from January to February, with an annual life cycle. This period roughly agrees with the period from February to March when we could collect mature swimming epitokes under the laboratory culture of the Thailand population in the present study. A similar reproductive period of this species has been suggested by Lee and Glasby (2015) who collected epitokes from mud flats in Singapore in December (four individuals), January (one), and April (one) of which some of their materials were not fully matured.

The east coast of the Malay Peninsula faces the South China Sea, where the northeast monsoon is dominant in a period from October to early March, whereas the southwest monsoon is dominant from late May to September (Akhir et al. 2011). The rainfall amount is usually the highest during the early northeast monsoon season (November and December) (Fig. 8B; Malaysian Meteorological Department 2018). The reproductive period of *N. glandicineta* coincides with the timing just after the rainy season. On the other hand, the reproductive period of this species also coincides with a period (one of two annual peaks), with the highest sea level at high tide, when the seawater can enter the uppermost reaches of estuaries (Fig. 8C). Ascertaining the environmental factors that affects the determination of the reproductive period in tropical estuaries would be an interesting future study.

Fig. 8C indicates that our choice of the sampling dates in April, May, August, and September in 2018 was inappropriate because the sea level at night on the high tides during these sampling dates was considerably less than the monthly maximum height of the sea level. Therefore, we cannot rule out the possibility that the swimming epitokes may appear in these months.

Fauvel (1932) found the 'subepitokous' males of *N. glandicineta*, which were collected from Vizagapatam on the eastern coast of India (near the type locality of this species) in May to June 1926. This suggests that the reproductive season in the type locality of this species may be different from that in the eastern Malay Peninsula. Whether the different reproductive seasons between geographically separated local populations could cause reproductive isolation between them, leading to speciation, is another interesting topic of study.

Fauvel (1932) also found no epitokous modification in a few females full of eggs and a fragment of a male filled with sperm among the many specimens collected from

India and Thailand (Taléh-Sap = Songkhla Lagoon). Therefore, this suggests that some cryptic species may coexist with *N. glandicineta*.

Early development

The early development of *Neanthes glandicineta* is first described in the present study (Fig. 9). The result demonstrated that the relatively small eggs (100–140 μm in diameter) formed a jelly layer just after fertilisation, and developed into trochophores, which hatched out of the jelly layer, entering a free-swimming larval life. This process of the embryonic development is almost the same as the relatively small (130–170 μm in diameter) eggs of the temperate estuarine nereidid, *Hediste diadroma* Sato & Nakashima, 2003 (Kagawa 1955, as *Neanthes japonica*; Sato and Tsuchiya 1991: small-egg type of *N. japonica*; Sato 1999: the small-egg form of *N. japonica*; Tosuji and Sato 2006; Sato 2017) in which a jelly layer formed just after fertilisation by the secretion of jelly substance from numerous cortical alveoli arranged in the egg surface layer (cortex) (Sato and Osanai 1986: *N. japonica*). Another temperate estuarine species, *H. japonica* (Izuka, 1908) with a relatively large egg diameter (180–210 μm) has a similar development also (Izuka 1908; Tosuji and Sato 2006; Sato 2017). However, the development of *N. glandicineta* could successfully progress under a relatively low salinity (15 psu); in contrast to that of *H. diadroma* and *H. japonica*, which both had a favourable salinity range of 22–30 psu and could not develop under 15 psu salinity (Sato and Tsuchiya 1987: small-egg type of *N. japonica*; Tosuji and Sato 2006). The tolerance of developing embryos against low salinity in *N. glandicineta* seems to be adaptive for its reproduction within an estuary with variable salinity.

The result indicates that the free-swimming larval phase in *N. glandicineta* is relatively short (two days in 25–30 °C): the shift from planktic to demersal larvae and the larval settlement on the bottom as crawling juveniles occur during the 3-chaetiger nectochaeta stage, when the lipid drops (maternal nutrients) disappear. On the other hand, in *H. diadroma* which has a catadromous life history (Sato 2017; Kan et al. 2020), the larval settlement occurred at the 5- to 8-chaetiger nectochaeta stage after a relatively long larval phase (more than 30 days in 15 °C), though the planktic larval life shifted to the demersal one, together with the disappearance of lipid drops during the 3-chaetiger nectochaeta, as in *N. glandicineta* (Tosuji and Sato 2006; Kan et al. 2020). The short period of planktic larval phase in *N. glandicineta* may be adaptive for preventing larvae from being washed out to sea.

These results indicate that the life cycle of *N. glandicineta* may be usually completed within an estuary with a limited larval dispersal ability.

Acknowledgements

This work was partially supported by the Research Acculturation Collaborative Grant (RACE/2015/56038) and the Higher Institution Centre of Excellence of Malaysia. We sincerely acknowledge Prof. Dr. Zaidi Che Cob, Prof. Dr. Zainudin Bachok, Azwarina

Mohd Azmi Ramasamy, Che Mohd Zan Husin, Yuzwan Mohamad, Mr. Abdul Rahman Ali (boatman), Rabaah Hamzah, Nazifi Jesop, Syazmeer Dzulkifli, Adilah Husna Termizi, and Najua Ismail for their support in sample collection and image editing. We deeply thank the staff of the Laboratory of Biodiversity, Institute of Oceanography and Environment, South China Sea Repository and Reference Centre, and Faculty of Science, Kagoshima University for providing facilities for the taxonomic work. Special thanks to the Malaysian Meteorological Department of the Ministry of Environment and Water Malaysia for providing the dataset to be used in this publication.

References

- Akhir MF, Sinha PC, Hussain ML (2011) Seasonal variation of South China Sea physical characteristics of the east coast of Peninsular Malaysia from 2002–2010 datasets. *International Journal of Environmental Sciences* 2(2): 569–575.
- Angsupanich S, Rakkheaw S (1997) Seasonal variation of phytoplankton community in Thale Sap Songkhla, a lagoonal lake in southern Thailand. *Netherlands Journal of Aquatic Ecology* 30: 297–307. <https://doi.org/10.1007/BF02085873>
- Chan WMF (2009) New nereidid records (Annelida: Polychaeta) from mangroves and sediment flats of Singapore. *Raffles Bulletin of Zoology, Supplement* 22: 159–172.
- Clark RB (1961) The origin and formation of the heteronereis. *Biological Reviews* 36: 199–236. <https://doi.org/10.1111/j.1469-185X.1961.tb01584.x>
- Fauvel P (1932) Annelida Polychaeta of the Indian Museum. *Memoirs of the Indian Museum, Calcutta* 12(1): 1–262.
- Fauvel P (1939) Annélides polychètes de l'Indochine. *Commentationes Pontificia Academia Scientiarum* 3(10): 243–368.
- Fauvel P (1953) The Fauna of India Including Pakistan, Ceylon, Burma and Malaya. Annelida Polychaeta. The Indian Press, Allahabad, 507 pp.
- Hanafiah Z, Sato M, Nakashima H, Tosuji H (2006) Reproductive swarming of sympatric nereidid polychaetes in an estuary of the Omuta-gawa River in Kyushu, Japan, with special reference to simultaneous swarming of two *Hediste* species. *Zoological science* 23(2): 205–217. <https://doi.org/10.2108/zsj.23.205>
- Hartmann-Schröder G (1985) Revision der Gattung *Ceratonereis* Kinberg (Nereididae, Polychaeta) (Mit besonderer Berücksichtigung der Arten mit eingeschnittenem Prostomium). *Mitteilungen aus dem Hamburgischen zoologischen Museum und Institut* 82: 37–59.
- Hsueh PW (2019) *Neanthes* (Annelida: Nereididae) from Taiwanese waters, with description of seven new species and one new species record. *Zootaxa* 4544(1): 173–198. <https://doi.org/10.11646/zootaxa.4554.1.5>.
- Ibrahim NE, Ibrahim YS, Sato M (2019) New record of an estuarine polychaete, *Neanthes glandicincta* (Annelida, Nereididae) on the eastern coast of Peninsular Malaysia. *ZooKeys* 831: 81–94. <https://doi.org/10.3897/zookeys.831.28588>
- Izuka A (1908) On the breeding habit and development of *Nereis japonica* n. sp. *Annotationes Zoologicae Japonenses* 6: 295–305.

- Kagawa Y (1955) Note on the optimum salinities, studied in the adult and larva of the brackish-water polychaete worm, *Nereis japonica*. Journal of Gakugei Collection Tokushima University, Natural Science 6: 11–16.
- Kan K, Kuroki Y, Sato M, Tosuji H (2020) Larval recruitment process in the catadromous life history of *Hediste diadroma* (Nereididae, Annelida) in an estuary in Kagoshima Bay, Southern Japan. Plankton and Benthos Research 15(1): 30–43. <https://doi.org/10.3800/pbr.15.30>
- Lee YL, Glasby CJ (2015) A new cryptic species of *Neanthes* (Annelida: Phyllodocida: Nereididae) from Singapore confused with *Neanthes glandicincta* Southern, 1921 and *Ceratonereis (Composetia) burmensis* (Monro, 1937). Raffles Bulletin of Zoology 31: 75–95.
- Misra A (1999) Polychaete. State Fauna Series 3: Fauna of West Bengal, Part 10: 125–225.
- Monro CCA (1937) On two new polychaetes from Indian Ocean. Annals and Magazine of Natural History Series 10(19): 531–538. <https://doi.org/10.1080/00222933708655297>
- Ng PKL, Corlett R, Tan HTW (2011) Singapore biodiversity: an encyclopedia of the natural environment and sustainable development. Editions Didier Millet in association with Raffles Museum of Biodiversity Research, Singapore, 552 pp.
- Olive PJW (1983) Annelida: Polychaeta. In: Adiyodi KG, Adiyodi KG (Eds) Reproductive Biology of Invertebrates. Volume I: Oogenesis, Oviposition, and Oosorption. John Wiley & Sons Ltd, New York, 357–422.
- Sato M (1999) Divergence of reproductive and developmental characteristics in *Hediste* (Polychaeta: Nereididae). In: Dorresteijn AWC, Westheide W (Eds) Reproductive Strategies and Developmental Patterns in Annelids. Developments in Hydrobiology (Vol. 142). Springer, Dordrecht, 129–143. https://doi.org/10.1007/978-94-017-2887-4_6
- Sato M (2017) Nereididae (Annelida) in Japan, with special reference to life-history differentiation among estuarine species. In: Motokawa M, Kajihara H (Eds) Species Diversity of Animals in Japan. Springer Japan, Tokyo, 477–512. https://doi.org/10.1007/978-4-431-56432-4_19
- Sato M, Nakashima A (2003) A review of Asian *Hediste* species complex (Nereididae, Polychaeta) with descriptions of two new species and a redescription of *Hediste japonica* (Izuka, 1908). Zoological Journal of the Linnean Society 137(3): 403–445. <https://doi.org/10.1046/j.1096-3642.2003.00059.x>
- Sato M, Osanai K (1986) Morphological identification of sperm receptors above egg microvilli in the polychaete, *Neanthes japonica*. Developmental Biology 113(2): 263–270. [https://doi.org/10.1016/0012-1606\(86\)90161-2](https://doi.org/10.1016/0012-1606(86)90161-2)
- Sato M, Tsuchiya M (1991) Two patterns of early development in nereidid polychaetes keying out to *Neanthes japonica* (Izuka). Ophelia Supplement 5: 371–382.
- Schroeder PC, Herman CO (1975) Annelida: Polychaeta. In: Glese AC, Pearse JS (Eds) Reproduction of Marine Invertebrates (Vol. 3). Academic Press, 213 pp. <https://doi.org/10.1016/B978-0-12-282503-3.50007-9>
- Southern R (1921) Polychaeta of the Chilka Lake and also of fresh and brackish waters in other parts of India. Memoirs of the Indian Museum 5: 563–659.
- Tosuji H, Sato M (2006) Salinity favorable for early development and gamete compatibility in two sympatric estuarine species of the genus *Hediste* (Polychaeta: Nereididae) in the Ariake Sea, Japan. Marine biology 148(3): 529–539. <https://doi.org/10.1007/s00227-005-0079-1>

- Villalobos-Guerrero TF, Bakken T (2018) Revision of the *Alitta virens* species complex (Annelida: Nereididae) from the North Pacific Ocean. *Zootaxa* 4483(2): 201–257. <https://doi.org/10.11646/zootaxa.4483.2.1>
- Worldwide Tides, Currents Predictor (2018) Online Tides and Currents Predictions (Kuala Terengganu). <https://tides.mobilegeographics.com> [Assessed on 6 August 2020]
- Wu SK (1967) The nereid worms of Taiwan. *Bulletin of the Institute of Zoology, Academia Sinica* 6: 47–76.
- Wu B, Sun R, Yang D (1985) *The Nereidae (polychaetous annelids) of the Chinese coast*. Springer/China Ocean Press, Beijing, 234 pp. [First published in 1981 in Chinese]

Life stages and morphological variations of *Limnocythere inopinata* (Crustacea, Ostracoda) from Lake Jiang-Co (northern Tibet): a bioculture experiment

Can Wang¹, Hailei Wang², Xingxing Kuang^{1,3}, Ganlin Guo⁴

1 Guangdong Provincial Key Laboratory of Soil and Groundwater Pollution Control, School of Environmental Science and Engineering, Southern University of Science and Technology, 518055, Shenzhen, China **2** MNR Key Laboratory of Saline Lake Resources and Environment, Institute of Mineral Resources, Chinese Academy of Geological Sciences, 100037, Beijing, China **3** Shenzhen Municipal Engineering Lab of Environmental IoT Technologies, Southern University of Science and Technology, 518055, Shenzhen, China **4** Jiangsu Key Laboratory of Marine Biotechnology, Jiangsu Ocean University, 222005, Lianyungang, China

Corresponding author: Hailei Wang (wanghailei77@126.com)

Academic editor: I. Karanovic | Received 1 July 2020 | Accepted 16 December 2020 | Published 18 January 2021

<http://zoobank.org/5C39D73C-76B7-4886-8D01-43297369D401>

Citation: Wang C, Wang H, Kuang X, Guo G (2021) Life stages and morphological variations of *Limnocythere inopinata* (Crustacea, Ostracoda) from Lake Jiang-Co (northern Tibet): a bioculture experiment. ZooKeys 1011: 25–40. <https://doi.org/10.3897/zookeys.1011.56065>

Abstract

Limnocythere inopinata (Baird, 1843) is a Holarctic species, abundant in a number of Recent and fossil ostracod assemblages, and has many important taxonomic and (paleo)ecological applications. However, the life cycle and morphological characteristics of the living *L. inopinata* are still unclear. A bioculture experiment was designed to study life stages and morphological variations from stage A-8 to adult in this species. The living animals were collected from Lake Jiang-Co, in the northern Tibetan Plateau. Results reveal that this species possesses a special growth pattern with the maximum size increase occurring at the transition from the instars A-5 to A-4. The growth pattern deviates from Brooks' rule and one population from Lake Dali, eastern Mongolian Plateau. This suggests that the life history of *L. inopinata* may be influenced by environmental factors. Some morphological differences between Lake Jiang-Co and European populations of *L. inopinata* are also uncovered. Therefore, a detailed morphological description of this population is provided, but refrain from erecting a new species at the present stage because those differences appear to be inconsistent.

Keywords

Cytheroidea, growth pattern, morphological characteristics, Tibetan Plateau

Introduction

Limnocythere inopinata (Baird, 1843), belonging to the family Limnocytheridae, is widely distributed in the Holarctic. Living populations of *L. inopinata* have been reported from Europe, Asia, and Africa. The European populations include: Austria (Löffler 1990; Yin et al. 1999; Rossi et al. 2010), Germany (von Grafenstein et al. 1999; Frenzel et al. 2010; Scharf et al. 2013), Greece (Frogley et al. 2001), Iceland (Alkalaj et al. 2019), Italy (Rossi et al. 2010; Marta et al. 2017), Poland (Szlauder-Lukaszewska 2014, 2015a, b), Spain (Mezquita et al. 1999; Rodríguez-Pérez and Baltanás 2008; Martínez-García et al. 2015), Sweden (Iglukowska and Namiotko 2012), Switzerland (Decrouy et al. 2012, 2014), Turkey (Külköylüoğlu et al. 2016; McCormack et al. 2019), and United Kingdom (Benzie 1989; Holmes et al. 2010). The Asian populations were recorded from China (Mischke et al. 2003; Zhang et al. 2015; Akita et al. 2016), India (Kramer et al. 2014), Israel (Mischke et al. 2012), and Jordan (Mischke et al. 2012). Finally, the African populations are known from Algeria (Ghaouaci et al. 2017), Egypt (Keatings et al. 2010), and Nigeria (Roberts et al. 2002).

The ecological characteristics of *L. inopinata* have been commonly used to infer paleoecological conditions (e.g., Shen et al. 2001; Poberezhnaya et al. 2006; McCormack et al. 2019). This species has been reported from a variety of water bodies (Geiger 1994), including ponds, swamps, lakes, and rivers. It is commonly distributed in shallow waters, while a few, less abundant, populations were found in deep water, e.g., from a depth of 64 m in the Baltic Sea (Hiller 1972). *Limnocythere inopinata* has salinity preference range between 0.50‰ and 9.00‰ (Usskilat 1975; Kempf 1986; Holmes et al. 1999) and a wide temperature range between 0.50 °C and 35.00 °C (Karan-Žnidaršič and Petrov 2007; Frenzel et al. 2010; Külköylüoğlu et al. 2016). *Limnocythere inopinata* from the Tibetan Plateau (TP) is especially noted for its preference of polyhaline waters (> 10‰; see Akita et al. 2016). The carapace morphology of this species is influenced by environmental factors (Carbonel et al. 1988; Yin et al. 1999). Yang et al. (2008) reported that extremely high silica values in low salinity water bodies may cause knot(s) in the shell of *L. inopinata*. Despite these studies, the life cycle and morphological characteristics of this species are still unknown.

The ontogeny of the Ostracoda is important for understanding their evolution. Watabe and Kaesler (2004) noted that the degree of adherence to Brooks' rule during the ontogeny of the Ostracoda is related to the heterochrony in evolution. Brooks' rule was the first estimation of growth patterns in crustaceans, and it predicts that animals will double in volume following each moult and thus present the linear dimension of growing by the cube root of two, i.e., 1.26 (Brooks 1886; Teissier 1960).

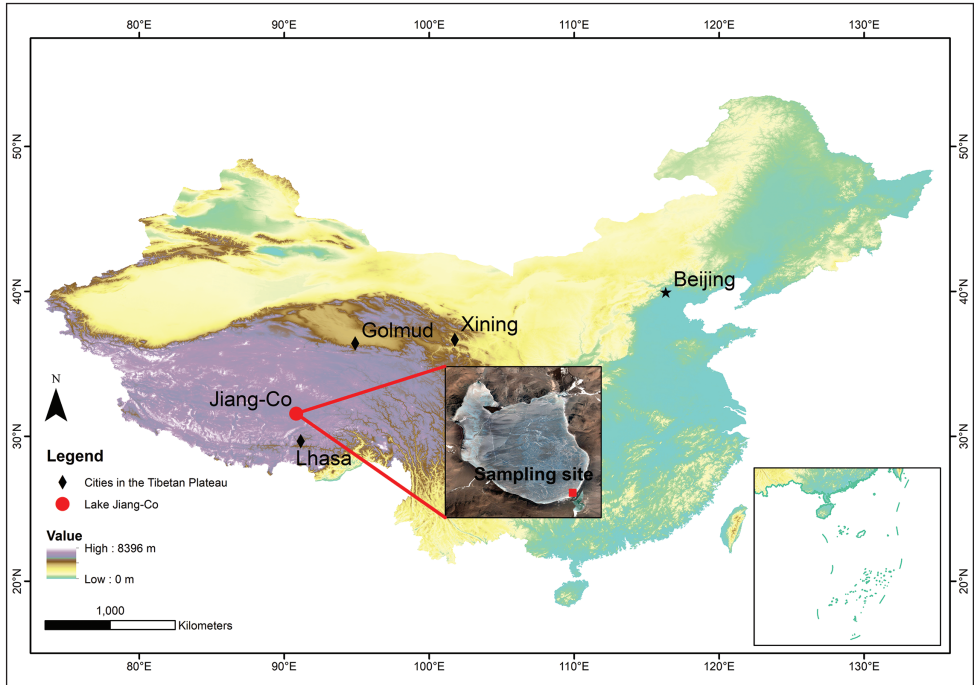


Figure 1. Map of the location of Lake Jiang-Co and sampling site.

Here we study a biocultured population of *L. inopinata* collected from Lake Jiang-Co. The aim was to clarify the life stages and morphological variations from A-8 stage to adult, and to compare our data on growth rate (length and height measurements of the shell) with the Brooks's rule and with the growth rate of the same species from Lake Dali, eastern Mongolian Plateau (MP) (Zhai et al. 2015). We also describe shell and soft parts of the Lake Jiang-Co population and compare this with the European population (Yin et al. 1999; Meisch 2000).

Materials and methods

Lake Jiang-Co (31°31'–31°35'N, 90°47'–90°52'E) is a brackish water lake in northern TP (Fig. 1). The lake area is approximately 40.29 km². There are no inflow and outflow rivers. In this region, annual mean precipitation ranges between 300 and 600 mm, annual mean evaporation is greater than 1000 mm, and the annual mean temperature ranges between -0.30 and 2.40 °C from 1987 to 2016 according to Yang et al. (2018).

Living *L. inopinata* were collected with surface sediments from the shores of Lake Jiang-Co in September 2016, using a plankton net with a mesh size of 200 µm. Salinity was 0.59‰ and the temperature of the bottom water was 17.40 °C. Specimens, all females, were sorted under the Nikon 90i. No males were recorded in the samples.

Individuals were cultured from indoor temperatures (from 9 to 14 °C) in the laboratory. The culturing water was collected from the lake and filtered through 10–20 µm filter papers. Culture was fed with *Chlorella vulgaris*.

Limnocythere inopinata individuals were hand-picked from biocultured populations, covering all eight juvenile stages (A-8 to A-1) and the adult stage (A). The A-8 to A stages were preliminarily determined by different size range of the left valve (i.e., length and height), based on approximately 200 individuals. Carapace length and height of every stage were measured under the microscope Nikon SME 1500 equipped with NIS-Element BR 3.1. In order to ensure that we found the true A-1 and A stages, twenty A-1 individuals and twenty adults were separately placed in eight glass dishes to observe if these individuals moulted and grew. If most of A-1 individuals moulted, and most of adults did not moult, it suggested that our division of nine stages could be trusted. We observed that most of A-1 individuals moulted and most of the adults did not do so. The size range of the left valve of A-1 and A stages was finally confirmed by the mean value of moulted A-1 individuals and non-moulted adults. Microscope and Scanning Electron Microscope (SEM) photographs of A-8 to A stages were taken by Nikon SME 1500 and Zeiss Ultra Plus SEM, respectively.

The estimation method of growth ratios of mean length and height for each ontogenetic transition follows Forel (2015):

$$K_L = L_{m+1} / L_m,$$

$$K_H = H_{m+1} / H_m,$$

where K_L and K_H are growth ratios of mean length and height, L_m and H_m are respectively mean length and height at stage m , and L_{m+1} and H_{m+1} are respectively mean length and height at stage $m+1$. We also conducted a linear regression and Pearson's chi-squared test on all data of carapace sizes.

The adults of *L. inopinata* were dissected under 96% ethanol in the glass dish and the soft parts were sealed by 96% ethanol in the glass bottle according to Namiotko et al. (2011), and their appendages were photographed. The descriptive terminology for the hard and soft parts followed Meisch (2000). All specimens are deposited in the Key Laboratory of Saline Lake Resources and Environment, Institute of Mineral Resources, Chinese Academy of Geological Sciences, Beijing, China.

Results

Life stages of *L. inopinata*

Length versus height of left valves and microscope photographs of *L. inopinata* covering groupings of instars A-8 to A-1 and adults are shown on the Fig. 2A. Growth ratios of mean length and height of this species from A-8 stage to adult compared with Brooks' rule are presented on the Fig. 2B.

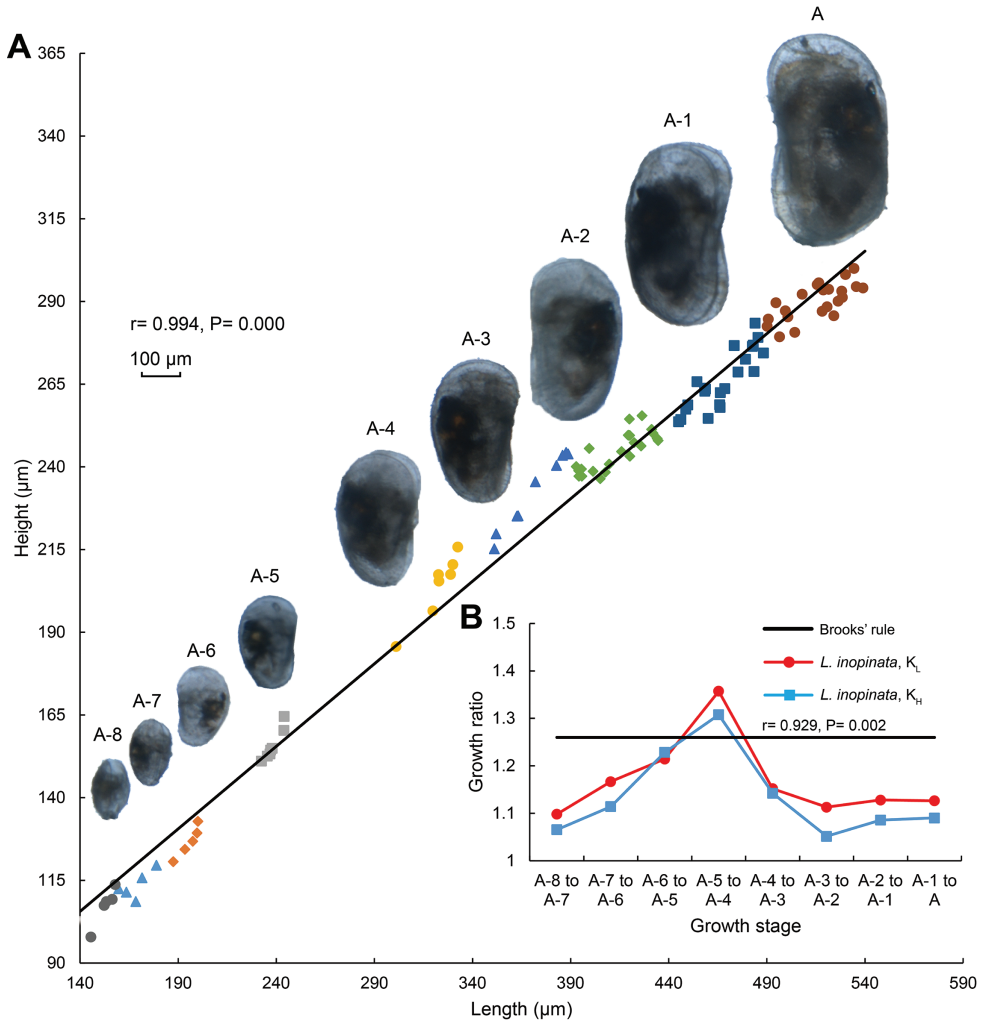


Figure 2. **A** Length versus height of left valves and microscope photographs of *L. inopinata* from A-8 stage to adult **B** Plot demonstrating the growth ratio elements K_L and K_H of *L. inopinata* from A-8 stage to adult. $K_L = L_{m+1} / L_m$, $K_H = H_{m+1} / H_m$, where K_L and K_H are growth ratios of mean length and height, L_m and H_m are respectively mean length and height at stage m , and L_{m+1} and H_{m+1} are respectively mean length and height at stage $m+1$. The black line suggests a growth ratio of 1.26, the value predicted by Brooks' rule. All individuals are from the indoor bioculture laboratory.

As the individuals grew, carapace length increased, ranging from 0.153 mm to 0.526 mm. Shell height also increased, ranging from 0.107 mm to 0.209 mm (Table 1). Individual sizes were variable within a certain growth stage: that of the instar A-4 to the adult stage were more variable than those of the A-8 to the A-5. Instar A-5 clearly separated from the instars A-4 and A-6, while there were some small overlaps occurring in contiguous growth stages, such as between the instars A-2 and A-3. Carapace length displayed a significant positive correlation with the height ($r = 0.994, P = 0.000$).

Table 1. Mean length and height of left valves of *L. inopinata* from A-8 stage to adult.

Stage of growth	n	Size	
		Length (mm)	Height (mm)
adult	12	0.526 ± 0.025	0.290 ± 0.009
A-1	12	0.467 ± 0.022	0.266 ± 0.012
A-2	12	0.414 ± 0.021	0.245 ± 0.008
A-3	9	0.372 ± 0.021	0.233 ± 0.017
A-4	7	0.323 ± 0.021	0.204 ± 0.018
A-5	7	0.238 ± 0.006	0.156 ± 0.005
A-6	5	0.196 ± 0.008	0.127 ± 0.006
A-7	5	0.168 ± 0.009	0.114 ± 0.005
A-8	5	0.153 ± 0.008	0.107 ± 0.009

Table 2. K_L and K_H of *L. inopinata* from A-8 stage to adult.

Phase of growth	Growth ratio	
	K_L	K_H
A-1 to adult	1.126	1.090
A-2 to A-1	1.128	1.086
A-3 to A-2	1.113	1.052
A-4 to A-3	1.152	1.142
A-5 to A-4	1.357	1.308
A-6 to A-5	1.214	1.228
A-7 to A-6	1.167	1.114
A-8 to A-7	1.098	1.065
Mean growth ratio	1.169	1.136

The K_L and K_H values for *L. inopinata* during ontogeny were generally lower than predicted by Brooks' rule except for the instars A-5 to A-4. Values ranged from 1.098 to 1.357 for K_L , and from 1.052 to 1.308 for K_H (Table 2), and were significantly positively correlated ($r = 0.929$, $P = 0.002$). Gradually increase was observed in K_L and K_H during the instars A-8 to A-4, followed by small change from the instar A-4 to the adult stage. The maximum values of K_L and K_H occurred at the transition from the instars A-5 to A-4, and were higher than 1.26, as predicted by Brooks' rule. The growth pattern of *L. inopinata* does not appear to follow the predictions using Brooks' rule.

The K_L values of the *L. inopinata* population in Lake Jiang-Co from the A-8 to the adult was compared with values obtained for a population from Lake Dali (Zhai et al. 2015) (Fig. 3), a marginal lake, located at the eastern part of MP (43°13'–43°23'N, 116°29'–116°45'E) with a surface area of 192 km² (Zhai et al. 2015) (Fig. 3A). Generally, the mean K_L values for both populations were lower than predicted by Brooks' rule, but that for the population from Lake Dali were higher than that from the Lake Jiang-Co (Fig. 3B). In addition, the growth pattern observed in Lake Dali was less varied: K_L varies from 1.153 to 1.327, and the maximum value of K_L was observed at the transition from the instar A-8 to the instar A-7. The maximum K_L was followed by a remarkable decline to a low K_L , followed by a relatively stable value, demonstrating that the *L. inopinata* populations in Lake Jiang-Co and Dali experience different growth patterns.

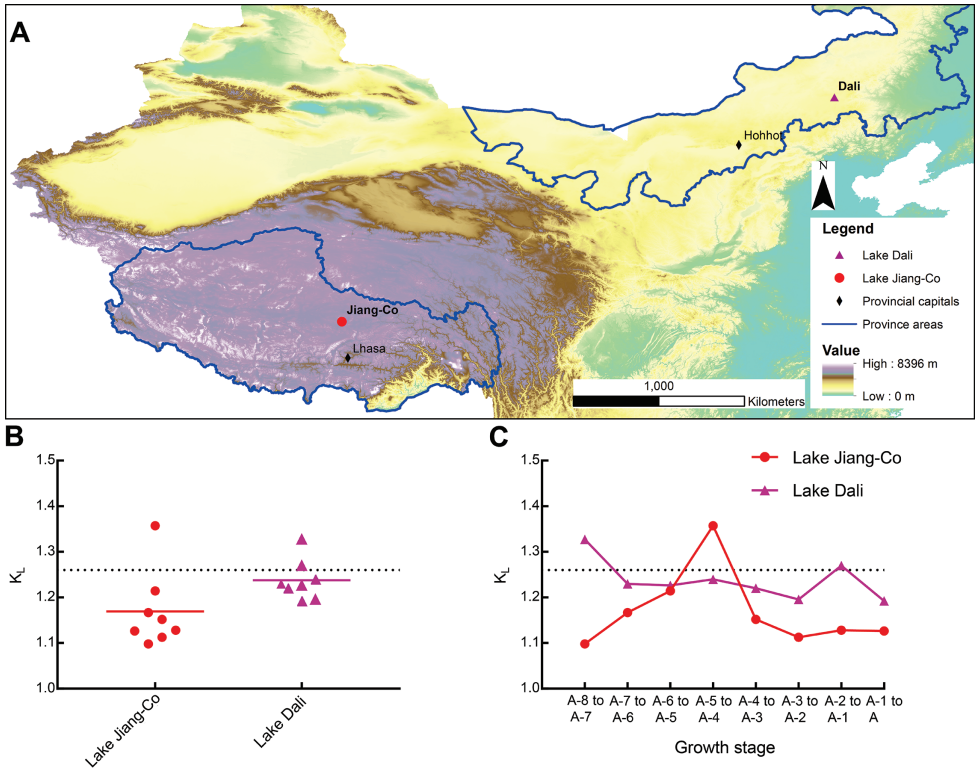


Figure 3. **A** Locations of Lake Jiang-Co and Lake Dali **B** scatter plot with mean value of K_L of *L. inopinata* populations from A-8 stage to adult in Lake Jiang-Co and Lake Dali (Zhai et al. 2015). The rounded dot and triangle represent the growth ratio between adjacent instars **C** comparison between K_L of *L. inopinata* populations from A-8 stage to adult in Lake Jiang-Co and Lake Dali (Zhai et al. 2015). The grey dotted lines suggest a growth ratio of 1.26, the value predicted by Brooks' rule.

Morphological description of *Limnocythere inopinata*

Figures 4, 5

Material examined and locality. Shells of *L. inopinata* from the instar A-8 to the adult stage collected from an indoor biocultured population, which was originally sampled from Lake Jiang-Co. The appendages of six adult females were selected for examination.

Description of shell. All the valves were thin and semi-transparent (Fig. 4). Generally, the carapace of instars A-8 and A-7 were too soft to remain intact after dissection. These individuals were marginally broken in ventral view, but the valve surface was ornamented with rounded pits and a reticulate pattern of ridges. Each valve had a medio-dorsal transverse groove at approximately the middle of its length. The groove of the instars A-6 to the adult stage were more obvious than that of the instars A-8 and A-7. The dorsal margin was slightly rounded in the instars A-8 to A-3 and almost straight in the instar A-2 to the adult stage. The valves of the instars A-6 to A-3 had

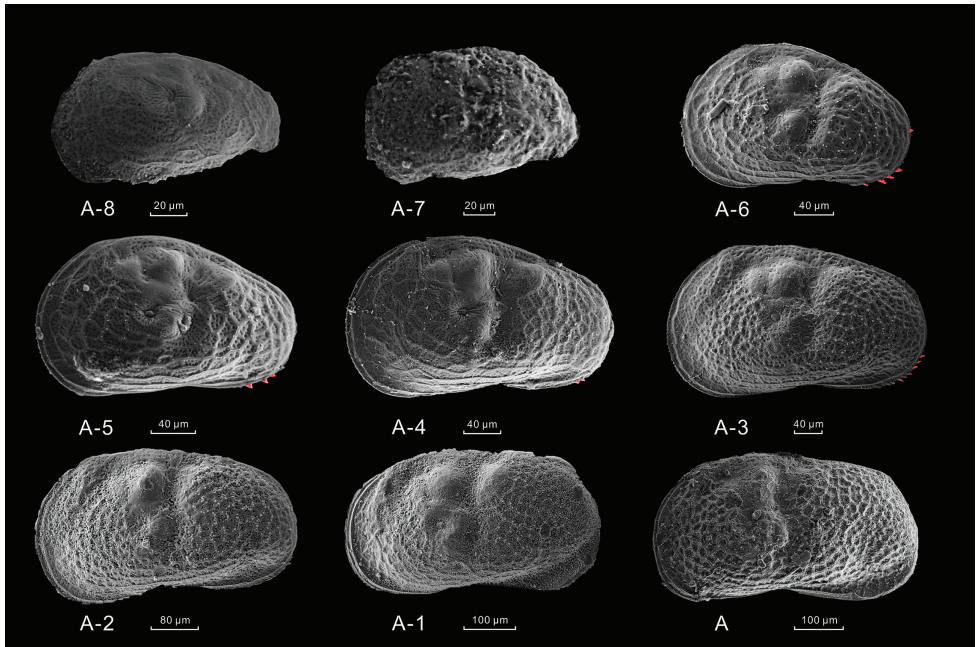


Figure 4. SEM photographs of *L. inopinata* describing carapace morphological features of different developmental stage. All the left valves are from indoor bioculture. The red parts of the instars A-6 to A-3 represent the marginal denticles.

a clear postero-ventral row of marginal denticles, while that trait was faint in the A-2 instar to the adult stage.

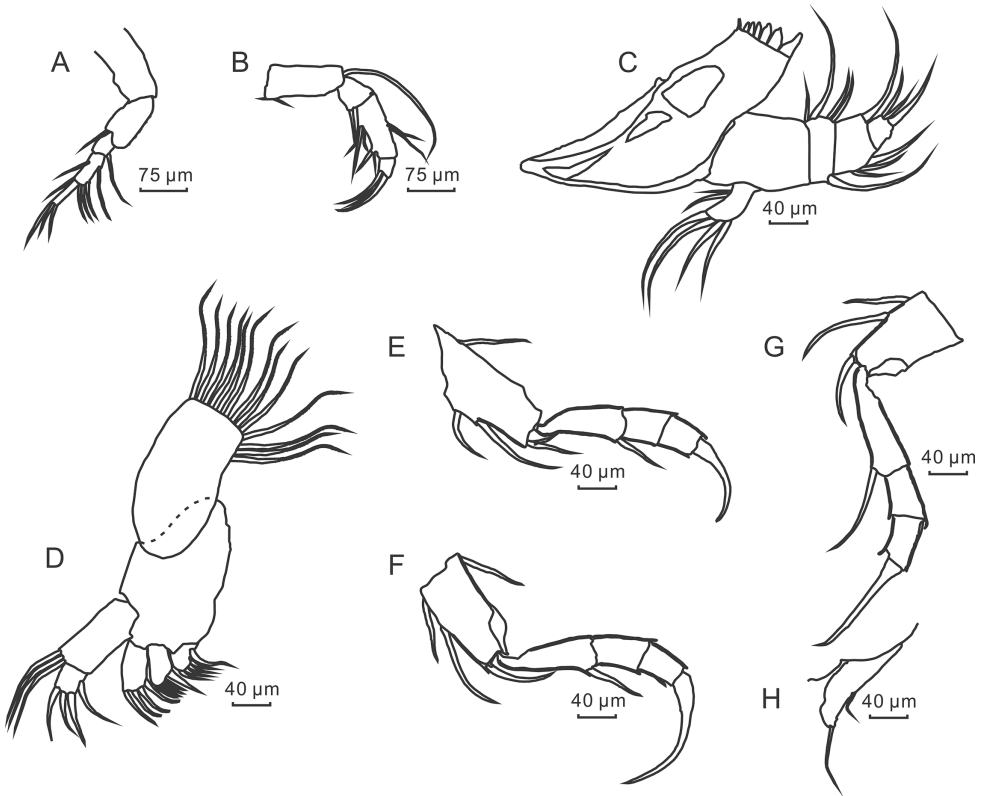
Description of the soft parts of adult. Antennule (Fig. 5A) symmetrical, uniramous, 5-segmented. The lengths of the segments, from proximal to distal ones, being 73.6 μm , 58.2 μm , 18.0 μm , 39.8 μm , and 33.4 μm , respectively (Table 3). Armature of segments as follows: segment II with one antero-apical seta; segment III with one postero-apical seta; segment IV with one postero-medial seta, and one anterior and three posterior setae at the apical part; segment V with three claws, lengths 53.9 μm , 41.4 μm , and 41.2 μm , respectively.

Antenna (Fig. 5B) biramous, with a nearly rectangular protopod, 78.6 μm in length (Table 3) with two ventro-basal setae. The exopod degenerated to a spinneret seta. The endopod well-developed and consisting of three segments, 34.5 μm , 66.1 μm , and 18.0 μm in length. Armature of endopod segments as follows: segment I with one postero-apical seta; segment II with two antero-medial setae, three postero-medial setae, and two postero-apical setae; segment III armed with three claws, lengths 67.9 μm , 57.5 μm , and 52.1 μm , respectively.

Mandible (Fig. 5C) with two protopodal segments, i.e., the coxa and the basis, the coxa nearly trapezoidal and the basis smaller and nearly rectangular. The exopodal branchial plate greatly reduced and unsegmented with two postero-medial setae and four apical setae. The endopodal part of the palp well-developed and comprising of three segments. Armature of endopod segments as follows: segment I with two postero-proximal setae,

Table 3. Length of adult appendage segments and terminal segment claws of *L. inopinata*. A1, antennule; A2, antenna; T1, first thoracopod; T2, second thoracopod; T3, third thoracopod; UR, uropodal rami.

Appendage	Segment I (μm)	Segment II (μm)	Segment III (μm)	Segment IV (μm)	Segment V (μm)	Claw 1 (μm)	Claw 2 (μm)	Claw 3 (μm)
A1	73.6	58.2	18.0	39.8	33.4	53.9	41.4	41.2
A2	78.6	34.5	66.1	18.0	–	67.9	57.5	52.1
T1	64.3	51.6	24.7	27.9	–	81.4	40.4	–
T2	58.0	54.7	20.4	29.6	–	67.7	–	–
T3	62.0	57.0	25.2	25.7	–	95.4	–	–
UR	39.2	–	–	–	–	–	–	–

**Figure 5.** Appendage morphology of *L. inopinata*, adult female **A** antennule **B** antenna **C** mandible **D** maxilla **E** first thoracopod **F** second thoracopod **G** third thoracopod **H** uropodal rami.

and one antero-distal seta and two postero-distal setae; segment II with three antero-medial setae and one postero-apical seta; segment III with three antero-apical setae.

Maxillula (Fig. 5D) with a protopod. The protopod bearing three endites, each armed with four or five setae. The exopod forming a well-developed branchial plate. The endopod constituting a palp with two segments, of which segment I bearing three postero-apical setae and segment II ornamented with four apical setae.

First thoracopod (Fig. 5E) uniramous with a protopod, length 64.3 μm (Table 3), and developing two anterior setae, one posterior seta and one or two apical seta(e). The

endopod composed of four segments, of which proximal three segments being 51.6 μm , 24.7 μm , and 27.9 μm in length. Segment III ornamented with two different morphological characteristics, one with a claw which segment IV fused with the terminal claw ~ 60.0 μm in length, and the other bearing two setae, of which one approximately twice as long as the other, with lengths 81.4 μm and 40.4 μm , respectively (see the Suppl. material 1: Fig. S1).

Second thoracopod (Fig. 5F) uniramous, bearing a protopod with length 58.0 μm (Table 3) and armed with two anterior setae and one posterior seta, and one apical seta. The endopod composed of four segments, of which proximal three segments being 54.7 μm , 20.4 μm , and 29.6 μm in length. Segment I bearing one antero-apical seta and segment IV fused with the terminal claw, being 67.7 μm in total length.

Third thoracopod (Fig. 5G) uniramous with a protopod, with a length of 62.0 μm (Table 3), and with two anterior setae and one apical seta. The endopod composed of four segments, of which proximal three segments being 57.0 μm , 25.2 μm , and 25.7 μm in length. Segment I bearing one antero-apical seta and segment IV fused with the terminal claw, being 95.4 μm in length.

Uropodal rami (Fig. 5H) reduced to a single segment, 39.2 μm in length (Table 3), bearing one postero-medial seta and one terminal seta.

Discussion

Life stages of *L. inopinata*

Like other arthropods, ostracods grow by moulting. From egg to adult, the podocopid Ostracoda usually undergo eight moulting stages. Many studies on life cycle have been published, including on *Heterocypris incongruens* Ramdohr, 1808 (Schreiber 1922), *Darwinula stevensoni* Brady & Robertson, 1870 (Scheerer-Ostermeyer 1940), *Cypridopsis vidua* O.F. Müller, 1776 (Kesling 1951), *Cyprideis torosa* Jones, 1850 (Weygoldt 1960), and *Eucypris virens* Jurine, 1820 (Smith and Martens 2000).

Based on our results, *L. inopinata* has a special growth pattern with a significant variation from Inner Mongolia populations at the transition from the instars A-5 to A-4. Carapace length is significantly positively correlated with the height ($r = 0.994$, $P = 0.000$). This phenomenon suggests that the shell length and height of *L. inopinata* are interdependent, which is in accordance with data on most other ostracod species, such as the study on *Eukloedenella adcapitidolorella* (Forel 2015). However, in the ontogeny of *L. inopinata*, the instar A-5 is a very special growth stage, and there is no overlap in carapace size between the instars A-6, A-5, and A-4. This usually corresponds to significant development of soft parts, such as new appendages development (Meisch 2000; Smith and Martens 2000). Slight overlap occurs in other adjacent growth stages. Compared with the data published in Zhai et al. (2015), *L. inopinata* population living in MP has a less varied growth pattern, including the instars A-5 moulting to A-4. This indicates that there is an intraspecific difference in growth pattern of *L. inopinata*.

Yin et al. (1999) pointed out that *L. inopinata* populations, which is originally collected from Europe and China, has different morphological traits for both the valves

(shape and size) and soft parts. Several studies suggested that the length of *L. inopinata* valves can be influenced by water salinity, i.e., species adapting to variable environment by adjusting body size for maintaining high fitness, a well-known life history strategy (Yin et al. 2001; Zhang et al. 2004; Xu et al. 2012). These studies only dealt with the specimens from Qinghai-Tibet Plateau. However, the difference in growth pattern between *L. inopinata* populations from Lake Jiang-Co and Lake Dali is possibly correlated with different water parameters, e.g., 0.59 vs. 7.60‰ salinity of Lake Jiang-Co and Lake Dali, respectively. It is reasonable to infer that the growth pattern of *L. inopinata* population living in a water with lower salinity condition is more volatile than in a higher salinity water body.

Brooks' rule predicts that the growth ratio of crustaceans during its growth process is 1.26 (Brooks 1886; Teissier 1960). Although the mechanism of this pattern is still unclear, the growth of ostracods somewhat deviates from this prediction (e.g., Kesling and Takagi 1961; Kesling and Crafts 1962). Danielopol et al. (2008) reviewed these studies and recorded values ranging from 1.210 to 1.370 for non-marine ostracod species. However, an intraspecific difference is likely to exist in growth pattern of different populations. This may be due to different life history strategies, corresponding to variable environmental conditions. Additional studies on more species are necessary to prove this hypothesis.

Comparisons between morphology of different *L. inopinata* populations

All the morphological characteristics of these populations have been compared with the European populations as described by Yin et al. (1999), Meisch (2000). Differences that occur in the chaetotaxy of the antenna, first thoracopod, and third thoracopod are significant.

Compared with the antenna of the European *L. inopinata* female (Yin et al. 1999; Meisch 2000), Lake Jiang-Co females have segment II carrying an additional postero-apical seta, while the chaetotaxy of the antenna is similar to the population studied by Yin et al. (1999). In our specimens, the protopod of the third thoracopod is unarmed, while there is one seta at the same place in the European *L. inopinata*.

The most obvious difference occurs in the first thoracopod. *Limnocythere inopinata* from Lake Jiang-Co has two types of chaetotaxy on the protopod and the terminal segment. One type is similar with the populations illustrated in Yin et al. (1999) and Meisch (2000), while the other is very different. The protopod of former one is armed with two apical setae and the terminal segment is fused with the claw it carries. In the latter type, the protopod bears only one apical seta and the terminal segment is armed with two setae. It is observed in one of the six dissected specimens. However, at the present moment with the lack of DNA data we cannot claim with great certainty that *L. inopinata* is actually a species complex.

Conclusions

This study represents a bioculture experiment on *L. inopinata* in order to better understand its life stages and morphological variations from the A-8 to the adult. The living

animals were collected from Lake Jiang-Co, northern Tibetan Plateau. *Limnocythere inopinata* has a special growth pattern in comparison to the prediction of Brooks' rule and the growth pattern of *L. inopinata* population in Lake Dali, eastern MP. The maximum growth occurs in the instars A-5 moulting to the A-4. This indicates that difference in growth pattern between populations may be attributed to different life history strategies as adaptation to environmental conditions. The adults of *L. inopinata* from Lake Jiang-Co differ from European *L. inopinata* in the morphological characteristics of the appendages with the most obvious difference appearing in the first thoracopod.

Acknowledgements

This study was supported by the National Natural Science Foundation of China (41372179, 91747204), the Special Funds for Basic Scientific Research, Chinese Academy of Geological Sciences (JYYWF20182701), Guangdong Provincial Key Laboratory of Soil and Groundwater Pollution Control (No. 2017B030301012), and High-level Special Funding of the Southern University of Science and Technology (Grant No. G02296302, G02296402). We thank Dayou Zhai for kindly providing valuable data. The manuscript benefited from constructive comments of Ivana Karanovic, Dayou Zhai, and Hayato Tanaka.

References

- Akita LG, Frenzel P, Wang J, Börner N, Peng P (2016) Spatial distribution and ecology of the Recent Ostracoda from Tangra Yumco and adjacent waters on the southern Tibetan Plateau: a key to palaeoenvironmental reconstruction. *Limnologia* 59: 21–43. <https://doi.org/10.1016/j.limno.2016.03.005>
- Alkalaj J, Hrafnisdottir T, Ingimarsson F, Smith RJ, Kreiling AK, Mischke S (2019) Distribution of Recent non-marine ostracods in Icelandic lakes, springs, and cave pools. *Journal of Crustacean Biology* 39(3): 202–212. <https://doi.org/10.1093/jcobiol/ruz008>
- Benzie JA (1989) The distribution and habitat preference of ostracods (Crustacea: Ostracoda) in a coastal sand-dune lake, Loch of Strathbeg, north-east Scotland. *Freshwater Biology* 22(2): 309–321. <https://doi.org/10.1111/j.1365-2427.1989.tb01104.x>
- Brooks WK (1886) Report on the Stomatopoda dredged by HMS “Challenger” during the years 1873–1876. Report on the scientific results of the voyage of HMS. Challenger *Zoology* 16: 1–116. <https://doi.org/10.5962/bhl.title.9891>
- Carbonel P, Colin JP, Danielopol DL, Löffler H, Neustrueva I (1988) Paleoecology of limnic ostracodes: a review of some major topics. *Palaeogeography, Palaeoclimatology, Palaeoecology* 62(1–4): 413–461. [https://doi.org/10.1016/0031-0182\(88\)90066-1](https://doi.org/10.1016/0031-0182(88)90066-1)
- Danielopol DL, Baltanás A, Namiotko T, Geiger W, Pichler M, Reina M, Roidmayr G (2008) Developmental trajectories in geographically separated populations of non-marine ostracods: morphometric applications for palaeoecological studies. *Senckenbergiana lethaea* 88(1): 183–193. <https://doi.org/10.1007/BF03043988>

- Decrouy L, Vennemann TW, Ariztegui D (2012) Sediment penetration depths of epi- and in-faunal ostracods from Lake Geneva (Switzerland). *Hydrobiologia* 688(1): 5–23. <https://doi.org/10.1007/s10750-010-0561-8>
- Decrouy L, Vennemann TW (2014) Life histories and distribution of ostracods with depth in western Lake Geneva (Petit-Lac), Switzerland: a reconnaissance study. *Crustaceana* 87(8–9): 1095–1123. <https://doi.org/10.1163/15685403-00003344>
- Forel MB (2015) Heterochronic growth of ostracods (Crustacea) from microbial deposits in the aftermath of the end-Permian extinction. *Journal of Systematic Palaeontology* 13(4): 315–349. <https://doi.org/10.1080/14772019.2014.902400>
- Frenzel P, Keyser D, Viehberg FA (2010) An illustrated key and (palaeo) ecological primer for Postglacial to Recent Ostracoda (Crustacea) of the Baltic Sea. *Boreas* 39(3): 567–575. <https://doi.org/10.1111/j.1502-3885.2009.00135.x>
- Frogley MR, Griffiths HI, Heaton TH (2001) Historical biogeography and Late Quaternary environmental change of Lake Pamvotis, Ioannina (north-western Greece): evidence from ostracods. *Journal of Biogeography* 28(6): 745–756. <https://doi.org/10.1046/j.1365-2699.2001.00582.x>
- Geiger W (1994) An ecophysiological approach to the clonal ecology of *Limnocythere inopinata*. In: Horne DJ, Martens K (Eds) *The evolutionary ecology of reproductive modes in nonmarine Ostracoda*. University of Greenwich Press, Greenwich, 23–26.
- Ghaouaci S, Yavuzatmaca M, Külköylüoğlu O, Amarouayache M (2017) An annotated checklist of the non-marine ostracods (Crustacea) of Algeria with some ecological notes. *Zootaxa* 4290(1): 140–154. <https://doi.org/10.11646/zootaxa.4290.1.8>
- Hiller D (1972) Untersuchungen zur Biologie und zur ökologie limnischer Ostracoden aus der Umgebung von Hamburg. *Archiv für Hydrobiologie* 40(4): 400–497.
- Holmes JA, Allen MJ, Street-Perrott FA, Ivanovich M, Perrott RA, Waller MP (1999) Late Holocene palaeolimnology of Bal Lake, northern Nigeria, a multidisciplinary study. *Palaeogeography, Palaeoclimatology, Palaeoecology* 148(1–3): 169–185. [https://doi.org/10.1016/S0031-0182\(98\)00182-5](https://doi.org/10.1016/S0031-0182(98)00182-5)
- Holmes J, Sayer CD, Liptrot E, Hoare DJ (2010) Complex controls on ostracod palaeoecology in a shallow coastal brackish-water lake: implications for palaeosalinity reconstruction. *Freshwater Biology* 55(12): 2484–2498. <https://doi.org/10.1111/j.1365-2427.2010.02478.x>
- Karan-Žnidaršič T, Petrov B (2007) Non-marine Ostracoda (Crustacea) of Banat district in Serbia. *Hydrobiologia* 585: 57–66. <https://doi.org/10.1007/s10750-007-0628-3>
- Keatings K, Holmes J, Flower R, Horne D, Whittaker JE, Abu-Zied RH (2010) Ostracods and the Holocene palaeolimnology of Lake Qarun, with special reference to past human-environment interactions in the Faiyum (Egypt). *Hydrobiologia* 654(1): 155–176. <https://doi.org/10.1007/s10750-010-0379-4>
- Kempf EK (1986) Late Quaternary environmental changes in the eastern Sahara (Libyan Desert) documented by an ostracode diagram. *Centre National de la Recherche Scientifique* 197: 235–238.
- Kesling RV (1951) The morphology ostracod molt stages. *Illinois Biological Monographs* 21: 1–126. <https://doi.org/10.5962/bhl.title.50392>
- Kesling RV, Takagi RS (1961) Evaluation of Przibram's law for ostracods by use of the Zeuthen Cartesian-diver weighing technique. *Contribution from the Museum of Paleontology, University of Michigan* 17: 1–58.

- Kesling RV, Crafts FC (1962) Ontogenetic increase in Archimedean weight of the ostracod *Chlamydotheca unispinosa* (Baird). *American Midland Naturalist* 68: 149–153. <https://doi.org/10.2307/2422641>
- Kramer M, Kotliá BS, Wünnemann B (2014) A late quaternary ostracod record from the Tso Kar basin (North India) with a note on the distribution of recent species. *Journal of paleolimnology* 51(4): 549–565. <https://doi.org/10.1007/s10933-014-9773-7>
- Külköylüoğlu O, Yavuzatmaca M, Sarı N, Akdemir D (2016) Elevational distribution and species diversity of freshwater Ostracoda (Crustacea) in Çankırı region (Turkey). *Journal of Freshwater Ecology* 31(2): 219–230. <https://doi.org/10.1080/02705060.2015.1050467>
- Iglikowska A, Namiotko T (2012) The non-marine Ostracoda of Lapland: changes over the past century. *Journal of Limnology* 71(2): e26. <https://doi.org/10.4081/jlimnol.2012.e26>
- Löffler H (1990) Paleolimnology of Neusiedlersee, Austria. *Hydrobiologia* 214(1): 229–238. <https://doi.org/10.1007/BF00050955>
- Marchegiano M, Gliozzi E, Ceschin S, Mazzini I, Adatte T, Mazza R, Ariztegui D (2017) Ecology and distribution of living ostracod assemblages in a shallow endorheic lake: the example of the Lake Trasimeno (Umbria, central Italy). *Journal of Limnology* 76: 469–487. <https://doi.org/10.4081/jlimnol.2017.1478>
- Martínez-García B, Suarez-Hernando O, Mendicoa J, Murelaga X (2015) Living ostracod species from permanent and semi-permanent ponds of Bardenas Reales de Navarra (Northern Spain) with remarks on their ecological requirements. *Ameghiniana* 52(6): 598–612. <https://doi.org/10.5710/AMGH.17.07.2015.2895>
- McCormack J, Akdemir D, Immenhauser A, Kwiecien O (2019) Ostracods as ecological and isotopic indicators of lake water salinity changes: the Lake Van example. *Biogeosciences* 16(10): 2095–2114. <https://doi.org/10.5194/bg-16-2095-2019>
- Mezquita F, Griffiths HI, Sanz S, Soria JM, Piñón A (1999) Ecology and distribution of ostracods associated with flowing waters in the eastern Iberian Peninsula. *Journal of Crustacean Biology* 19(2): 344–354. <https://doi.org/10.1163/193724099X00150>
- Mischke S, Herzsuh U, Kürschner H, Fuchs D, Zhang J, Meng F, Sun Z (2003) Sub-recent Ostracoda from Qilian Mountains (NW China) and their ecological significance. *Limnologia* 33(4): 280–292. [https://doi.org/10.1016/S0075-9511\(03\)80023-3](https://doi.org/10.1016/S0075-9511(03)80023-3)
- Mischke S, Ginat H, Al-Saqarat B, Almogi-Labin A (2012) Ostracods from water bodies in hyperarid Israel and Jordan as habitat and water chemistry indicators. *Ecological Indicators* 14(1): 87–99. <https://doi.org/10.1016/j.ecolind.2011.07.017>
- Meisch C (2000) *Freshwater Ostracoda of Western and Central Europe*. Heidelberg.
- Namiotko T, Dan D, Baltanás A (2011) Soft body morphology, dissection and slide-preparation of Ostracoda: a primer. *Joansea – Geologie und Palaontologie* 11: 327–343.
- Poberezhnaya AE, Fedotov AP, Sitnikova TY, Semenov MY, Ziborova GA, Otinova EL, Khabuev AV (2006) Paleoecological and paleoenvironmental record of the Late Pleistocene record of Lake Khubsugul (Mongolia) based on ostracod remains. *Journal of Paleolimnology* 36(2): 133–149. <https://doi.org/10.1007/s10933-006-0009-3>
- Roberts JH, Holmes JA, Swan AR (2002) Ecophenotypy in *Limnocythere inopinata* (Ostracoda) from the late Holocene of Kajemarum Oasis (north-eastern Nigeria). *Palaeogeography, Palaeoclimatology, Palaeoecology* 185(1–2): 41–52. [https://doi.org/10.1016/S0031-0182\(02\)00254-7](https://doi.org/10.1016/S0031-0182(02)00254-7)

- Rodríguez-Pérez H, Baltanás Á (2008) Ecology and production of *Heterocypris exigua* and *Plesiocypridopsis newtoni* (Crustacea, Ostracoda) in an oligohaline hypertrophic shallow lake. *Fundamental and Applied Limnology/Archiv für Hydrobiologie* 172(1): 13–26. <https://doi.org/10.1127/1863-9135/2008/0172-0013>
- Rossi V, Piotti A, Geiger W, Benassi G, Menozzi P (2010) Genetic Structure of Austrian and Italian Populations of *Limnocythere inopinata* (Crustacea, Ostracoda): A Potential Case of Post-Glacial Parthenogenetic Invader? *Annales Zoologici Fennici* 47: 133–143. <https://doi.org/10.5735/086.047.0206>
- Scharf B, Brunke M (2013) The recolonization of the river Elbe with benthic and hyporheic Ostracoda (Crustacea) after the reunion of Germany in 1989. *International review of hydrobiology* 98(6): 305–312. <https://doi.org/10.1002/iroh.201201617>
- Scheerer-Ostermeyer E (1940) Beitrag zur Entwicklungsgeschichte der Süßwasserosttrakoden. *Zoologische Jahrbücher, Abteilung für Anatomie und Ontogenie der Tiere* 66: 349–370.
- Schreiber E (1992) Beiträge zur Kenntnis der Morphologie, Entwicklung und Lebensweise der Süßwasser-Ostracoden. *Zoologische Jahrbücher. Abteilung für Anatomie und Ontogenie der Tiere* 43(4): 485–583.
- Shen J, Matsumoto R, Wang S, Zhu Y (2001) Quantitative reconstruction of the paleosalinity in the Daihai Lake, Inner Mongolia, China. *Chinese Science Bulletin* 46(1): 73–76. <https://doi.org/10.1007/BF03183214>
- Smith RJ, Martens K (2000) The Ontogeny of the Cypridid Ostracod *Eucypris virens* (Jurine 1820) (Crustacea, Ostracoda). *Hydrobiologia* 419:31–63. <https://doi.org/10.1023/A:1003985908460>
- Szlauer-Łukaszewska A (2014) The dynamics of seasonal ostracod density in groyne fields of the Oder River (Poland). *Journal of Limnology* 73(2): 298–311. <https://doi.org/10.4081/jlimnol.2014.865>
- Szlauer-Łukaszewska A (2015a) Effects of river bed regulation on habitats and communities: A case study for ostracods in the Oder River, Poland. *International Review of Hydrobiology* 100(2): 69–78. <https://doi.org/10.1002/iroh.201401738>
- Szlauer-Łukaszewska A (2015b) Substrate type as a factor affecting the ostracod assemblages in groyne fields of the Oder River (Poland). *North-Western Journal of Zoology* 11(2): 274–287. <https://doi.org/10.4081/jlimnol.2014.865>
- Teissier G (1960) Reticulate growth. In: Waterman TH (Ed.) *The Physiology of Crustacea*. Academic Press, New York, 541–544.
- Usskilat F (1975) Untersuchungen am Oligohalinikum der Schlei: 2. Die Ostracodengemeinschaften des Haddebyer und Selke Noores (Schlei). *Kieler Meeresforschungen* 31: 151–178.
- Von Grafenstein U, Erlernkeuser H, Trimborn P (1999) Oxygen and carbon isotopes in modern fresh-water ostracod valves: assessing vital offsets and autecological effects of interest for palaeoclimate studies. *Palaeogeography, Palaeoclimatology, Palaeoecology* 148(1–3): 133–152. [https://doi.org/10.1016/S0031-0182\(98\)00180-1](https://doi.org/10.1016/S0031-0182(98)00180-1)
- Watabe K, Kaesler RL (2004) Ontogeny of a new species of Paraparchites (Ostracoda) from the lower Permian Speiser Shale in Kansas. *Journal of Paleontology* 78(3): 603–611. [https://doi.org/10.1666/0022-3360\(2004\)078%3C0603:OOANSO%3E2.0.CO;2](https://doi.org/10.1666/0022-3360(2004)078%3C0603:OOANSO%3E2.0.CO;2)
- Weygoldt P (1960) Embryologische Untersuchungen an Ostrakoden: Die Entwicklung von *Cyprideis litoralis* (G. S. Brady) (Ostracoda, Podocopa, Cytheridae). *Zoologische Jahrbücher. Abteilung B (Anatomie und Ontogenie der Tiere)* 78(3): 369–426.

- Xu X, Wang Y, Shen J, Wang Y (2012) Discussions on feasibility of paleo-salinity reconstruction of Lake Qinghai water by variations in body length of ostracod valves. *Acta Sedimentologica Sinica* 30(6): 1072–1079. [in Chinese with English abstract]
- Yang M, Dawa Z, Jiang Y, Gema Q (2018) Characteristics of modern climate change and climate humidification in Naqu area. *Tibet Science and Technology* 2: 63–65. [in Chinese]
- Yang F, Dong N, Qiao Z, Sun Z, Ren Y (2008) Taxonomy and Habitat of Quaternary Limnocythere (Ostracoda) from the Qaidam Basin and the Qinghaihu Lake, Qinghai. *Acta Micropalaeontologica Sinica* 25(4): 316–332. [in Chinese with English abstract]
- Yin Y, Geiger W, Martens K (1999) Effects of genotype and environment on phenotypic variability in *Limnocythere inopinata* (Crustacea: Ostracoda). *Hydrobiologia* 400: 85–114. <https://doi.org/10.1023/A:1003759125903>
- Yin Y, Li W, Yang X, Wang S, Li S, Xia W (2001) Morphological response of *Limnocythere inopinata* to hydrochemical environmental factors. *Science in China (Series D)* 31: 252–257. [in Chinese]
- Zhai D, Xiao J, Fan J, Wen R, Pang Q (2015) Differential transport and preservation of the in-stars of *Limnocythere inopinata* (Crustacea, Ostracoda) in three large brackish lakes in northern China. *Hydrobiologia* 747(1): 1–18. <https://doi.org/10.1007/s10750-014-2118-8>
- Zhang E, Shen J, Wang S, Yin Y, Zhu Y, Xia W (2004) Quantitative reconstruction of the paleosalinity at Qinghai Lake in the past 900 years. *Chinese Science Bulletin* 49(7): 730–734. <https://doi.org/10.1007/BF03184273>
- Zhang W, Mischke S, Zhang C, Zhang H, Wang P (2015) Sub-Recent Sexual Populations of *Limnocythere inopinata* Recorded for the First Time from > 3500 m Altitude on the Tibetan Plateau. *Acta Geologica Sinica (English Edition)* 89(3): 1041–1042. <https://doi.org/10.1111/1755-6724.12497>

Supplementary material I

Figure S1

Authors: Can Wang, Hailei Wang, Xingxing Kuang, Ganlin Guo

Data type: png image

Explanation note: Another morphological type of first thoracopod of *L. inopinata*, adult female. Protopod with one apical seta, and distal segment with two posterior setae, the well-developed seta approximately twice as long as smaller one.

Copyright notice: This dataset is made available under the Open Database License (<http://opendatacommons.org/licenses/odbl/1.0/>). The Open Database License (ODbL) is a license agreement intended to allow users to freely share, modify, and use this Dataset while maintaining this same freedom for others, provided that the original source and author(s) are credited.

Link: <https://doi.org/10.3897/zookeys.1011.56065.suppl1>

A new *Parazuphium* Jeannel, 1942 species (Coleoptera, Carabidae) from the Zagros Mountains in Iran

David W. Wrase¹, Thorsten Assmann²

1 Oderstraße 2, D-15306, Gusow-Platkow, Germany **2** Institute of Ecology, Leuphana University Lüneburg, Universitätsallee 1, D-21331, Lüneburg, Germany

Corresponding author: David W. Wrase (carterus@gmx.de)

Academic editor: B. Guéorguiev | Received 8 October 2020 | Accepted 16 December 2020 | Published 15 January 2021

<http://zoobank.org/E8A208E4-1FE6-4855-8FFC-34671103342E>

Citation: Wrase DW, Assmann T (2021) A new *Parazuphium* Jeannel, 1942 species (Coleoptera, Carabidae) from the Zagros Mountains in Iran. ZooKeys 1011: 41–50. <https://doi.org/10.3897/zookeys.1011.59449>

Abstract

Parazuphium weigeli **sp. nov.** is described from the Zagros Mountains in Iran. The microphthalmic species was found in a subalpine site under a deeply embedded stone close to a snow field. It resembles *P. salmoni* Assmann, Renan & Wrase, 2015, but differs by shape of pronotum and its punctuation, eye size, body proportions, and shape of median lobe of aedeagus and preputial sclerites. An identification key to the known species from Iran is given.

Keywords

Identification key, microphthalmic species, subalpine habitats, Zuphiini

Introduction

The ground beetle fauna of Iran was compiled by Azadbakhsh and Nozari (2015) in catalogue form. However, soon after the publication of this work, it became clear that the fauna of this large country with its numerous climatic zones and diverse habitats has not been sufficiently studied. Several ground beetle species have since been described (e.g., Azadbakhsh and Wrase 2016; Wrase and Schnitter 2017; Casale and Wrase 2018; Muilwijk et al. 2018; Muilwijk et al. 2019).

We compared two specimens of *Parazuphium* collected from the Zagros Mountains with the other known *Parazuphium* species from the Palaearctic, but it was clear

they represented a new species. The description of this new species is given below, and we offer an identification key of the species known from Iran to support further work on ground beetles in this country.

Material and methods

The material examined is housed in the collections listed below:

NKME Naturkundemuseum Erfurt, Germany;

cWR Working collection David W. Wrase, Gusow-Platkow, Germany (part of Zoologische Staatssammlung München, Germany).

Dissections were made using standard techniques; genitalia were preserved in “Lompe solution” on acetate labels (Lompe 1989) or in Euparal, and pinned beneath the specimens from which they had been removed.

The following measurements were used:

- BL** Body length: maximal linear distance from the tip of the mandibles to the apex of the right elytron;
- HW** Head width: maximal linear distance;
- A1L–A4L** Length of the antennomeres: from the basal excision to the tip of the given segment (A1L, A2L, A3L, and A4L refer to the length of the antennomeres I (scapus), II, III and IV, respectively);
- PL** Pronotum length: from the anterior to the posterior margin along the midline;
- EL** Elytra length: maximal linear distance from the end of the scutellum to the apex of the right elytron;
- PW** Pronotum width: greatest linear transverse distance across the pronotum;
- EW** Elytra width: maximum distance across the elytra;
- PEW** Prebasal excision width: shortest distance between the two outer pronotal margins;
- PBaW** Pronotal base width: width between the tips of the hind angles at the insertion of the seta.

These measurements were made at magnifications of $\times 25$ and $\times 50$, using an ocular micrometre in a Leica MZ 16 stereo binocular microscope. Microsculpture was examined at a magnification of $\times 100$.

The photos were prepared with an Olympus E-330 digital camera in combination with a Leica MZ 95 stereo binocular microscope. Stacking (up to ~ 100 layers) was done with the software Picolay (www.picolay.de). Drawings were made with a drawing tube attached to the Leica MZ 95.

Labels of type specimens are cited as originally given, and different lines are separated by a forward slash (/).

Types are deposited in Naturkundemuseum Erfurt, Germany (NKME) and collections of David W. Wrase in Zoologische Staatssammlung München (cWR).

Results

Parazuphium weigeli sp. nov.

<http://zoobank.org/69A63791-3CDF-4CCF-A0AE-B359EC350BF7>

Types. *Holotype* male: “Iran Zagros Mts., P. Chahar / Mahall va Bachtari, Asad / Abad 5 km SW, 32°20'30"N, 50°32'59"E, snow field, high pasture, 19.IV.2018, 2500- / 2770 m, leg. A.Weigel” (NKME; left and right antennomeres X and XI are missing). Paratype: 1 female, same data as HT (cWR).

Diagnosis. A microphthalmic, depigmented, brachypterous *Parazuphium* species with short, robust legs and moderately long antennae. Median lobe of aedeagus with three sclerites. For habitus see Fig. 1.

Description. BL 3.7–3.9 mm; EW 1.3–1.4 mm.

Colour: Light yellowish to brownish.

Head large, slightly triangular, with rounded tempora. Eyes small and flat, $\sim 1/3$ as long as tempora (dorsal view) (Figs 1, 2a). Antennae moderately long, scapus (antennomere I) somewhat shorter than width of head ($A1L/HW$ 0.82–0.83), $\sim 5 \times$ as long as antennomere II ($A1L/A2L$ 4.7–5.17), antennomere II somewhat longer than $1/2$ antennomere III ($A2L/A3L$ 0.54–0.58), antennomere III somewhat shorter than antennomere IV ($A3L/A4L$ 0.92). Neck somewhat wider than $1/3$ of head width. Surface moderately shiny, punctures somewhat indistinct and scattered, setae also fine and scattered. Microsculpture consisting of isodiametric meshes.

Pronotum somewhat wider than head (HW/PW 0.88–0.91), slightly longer than wide (PW/PL 0.92), widest at approximately the apical $1/6$, where lateral seta is inserted. Anterior margin almost rectilinear, somewhat excavated at insertion of neck. Anterior angles rounded, but hardly prominent. Lateral margin in apical $2/3$ continuously rounded, concavely curved at the prebasal excision. Posterior angles obtuse and weakly prominent ($PBaW/PEW$ 1.02–1.05), distinctly shifted forward due to a strong excision of the basal margin (Fig. 4A). Disc flat, median line medially somewhat excavated. Median sulcus fine, impressed on the posterior margin, not reaching the basal margin. Regularly and more strongly punctate and setose than head, microsculpture with irregular transverse meshes.

Elytra short (EL/EW 1.28–1.31), subparallel, distinctly widening to the apex. Apical margin sinuous (Fig. 2b). Striae weak, only intimated, somewhat irregular, internal intervals weakly convex. Punctuation denser than on pronotum, somewhat wrinkled. Surface with setosity formed by short fine setae (somewhat denser than on pronotum), inclined backwards, setae at apex somewhat longer. Series umbilicata consists of eight (five long and three short) humeral and five (three long and two short) apical setae. Surface moderately shiny, microsculpture with irregular meshes. Brachypterous.



Figure 1. Habitus of *Parazuphium weigeli* sp. nov., paratype, female.

Legs robust and short, protibia somewhat curved inwards, mesotibia bent slightly outwards, metatibia straight. Male protarsomeres I–IV enlarged and with adhesive setae beneath.

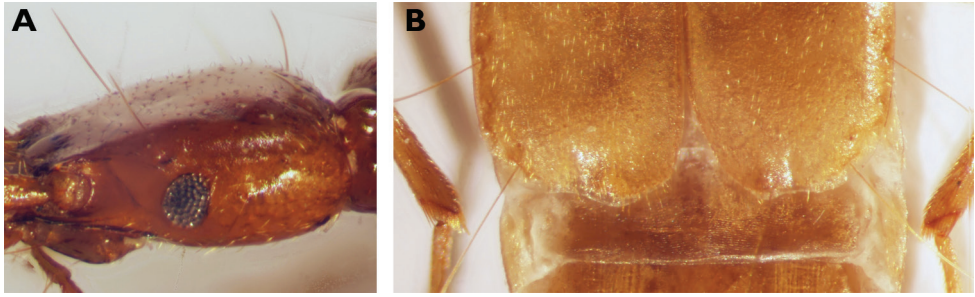


Figure 2. *Parazuphium weigeli* sp. nov. **A** head in lateral view (holotype) **B** apex of elytra (paratype).

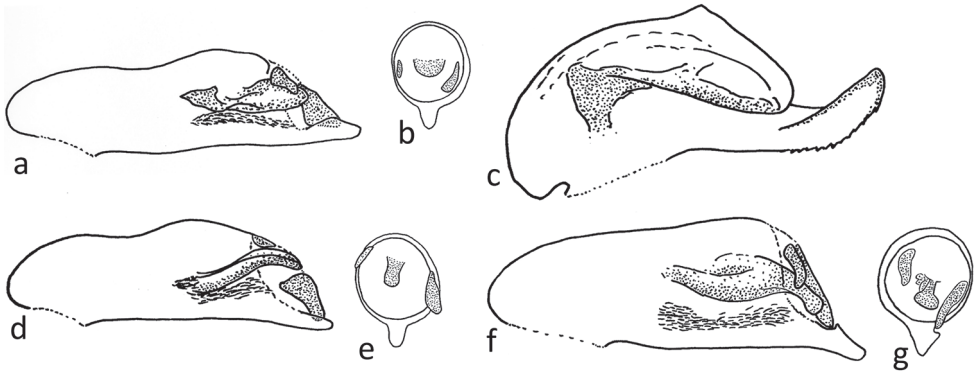


Figure 3. Median lobe of aedeagus of *Parazuphium* **a, c, d, f** lateral views **b, e, g** view onto oroficium (preputial field) **a, b** *P. weigeli* sp. nov. **c** *P. damascenum* **d, e** *P. salmoni* **f, g** *P. chevrolatii*.

Median lobe of aedeagus – 0.75 mm long, strongly sclerotised. Dorsal side sinuous, apex pointed. Preputial field with three sclerites; the central one large, prolonged, at the tip spoon-like rounded, but central and basal part irregularly shaped; the left one rudimentary; the right one triangular (Fig. 3a, b). Left paramere rounded, larger than the strongly reduced right one.

Comparisons. The new species belongs to the genus *Parazuphium* because of small, numerous, erect setae on the scapus, one pair of supraorbital setae, a sinuous apical margin of the elytra, and a tube-shaped median lobe of the aedeagus with small sclerites on the preputial field.

In its characters it is similar to *P. salmoni* Assmann, Renan & Wrase, 2015. It shares with it the small eyes, strong and relatively short legs, moderately long antennae, metatibia straight in both sexes, similar body indices, brachyptery, and the colour. It differs from *P. salmoni* by the following features: (1) eyes larger (eye diameter in dorsal view $\sim 1/3$ of temple length, in *P. salmoni* $\sim 1/4$); (2) antennomere I shorter in relation to antennomere II, $\sim 5 \times$ as long as antennomere II (in *P. salmoni* $5.5\text{--}6 \times$) (measured from the basal incision of the antennomeres to the apex); (3) pronotum more slender in relation to head (HW/PW 0.88–0.91, in *P. salmoni* 0.83–0.85); (4) hind angles less prominent (Fig. 4); (5) punctuation

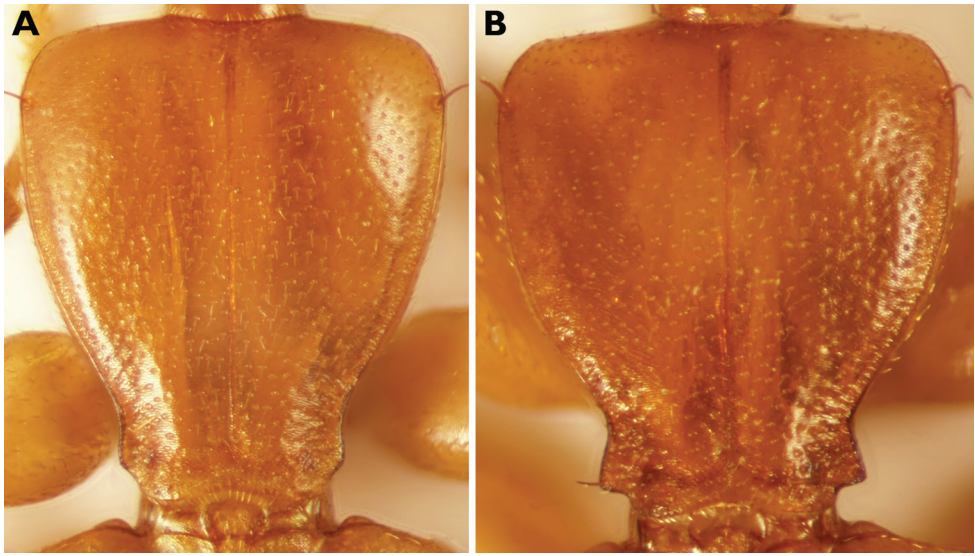


Figure 4. Pronotum of *Parazuphium* **A** *P. weigeli* sp. nov. **B** *P. salmoni*.

of pronotum less prominent (Fig. 4); (6) microsculpture of pronotum weaker and transverse (in *P. salmoni* isodiametric); (7) median lobe of aedeagus not downwardly bent and with different configuration and shape of the sclerites of the preputial field (Fig. 3a, b vs. Fig. 3d, e).

The new species differs from *P. damascenum* (Fairmaire, 1897) by (1) straight metatibia in both genders; (2) smaller and flat eyes; (3) brachyptery, (4) deviating shape of median lobe of aedeagus and its sclerites (Fig. 3a–c).

Parazuphium weigeli sp. nov. differs from *P. chevrolatii* by: (1) smaller eyes; (2) antennomere I shorter, shorter than head width; (3) weakly developed elytral intervals; (4) slender median lobe of aedeagus without an excision at the base of prolonged apical tip (Fig. 3a, b vs. Fig. 3f, g).

The other microphthalmic species of the genus (*P. angusticolum* Hürka, 1982, *P. baeticum* (K. & J. Daniel, 1898), *P. punicum* (K. & J. Daniel, 1898), *P. ramirezi* J. & E. Vives, 1976) differ from *P. weigeli* sp. nov. by their (1) slender legs, (2) longer body lengths, (3) deviating proportions of antennomeres, (4) shape of median lobe of aedeagus and number and shape of sclerites (cf. Hürka 1982, 1987). These species occur exclusively in the south-western part of the Palaearctic (Morocco, Spain, and Sicily) (Huber and Marggi 2017).

Habitat. Habitat is a subalpine grassland in 2500–2770 m a.s.l. The specimens were found under a large stone, deeply embedded in the soil, close to a snow field (Fig. 5).

Dispersal power. Brachypterous.

Distribution. Known so far only from the type locality. As the species is incapable of flight, its dispersal power is strongly limited, and a wider distribution range outside the Zagros Mountains is unlikely. Further studies may show if the occurrence of the species is restricted to high altitudes.



Figure 5. Habitat of *Parazuphium weigeli* sp. nov. **A** landscape **B** microhabitat with the stone under which the two individuals were found. Photographs by Andreas Weigel.

Etymology. Latinised patronym based on the surname of our colleague and friend, Andreas Weigel (Pößneck, Germany), specialist of Cerambycidae. He collected the first specimens of this new species and contributed to carabidology with numerous records of ground beetles, including new taxa.

Identification key to the known *Parazuphium* species from Iran

The genus *Parazuphium* can be easily distinguished from the other genera of the tribe by the following features: (1) scapus of antennae with moderately long setae which poke (more or less at a right angle) out of the normal hairs; these setae are shorter than the large apical seta but longer than the regular vertically protruding bristles (Assmann et al. 2015: fig. 5). (2) Median lobe of aedeagus compact and heavily sclerotised, with a small membranous preputial field. (3) Two pairs of supraorbital setae (the posterior pair located in the basal quarter of the head). (4) Apical margin of elytra sinuous. (5) Genital segment almost rectangular, sometimes bilaterally symmetrical, but not rounded, and heavily sclerotised.

- 1 Metatibia strongly curved, especially in males (Assmann et al. 2015: fig. 10a, b). Eyes larger, laterally protruding. Median lobe of aedeagus with tip bent upwards and lower side like a saw blade (Fig. 3c). Body length 3.5–5.2 mm..... *Parazuphium damascenum* (Fairmaire, 1897)
- Metatibia almost straight in both genders (Fig. 1; Assmann et al. 2015: fig. 10c, d). Eyes of variable size (Fig. 2a; Assmann et al. 2015: fig. 11a, b) **2**
- 2 Eyes strongly reduced (Fig. 2a), temples at least 3 × as long as eyes (dorsal view). Antennae shorter, scapus shorter than the head width, antennomere II < 2 × as long as wide. Median lobe of aedeagus with different configuration and shape of the sclerites of the preputial field (Fig. 3a, b). Body length 3.7–3.9 mm..... *Parazuphium weigeli* sp. nov.
- Eyes of variable size (Assmann et al. 2015: fig. 11a, b), but shorter than temples (dorsal view). Antennae elongate, scapus longer than head width, antennomere II ~ 2 × as long as wide. Median lobe of aedeagus with an excision at the base of prolonged apical tip (Fig. 3f, g). Body length 4–6.5 mm *Parazuphium chevrolatii* Castelnau de Laporte, 1833

Acknowledgements

We would like to thank Andreas Weigel (Pößneck) for the carabid specimens he provided to DWW and for permission to use his habitat photographs. Thanks also to Hongliang Shi (Beijing), Ilya Kabak (Saint Petersburg), and Borislav Guéorguiev (Sofia) for their comments during the review process.

References

- Assmann T, Austin K, Boutaud E, Buse J, Chikatunov V, Drees C, Felix RFFL, Friedman ALL, Khoury F, Marcus T, Renan I, Schmidt C, Wrase DW (2015) The ground beetle supertribe Zuphiitae in the southern Levant (Coleoptera: Carabidae). *Spixiana* 38: 237–262. https://pfeil-verlag.de/wp-content/uploads/2016/07/spix38_2_10.pdf

- Azadbakhsh S, Nozari J (2015) Checklist of the Iranian ground beetles (Coleoptera; Carabidae). *Zootaxa* 4024: 1–108. <https://doi.org/10.11646/zootaxa.4024.1.1>
- Azadbakhsh S, Wrase DW (2016) A new species of the genus *Acinopus* Dejean, 1821 from west of Iran (Coleoptera; Carabidae; Harpalini) with a key to species of Iran. *Zootaxa* 4147: 583–588. <https://doi.org/10.11646/zootaxa.4147.5.6>
- Casale A, Wrase DW (2018) New or little known Sphodrini from Iran (Coleoptera: Carabidae: Sphodrini). *Annales de la Société entomologique de France (N.S.)* 54: 309–317. <https://doi.org/10.1080/00379271.2018.1492689>
- Huber C, Marggi W (2017) Tribe Zuphiini Bonelli, 1810. In: Löbl I, Löbl D (Eds) *Catalogue of Palearctic Coleoptera, Volume 1 (revised and updated edition, Archostemata – Myxophaga – Adephaga)*. Brill, Leiden, Boston, 835–838.
- Hůrka K (1982) Taxonomic notes on *Parazuphium*, with descriptions of three new taxa (Coleoptera, Carabidae). *Acta Entomologica Bohemoslovaca* 79: 281–288.
- Hůrka K (1987) Separation of *Parazuphium* (*P.*) *chevolati* and *P.* (*P.*) *maroccanum*, and description of a new subspecies (Col., Carabidae, Zuphiini). *Acta Entomologica Bohemoslovaca* 84: 469–473.
- Lompe A (1989) Ein bewährtes Einbettungsmittel für Insektenpräparate. In: Lohse GA, Lucht WH (Eds) *Die Käfer Mitteleuropas, 1. Supplementband mit Katalogteil*. Goecke und Evers, Krefeld, 17–18.
- Muilwijk J, Kabak I, Serri S (2018) *Microdaccus bushebricus* sp. n., a new carabid species from Iran (Coleoptera, Carabidae: Lebiini). *Entomological Review* 98: 1177–1180. <https://doi.org/10.1134/S001387381809004X>
- Muilwijk J, Lohaj R, Seiedy M (2019) A new species of the genus *Laemostenus* (Coleoptera: Carabidae) from Zagros Mountains, Iran. *Journal of Entomological Society of Iran* 38: 401–407. <https://www.magiran.com/paper/2004013/?lang=en>
- Wrase DW, Schnitter PH (2017) Description of a new *Nebria* (*Eunebria*) species from Iran (Coleoptera, Carabidae: Nebriini) and faunistic data for *Nebria* (*Eunebria*) *xanthacra xanthacra* Chaudoir, 1850. *Linzer biologische Beiträge* 49: 927–935. https://www.zobodat.at/pdf/LBB_0049_1_0927-0935.pdf

New species of *Limnophyes* Eaton (Diptera, Chironomidae) from China and synonymy of *L. fuscipygmus* Tokunaga, 1940

Wenbin Liu¹, Cong Zhao¹, Fanqing Kong², Chuncai Yan¹, Xinhua Wang³

1 Tianjin Key Laboratory of Conservation and Utilization of Animal Diversity, Tianjin Normal University, Tianjin, 300387, China **2** Ecological Environment Monitoring and Scientific Research Center of Haihe River Basin and Beihai Sea Area, Ministry of Ecological Environment, Tianjin, 300170, China **3** College of Life Science, Nankai University, Tianjin 300071, China

Corresponding author: Chuncai Yan (skyycc@tjnu.edu.cn)

Academic editor: F.L. da Silva | Received 26 September 2020 | Accepted 15 December 2020 | Published 18 January 2021

<http://zoobank.org/F6406B42-0B89-4673-8FE5-E402682F5BF8>

Citation: Liu W, Zhao C, Kong F, Yan C, Wang X (2021) New species of *Limnophyes* Eaton (Diptera, Chironomidae) from China and synonymy of *L. fuscipygmus* Tokunaga, 1940. ZooKeys 1011: 51–61. <https://doi.org/10.3897/zookeys.1011.58993>

Abstract

Two new species, *L. minerus* Liu & Yan, **sp. nov.** and *L. subtilus* Liu & Yan, **sp. nov.** are described and illustrated as adult males. *Limnophyes minimus* (Meigen, 1818) is assigned as a senior synonym of *L. minerus* Tokunaga, 1940. A key to males of *Limnophyes* from China is presented.

Keywords

Identification key, morphology, synonymy, systematics, taxonomy

Introduction

Limnophyes was erected by Eaton (1875) with *Limnophyes pusillus* Eaton, 1875 as type species. Sæther (1990a, b) reviewed the Holarctic, Afrotropical and Neotropical members of this genus. Subsequently, the genus in different life stages and geographical areas were studied by a number of authors (Wang 2000; Chaudhuri et al. 2001; Langton and Moubayed 2001; Yamamoto 2004; Makarchenko et al. 2005; Mendes et al. 2007;

Murray 2007; Makarchenko and Makarchenko 2011; Moubayed 2011; Pinho and Andersen 2015; Song et al. 2020). To date, the genus comprises more than 90 species recorded worldwide (Ashe and O'Connor 2012; Song et al. 2020). However, although 28 species of *Limnophyes* have been recorded in Japan, only four of these are widespread Holarctic species. Most likely, many of the remaining Japanese names are synonymous with names from other regions, and a revision is desirable (Przhiboro and Sæther 2007).

To date, 16 species of the genus from China were described or recorded including two larvae, *L. pentaplastus* (Kieffer, 1921) and *L. pumilio* (Holmgren, 1869) (Wang and Sæther 1993; Wang 1997; Wang 2000; Song et al. 2020).

In this study we describe two new species of *Limnophyes* from Oriental China as male adults, provide a key to the known adult males of the genus from China, and suggest that *L. fuscipygmus* Tokunaga, 1940 from China be considered a synonym of *L. minimus* (Meigen, 1818).

Methods and material

The morphological nomenclature follows Sæther (1980). The material examined was mounted on slides following the procedure outlined by Sæther (1969). All samples have been stored in 85% ethanol prior to preparation. Color is described as observed in specimens mounted in Canada balsam on slides. Measurements are given as ranges followed by the arithmetic mean when four or more species were measured, followed by the number of specimens measured (*N*) in parentheses. All types are deposited in the College of Life Sciences, Nankai University, China (BDN).

Abbreviations used in text as follows: AR, antennal ratio = length of ultimate flagellomere/combined lengths of flagellomeres one to penultimate; fe, femur; HR, hypopygium ratio = gonocoxite length/gonostylus length; HV, hypopygium value = body length/gonostylus length \times 10; LR, leg ratio = tarsomere length/tibia length; LR₁, tarsomere I length/tibia length; p1–3, Legs (1–fore, 2–mid, 3–hind); R, Radius; R₁, Radius 1; R₄₊₅, Radius four and five; Cu₂, the second Cubitus; Ta1–5, tarsomeres 1–5; Ti, tibia; VR, ratio of length of Cu/length of M; BV, Length of (femur + tibia + ta1) / length of (ta2 + ta3 + ta4 + ta5); SV, Length of (femur + tibia) / length of ta; BR, longest seta on tarsomere 1/minimum width of tarsomere 1.

Taxonomy

Limnophyes minerus Liu & Yan, sp. nov.

<http://zoobank.org/559838A7-DBA7-4578-8408-841097D8A54F>

Figs 1–4

Type material. *Holotype* male (BDN No. 13105), CHINA: Sichuan Province, Kangding County, Wasi River, 30.051°N, 101.964°E, 3124 m a.s.l., light trap, 15.vi.1996,

X. Wang. **Paratype:** 1 male, Sichuan Province, Daocheng County, Sangdui Town, 29.038°N, 100.297°E, 3447 m a.s.l., sweep net, 11.vi.1996, X. Wang; 1 male, Hubei Province, Wufeng County, Houhe River, 30.199°N, 110.675°E, 1723 m a.s.l., sweep net, 1.vii.1997, B. Ji.

Diagnostic characters. The species can be separated from other members of the genus by having minute inferior volsella, virga consisting of one tapering spine, no lanceolate setae, and AR 0.24–0.27.

Etymology. From the Latin, *minerus*, minute or tiny, referring to the reduced inferior volsella, adjective in the nominative singular.

Description. Male ($N = 3$).

Total length 1.68–1.80 mm. Wing length 0.95–1.25 mm. Total length / wing length 1.44–1.76. Wing length / length of profemur 2.57–3.20.

Coloration. Head and thorax dark brown. Abdomen and legs brown. Wing nearly transparent.

Head. Antenna with 13 flagellomeres. AR 0.24–0.27. Ultimate flagellomere 79–98 μm long. Temporal setae 4–5, including 1 inner vertical, 1–3 outer verticals and 1–2 postorbitals. Clypeus with 10–21 setae. Tentorium 110–120 μm long, 14–18 μm wide. Palpomere lengths (in μm): 17–20, 22–25, 42–55, 35–52, 79–95. Length ratio of palpomeres 5/3 1.73–1.91.

Wing (Fig. 1). Anal lobe reduced. VR 1.22–1.30. Brachiolum with one seta. R with 1–3 setae. Costal extension 40–50 μm long. Squama with 2–4 setae.

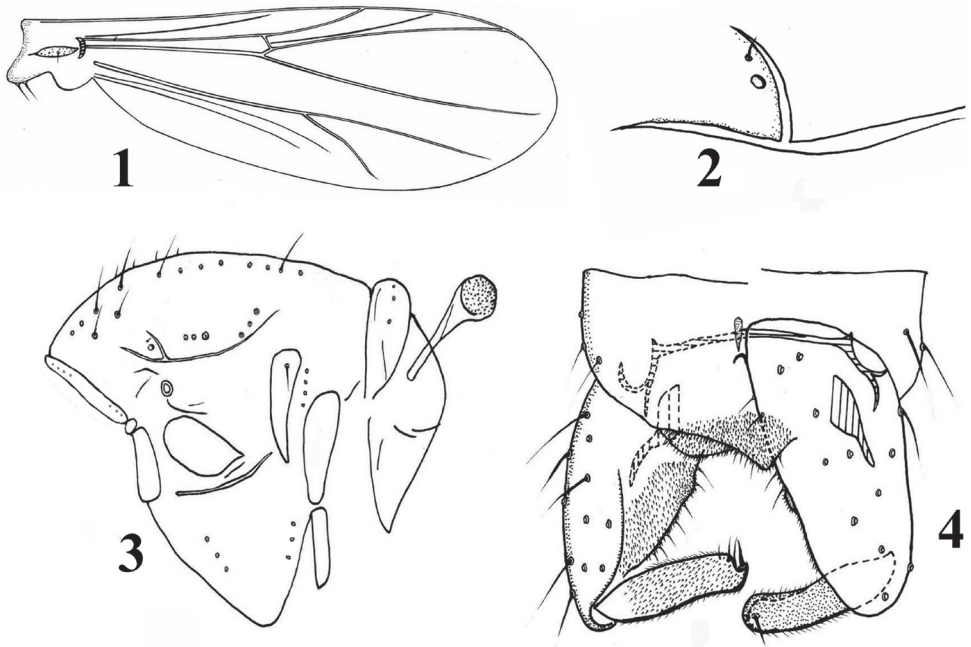
Thorax (Figs 2, 3). Anteprenotum with 2–4 median setae, and 2–3 lateral setae. Humeral pit (Fig. 3) small, with sclerotized anterior margin. Dorsocentrals 14–16, with 0–1 non-lanceolate humeral, and 14–15 non-lanceolate dorsocentrals. Preepisternum with 3 setae in anterior and posterior respectively. Acrostichals 4, prealars 4–5, supraalar 1, posterior anepisternum II with 3–4 setae, epimeron II with 4 setae, median anepisternum II with one seta; scutellum with 9 setae.

Legs ($N = 2$). Spur of fore tibia 33–37 μm long, of mid tibia 17–23 μm and 13–18 μm long, of hind tibia 37–38 μm and 13–15 μm long. Setae of tibial comb 28–30 μm long, comb with 11 teeth. Width at apex of fore tibia 25–26 μm , of mid tibia 24–25 μm , of hind tibia 30 μm . Lengths and proportions of legs in Table 1.

Hypopygium (Fig. 4). “Anal point” bluntly triangular, with 8–13 weak setae. Laterosternite IX with 2–3 setae. Phallapodeme 25–32 μm long; transverse sternapodeme 63–75 μm long. Virga 17–19 μm long, consisting of one tapering spine. Gonocoxite

Table 1. Lengths (in μm) and proportions of leg segments of male *L. minerus* Liu & Yan, sp. nov. ($N = 3$).

	fe	ti	ta ₁	ta ₂	ta ₃	ta ₄
P	310–390	430–510	220–240	130–140	80–95	45–50
P ₁ ^l	380–420	370–470	150–200	85–100	40–60	40–45
P ₃	390–450	420–510	230–280	110–120	95–130	50
	ta ₅	LR	BV	SV	BR	
P ₁	45–60	0.47–0.52	3.20–3.34	3.36–3.75	2.20–2.25	
P ₂	35–50	0.43–0.47	3.92–5.45	4.45–5.00	2.00–2.33	
P ₃	45–60	0.55–0.56	3.41–3.47	3.43–3.52	2.50–2.67	



Figures 1–4. *Limnophyes minerus* Liu & Yan, sp. nov., male **1** wing **2** humeral area of the thorax **3** thorax **4** hypopygium.

113–125 μm long. Inferior volsella minute. Gonostylus 65–73 μm long, with pointed crista dorsalis. Megaseta 10–16 μm long. HR 1.55–1.89, HV 2.58–2.73.

Remarks. The new species can be separated from other members of the genus by having a minute inferior volsella. The characters of the new species closely resemble *L. ninae* Sæther, 1975 (Sæther 1975, 1990a). However, the new species differs from the latter on the basis of following characters: (1) the humeral pit of the new species lacking lanceolate prescutellars, whereas in *L. ninae* the humeral pit has lanceolate setae inside the margin; (2) virga consisting of three spines with the median much shorter in *L. ninae*, whereas the new species has a single virga; (3) the AR of new species (0.24–0.27) is much lower than in *L. ninae* (0.62–0.77).

Distribution. The new species was collected in a subtropical mountain area in Hubei and Sichuan Provinces in Oriental China.

Limnophyes minimus (Meigen, 1818)

Chironomus minimus Meigen, 1818: 47.

Limnophyes pusillus Eaton, 1875: 60; Goetghebuer 1932: 196; 1940–50: 140; Brundin 1947: 83.

Spaniotoma (Limnophyes) pusilla (Eaton); Edwards, 1929: 355.

Limnophyes minimus (Meigen); Goetghebuer 1932: 108, 1940–50: 137.

Limnophyes interruptus Goetghebuer, 1938: 463.

Limnophyes immucronatus Sæther, 1969: 103.

Limnophyes hudsoni Sæther, 1975: 1032.

Limnophyes natalensis (Kieffer); Freeman 1957: 344, pro parte, (misidentified)

Limnophyes minimus (Meigen); Sæther 1990: 59; Wang and Sæther 1993: 216; Wang 2000: 636; Yamamoto 2004: 46; Makarchenko et al. 2005: 403, 2011: 115, Langton and Pinder 2007: 114.

Limnophyes fuscipygmus Wang, 2000: 636, *nec* Tokunaga, 1940: 287 syn. nov.

Material examined. Fujian Province, Fuzhou Agricultural University Campus, sweep net, 5 males, 22.iv.1993, W. Bu; Fujian Province, Nanping County, Maodi Town, sweep net, 4 males, 22.ix.2002, Z. Liu; Fujian Province, Shanghang County, Mt. Buyun, light trap, 5 males, 6.v.1993, W. Bu; Fujian Province, Wuyishan Natural Reserve Area, light trap, 31 males, 25.iv.1993, W. Bu; Guangxi Autonomous Region, Jinxiu County, Luoxiang Town, sweep net, 2 males, 9.vi.1990, X. Wang; Guangxi Autonomous Region, Longsheng County, sweep net, 5 males, 24.v.1990, X. Wang; Guizhou Province, Daozhen County, Dashahe Natural Reserve Area, sweep net, 1 male, 22.v.2004, H. Tang; Guizhou Province, Daozhen County, Xiaoshahe River, sweep net, 1 male, 25.v.2004, H. Tang; Hebei Province, Chengde City, Beidai River, sweep net, 1 male, viii.1986, X. Wang; Hebei Province, Chengde City, Saihanba Forest Park, sweep net, 1 male, 15.vii.2001, Y. Guo; Henan Province, Luanchuan County, Longyuwan Park, sweep net, 1 male, 13.vii.1996, J. Li; Henan Province, Baiyunshan Forest Farm, sweep net, 3 males, 16.vii.1996, J. Li; Henan Province, Song County, Baiyunshan Forest Farm, sweep net, 3 males, 16.vii.1996, J. Li; Hubei Province, Hefeng County, Mt. Fenshui, light trap, 3 males, 16.vii.1997, B. Ji; Hubei Province, Lifeng County, Houhe River, sweep net, 2 males, 30.vi.1997, B. Ji; Hubei Province, Lichuan County, Mt. Xingdou, sweep net, 3 males, 30.vi.1997, B. Ji; Hubei Province, Xianfeng County, Pingbaying Park, sweep net, 3 males, 25.vi.1997, B. Ji; Jiangxi Province, Poyang Lake, sweep net, 4 males, 12.vi.2004, C. Yan; Jiangxi Province, Yifeng County, Mt. Gongshan, sweep net, 2 males, 8.vi.2004, C. Yan; Jiangxi Province, Wuyishan Natural Reserve Area, light trap, 2 males, 13.vi.2004, C. Yan; Ningxia Autonomous Region, Mt. Liupan, Erlonghe Forest Farm, sweep net, 6 males, 7.viii.1987, X. Wang; Shanxi Province, Ningshan County, Huoditang Forest Farm, sweep net, 2 males, 12.viii.1994, W. Bu; Sichuan Province, Ganzi City, Yajiang River, light trap, 2 males, 14.vi.1996, X. Wang; Sichuan Province, Kangding City, Wasi River, light trap, 2 males, 15.vi.1996, X. Wang; Sichuan Province, Litang County, Zhaisang Region, sweep net, 2 males, 11.vi.1996, X. Wang; Sichuan Province, Mt. Emei, sweep net, 1 male, 17.v.1987, X. Wang; Xizang Autonomous Region, Xiazayu County, sweep net, 2 males, 24.iv.1988, C. Deng; Xizang Autonomous Region, Shigatse City, Zhangmu Town, sweep net, 6 males, 18.ix.1987, C. Deng; Yunnan Province, Fumin County, Daying Town, sweep net, 1 male, 1.vi.1996, X. Wang; Yunnan Province, Wuding County, Mashan Town, sweep net, 1 male, 1.vi.1996, X. Wang; Zhejiang Province, Baishanzu Natural Reserve

Area, light trap, 2 males, 18.iv.1994, H. Zou; Zhejiang Province, Tianmushan Natural Reserve Area, light trap, 1 male, 17.viii.1999, H. Zou.

Remarks. *Limnophyes minimus* (Meigen, 1818) is one of the dominant species of *Limnophyes* in China. Of all the specimens examined, some variation can be found. One specimen from Guangxi Province had a strongly reduced anal lobe, antenna with 10 segments, and LR_1 of 0.59, i.e., outside the range of 0.45–0.55. Two specimens from Sichuan and Yunnan provinces have AR 0.20 and 0.30, both lower than the minimum value of Sæther's description (AR 0.48). One specimen from Fujian Province had 9-segmented antenna, and high length ratio of palpomeres 5/3 (2.11).

Tokunaga (1940) described the species *L. fuscipygmus* based on materials from Taiwan Province, China. The holotype specimen of *L. fuscipygmus* mainly agrees with the description of *L. minimus* by Sæther (1975: 1032, figs 2–4), especially the characters of humeral pit, anal point, inferior volsella, and gonostylus. Consequently, it must be considered a junior synonym of *L. minimus*.

Distribution. The species is widespread, and it has been recorded in all the six Chinese geographical regions. It occurs both in Palaeartic and Oriental China.

***Limnophyes subtilus* Liu & Yan, sp. nov.**

<http://zoobank.org/56360531-A0B1-4140-8CB9-711A0E6672C7>

Figs 5–8

Type material. *Holotype* male (BDN No. 12222), CHINA: Sichuan Province, Daocheng County, Daocheng River, 29.112°N, 100.146°E, 2492 m a.s.l., sweep net, 11.vi.1996, X. Wang. *Paratype*: 5 males, as holotype.

Diagnostic characters. The new species can be separated from other members of the genus by having 9–21 lanceolate humerals, 7–9 lanceolate prescutellars, megaseta hair-like, virga very slender, and anal lobe moderately developed.

Etymology. From the Latin, *subtilus*, thin, slender, referring to the shape of the virga, adjective in the nominative singular.

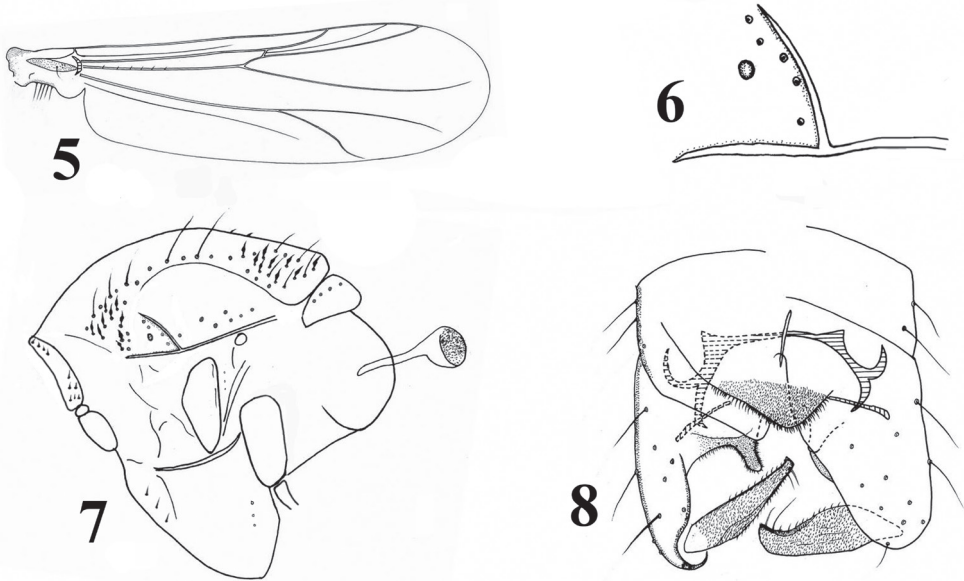
Description. Male ($N = 6$).

Total length 2.53–2.83, 2.67 mm. Wing length 1.56–1.73, 1.63 mm. Total length / wing length 1.54–1.74, 1.64. Wing length / length of profemur 2.97–3.16, 3.05.

Coloration. Head, thorax and legs dark brown. Abdomen yellowish brown. Wing nearly transparent.

Head. Antenna with 13 flagellomeres. AR 0.76–0.88, 0.83. Ultimate flagellomere 295–330, 310 μm long. Temporal setae 5–7, 6, including 1 inner vertical, 2 outer verticals and 2–4, 3 postorbitals. Clypeus with 14–18, 16 setae. Tentorium 132–140, 136 μm long, 22 μm wide. Palpomere lengths (in μm): 25–31, 28; 40–45, 43; 79–95, 86; 78–90, 85; 120–128, 125. Length ratio of palpomeres 5/3 1.26–1.62, 1.44.

Wing (Fig. 5). Anal lobe moderately developed. VR 1.20–1.29, 1.26. Brachiolum with one seta. R with 5–6, 5 setae. Costal extension 22–40, 31 μm long. Squama with 6–8, 7 setae.



Figures 5–8. *Limnophyes subtilis* Liu & Yan, sp. nov., male **5** wing **6** humeral area of the thorax **7** thorax **8** hypopygium.

Table 2. Lengths (in μm) and proportions of leg segments of male *L. subtilis* Liu & Yan, sp. nov. ($N = 6$).

	fe	ti	ta ₁	ta ₂	ta ₃	ta ₄
P ₁	540–580, 560	690–730, 712	340–360, 352	200–230, 215	130–140, 132	80–90, 87
P ₂	590–620, 602	620–650, 632	270–290, 280	170–180, 178	120	60–80, 72
P ₃	590–630, 605	730–760, 745	420–440, 432	220	190–200, 192	95–100, 98
	ta ₅	LR	BV	SV	BR	
P ₁	80	0.49	3.04–3.25, 3.20	3.61–3.64, 3.62	1.84–2.00, 1.88	
P ₂	55–70, 64	0.44–0.45, 0.44	3.47–3.55, 3.49	4.38–4.48, 4.41	2.50	
P ₃	80	0.55–0.60, 0.58	2.97–3.05, 3.02	3.13–3.16, 3.14	2.00–2.60, 2.38	

Thorax (Figs 6, 7). Antepronotum with 3–4, 4 median and 4–6, 5 lateral setae. Humeral pit (Fig. 7) rounded, with sclerotized posterior margin. Dorsocentrals 43–47, 45, including 9–21, 14 lanceolate humerals, 6–10, 8 non-lanceolate humerals, 14–19, 15 other non-lanceolate dorsocentrals, and 7–9, 8 lanceolate prescutellars. Preepisternum with 2–3, 3 setae in anterior row, and posterior with 3 setae. Acrostichals 2–6, 5; prealars 4–10, 7; supraalar 1; posterior anepisternum II with 2–4, 3 setae; epimeron II with 3 setae; scutellum with 6–9, 8 setae.

Legs. Spur of fore tibia 44 μm , of mid tibia 17–19, 18 μm and 14–18, 16 μm long, of hind tibia 37–45, 41 μm and 13–22, 17 μm long. Tibial comb 42–45, 44 μm long, comb with 13 teeth. Width at apex of fore tibia 31–40, 35 μm , of mid tibia 31–33, 32 μm , of hind tibia 31–40, 35 μm . Lengths and proportions of legs in Table 2.

Hypopygium (Fig. 8). “Anal point” broadly rounded, with 17–32 setae. Laterosternite IX with 3–5, 4 setae. Phallapodeme 43–62, 50 μm long; transverse sterna-

podeme 68–83, 77 μm long. Virga 32–35, 33 μm long, consisting of slender single spine. Gonocoxite 141–148, 144 μm long. Inferior volsella with developed digitiform dorsal lobe. Gonostylus 84–98, 91 μm long, with pointed crista dorsalis. Megaseta hair-like, 17–20, 19 μm long. HR 1.46–1.68, 1.59; HV 2.81–3.15, 2.95.

Remarks. The characters of the new species mainly agree with *L. eltoni* (Edwards, 1922) (Sæther 1990b). However, the new species differs from the latter on the basis of following characters: (1) the obvious costal extension of the new species (22–40 μm), shorter than for *L. eltoni* (77–94 μm); (2) “Anal point” of *L. eltoni* strongly projecting with apical notch, whereas in the new species it is not notched; (3) the new species has hair-like megaseta in the gonostylus, whereas the megaseta of *L. eltoni* is spine-like, subapically.

Distribution. The species were collected in a subtropical mountain area in Sichuan Province in Oriental China.

Key to adult males of *Limnophyes* from China

- 1 Preepisternum with dorsocentral to posterocentral group of setae, no anterior setae..... *L. brachytomus* (Kieffer)
- Preepisternum with anterior row of setae, with or without additional dorso-central to posterocentral setae 2
- 2 Dorsocentral without lanceolate humerals and/or prescutellars 3
- Dorsocentral with lanceolate humerals and/or prescutellars 6
- 3 “Anal point” strongly bifid, inferior volsella triangular
..... *L. verpus* Wang & Sæther
- “Anal point” not bifid, inferior volsella not triangular 4
- 4 First abdominal segment pale..... *L. palleocestus* Wang & Sæther
- First abdominal segment brown..... 5
- 5 Inferior volsella very small or absent..... *L. minerus* Liu & Yan, sp. nov.
- Inferior volsella moderately large, rectangular *L. minimus* (Meigen)
- 6 More than 13 lanceolate humerals and lanceolate prescutellars combined... 7
- Less than 10 lanceolate humerals and lanceolate prescutellars combined... 11
- 7 Virga very slender, anal lobe slightly projecting.....
..... *L. subtilus* Liu & Yan, sp. nov.
- Virga not slender, anal lobe reduced or right angled..... 8
- 8 Lanceolate prescutellars absent..... *L. pumilio* (Holmgren)
- Lanceolate prescutellars present..... 9
- 9 Megaseta long, bristle-like..... *L. optimus* Wang & Sæther
- Megaseta absent or hair-like..... 10
- 10 “Anal point” apically notched, AR 0.49–0.79 *L. pentaplastus* (Kieffer)
- “Anal point” apically not notched, AR 0.18–0.30 *L. gurgicola* (Edwards)
- 11 Gonostylus with strongly triangular protrusive middle part
..... *L. triangulus* Wang
- Gonostylus without such strongly triangular protrusive middle part 12

- 12 Gonostylus with rounded crista dorsalis.....*L. orbicristatus* Wang & Sæther
 – Gonostylus often with pointed crista dorsalis..... 13
 13 “Anal point” pronounced parallel-sided, dorsal lobe of inferior volsella triangular *L. habilis* (Walker)
 – “Anal point” not parallel-sided, dorsal lobe of inferior volsella not triangular...14
 14 Thorax with scalpellate acrostichals, virga with 3 spines
 *L. aquamatus* Andersen
 – Thorax without scalpellate acrostichals, virga with 1 or 2 spines..... 15
 15 Flagellum with 11–12 flagellomeres, a strong tubercle in place of humeral pit..... *L. bullus* Wang & Sæther
 – Flagellum with 13 flagellomeres, humeral pit not as above..... 16
 16 Virga consisting of two fused spines, “Anal point” relatively small, broad-based, bluntly triangular *L. nudus* Song, Zheng, Wang & Qi
 – Virga consisting of one simple spine, “Anal point” strong to moderately projecting with or without apical notch *L. difficilis* Brundin

Acknowledgements

We are grateful to Mrs Li Yu-Fen who made the slide preparations. Financial support from the National Natural Science Foundation of China granted No., 31672324, 31801994. Natural Science Foundation of Tianjin (18JJCQNJC14700, 18JCYB-JC96100, S20QNS624), Freshwater ecological monitoring and assessment of Haihe River Basin (2020) and Tianjin Normal University Foundation (5RL104, 043135202-XB1715, 043135202-XK1706; 135305JF79) are acknowledged with thanks.

References

- Ashe P, O'Connor JP (2012) A world catalogue of Chironomidae (Diptera). Part 2. Orthocladiinae. Irish Biogeographical Society & National Museum of Ireland, Dublin, 968 pp.
- Brundin L (1947) Zur Kenntnis der schwedischen Chironomiden. Arkiv för Zoologi 41: 1–22.
- Chaudhuri PK, Hazra N, Alfred JRB (2001) A checklist of chironomid midges (Diptera: Chironomidae) of the Indian subcontinent. Oriental Insects 35: 335–372. <https://doi.org/10.1080/00305316.2001.10417312>
- Eaton AE (1875) Breves dipterarum uniusque lepidopterarum Insulae Kerguelensi indigenarum diagnoses. Entomologist's Monthly Magazine 12: 58–61.
- Edwards FW (1929) British non-biting midges (Diptera, Chironomidae). Transactions of the Entomological Society of London 77: 279–430. <https://doi.org/10.1111/j.1365-2311.1929.tb00692.x>
- Freeman P (1957) A study of the Chironomidae (Diptera) of Africa South of the Sahara. III. Bulletin of the British Museum (Natural History) Entomology 5: 323–426. <https://doi.org/10.5962/bhl.part.1515>

- Goetghebuer M (1932) Diptères. Chironomidae IV. (Orthocladiinae, Corynoneurinae, Clunioninae, Diamesinae). Faune de France 23: 1–204.
- Goetghebuer M (1938) Quelques Chironomides nouveaux de l'Europe. Bulletin et Annales de la Société royale Belge d'Entomologie 78: 453–464.
- Goetghebuer M (1940–50) Tendipedidae (Chironomidae). F. Subfamille Orthocladiinae. A. Die Imagines. In: Lindner E (Ed.) Die Fliegen der palaearktischen Region 13g, 208 pp.
- Langton PH, Moubayed J (2001) *Limnophyes roquehautensis* sp. n. and *L. inanispatina* sp. n. from southern France (Diptera, Chironomidae). Nouvelle Revue d'Entomologie 18: 3–8.
- Langton PH, Pinder LCV (2007) Keys to the adult male Chironomidae of Britain and Ireland. Volume 1. Introductory text, keys, references, checklist and index; Volume 2. Illustrations of the hypopygia and a supplement identifying sixteen species recently recorded from Britain and Ireland. Freshwater Biological Association, Scientific Publication 64, 231 plus 168 pp.
- Makarchenko EA, Makarchenko MA, Zorina OV, Sergeeva IV (2005) Pervye itogi izucheniya fauny i taksonomii khironomid (Diptera, Chironomidae) rossiiskogo Dal'nego Vostoka [Preliminary data on fauna and taxonomy of chironomids (Diptera, Chironomidae) of the Russian Far East]. In: Makarchenko EA (Ed.) Chteniya pamyati Vladimira Yakovlevitsha Levanidova [V. Ya. Levanidov's Biennial Memorial Meetings] 3: 394–420. Vladivostok: Dal'nauka Publishers [in Russian with English summary]
- Makarchenko EA, Makarchenko MA (2011) Fauna and distribution of the Orthocladiinae of the Russian Far East. In: Wang X, Liu W (Eds) Proceedings of the 17th International Symposium on Chironomidae, 107–125.
- Meigen JW (1818) Systematische Beschreibung der bekannten europäischen zweiflügeligen Insekten. Erster Teil. F.W. Forstmann, Aachen, i–xxxvi + 1–3332 [+ 1], pl. 1–11.] <https://doi.org/10.5962/bhl.title.13731>
- Mendes HF, Andersen T, Pinho LC (2007) *Corytibacladius* Oliveira, Messias & Santos, 1995, a junior synonym of *Limnophyes* Eaton, 1875 (Diptera: Chironomidae: Orthocladiinae). Aquatic Insects 29: 255–261. <https://doi.org/10.1080/01650420701411481>
- Moubayed BJ (2011) Description of *Limnophyes tyrrheneus* sp. n. from pozzines of the mountain lake Ninu in Corsica [Diptera, Chironomidae, Orthocladiinae]. Ephemera 13(2): 71–78.
- Murray DA (2007) *Limnophyes platystylus* new species (Diptera: Chironomidae, Orthocladiinae) from Ireland. In: Andersen, T. (Ed.) Contributions to the Systematics and Ecology of Aquatic Diptera –A Tribute to Ole A. Sæther. Columbus, Ohio: The Caddis Press, Columbus, Ohio, 215–218.
- Pinho LC, Andersen T (2015) *Limnophyes guarani* sp. n., a new hygropetric Orthocladiinae from southern Brazil (Diptera: Chironomidae). Zootaxa 3948(1): 137–144. <https://doi.org/10.11646/zootaxa.3948.1.9>
- Przhiboro A, Sæther OA (2007) *Limnophyes* (Diptera: Chironomidae) from northwestern Russia. Aquatic insects 29(1): 49–58. <https://doi.org/10.1080/01650420701225691>
- Sæther OA (1969) Some Nearctic Podonominae, Diamesinae, and Orthocladiinae (Diptera: Chironomidae). Bulletin of the Fisheries Research Board of Canada 170: 1–154.
- Sæther OA (1975) Twelve new species of *Limnophyes* Eaton, with keys to Nearctic males of the genus (Diptera: Chironomidae). The Canadian Entomologist 107: 1029–1056. <https://doi.org/10.4039/Ent1071029-10>

- Sæther OA (1980) Glossary of chironomid morphology terminology (Diptera: Chironomidae). Entomologica scandinavica Supplement 14: 1–51.
- Sæther OA (1990a) A review of the genus *Limnophyes* Eaton from the Holarctic and Afrotropical regions (Diptera: Chironomidae, Orthocladiinae) Entomologica scandinavica 35: 1–135.
- Sæther OA (1990b) A revision of the Neotropical types described as *Spaniotoma* (*Limnophyes*) by Edwards 1931, with the description of *Edwardsidia* gen. n. (Diptera: Chironomidae). Entomologica Scandinavica 21: 305–319. <https://doi.org/10.1163/187631290X00229>
- Song C, Zheng J, Wang X, Qi X (2020) A new species of *Limnophyes* Eaton (Diptera: Chironomidae) from Xizang, China. Zootaxa 4722(3): 295–300. <https://doi.org/10.11646/zootaxa.4722.3.7>
- Tokunaga M (1940) Chironomidae from Japan (Diptera), XII. New or little-known Ceratopogonidae and Chironomidae. Phillipine Journal of Science 72: 255–317.
- Wang X (1997) A new species of *Limnophyes* Eaton from China (Diptera: Chironomidae). Acta Scientiarum Naturalium University Nankaiensis 30(4): 5–7.
- Wang X (2000) A revised checklist of Chironomidae from China (Diptera). In: Hoffrichter O (Ed.) Late 20th Century Research on Chironomidae. An Anthology from the 13th International Symposium on Chironomidae. Shaker Verlag, Aachen, 629–652.
- Wang X, Sæther OA (1993) *Limnophyes* Eaton from China, with description of five new species (Diptera: Chironomidae). Entomologica scandinavica 24: 215–226. <https://doi.org/10.1163/187631293X00316>
- Yamamoto M (2004) A catalog of Japanese Orthocladiinae (Diptera: Chironomidae). Maku-nagi, Acta Dipterologica 21: 1–121.

Records of *Parochlus steinenii* in the Maritime Antarctic and sub-Antarctic regions

Melisa Gañan^{1,3}, Tamara Contador^{1,2,3}, Javier Rendoll^{1,2}, Felipe Simoes^{4,5}, Carolina Pérez^{1,2}, Gillian Graham⁶, Simón Castillo⁷, James Kennedy^{1,2,6}, Peter Convey⁴

1 Wankara Sub-Antarctic and Antarctic Freshwater Ecosystems Laboratory, Sub-Antarctic Biocultural, Conservation Program, Universidad de Magallanes, Puerto Williams, Teniente Muñoz 166, Chile **2** Institute of Ecology and Biodiversity, Universidad de Chile, Santiago, Las Palmeras 3425, Chile **3** Núcleo Milenio de Salmónidos Invasores (INVASAL) Iniciativa Científica Milenio, ICM, Núcleo Científico Milenio, Concepción, Chile **4** British Antarctic Survey, NERC, High Cross, Madingley Road, Cambridge CB3 0ET, UK **5** Department of Zoology, Museum of Zoology, University of Cambridge, Downing Street, Cambridge CB2 3EJ, UK **6** Department of Biological Sciences, University of North Texas, 1511W Sycamore, Denton, TX 76201, USA **7** Department of Ecology, Pontificia Universidad Católica, Facultad de Ciencias Biológicas. Avda. Libertador Bernardo O'Higgins 340, Santiago, Chile

Corresponding author: Melisa Gañan (melysa_gm@yahoo.es); Tamara Contador (tamara.contador@umag.cl)

Academic editor: F. Laurindo da Silva | Received 23 July 2020 | Accepted 7 October 2020 | Published 18 January 2021

<http://zoobank.org/BC17D44D-A149-4453-845E-9C909CCC35E8>

Citation: Gañan M, Contador T, Rendoll J, Simoes F, Pérez C, Graham G, Castillo S, Kennedy J, Convey P (2021) Records of *Parochlus steinenii* in the Maritime Antarctic and sub-Antarctic regions. ZooKeys 1011: 63–71. <https://doi.org/10.3897/zookeys.1011.56833>

Abstract

This study provides the summary of the reports of the geographical distribution in the Maritime Antarctic and sub-Antarctic regions of *Parochlus steinenii* (Gercke, 1889) (Diptera, Chironomidae), the only flying insect occurring naturally in the Antarctic continent. The distribution encompasses the South Shetland Islands (Maritime Antarctic), South Georgia (sub-Antarctic), and parts of the Cape Horn Biosphere Reserve (CHBR, southern Chile). In total 78 occurrence records were identified, 53 from our own records, 19 from the literature, and six from other data present in GBIF. Of the 78 records, 66 are from the South Shetland Islands, eight are from South Georgia, and four from the CHBR. This database was developed as one of the main objectives of two Chilean-funded research projects addressing understanding the effects of climate change on sub-Antarctic and Antarctic insects. It provides dataset documenting the distribution of *Parochlus steinenii* in the Maritime Antarctic, the sub-Antarctic, and the CHBR in southern South America (Chile). The complete dataset is available in Darwin Core Archive format via the Global Biodiversity Information Facility (GBIF).

Keywords

Cape Horn Biosphere Reserve, *Parochlus steinenii*, South Georgia, South Shetland Islands, winged Antarctic midge

Project details

Project title: This database was developed as part of the main objectives of two Chilean-funded research projects aiming towards better understanding the effects of climate change in sub-Antarctic and Antarctic insects:

- Dipterans in sub-Antarctic and Antarctic regions: are they ready for the changes?
- Addressing global warming scenarios in freshwater ecosystems using aquatic insects as model organisms in the Magellanic sub-Antarctic and Antarctic regions.

Personnel: Melisa Gañan (Data Collector, Data Manager, Data Publisher), Tamara Contador (Principal Investigator, Data Collector, Data Manager, Data Publisher), Javier Rendoll (Data Collector, Data Manager), Felipe Simoes (Data Collector, Data Manager), Carolina Pérez (Data Collector, Data Manager), Gillian Graham (Data Collector), Simón Castillo (Data Collector), James Kennedy (Data Collector, Data Manager) and Peter Convey (Data Collector, Data Manager).

Funding: INACH RT-48_16 and Fondecyt de Iniciación 11130451.

Study area descriptions/descriptor: The study area (Fig. 1) includes: 1. The South Shetland Islands and part of the north-west coast of the Antarctic Peninsula (Antarctic Conservation Biogeographic Region (ACBR) 3, Terauds et al. 2012; Terauds and Lee 2016); 2. The sub-Antarctic island of South Georgia; 3. Navarino Island, Cape Horn National Park, and Diego Ramírez Marine Park (Cape Horn Biosphere Reserve, Magallanes sub-Antarctic region, Rozzi et al. 2012).

Design description: The study was conducted throughout the latitudinal and environmental gradient that includes the southern tip of South America in the sub-Antarctic Magellanic ecoregion (54–57°S), and the Scotia Arc distribution of *Parochlus steinenii* (*P. steinenii*) in the sub-Antarctic (South Georgia, 53–54°S) and Maritime Antarctic (South Shetland Islands, 63–64°S) regions. The geographical range of the study involves both small-scale (microhabitats and environmental gradients) and the larger spatial scale 10-degree latitudinal gradient.

The specific locations surveyed were: 1. On the maritime Antarctic South Shetland Islands, ice-free areas on Deception, Livingston, Greenwich, Robert, Nelson, King George Islands, and the north-west coast of Antarctic Peninsula (Trinity Peninsula and Litchfield Island). These areas are characterized by a geomorphology which includes periglacial landforms, with numerous temporary shallow meltwater ponds and permanent lakes (typically smaller than 100 m²), which are ice-covered for 9–10 months of the year (Contador et al. 2020); 2. In South Georgia, which is the largest island on the Scotia

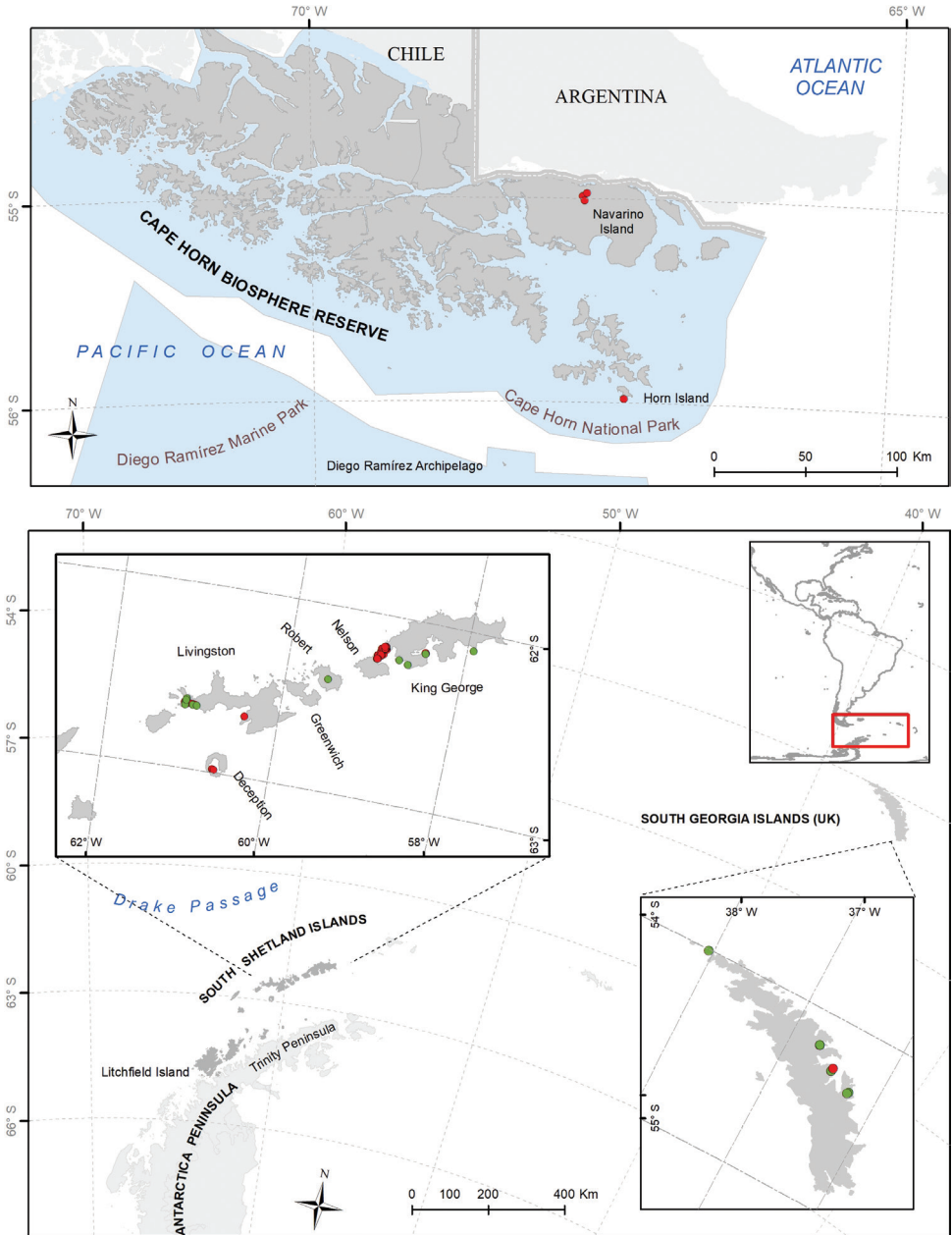


Figure 1. Map of study area. The red circles correspond to the records of *Parochlus steinenii* found in this study, the green circles correspond to the bibliographic records.

Arc, with much of the barren, mountainous and highly glacial territory (Regional ecosystem profile – Polar and Sub-polar Region 2017), we surveyed accessible lakes near the British Antarctic Survey research station; 3. In CHBR, we surveyed the north coast of

Navarino Island, with freshwater systems that present altitudinal gradients with marked slopes in an altitudinal range that extends between 1000 m and sea level, and where the thermal ranges change drastically along of the altitudinal profile (Contador 2011; Contador et al. 2015). We also surveyed Horn Island in the southernmost of the Cape Horn archipelago, and the Diego Ramirez archipelago, both made up of low-lying islets and marked by strong winds throughout the year (Pisano 1980, Pisano and Schlatter 1981).

Field expeditions were organized by the Chilean Antarctic Institute (INACH) in South Shetland Islands; by the British Antarctic Survey in South Georgia; and by the Sub-Antarctic Biocultural Conservation Program of the Universidad de Magallanes in CHBR.

Taxonomic coverage

General taxonomic coverage description: The dataset reports occurrences of the species *Parochlus steinenii* (Gercke, 1889) (Diptera: Chironomidae: Podonominae), also known as the winged Antarctic midge. *P. steinenii* is recorded from freshwater ecosystems through the ice-free areas of the South Shetland Islands in the Maritime Antarctic, on sub-Antarctic South Georgia, and in Navarino and Horn islands in the CHBR. Knowing these presences is of great importance since *P. steinenii* has been proposed as an effective native sentinel species and indicator of climate change in Antarctica (Contador et al. 2020).

Taxonomic ranks

Kingdom Animalia

Phylum Arthropoda

Class Insecta

Order Diptera

Family Chironomidae

Subfamily Podonominae

Tribe Podonomini

Genus *Parochlus*

Species *Parochlus steinenii*

Common name: winged Antarctic midge

Spatial coverage

General spatial coverage: The dataset comprises the South Shetland Islands, specifically King George, Nelson, Robert, Livingston and Deception islands in the Maritime Antarctic, South Georgia in the sub-Antarctic, and Horn and Navarino islands in the CHBR (southern South America, Chile).

Coordinates: The areas surveyed lie within the polygon 53–63°S latitude and 35–69°W longitude.

Temporal coverage

January 1, 2014–February 25, 2019.

Natural collections description

Parent collection identifier: UMAG: WANKARA LABORATORY

Collection name: Colección de Invertebrados Antárticos y Subantárticos del Laboratorio Dulceacuícola Wankara de la Universidad de Magallanes, Puerto Williams

Collection identifier: urn:UMAG:WANKARA:Inv:Dip:AQ:Pstei and urn:UMAG:WANKARA:Inv:Dip:CL:Pstei

Specimen preservation method: 95% alcohol

Curatorial unit: 20 individuals per 5 ml glass vials

Methods

Survey and sampling: Intensive field surveys through accessible ice-free areas in the South Shetland Islands, through lakes on South Georgia, and lakes on Horn Island, Navarino Island, and Diego Ramírez archipelago were conducted. For each sample site, the presence of *P. steinenii* was assessed and reference collection of individuals was made, the macrohabitat was described, and the climatic and water variables were recorded. Survey data were combined with information from a careful bibliographic review.

Sampling description: All sites were sampled for a period of 4–6 h, depending on climatic conditions and logistic support. We assessed the presence of *P. steinenii* as larvae, pupae, or adults by searching close to the shoreline of lakes and streams, and specifically under rocks and vegetation, and in sediments (Fig. 2). We manually extracted specimens from rocks and mosses and sometimes with the use of an entomological aspirator. Each site visited was georeferenced using a Garmin 78SC GPS receiver. Water body typology and macrohabitat were described following Hahn and Reinhardt (2006). Climatic variables (air temperature, wind speed, and relative humidity) were measured using an anemometer (Kestrel 3000 Env) and water variables (pH, conductivity, water temperature, and dissolved oxygen) were measured using a YSI 605 595 Professional Plus multimeter. We additionally sourced all available information from the existing literature (see Torres 1956; Wirth and Gressitt 1967; Brundin 1970; Edwards and Usher 1985; Rauschert 1985; Shimada et al. 1991; Richard et al. 1994; Convey and Block 1996; Allegrucci et al. 2006; Hahn and Reinhardt 2006; Toro et al. 2006; Agius et al. 2008; Rico and Quesada 2013).

Fieldwork in the Antarctic was conducted during six austral summer seasons (2013/14, 2014/15, 2015/16, 2016/17, 2017/18 and 2018/19). In South Georgia fieldwork was conducted in the Austral summer of 2018 and in the Magellanic sub-Antarctic Region in the Austral summer of 2016.



Figure 2. *Parochlus steinenii* (Fildes Bay, South Shetland Islands). **a** Female (up) and male (down) adult **b** larva **c** pupa **d** group of adults on a stone.

Living individuals were transported to the laboratory for phenology and physiologic studies, while some individuals were immediately preserved in alcohol (95%) for genetic studies. Samples were transported to the Wankara Subantarctic and Antarctic Freshwater Studies Laboratory at Magallanes University in Puerto Williams, Chile. Characteristics of the species according to the taxonomic key of Wirth and Gressitt (1967) were verified in the laboratory. To date, the species was not recorded in any extensive terrestrial/freshwater study along the Diego Ramírez Island, South Orkney Islands, or north-west coast of the Antarctic Peninsula (Chown and Convey 2016; Contador et al. 2020).

Quality control description: Each record of the species obtained in the field was georeferenced using a Garmin 78SC GPS receiver. Most records obtained from literature included geographical coordinates. Otherwise, we assigned a georeference record by identification of the body of water described in the study.

Geographic names used for records presented here follow the official name used in the maps prepared by the SCAR Composite Gazetteer of Antarctica (CGA) and by the Military Geographical Institute (IGM) of Chile. For sites lacking formal names, unofficial names were assigned.

Data resources: The data set of this article is deposited at GBIF, the Global Biodiversity Information Facility, <https://www.gbif.org/dataset/30c49fbf-4e2e-482e-bb49-4d294bc332cb>, <https://doi.org/10.15468/2cfwd7>.

Datasets

Dataset description

Object name: Darwin Core Archive Presence *Parochlus steinenii* AQ_CL

Character encoding: UTF-8

Format name: Darwin Core Archive format

Format version: 1.0

Distribution: <https://www.gbif.org/dataset/30c49fbf-4e2e-482e-bb49-4d294bc332cb>

Publication date of data: 2020-05-27

Language: English

Licenses of use: Creative Commons Attribution (CC-BY) 4.0 License

Metadata language: English

Date of metadata creation: 2020-05-27

Hierarchy level: Dataset

Acknowledgements

This project was funded by Chile's National Fund for Scientific and Technological Development (FONDECYT), the Chilean Antarctic Institute (INACH), and CONICYT PIA Apoyo CCTE (projects 11130451, RT_48_16, and AFB170008, respectively). Felipe was funded by Conselho Nacional de Desenvolvimento Científico e Tecnológico and the Cambridge Trust, PhD scholarship Process no. 233923/2014-4.

Peter C. was supported by NERC core funding to the British Antarctic Survey (BAS) "Biodiversity Evolution and Adaptation" Team. Gonzalo Arriagada produced the photographs of *Parochlus steinenii* larvae, pupae and adults used in Fig. 2. In Fig. 1, coastline_high_res_line, and seamask_high_res_polygon layers were downloaded from the Antarctic Digital Database (ADD version 7; <http://www.add.scar.org>).

References

- Agius J, Gibson J, Rico E, Quesada A (2009) Paleolimnological evidence confirms that *Parochlus steinenii* (Gerke) is not a recent introduction to the Antarctic Peninsula Region. Chironomus Newsletter of Chironomidae Research 22: 18–21. <https://doi.org/10.5324/cjcr.v0i22.604>
- Allegrucci G, Carchini G, Todisco V, Convey P, Sbordoni V (2006) A molecular phylogeny of Antarctic Chironomidae and its implications for biogeographical history. Polar Biology 29: 320–326. <https://doi.org/10.1007/s00300-005-0056-7>
- Brundin L (1970) Diptera: Chironomidae of South Georgia. Pacific Insects Monograph 23: 276–276.

- Chown SL, Convey P (2016) Antarctic entomology. *Annual Review of Entomology* 61: 119–137. <https://doi.org/10.1146/annurev-ento-010715-023537>
- Contador T (2011) Benthic macroinvertebrates of temperate, sub-Antarctic streams: the effects of altitudinal zoning and temperature on the phenology of aquatic insects associated to the Róbalo river, Navarino Island (55°S), Chile. PhD Thesis. University of North Texas, Denton, 140 pp.
- Contador T, Kennedy JH, Rozzi R, Villarroel JO (2015) Sharp altitudinal gradients in Magellanic Sub-Antarctic streams: patterns along a fluvial system in the Cape Horn Biosphere Reserve (55°S). *Polar Biology* 38: 1853–1866. <https://doi.org/10.1007/s00300-015-1746-4>
- Contador T, Gañan M, Bizama G, Fuentes-Jaque G, Morales L, Rendoll J, Simoes F, Kennedy J, Rozzi R, Convey P (2020) Assessing distribution shifts and ecophysiological characteristics of the only Antarctic winged midge under climate change scenarios. *Scientific Reports* 10: e9087. <https://doi.org/10.1038/s41598-020-65571-3>
- Convey P, Block W (1996) Antarctic Diptera: ecology, physiology and distribution. *European Journal of Entomology* 93: 1–13.
- Edwards M, Usher MB (1985) The winged Antarctic midge *Parochlus steinenii* (Gerke) (Diptera: Chironomidae) in the South Shetland Islands. *Biological Journal of the Linnean Society* 26: 83–93. <https://doi.org/10.1111/j.1095-8312.1985.tb01553.x>
- Hahn S, Reinhardt K (2006) Habitat preference and reproductive traits in the Antarctic midge *Parochlus steinenii* (Diptera: Chironomidae). *Antarctic Science* 18: 175–181. <https://doi.org/10.1017/S0954102006000204>
- Pisano E (1980) Catálogo de la flora vascular del archipiélago del Cabo de Hornos. *Anales Del Instituto de La Patagonia (Chile)* 11: 151–189.
- Pisano E, Schlatter R (1981) Vegetación y flora de las islas Diego Ramirez (Chile). I. Características y Relaciones de la flora vascular. *Anales del Instituto de La Patagonia* 12: 183–194.
- Rauschert M (1985) Beobachtungen an der Chironomide *Parochlus steinenii* auf der Insel King George (Südshetlandinseln, Antarktis) (Diptera, Chironomidae). *Deutsche Entomologische Zeitschrift* 32: 183–188. <https://doi.org/10.1002/mmnd.19850320125>
- Regional ecosystem profile – Polar and Sub-polar Region (2017) EU Outermost Regions and Overseas Countries and Territories, Claire-Sophie Azam, Cédric Marteau, Vincent Piton, Cynthia Borot, Paul Tixier. *Terres australes et antarctiques françaises (TAAF)*. BEST, Service contract 07.0307.2013/666363/SER/B2, European Commission, 225 pp. [+ 31 Annexes, 24–27]
- Richard KJ, Convey P, Block W (1994) The terrestrial arthropod fauna of the Byers Peninsula, Livingston Island, South Shetland Islands. *Polar Biology* 14: 371–379. <https://doi.org/10.1007/BF00240257>
- Rico E, Quesada A (2013) Distribution and ecology of chironomids (Diptera, Chironomidae) on Byers Peninsula, Maritime Antarctica. *Antarctic Science* 25: 288–291. <https://doi.org/10.1017/S095410201200096X>
- Rozzi R, Armesto JJ, Gutiérrez J, Massardo F, Likens G, Anderson CB, Poole A, Moses K, Hargrove G, Mansilla A, Kennedy JH, Willson M, Jax K, Jones C, Callicott JB, Kalin MT (2012) Integrating ecology and environmental ethics: Earth stewardship in the southern end of the Americas. *BioScience* 62: 226–236. <https://doi.org/10.1525/bio.2012.62.3.4>

- Shimada K, Ohyama Y, Pan CX (1991) Cold-hardiness of the Antarctic winged midge *Parochlus steinenii* during the active season at King George Island. *Polar Biology* 11: 311–314. <https://doi.org/10.1007/BF00239023>
- Simões F (2019) Ecophysiology, morphology and phylogeography of insects in the Scotia Arc. PhD Thesis. University of Cambridge, Cambridge, 191 pp.
- Terauds A, Chown S, Morgan F, Peat J, Watts D, Keys H, Convey P, Bergstrom D (2012) Conservation biogeography of the Antarctic. *Diversity and Distributions* 18: 726–741. <https://doi.org/10.1111/j.1472-4642.2012.00925.x>
- Terauds A, Lee JR (2016) Antarctic biogeography revisited: updating the Antarctic Conservation Biogeographic Regions. *Diversity and Distributions* 22: 836–840. <https://doi.org/10.1111/ddi.12453>
- Torres BA (1956) Primer hallazgo de Tendipedidos alados en la región Antártica. Podonominae, una nueva subfamilia para la citada región. *Anales de la Sociedad Científica Argentina* 161: 41–52.
- Wirth WW, Gressitt JL (1967) Diptera: Chironomidae (Midges). In: Gressitt JL (Ed.) *Entomology of Antarctica*, vol. 10, Antarctic Research Series. American Geophysical Union, Washington, 197–203. <https://doi.org/10.1029/AR010p0197>

Records from other data published in GBIF

- Hårsaker K, Aspaas AM, Dolmen D, Ekrem T, Munkeby TB, Stur E, Frode Ø, Aagaard K, Finstad AG (2020) Terrestrial and limnic invertebrates systematic collection, NTNU University Museum. Version 1.290. NTNU University Museum. Occurrence dataset. <https://doi.org/10.15468/fsreqb> [accessed via GBIF.org on 02.10.2020]
- The International Barcode of Life Consortium (2016) International Barcode of Life project (iBOL). Occurrence dataset. <https://doi.org/10.15468/inycg6> [accessed via GBIF.org on 02.10.2020]

Description of the male of *Xystromutilla bucki* Suárez, 1960 (Hymenoptera, Mutillidae), including new information on the biology of the genus

Roberto A. Cambra¹, Caroline Nepomuceno Queiros², Jean P. Alves De Deus², Kevin A. Williams³, Pedro R. Bartholomay⁴, Jucélia Iantas⁵, Michele C. Nether⁶, Kenji Nishida⁷, Yostin J. Añino¹, Daisy Saavedra¹, Maria L. Tunes Buschini²

1 Museo de Invertebrados G. B. Fairchild, Estafeta Universitaria Apartado 00017, Universidad de Panamá, Panamá 0824, Panamá **2** Laboratório de Biologia e Ecologia de Vespas e Abelhas, Universidade Estadual do Centro-Oeste, Rua Simeão Camargo Varela de Sá 03, Vila Carli, 85040-080, Guarapuava, Paraná, Brazil **3** Plant Pest Diagnostics Center, California Department of Food & Agriculture, 3294 Meadowview Road, Sacramento, CA 95832, USA **4** Instituto Nacional da Mata Atlântica, Av. José Ruschi n^o4, Santa Teresa, Espírito Santo, Brazil **5** Centro Universitário de União da Vitória – UNIUV – Avenida Bento Munhoz da Rocha Neto, 3856,84600-000, União da Vitória (PR), Brazil **6** Universidade Federal do Paraná, Campus Pontal do Paraná, Centro de Estudos do Mar Avenida Beira-mar, s/n CEP: 83255976 Pontal do Sul, Pontal do Parana, Paraná, Brazil **7** Collaborator, Museo de Zoología, Universidad de Costa Rica; and Estación Biológica Monteverde (EBM), Monteverde, Puntarenas, Costa Rica

Corresponding author: Roberto A. Cambra (cambramiup60@gmail.com); Yostin J. Añino (yostin0660@gmail.com)

Academic editor: K. van Achterberg | Received 19 November 2020 | Accepted 11 December 2020 | Published 18 January 2021

<http://zoobank.org/8CCD5721-D1FE-47F2-BBEC-08D80E4ACA22>

Citation: Cambra RA, Queiros CN, De Deus JPA, Williams KA, Bartholomay PR, Iantas J, Nether MC, Nishida K, Añino YJ, Saavedra D, Buschini MLT (2021) Description of the male of *Xystromutilla bucki* Suárez, 1960 (Hymenoptera, Mutillidae), including new information on the biology of the genus. ZooKeys 1011: 73–84. <https://doi.org/10.3897/zookeys.1011.60944>

Abstract

The male of *Xystromutilla bucki* Suárez, 1960 is described and associated with the female based on couples reared from trap-nests occupied by *Auplopus subaurarius* Dreisbach, 1963 (Hymenoptera: Pompilidae). Information on the diapause of *X. bucki* and *Pseudomethoca* nr. *chontalensis* (Cameron, 1895) (Hymenoptera: Mutillidae) is presented. Seasonal and annual variation in the abundance of *X. turrialba* Casal, 1969 are also given.

Keywords

Auplopus, diapause, Neotropical, Pepsinae, *Pseudomethoca*, seasonal abundance, Sphaerophthalminae, spider wasps, velvet ants

Introduction

Xystromutilla André, 1905 (Mutillidae: Sphaerophthalminae) belongs to the tribe Sphaerophthalmini (Brothers and Lelej 2017). This Neotropical genus has 14 described species (Bartholomay et al. 2019; Pagliano et al. 2020), two from Central America and 12 from South America, with only *X. turrialba* Casal, 1969 and *X. carpenteri* Cambra & Quintero, 2004 known from both sexes (Cambra and Quintero 2004). Morato (1994) mentioned rearing male and female specimens of *X. asperiventris* André, 1905 from the same trap nests, but this male has not yet been described, although specimens were used by Brothers and Lelej (2017) in compiling the characters of *Xystromutilla*.

Four species of *Xystromutilla* have known hosts; three of these attack solitary aculeate wasps and one attacks a solitary bee. André (1906) mentioned a specimen of *X. aequatorialis* (André, 1906) with a label indicating it was a parasite of *Melitoma taurea* (Say) (as *Entechnia taurea* Say). Morato (1994) reared *X. asperiventris* André, 1905 from *Trypoxylon* (*Trypoxylon*) *nitidum* F. Smith, 1856, *Trypoxylon* (*Trypargilum*) *lactitarse* de Saussure, 1867, *Trypoxylon* aff. *unguicorne* Richards, 1934 (Crabronidae), and *Podium rufipes* Fabricius, 1804 (Sphecidae); Rodríguez and Matías (1996) recorded *X. turrialba* from *Trypoxylon* sp. and *Podium* sp.; and Cambra and Quintero (2004) mentioned that *X. hansonii* Cambra & Quintero, 2004 was reared from a species of Eumeninae (Vespidae).

In this paper, we present the male description and host association for *X. bucki* Suárez, 1960. Information on diapause for Neotropical Mutillidae is provided, as well as seasonal and annual variation in the abundance of *X. turrialba*.

Materials and methods

The study of *Xystromutilla bucki* Suárez, 1960 was carried out from August 2018 to August 2019 in the municipality of Guarapuava, state of Paraná (PR), southern Brazil. Information on the study site and sampling methods with trap-nests were discussed in Cambra et al. (2017).

The study site for flight seasonality of *Xystromutilla turrialba* Casal, 1969 was the field station of the Smithsonian Tropical Research Institute (STRI) on Barro Colorado Island (BCI). Information on the study site and sampling methods with Malaise traps were discussed in Cambra et al. (2018).

Photographs of genitalia were made with an Olympus Stylus digital camera using an Olympus BX53F stereomicroscope, with further image processing done using ArcSoft PhotoStudio. The genitalia were stored in a glass vial and placed on the specimen pin. Measurements of the male specimen were made with a calibrated micrometer scale attached to an ocular lens of the stereomicroscope.

The specimens of *Xystromutilla bucki* were identified by authors K.A.W., P.R.B. and R.A.C., while the specimens of *Auplopus subaurarius* Dreisbach, 1963 by R.A.C. and Eduardo Fernando dos Santos. The specimens examined are deposited in Museo de Invertebrados G. B. Fairchild, University of Panama, Panama (MIUP) and in the

entomological collection of Laboratório de Biologia e Ecologia de Vespas e Abelhas, Universidade Estadual do Centro-Oeste, Guarapuava (PR), Brazil (UNICENTRO). The specimens of *Pseudomethoca* nr. *chontalensis* are deposited in Museo de Zoología, Universidad de Costa Rica, San José, Costa Rica (MZUCR).

Results

Taxonomy

Xystromutilla bucki Suárez, 1960

Figs 1–8

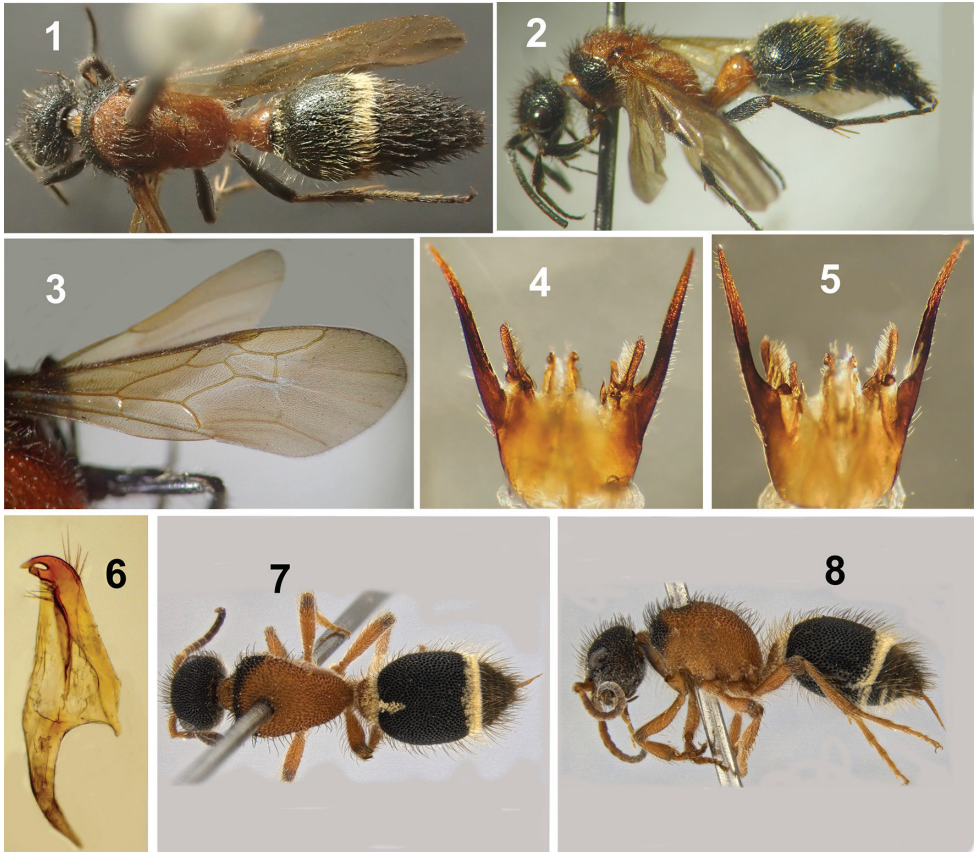
Xystromutilla bucki Suárez, 1960: 453–455, ♀, holotype, Porto Alegre, [Rio Grande do Sul], Brasil, 19.iii.1952, P. Buck (Colección Suárez; now in Museo Nacional de Ciencias Naturales, Madrid, Spain).

Diagnosis. Male (Figs 1–6). This species can be recognized by its unique coloration, wherein the meso-metathorax, propodeum and first metasomal segment are orange-red; wings subhyaline. The following morphological characters are also useful for diagnosis: head with simple setae; mandible ventrally with a strong basal tooth; sternum 1 without a spine; hypopygium posterior margin with a small denticle medially; paramere almost straight and cuspis finger-shaped. Other described males of *Xystromutilla* have black integument, fore wings partly or totally fuscous, sternum 1 with a basal spine, hypopygium with medial spine on the apical margin, paramere lyre-shaped and cuspis elongate spoon-shaped. These morphological characters are not present in males of *X. bucki*. **Female** (Figs 7, 8). Head, pronotum and metasomal segment 1 orange-red, rest of metasoma black; head with simple setae only; humeral angles of pronotum rounded, not carinate; integument of basal half of tergum 2 without carinae.

Description. Male (hitherto unknown). (Figs 1, 2). **Body length.** 10.1 mm.

Body Color. Integument black, except apical half of mandible, meso-metathorax, propodeum and first metasomal segment orange-red; tibial spurs white; wings subhyaline, without infuscated area; head, pronotum, mesoscutum and scutellum with long, semierect simple black setae; meso-metapleura and propodeum mostly with long, semierect simple pale white setae; fore legs mostly with simple black setae, mid and hind legs mostly with simple pale white setae and few black setae; metasomal segments one and two with long semierect simple pale white setae, posterior margin of metasomal segment 2 with dense and decumbent band of plumose white setae; metasomal segments 3 to 7 with long, semierect black setae, posterior margins of metasomal segments 3 and 4 with decumbent plumose black setae mostly hidden by simple setae.

Head. Rectangular in dorsal view, frons, vertex and gena with medium-sized, very close punctures; distance between eye margin and lateral ocellus $2.77 \times$ as long as diameter of ocellus; flagellomere I $1.9 \times$ pedicel length; flagellomere II $2.2 \times$ pedicel



Figures 1–8. *Xystromutilla bucki* 1–6 male: 1 dorsal view 2 lateral view 3 right wings 4 genitalia, dorsal view 5 genitalia, ventral view 6 penis valve, lateral view 7, 8 female: 7 dorsal view 8 lateral view.

length; clypeus bidentate medially on anterior margin; mandible apically obliquely tridentate, ventrally with a strong tooth near base.

Mesosoma. Pronotum, mesoscutum, scutellum and mesopleuron with medium-sized, contiguous punctures, metapleuron impunctate; tegula glabrous, except anterior and inner margins setigerously punctate; propodeum totally reticulate; notaulus incomplete, not reaching anterior margin of mesoscutum; scutellum convex; fore wing (Fig. 3) with two submarginal cells; coxae without denticle, tubercle or carina.

Metasoma. First segment petiolate, tergum 1 dorsal face $1.47 \times$ as long as wide; tergum 1–2 and sternum 2 and 7 mostly with medium-sized close punctures; metasomal segments 3–6 with small, close punctures; tergum 7 basal half with small punctures, apical half mostly without punctures; sternum 1 without a spine near base, with two longitudinal carinae diverging posteriorly; hypopygium posterior margin not straight, with a small denticle medially.

Genitalia. Parameres (Figs 4, 5) almost straight, not lyre-shaped; basal half in lateral view broad, distal half gradually narrowing toward apex and slightly curved upwards, ending in a sharp point; dorsal surface with five long setae at end of basal broad

half; very short sparse setae elsewhere; digitus and cuspis (Figs 4, 5) finger-shaped, digitus with inconspicuous and sparse setae, cuspis laterally flattened with dense long setae on inner surface; penial valve (Fig. 6) with an apical tooth and preapical projection with blunt apex, apical dorsal edge with five long setae and near to base of preapical projection with six long setae.

Material examined. BRAZIL: **Santa Catarina:** Porto União, nest 371 (1) (5 mm hole diameter), 13.i.2012–14.ii.2012, J. Iantas, 1 ♀ (MIUP) (reared from nest of *Auplopus subaurarius* Dreisbach, 1963). **Rio Grande do Sul:** Cambara do Sul, Itaim-bezinho, 10.iii.2000, col. R. da Cunha, 1 ♀ (MIUP); Guaíba, 116 – km 307, col. F.V. Borges: 15.i.1998, 1 ♂ (MIUP); 30.ix.1999, 1 ♂ (MIUP); São Francisco de Paula, CPCN Pro-Mata, col. B. Harter: 4.viii.1997, 1 ♂ (MIUP); 6.i.1998, 1 ♂ (MIUP). **Paraná:** Turvo, 25°01'55"S, 51°31'53"W, col. M.C. Nether: 22.xii.2012, 2 ♂ (nest 223) (MIUP); 22.ii.2013, 1 ♂ (nest 552) (MIUP); Guarapuava, 25°21'55"S, 51°27'58"W, 24.i.2013, col. M.C. Nether, 1 ♂ (nest 447) (MIUP); Guarapuava, 25°24'09.7"S, 51°24'45.5"W, 11.iii.2019, col. C. Queiros and J. De Deus, 6 ♂, 1 ♀ (nests 353, 460) (UNICENTRO); Guarapuava, 25°39'S, 51°42'W, 10.v.2019, col. C. Queiros and J. De Deus, 1 ♀ (nest 365) (UNICENTRO)

Distribution. Brazil (Paraná, Rio Grande do Sul, Santa Catarina).

Biology. This is the first record of Pompilidae as a host of *Xystromutilla*. In the Araucaria forest fragments, 66 trap-nests of *Auplopus subaurarius* Dreisbach were examined. Of these nests, *X. bucki* parasitized three of them, all of which were in bamboo, 1.3 cm in diameter and 18.2 cm in length. One of the nests had nine cells, six of which were parasitized by *Xystromutilla* (five males and one female emerged) and two by *Photocryptus* sp. (Ichneumonidae: Cryptinae). The other two parasitized nests contained one cell each, from which emerged a male and a female. Therefore, six males and two females emerged in total from the nests. The males were larger bodied with average head width 0.3 mm (n = 6; SD = 0.01 mm) and the females 0.2 mm (n = 2; SD = 0.06 mm).

We found in *Xystromutilla bucki* that the average time between nest collection and adult wasp emergence, for seven of the eight specimens reared, was 265 days (n = 7; SD = 4.2 days), with immatures exhibiting diapause at the prepupal stage (6 males, 1 female). Only one female (from the one-celled nest) did not enter into diapause, but rather emerged 11 days after nest collection.

Xystromutilla turrialba Casal, 1969

Xystromutilla turrialba Casal, 1969, Physis 29: 47, holotype female, Turrialba, Costa Rica, USNM.

Material examined. (81 specimens, MIUP): PANAMÁ, Barro Colorado Island: iv.2001, 15 males; v.2001, 5 males; v.2002, 2 males; vi.2002, 5 males; vii.2002, 1 male; iii.2003, 14 males, 1 female; iv.2003, 27 males, 1 female; v.2003, 5 males; ii.2004, 2 males; iv.2004, 2 males; v.2004, 1 male.

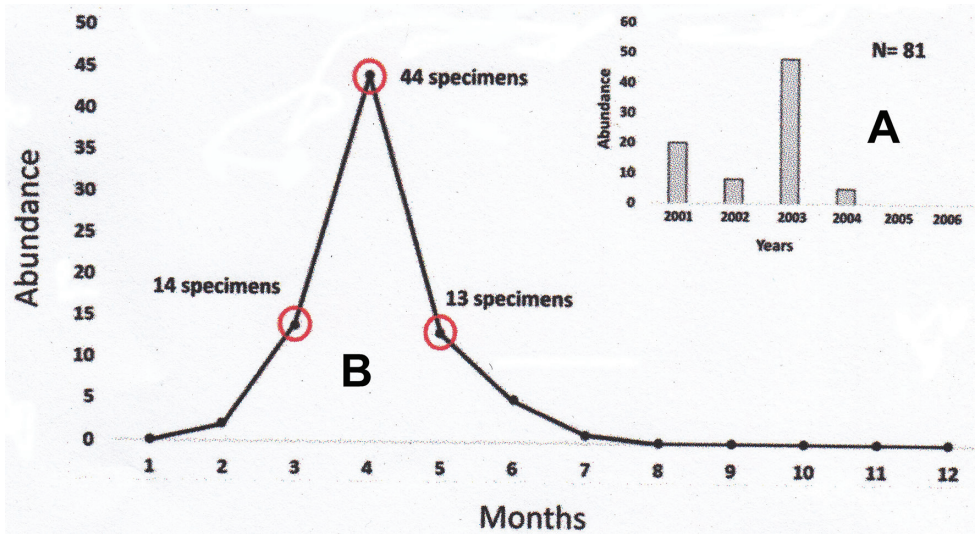


Figure 9. **A** total *Xystromutilla turrialba* specimens captured by year (2001–2006) **B** total *Xystromutilla turrialba* specimens captured by month (2001–2006).

Distribution. Honduras, Nicaragua, Costa Rica, Panama (Casal 1969; Cambra and Quintero 2004).

Seasonal and annual abundance. A total of 81 specimens of *Xystromutilla turrialba* (79 males and 2 females) were captured over six continuous sampling years (2001–2006) with ten Malaise traps on Barro Colorado Island (BCI), Panama. The years with the greatest abundance of specimens were 2001 and 2003; samples were not captured during 2005 and 2006 (Fig. 9A). Specimens of *X. turrialba* were captured only in the months from February to July, with greatest abundance from March to May with 71 (87.6%) specimens captured, peaking during April with 44 specimens (54.3%) (Fig. 9B). The greater abundance of *X. turrialba* during April is similar to results found for *Dasymutilla* Ashmead, 1899 and *Ephuta* Say, 1836 (Mutillidae) species on BCI (Cambra et al. 2018; Añino et al. 2020). The only two females of *X. turrialba* were captured in March and April, and their relatively small number compared to that of males on BCI is due to the sampling methodology, since females are apterous. The under-representation of females is not seen in hand-net and trap-nest samples from Panama, in which 14 females and 16 males of *X. turrialba* were captured during all months of the year except November (Cambra and Quintero 1992, 2004).

Discussion

Both sexes of *Xystromutilla bucki* are morphologically similar to some species of the genus *Sphaerophthalma* Blake, 1871, especially those recorded from Central and South America (Williams and Pitts 2007). Brothers (2006) presented a key for the Neotropi-

cal genera of Mutillidae, placing both *Xystromutilla* and *Sphaerophthalma* in the same couplet and separating them based on the presence or absence of plumose setae on the head, as well as the shape of the first metasomal tergum. It is important to note that *Sphaerophthalma* is a sort of “dumping ground” genus for nocturnal species of velvet ants in South America and many of its species will likely be placed in different genera in the future (KAW, PRB and RAC, pers. obs.). Sexual associations are of great importance to understand the phylogenetic relationships of *Xystromutilla*, *Sphaerophthalma* and any other genera to be dismembered from the latter, as well as to have a better knowledge of the morphological characteristics that delimit Sphaerophthalmini genera in the New World.

Little information exists on overwintering/diapause in Mutillidae. Mickel (1928) summarized earlier information from several sources in compiling a typical mutillid life history and stated that “in colder latitudes the winter is passed in the prepupal stage”. Bohart and McSwain (1939) mentioned prepupal overwintering for *Dasymutilla sackenii* (Cresson, 1865) from California. Brothers (1972, 1978) observed diapause in the fifth larval instar (prepupa) of some *Pseudomethoca frigida* (Smith, 1855) and *Myrmosula parvula* (Fox, 1893) kept in the laboratory. Brothers (1972) also presented a summary of unpublished observations by Cottrell, indicating that some individuals of *Dasymutilla bioculata* (Cresson, 1865) may diapause as prepupae for more than one season. Our finding of prepupal diapause in *Xystromutilla bucki* represents the first record for a Neotropical mutillid species and reinforces the apparently general occurrence of such diapause where environmental conditions are appropriate.

Apart from prepupal diapause, there are a few records of hibernation/diapause by adults. Potts and Smith (1944) recorded hibernation in two adult females of *Dasymutilla aureola pacifica* (Cresson, 1875) from California; Evans and Miller (1970) indicated some degree of overwintering by three adult females (marked the previous summer of 1968) of *D. nigripes* (Fabricius, 1787) collected in the summer of 1969 in Michigan; and Hennessey (2002) recorded overwintering by adult females of *D. nigripes* (Fabricius), *D. vesta* (Cresson, 1865) and *Timulla vagans* (Fabricius, 1798) in a deciduous forest in Maryland. The following observations on *Pseudomethoca* nr. *chontalensis* (Cameron, 1895), det. R. Cambra, by Kenji Nishida (unpublished data) are also relevant here. On January 25, 2015, fifteen adult females of *P.* nr. *chontalensis* (with two dark morphs) were found inside a hollow and dry twig of *Quercus insignis* (Fagaceae) (Figs 10, 11). The twig was found on the ground in a relatively open area of the forest in EBM, Monteverde at 1530 m, Pacific slope, Costa Rica; the weather this time of the year is windy and cold, and the temperature was no higher than 16 °C during the morning or afternoon and 12 °C during the night. The twig on the ground used as ‘shelter’ was an old, empty, cut-off branch made by a female Cerambycidae (Coleoptera) larva (det. K. Nishida), which had probably eaten much of the interior of the twig. No traces or remains of larvae, prepupae, or pupae of any other insect were found, suggesting that the mutillids did not emerge inside the twig. When the twig was manually opened, the 15 mutillids were observed well grouped, with some on top of the others. Two fell to the ground and escaped into the litter; the other 13 (three



Figures 10, 11. *Pseudomethoca* nr. *chontalensis* inside of hollow *Quercus insignis* twig (manually opened).

groups, of six, four, and three specimens) remained motionless within the twig. On February 5, 2015, all the females began to move and left the twig. The temperature was between 24 and 28 °C. The 13 females remained grouped for 12 days. This immobile aggregation indicates a probable diapause in adult females of *P.* nr. *chontalensis*. Janvier (1933: 283) recorded a single male in the middle of a group of 46 female mutillids captured in Chile (identified as *Dimorphomutilla formosa* Mickel, 1938 by Quintero and Cambra 2001). Janvier did not mention how long they were grouped. We do not know of another record related to possible diapause in adults of Neotropical Mutillidae.

Mutillids are solitary wasps; in tropical forests they are generally widely dispersed. We do not know how *P.* nr. *chontalensis* females would form such an aggregation.

However, females and males of Mutillidae produce sounds that may be species specific (Tschuch 1993; Torrico-Bazoberry and Muñoz 2019). The function of stridulation in mutillids is unclear, although these sounds apparently act as warning/defensive signals (Schmidt and Blum 1977; Masters 1979; Polidori et al. 2012) and/or have roles in intra-specific communication (Bayliss and Brothers 1996; Torrico-Bazoberry and Muñoz 2019), but there is no evidence suggesting that such signals could be used in forming aggregations. Although we cannot definitively know the function of aggregation in *P. nr. chontalensis*, we suggest that it is a defensive strategy against potential predators while waiting for favorable environmental conditions for dispersal, mating and host searching activities.

Acknowledgements

We are grateful to Denis J. Brothers, University of KwaZulu-Natal, for making useful suggestions and corrections improving this work. We thank Vanessa Sánchez, University of Panama, and Donald Windsor, Smithsonian Tropical Research Institute, for the excellent assistance provided in the processing of the specimens of *X. turrialba* captured in BCI. The long-term Malaise trap sampling on BCI was instituted by John Pickering (University of Georgia, USA) and was supported by funding from the “Environmental Sciences Program” of the Smithsonian Institution.

References

- André E (1905) Nouvelles espèces de Mutillides d'Amérique. (Hym.). Zeitschrift für Systematische Hymenopterologie und Dipterologie 5: 361–376.
- André E (1906) Nouvelles espèces de Mutillides d'Amérique (Hym.). Zeitschrift für Systematische Hymenopterologie und Dipterologie 6: 33–48. [65–80, 161–169.]
- Añino YJ, Cambra RA, Windsor DM, Williams KA, Bartholomay PR, Quintero D, Sánchez V (2020) Seasonal and annual variation in the abundance of *Ephuta* Say (Hymenoptera: Mutillidae) in Panama. Revista de Biología Tropical 68(2): 573–579.
- Ashmead WH (1899) Superfamilies in the Hymenoptera and generic synopses of the families Thynnidae, Myrmosidae, and Mutillidae. Journal of the New York Entomological Society 7: 45–60. <https://www.biodiversitylibrary.org/page/9198707>
- Bartholomay PR, Williams KA, Cambra RA, Oliveira ML (2019) Does the genus *Dasymutilla* Ashmead occur in South America? The new genus *Quwitilla*, new combinations, and new distribution records from Neotropical velvet ants (Hymenoptera: Mutillidae). Zootaxa 4623(2): 261–282. <https://doi.org/10.11646/zootaxa.4623.2.3>
- Bayliss PS, Brothers DJ (1996) Biology of *Tricholabiodes* Radoszkowski in southern Africa, with a new synonymy and review of recent biological literature (Hymenoptera: Mutillidae). Journal of Hymenoptera Research 5: 249–258.
- Blake CA (1871) Synopsis of the Mutillidae of North America. Transactions of the American Entomological Society 3: 217–265. <https://doi.org/10.2307/25076249>

- Bohart GE, McSwain JW (1939) The life history of the sand wasp, *Bembix occidentalis beutenmuelleri* Fox and its parasites. Bulletin of the Southern Academy of Sciences 38: 84–97.
- Brothers DJ (1972) Biology and immature stages of *Pseudomethoca f. frigida*, with notes on other species (Hymenoptera: Mutillidae). The University of Kansas Science Bulletin 50(1): 1–38.
- Brothers DJ (1978) Biology and immature stages of *Myrmosula parvula* (Hymenoptera: Mutillidae). Journal of the Kansas Entomological Society 51(4): 698–710.
- Brothers DJ (2006) Mutillidae. In: Hanson P, Gauld I (Eds) Hymenoptera de la Región Tropical. Memoirs of the American entomological Institute 77: 586–594.
- Brothers DJ, Lelej AS (2017) Phylogeny and higher classification of Mutillidae (Hymenoptera) based on morphological reanalyses. Journal of Hymenoptera Research 60: 1–97. <https://doi.org/10.3897/jhr.60.20091>
- Cambra RA, Quintero D (1992) Velvet ants of Panama: distribution and systematics (Hymenoptera: Mutillidae). In: Quintero D, Aiello A (Eds) Insects of Panama and Mesoamerica: Selected Studies. Oxford University Press, Oxford, 459–478.
- Cambra RA, Quintero D (2004) New species of *Xystromutilla* André (Hymenoptera: Mutillidae) and the first illustrated key for the males of the genus. Transactions of the American Entomological Society 130(4): 463–478.
- Cambra RA, Tunes-Buschini ML, Quintero D, Brozoski F, Rudiak-Lustosa P (2017) *Ephuta icema* Casal, 1969 and its host *Auplopus subaurarius* Dreisbach, 1963 (Hymenoptera: Mutillidae, Pompilidae) from Brazil. Zootaxa 4272(2): 285–290. <https://doi.org/10.11646/zootaxa.4272.2.9>
- Cambra RA, Williams KA, Quintero D, Windsor D, Pickering J, Saavedra D (2018) *Dasymutilla* Ashmead (Hymenoptera, Mutillidae) in Panama: new species, sex associations and seasonal flight activity. Insecta Mundi 0608: 1–17.
- Cameron P (1894–1896) Biologia Centrali-Americana. Hymenoptera 2: 259–395.
- Casal OH (1969) Sobre *Xystromutilla* André, 1905 (Hymenoptera, Mutillidae). Physis 29: 47–50.
- Cresson ET (1865) Descriptions of some new species of *Mutilla* from California. Proceedings of the Entomological Society of Philadelphia 4: 385–390. <https://www.biodiversitylibrary.org/page/3328793>
- Cresson ET (1875) Descriptions of new species of *Mutilla*. Transactions of the American Entomological Society 5: 119–120. <https://doi.org/10.2307/25076298>
- Dreisbach RR (1963) New species of spider wasps, genus *Auplopus*, from the Americas South of the United States (Hymenoptera: Psammocharidae). Proceedings of the United States National Museum 114(3468): 137–211. [13 pls] <https://doi.org/10.5479/si.00963801.114-3468.137>
- Evans DA, Miller BR (1970) A note on adult overwintering of *Dasymutilla nigripes* in Michigan (Hymenoptera: Mutillidae). The Michigan Entomologist 2(3–4): 74–74.
- Fabricius JC (1787) Mantissa Insectorum, sistens eorum nuper detecta, adjectis characteribus genericis, differentiis specificis, emendationibus, obsevationibus. Hafniae, Proft. 1: 311–313. <https://doi.org/10.5962/bhl.title.11657>
- Fabricius JC (1798) Supplementum Entomologiae Systematicae. t. 5, 42–42. <https://www.biodiversitylibrary.org/page/42138538>
- Fabricius JC (1804) Systema Piezatorum secundum ordinis, genera, species, adjectis synonymis, locis, observationibus, descriptionibus. Brunswick: C. Reichard, [xiv + 15–439 + 30] 469 pp. <https://doi.org/10.5962/bhl.title.10490>

- Fox WJ (1893) New North American Aculeate Hymenoptera. Journal of the New York Entomological Society 1: 53–53. <https://www.biodiversitylibrary.org/page/33454707>
- Hennessey RD (2002) Population-level characteristics of *Dasymutilla nigripes*, *D. vesta*, and *Timulla vagans* (Hymenoptera: Mutillidae). Florida Entomologist 85(1): 245–253. [https://doi.org/10.1653/0015-4040\(2002\)085\[0245:PLCODN\]2.0.CO;2](https://doi.org/10.1653/0015-4040(2002)085[0245:PLCODN]2.0.CO;2)
- Janvier H (1933) Étude biologique de quelques hyménoptères du Chili. Annales des sciences naturelles. Zoologie et biologie animale (Ser. 10) 16: 209–356.
- Masters WM (1979) Insect disturbance stridulation: its defensive role. Behavioral Ecology and Sociobiology 5(2): 187–200. <https://doi.org/10.1007/BF00293305>
- Mickel CE (1928) Biological and taxonomic investigations on the mutillid wasps. Bulletin of the United States National Museum 143: 1–360. [+ 5 pls] <https://doi.org/10.5479/si.03629236.143.1>
- Mickel CE (1938) The Neotropical mutillid wasps of the genus *Dimorphomutilla* Ashmead (Hymenoptera). Revista de Entomologia, Rio de Janeiro 9: 349–364.
- Morato EF (1994) *Xystromutilla asperiventris* André, 1905 (Mutillidae) reared from sphecoid wasps in trap-nests, Manaus Amazonas, Brazil. Sphecos 28: 13–14.
- Pagliano G, Brothers DJ, Cambra RA, Lelej AS, Lo Cascio P, Matteini-Palmerini M, Scaramozzino PL, Williams KA, Romano M (2020 [“2018”]) Checklist of names in Mutillidae (Hymenoptera), with illustrations of selected species. Bollettino del Museo Regionale di Scienze Naturali di Torino 36(1–2): 5–427.
- Polidori C, Ruffato G, Borruso L, Settanni C, Pavan G (2012) [“2013”] Stridulatory organ and distress call in males and females of a small velvet ant (Hymenoptera: Mutillidae). Bioacoustics 22(2): 121–135. <https://doi.org/10.1080/09524622.2012.736241>
- Potts RW, Smith RF (1944) Hibernation of *Dasymutilla aureola pacifica*. The Pan-Pacific Entomologist 20(2): 60–60.
- Quintero D, Cambra RA (2001) On the identity of *Scaptopoda* F. Lynch Arribálzaga, new taxonomic changes and new distribution records for Neotropical Mutillidae (Hymenoptera), with notes on their biology. Transactions of the American Entomological Society 127(3): 291–304.
- Richards OW (1934) The American species of the genus *Trypoxylon* (hymenopt., sphecoidea). Transactions of the Royal Entomological Society of London 82(2): 173–362. <https://doi.org/10.1111/j.1365-2311.1934.tb00033.x>
- Rodríguez AR, Matías FA (1996) Diversidad de himenópteros usuarios de trampas-nidos, sus parasitoides y sus preferencias de anidación en Península Gigante. Thesis, Universidad de Panamá.
- Saussure H de (1867) Hymenoptera. In: Reise der österreichischen Fregatte Novara um die Erde. Zoologischer Theil 2: 1–138.
- Say T (1836) Descriptions of new species of North American Hymenoptera, and observations on some already described. Boston Journal of Natural History 1(3): 295–298. <https://www.biodiversitylibrary.org/page/32414019>
- Schmidt JO, Blum MS (1977) Adaptations and responses of *Dasymutilla occidentalis* (Hymenoptera: Mutillidae) to predators. Entomologia Experimentalis et Applicata 21(2): 99–111. <https://doi.org/10.1111/j.1570-7458.1977.tb02663.x>
- Smith F (1855) Catalogue of hymenopterous insects in the collection of the British Museum, part III. Mutillidae and Pompilidae. London, 63 pp. <https://www.biodiversitylibrary.org/page/9319972>

- Smith F (1856) Catalogue of hymenopterous insects in the collection of the British Museum, part IV, Sphecidae, Larridae and Crabronidae. London, 207–497. <https://doi.org/10.5962/bhl.title.20858>
- Suárez FJ (1960) Datos sobre mutílicos neotropicales I. Nuevas especies de Sphaerophthalminae (!) (Hymenoptera). EOS 36(4): 451–480.
- Torrico-Bazoberry D, Muñoz MI (2019) High-frequency components in the distress stridulation of Chilean endemic velvet ants (Hymenoptera: Mutillidae). Revista Chilena de Entomología 45(1): 5–13.
- Tschuch G (1993) Sound production in mutillid wasps (Mutillidae, Hymenoptera). Bioacoustics 5(1–2): 123–129. <https://doi.org/10.1080/09524622.1993.9753234>
- Williams KA, Pitts JP (2007) New species of the predominately temperate velvet ant genera *Lomachaeta* Mickel and *Sphaerophthalma* Blake from Central and northern South America (Hymenoptera: Mutillidae). Transactions of the American Entomological Society 133(3+4): 297–326. <https://doi.org/10.3157/0002-8320-133.3.297>

Description of a new species, *Sillago nigrofasciata* sp. nov. (Perciformes, Sillaginidae) from the southern coast of China

Jia-Guang Xiao¹, Zheng-Sen Yu², Na Song², Tian-Xiang Gao³

1 Laboratory of Marine Biology and Ecology, Third Institute of Oceanography, Ministry of Natural Resources, Xiamen 361005, China **2** Fisheries College, Ocean University of China, Qingdao 266003, China **3** Fisheries College, Zhejiang Ocean University, Zhoushan 316022, China

Corresponding author: Tian-Xiang Gao (gaotianxiang0611@163.com)

Academic editor: M.E. Bichuette | Received 6 August 2020 | Accepted 17 December 2020 | Published 18 January 2021

<http://zoobank.org/FCC7DDBC-D5C4-4AAE-95A3-DA536860C954>

Citation: Xiao J-G, Yu Z-S, Song N, Gao T-X (2021) Description of a new species, *Sillago nigrofasciata* sp. nov. (Perciformes, Sillaginidae) from the southern coast of China. ZooKeys 1011: 85–100. <https://doi.org/10.3897/zookeys.1011.57302>

Abstract

A new *Sillago* species, the black-banded sillago, *Sillago nigrofasciata* sp. nov., is described based on 302 specimens sampled from the southern coast of China. Morphological comparisons have been conducted between the new species and ten other *Sillago* species. The results show that the new species is characterized by a black mid-lateral band below the lateral line when fresh; other characteristics are similar to those of *Sillago sihama* but subtle differences exist on the swim bladder between *Sillago nigrofasciata* sp. nov. and *S. sihama*. A detailed description and illustrations are provided for the new species. The validity of this new species is also supported by a genetic comparison using sequences of the mitochondrial cytochrome c oxidase subunit I (COI) gene.

Keywords

DNA barcoding, molecular phylogenetic analyses, morphology, swim bladder, taxonomy

Introduction

The family Sillaginidae Richardson, 1846, commonly known as sand whiting or sand borer, is a small family of demersal marine fishes that primarily inhabit inshore waters with sandy substrates or estuarine areas of rivers throughout the Indo-West Pacific (IWP; McKay 1985; McKay 1992; Nelson et al. 2016). At present, it is generally agreed that this family consists of 36 species, among them, five new *Sillago* species were published successively after the overview of the FAO species catalogue (McKay 1992), including *S. caudicula* Kaga, Imamura & Nakaya, 2010; *S. sinica* Gao & Xue, 2011; *S. suzensis* Golani, Fricke & Tikochinski, 2014; *S. shaoi* Gao & Xiao, 2016; and *S. panhwari* Panhwar, 2018 (Kaga et al. 2010; Gao et al. 2011; Golani et al. 2014; Xiao et al. 2016; Panhwar et al. 2018).

Reliance only on morphology to identify fishes to the species level is challenging when the diagnostic characters are similar among related taxa. Species of the family Sillaginidae are easily identified due to similarity of shape and coloration pattern (Sano and Mochizuki 1984; McKay 1992). This external morphological similarity, however, has led to much confusion in their specific identification and many cryptic species have been concealed in the synonymy of those wide-ranging species (Cheng and Zheng 1987; Kwun and Kim 2010; Bae et al. 2013). As a widely distributed Sillaginidae species, *Sillago sihama* (Forsskål, 1775) exhibits many cryptic lineages across its Indo-West Pacific distribution (Cheng et al. 2020). In fact, these five recently identified *Sillago* species were all wrongly assigned to *S. sihama*.

The most important character commonly used to identify *Sillago* species is its swim bladder. McKay (1985) reported three subgenera of the genus *Sillago*: *Sillaginopodys* Fowler, 1933 (swim bladder reduced, no duct-like process); *Sillago* Cuvier, 1817 (swim bladder divided posteriorly into two tapering extensions, duct-like process present); and *Parasillago* McKay, 1985 (swim bladder with a single posterior extension and the duct-like process). McKay (1985) also described four species of the subgenus *Sillago* (*S. S. intermedius* Wongratana, 1977; *S. S. megacephalus* Lin, 1933; *S. S. parvisquamis* Gill, 1861; and *S. S. sihama* Forsskål, 1775). The presence of two posterior extensions of the swim bladder observed in five species suggested that they should belong to the subgenus *Sillago*. In addition, a redescription of *S. indica* McKay, Dutt & Sujatha, 1985, reassigns it to the subgenus *Sillago* (Kaga and Ho 2012). This subgeneric grading system is very useful in both classification and phylogenetic analysis. Sometimes, the swim bladders of some sibling species are very similar, making the identification of these species extremely difficult, and other evidence must be found. In the last decades, DNA barcoding has provided an independent means of testing the validity of existing taxonomic units, revealing cases of inappropriate synonymy and, consequently, the existence of numerous cryptic species (Hebert et al. 2003a, b; Burns et al. 2008; Locke et al. 2010; Gao et al. 2011). Cheng et al. (2020) performed a thorough phylogenetic analysis based on both morphological and genetic evidences. The results indicated that more cryptic species could be present in the family Sillaginidae, and there are at least eight clades within the *S. sihama* complex.

While undertaking a taxonomic review of the genus *Sillago* along the southern coast of China, we had an opportunity to examine 302 specimens collected from this northwest Pacific Ocean coastline. Based on morphological characteristics, those specimens were assigned to *S. sihama*; particularly, their swim bladders were very similar to those of *S. sihama* (McKay 1992: fig. 130, type locality Queensland). However, a high mean genetic distance was found between these sequences and those of *S. sihama* based on DNA barcoding sequences. In addition, morphological evidence indicated that they belong to an unrecognized species. Herein, we use molecular and morphological approaches to describe the new species, and reconstruct the relationships of the species in the genus. Our results confirm the genetic distinction of the know *Sillago* species and invoke the possibility of additional species of *Sillago*, which may be hiding in the *S. sihama* cryptic complex along the coast of China.

Materials and methods

Sampling

The unidentified specimens were collected from the southern coast of China, more precisely in Fuding (Fujian, 50 individuals), Xiamen (Fujian, 40 individuals), Changhua (Taiwan, 1 individuals), Chiayi (Taiwan, 17 tissues), Shantou (Guangdong, 6 individuals), Zhuhai (Guangdong, 18 individuals), Zhanjiang (Guangdong, 30 individuals), Beihai (Guangxi, 80 individuals), Fangchenggang (Guangxi, 50 individuals), Haikou (Hainan, 4 individuals), and Danzhou (Hainan, 6 individuals) (Fig. 1). All specimens were deposited at Fishery Ecology & Marine Biodiversity Laboratory, Fisheries College, Zhejiang Ocean University, Zhoushan (**ZJOU_FEBL**) and Fishery Ecology Laboratory, Fisheries College, Ocean University of China, Qingdao (**OUC_FEL**).

In this study, the recorded ten *Sillago* species with two posterior extensions of the swim bladder were referenced and compared to assign the new species (Table 1). Eight of them were used for genetic comparison altogether, including *S. indica*, *S. nigrofasciata* sp. nov., *S. panhwari*, *S. parvisquamis*, *S. sihama*, *S. shaoi*, *S. sinica*, and *S. suezensis*.

Morphological analysis

The genus and species classification followed McKay (1985), unless otherwise noted. The terminology of appendages of the swim bladder followed Shao et al. (1986) and Kaga and Ho (2012). In the descriptive section, the data of the holotypes were given first, while those of the paratypes followed in parentheses. General abbreviations used in this paper were:

- | | | | |
|-----------|--------------------------------|-----------|----------------------------------|
| A | the number of anal fin rays; | P | the number of pectoral fin rays; |
| C | the number of caudal fin rays. | SL | standard length; |
| D | the number of dorsal fin rays; | V | the number of ventral fin rays. |
| HL | head length; | | |

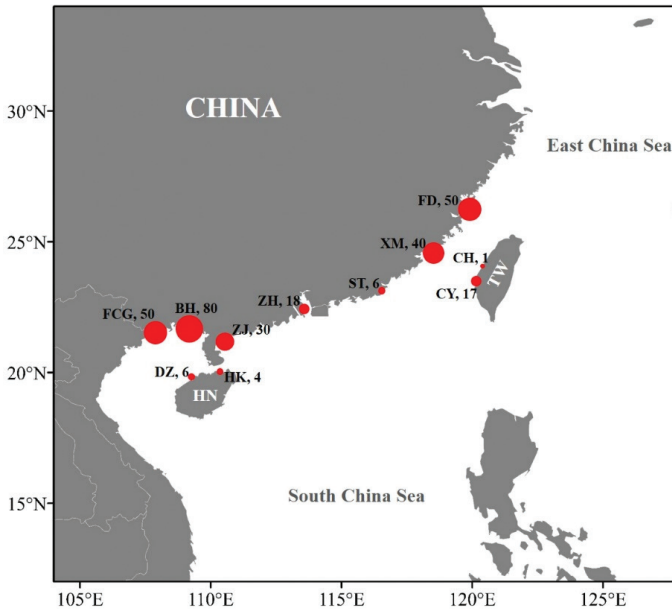


Figure 1. Sampling sites and corresponding sample sizes (represented by circle size and Arabic numerals) of *Sillago nigrofasciata* sp. nov. **HN**, Hainan Island; **TW**, Taiwan Island; **FD**, Fuding; **XM**, Xiamen; **ST**, Shantou; **ZH**, Zhuhai; **ZJ**, Zhanjiang; **BH**, Beihai; **FCG**, Fangchenggang; **DZ**, Danzhou; **HK**, Haikou; **CY**, Chiayi; **CH**, Changhua.

All measurements were made with dial calipers and dividers to the nearest 0.1 mm. The definition of the modified vertebrae followed McKay (1992). Gill rakers and swim bladders were examined in the dissected paratypes.

Genetic analysis

To analyze genetic differences between this new species and other congeners, mitochondrial (mt) DNA cytochrome oxidase subunit I (COI) fragments of *Sillago* spp. were amplified based on the method of Ward et al. (2005). Genomic DNA extraction and polymerase chain reaction (PCR) followed the protocols of Gao et al. (2011). Sequences were checked and aligned using DNASTAR software (DNASTAR Inc., Madison, WI, USA) and MEGA 5.0 (Tamura et al. 2011) was used to analyze the sequences, estimate the pairwise genetic distances, and construct a Neighbor-joining (NJ) tree under the Kimura 2-parameter (K2P) model. COI sequences of *S. nigrofasciata* sp. nov. obtained in the present study were submitted to GenBank with the following accession numbers: KU051808, KU051809, KU051812, MG571453–MG571458, MG911029–MG911030. Twenty-nine COI sequences were obtained from GenBank with the following accession numbers: *S. indica* (KM350229–KM350232), *S. panhwari* (MF571945, MF571947, KU051787 and KU051788), *S. parvisquamis* (HQ389247–HQ389249), *S. shaoi* (KU051872, KU051873,

Table 1. Comparison of *Sillago nigrofasciata* sp. nov. and other ten species of *Sillago* with two posterior extensions of the swim bladder.

	<i>Sillago nigrofasciata</i> sp. nov. ^a	<i>S. intermedius</i> ^b	<i>S. megalcephalus</i> ^b	<i>S. panhwar</i> ^{c,e}	<i>S. shao</i> ^d	<i>S. parvisquamis</i> ^b	<i>S. silhamad</i>	<i>S. caudiculat</i>	<i>S. sinice</i> ^d	<i>S. suezensis</i> ^g	<i>S. indicap</i> ^{d,h}
Dorsal fins	X-XII, I, 20-22	XI, I, 21-22	XI, I, 22	X-XII, I, 20-22	XI, I, 20-22	XII-XIII, I, 20-22	XI, I, 20-23	XI, I, 22-23	X-XI, I, 20-22	X-XII, I, 19-22	X-XI, I, 20-22
Anal fin	II, 20-22	II, 21-22	II, 23	II, 18-23	II, 21-22	II, 22-24	II, 21-23	II, 23-24	II, 21-23	II, 18-22	II, 21-23
Scales in lateral line	67-75	67-70	70	69-84	70-73	79-84	68-72	71	75-79	63-74	68-71
Scales above/below lateral line	4-6/9-12	6-7/8-9	5/10-11	4-5/7-10	5-6/10-12	7/11-12	5-6/10-12	5/11	5-6/9-11	-	5-6/10-12
Gill rakers first arch	2-4/5-8	-	-	3-4/7-8	3-4/5-6	1-2/7-9	3/8-9	4/11	2-4/6-8	3-4/8-10	3-4/7-8
Vertebrae	34-35	34	-	34	35	39-40	34	35-36	37-39	34	33-35
HL/SL (%)	25.1-30.8	30.0-31.0	33.0	27.9-35.0	26.1-31.0	25.9-27.7	24.0-30.0	29.0-30.1	24.7-29.8	26.6-27.0	27.5-32.4

Notes: a, this study; b, McKay 1985, 1992; c, Panhwar et al. 2018; d, Xiao et al. 2016; e, Kaga et al. 2010; f, Gao et al. 2011; g, Golani et al. 2014; h, Kaga and Ho 2012.

KU051879, KU051886, and KU051887), *S. sihama* (KU051813, KU051819, KU051857, KU051803, and KU051881), *S. sinica* (KU052012, KU052017, KU052023, KU052025, and KU052029), and *S. suezensis* (FJ155362–FJ155364). *Sillaginodes punctata* was selected as the outgroup for genetic analyses based on a previous phylogenetic hypothesis of Xiao et al. (2016).

Results

Genetic analysis of the COI gene

Forty specimens of eight *Sillago* species were used in the genetic analysis. There were no indels/insertions, and 185 variable sites were observed. Pairwise genetic distances (K2P) were shown in Table 2. Genetic distances among species ranged from 0.084 to 0.224, the intraspecific distances ranged from 0.000 to 0.004. The NJ tree based on the COI gene sequences revealed that all previously recognized and the newly discovered *S. nigrofasciata* sp. nov. individuals formed monophyletic groups (Fig. 2). Furthermore, a strong genetic divergence was detected between *S. nigrofasciata* sp. nov. and its plesiomorphic sister species *S. sihama*.

Taxonomic account

Family Sillaginidae Richardson, 1846

Sillago Cuvier, 1817

Sillago nigrofasciata sp. nov.

<http://zoobank.org/43E56C5F-C745-469E-9EE8-A221AEA5BFD5>

Figures 1–4, Tables 1–3

Type material. Holotype. OUC_FEL178001, 151.2 mm SL, coastal area of Fuding, Fujian Province, China, collected by Yuan Li, January 2014.

Paratypes. OUC_FEL178002–178030, 29 individuals, 134.4–161.4 mm SL, collection data same as for holotype; ZJOU_FEBL021255–021283, 29 individuals, 127.8–155.6 mm SL, coastal area of Xiamen, Fujian Province, collected by Jia-Guang Xiao, November 2015; ZJOU_FEBL021284, 1 individuals, 167.6 mm SL, coastal area of Changhua, Taiwan, collected by Shih-Chieh Shen, July 2014; OUC_FEL178051–178068, 18 individuals, 147.8–161.4 mm SL, coastal area of Zhuhai, Guangdong Province, collected by Bin-Bin Shan, December 2014; OUC_FEL178069–178098, 30 individuals, 120.3–163.0 mm SL, coastal area of Fangchenggang, Guangxi Province, collected by Dong-Ping Ji, December 2014.

Etymology. The specific name *nigrofasciata* is a compound adjective derived from the Latin words referring to the wide mid-lateral black longitudinal band of this species, a diagnostic character of the species.

Table 2. Net genetic distances (K2P) within (on the diagonal) and between (below the diagonal) the eight *Sillago* species.

	<i>S. suezensis</i>	<i>S. parvisquamis</i>	<i>S. indica</i>	<i>S. sinica</i>	<i>S. sibama</i>	<i>S. shaoi</i>	<i>S. panhwari</i>	<i>S. nigrofasciata</i> sp. nov.
<i>S. suezensis</i>	0.000±0.000							
<i>S. parvisquamis</i>	0.193±0.021	0.000±0.000						
<i>S. indica</i>	0.084±0.012	0.202±0.022	0.002±0.001					
<i>S. sinica</i>	0.211±0.023	0.168±0.019	0.214±0.023	0.001±0.001				
<i>S. sibama</i>	0.177±0.020	0.210±0.022	0.172±0.020	0.211±0.023	0.001±0.001			
<i>S. shaoi</i>	0.213±0.023	0.152±0.017	0.224±0.023	0.124±0.015	0.196±0.021	0.003±0.002		
<i>S. panhwari</i>	0.192±0.020	0.214±0.022	0.206±0.022	0.217±0.022	0.210±0.022	0.222±0.023	0.004±0.002	
<i>S. nigrofasciata</i> sp. nov.	0.204±0.022	0.194±0.021	0.216±0.022	0.192±0.021	0.181±0.019	0.196±0.021	0.198±0.021	0.001±0.001

**Figure 2.** **A** *Sillago nigrofasciata* sp. nov., OUC_FEL178001, holotype, 151.2 mm SL, Fuding, China, **B** *Sillago sibama*, ZJOU_FEBL021131, 131.0 mm SL, Zhangzhou, China.

Diagnosis. Relatively large body and usually with a wide mid-lateral black stripe from opercular to caudal peduncle; dorsal-fin rays X–XII (mostly XI), I+20–22, soft anal fin rays 20–22; scales in lateral line 67–75, scales above lateral line 4–6; gill rakers 2–4+5–8; vertebra: abdominal 14 or 15 (mostly 14), modified 3–7 (mostly 4 or 5), caudal 13–18, and total 34 or 35 (mostly 34) (Table 3). Swim bladder with two posterior extensions, the origin of the duct-like process at the terminus of swim bladder and start at the joint of roots of two posterior extensions (Fig. 4).

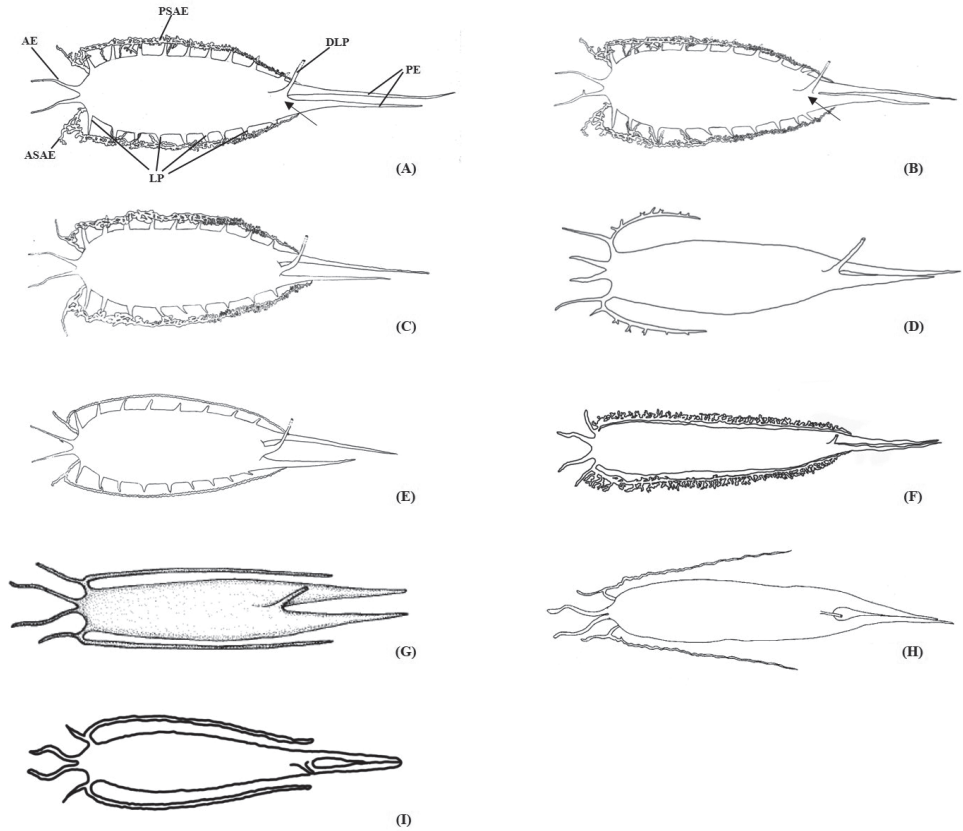


Figure 3. Swim bladders of nine *Sillago* species **A** *S. nigrofasciata* sp. nov. **B** *S. sibama* **C** *S. shaoi* **D** *S. sinica* **E** *S. indica* **F** *S. parvisquamis* **G** *S. intermedius* (McKay 1992) **H** *S. caudicula* (Kaga et al. 2010) **I** *S. suezensis* (sketch based on Golani et al. 2014). **AE**, anterior extension; **ASAE**, anterior sub-extension of anterolateral extension; **PSAE**, posterior sub-extension of anterolateral extension; **LP**, lateral processes; **DLP**, duct-like process; **PE**, posterior extension. Black arrows indicate differences between *S. nigrofasciata* sp. nov. and *S. sibama*.

Description. General body features are shown in Figure 3. Counts and measurements are given in Table 3. Body elongate, anterior slightly pyramidal, posterior cylindrical; anterodorsal profile smooth. Body depth 16.1% (13.4–17.4%) in SL. Head large, length 29.9% (25.1–30.8%) in SL. Snout long, 41.7% (39.6–52.7%) of HL. Eye moderate, its margin slightly covered with adipose eyelid, diameter 17.9% (16.5–24.9%) of HL. Interorbital region flat, interorbital width 23.5% (14.8–31.2%) of HL. Nostrils situated anterior to upper margin of eye; posterior margin of anterior nostril with single anteriorly directed flap; posterior nostril lacking flap. Mouth small, terminal, anterior tip of upper jaw situated at almost same position as tip of lower jaw. Upper jaw with small canines forming a wide tooth band becoming narrower posteriorly. Lower jaw with small canines, forming tooth band anteriorly, width same as upper jaw tooth band, tooth band gradually becoming narrower posteriorly, ending in one row.

Table 3. Morphometric measurements for type specimens of *Sillago nigrofasciata* sp. nov.

Morphometric measurements (mm) and counts	Holotype	Paratypes (n = 107)
Total weight (TW, g)	37.0	16.2–49.3
Total length (TL)	174.5	140.4–187.8
Standard length (SL)	151.2	121.0–163.0
Head length (HL)	45.3	33.7–46.5
Snout length (SL)	18.9	15.0–22.3
Eye diameter (ED)	8.1	6.8–11.6
Interorbital width (IW)	10.7	6.0–14.1
Postorbital length (PL)	17.0	12.9–19.1
Body depth (BD)	24.3	17.4–27.2
Body width (BW)	19.3	17.0–22.4
Length of caudal peduncle (LCP)	16.2	10.8–20.0
Depth of caudal peduncle (DCP)	9.9	7.1–11.1
Base of the 1 st dorsal fin	36.7	25.3–40.0
Base of the 2 nd dorsal fin	52.6	41.1–64.8
Base of the anal fin	54.2	42.8–58.2
Pectoral fin length	24.2	18.2–27.1
Ventral fin length	23.1	17.4–27.2
D	XI, I+21	X–XII, I+20–22
P	16	14–16
V	I+5	I+5
A	II+22	II+20–22
C	17	16–18
Gill rakers first arch	3+7	2–4+5–8
Vertebrae	34	34–35
Scales on lateral line	69	67–75
Scales above/below lateral line	6/11	4–6/9–12
As % of SL		
Body depth (BD)	16.1	13.4–17.4
Head length (HL)	29.9	25.1–30.8
Length of caudal peduncle (LCP)	10.7	7.9–13.4
As % of HL		
Eye diameter (ED)	17.9	16.5–24.9
Interorbital width (IW)	23.5	14.8–31.2
Snout length (SL)	41.7	39.6–52.7
Postorbital length (PL)	37.6	33.2–42.4
DCP/LCP	61.0	51.3–88.5

Palatine and tongue toothless. Vomer with three to four rows of canine teeth. Posterior margin of preopercle slightly serrated. Gill aperture large, lateral, extending to ventral side of head, stopping at middle bottom of opercle. Gill rakers on the first arch pointed but short. Caudal peduncle short, depth of caudal peduncle 61.0% (51.3–88.5%) of length of caudal peduncle.

Body covered with small or moderate sized ctenoid scales, and cheek scales cycloid, arranged in two or three rows. Lower part of pre-opercular-mandibular canal covered with cycloid scales. The base of pectoral fin and ventral fin lacking scales. Lateral line beginning above gill aperture and anterior portion of pectoral fin, extending along curve of dorsal edge to the end of body.

Two separated dorsal fins, first dorsal fin XI (X–XII), obviously higher than second, origin posterior to top of pectoral fin base, composed of spines, gradually shortening. Fin membrane with dense black spots. Base of second dorsal fin long, composed of a single spine and 21 (20–22) soft rays, originating mid-body, and not extending to

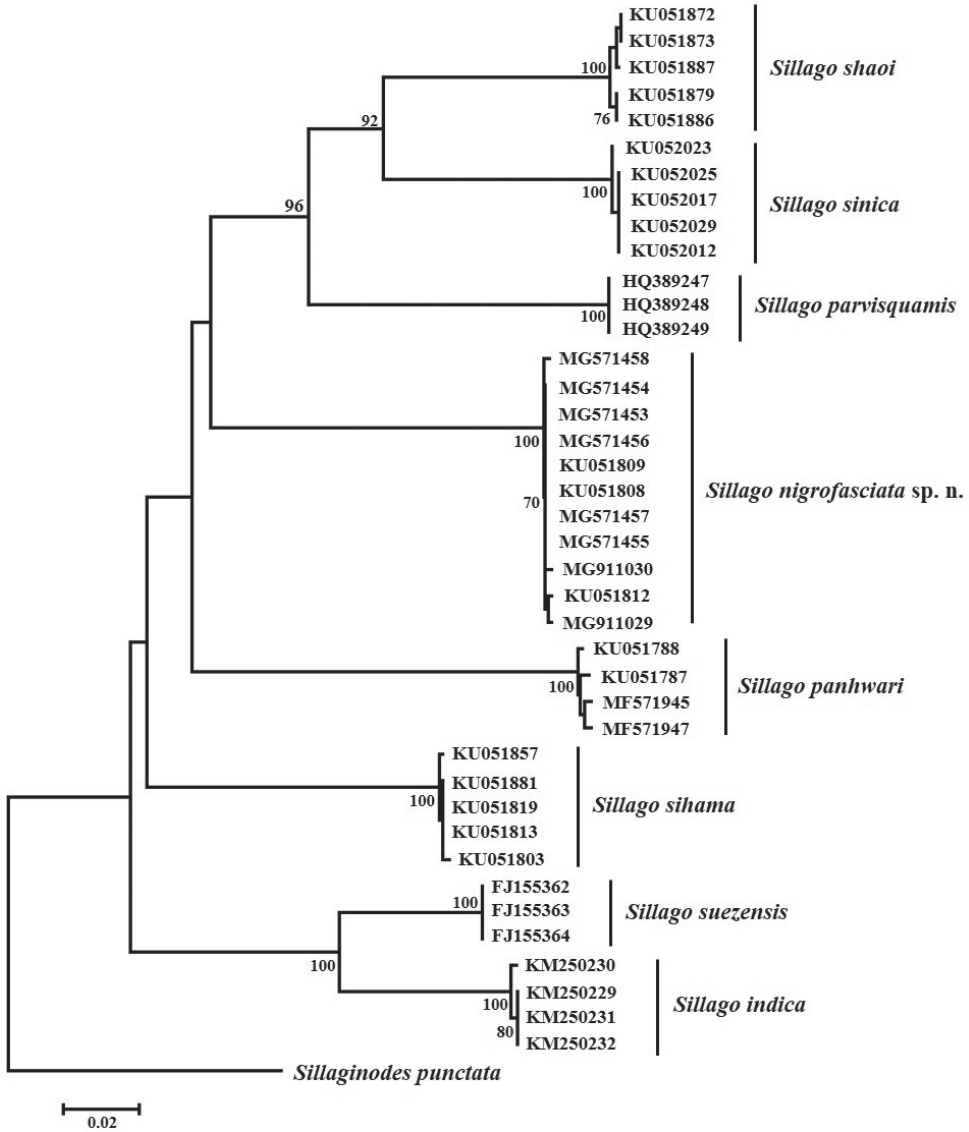


Figure 4. Neighbor-joining (NJ) tree for cytochrome oxidase subunit I (COI) gene sequences of eight species of *Sillago*. The NJ tree was constructed under the K2P model using *Sillaginodes punctata* as the outgroup. Bootstrap support values of > 70% from 1000 replicates are shown.

caudal fin origin when placed flat. Origins of anal fin slightly posterior to cloacal pore, with II+22 (20–22), not extending to caudal fin origin when placed flat. Pectoral fin 16 (14–16), slender. Two separated ventral fins broad, I+5, approximately triangular, and shorter than pectoral fin.

Color of fresh specimens. Upper surface of head dark brown and trunk bright brown, grading to silver on abdomen. Dorsal side of snout brownish gray. Cheek yel-

low, slightly silver posteriorly, with black dots amassed on the anterior inferior part of eyes. A wide faint stripe composed of tiny black dots on skin always present, from opercular to caudal peduncle. Dorsal fins yellowish hyaline, small dark dense spots on fin membrane. Pectoral, ventral, and anal fins yellowish hyaline with dark spots; caudal fin yellowish dusky with a black margin and grayish brown margin posteriorly, lobes usually broadly truncated posteriorly.

Swim bladder. Swim bladder large. Two anterior extensions diverging to terminate on either side of the basioccipital above the auditory capsule. Two posterior tapering extensions of the swim bladder penetrating into the caudal region, one usually longer than the other. Two anterolateral extensions originate anteriorly, each branch into anterior and posterior sub-extensions: the anterior one comprising a short, simple blind tubule and the posterior sub-extensions kinked, long and complex, extending along the abdominal wall ventral to the base of the posterior extensions, respectively, tangent but not interconnected. A single duct-like process originating from ventral surface of swim bladder extending to the urogenital opening and a sub-extension connecting with a sanguineous vesicle close to vertebra, of unknown function. Eight or nine lateral processes extending from entire lateral surface of main body of swim bladder, anterior three or four stout and horn-like, posterior five or six small and triangular in shape.

Habitat. Habitat is similar to *S. sihama* in nearshore areas and frequently entering estuaries for considerable periods, it is common along the beaches, sand bars, and mangrove creeks with sandy substrates. Depths ranging from 0 to 20 m, and frequently captured by trawling vessels.

Distribution. *Sillago nigrofasciata* sp. nov. was only found along the southern coast of China including the coastal waters of the South China Sea and the Taiwan Strait. Actually, its distribution range is similar to that of *S. sihama* in China (Fig. 1).

Comparisons. According to the subgeneric grading system in *Sillago* proposed by McKay (1985), we used the characters of swim bladder, especially, the number of the posterior extensions, to divide *Sillago* into several categories. This study confirmed the validity of a new species with two posterior extensions by comparison-elimination with other species in the same category. Among the ten known members of *Sillago* with two posterior extensions, *S. nigrofasciata* sp. nov. was easily distinguished from *S. intermedius* and *S. caudicula* by the body coloration (dusky black blotches were present on the body of *S. intermedius* and *S. caudicula*), from *S. parvisquamis* and *S. sinica* by the dusky spots on the second dorsal fin membranes (five or six rows in *S. parvisquamis* and three or four rows in *S. sinica*). Empirically, *S. nigrofasciata* sp. nov. could also be distinguished from *S. sihama*, *S. indica*, *S. panhwari*, and *S. suezensis* by the coloration of anal fin (the anal fin of *S. nigrofasciata* sp. nov. was usually yellowish with sparse black spots, the anal fin of *S. indica* was yellowish brown, but the anal fin of *S. sihama*, *S. panhwari*, and *S. suezensis* were hyaline; on the other hand, there were more black dots on skin and fins of *S. indica* than on *S. nigrofasciata* sp. nov. when fresh).

Moreover, by the primary diagnostic features (Table 1), *S. nigrofasciata* sp. nov. was easily distinguishable from other species by the following: *S. megacephalus* by having a smaller head (25.1–30.8% SL in *S. nigrofasciata* sp. nov. vs. 33.0% in *S. megacephalus*)

and less soft rays in anal fin (20–22 in *S. nigrofasciata* sp. nov. vs. 23 in *S. megecephalus*), from *S. parvisquamis* and *S. sinica* by having 34–35 total vertebrae (39–40 in *S. parvisquamis* and 37–39 in *S. sinica*), from *S. parvisquamis* and *S. sinica* can also be having 67–75 scales on lateral line (79–84 in *S. parvisquamis* and 75–79 in *S. sinica*), and from *S. caudicula* by gill rakers (4/11 in *S. caudicula*) and soft rays in anal fin (23–24 in *S. caudicula*).

As for the shape of swim bladder (Fig. 4), that of *S. suezensis* was always controversial (Kaga 2013). Based on its original description, the figures of the swim bladder (Golani et al. 2014: 418, fig. 4A–C) were stylized, lacking the details of those provided by McKay (1985, 1992) and Kaga and Ho (2012). However, the sequences of *S. suezensis* (Mediterranean population) and *S. sihama* (Hong Kong and southern Red Sea populations) showed a strong genetic divergence (Tikochinski et al. 2013). Here, those sequences were also cited to verify authenticity of *S. nigrofasciata* sp. nov. and dismissed *S. suezensis* (Fig. 2). The swim bladder of *S. panhwari* was described as having narrow anterior extensions joined at the origin, diverging to terminate on both sides of the basioccipital above the auditory capsule whereas the two posterior extensions penetrate into the caudal region, one usually longer than the other, and with a duct-like process (Panhwar et al. 2018). But based on the photo (Panhwar et al. 2018: fig. 3a), the swim bladder was flat and gasless, and the anterolateral extensions may be broken. Moreover, there was no description of the swim bladder of *S. megecephalus* by Lin (1933).

Sillago sihama was considered as having a wide Indo-Pacific distribution and consisting of more than one taxon. McKay (1992: 59, fig. 130) described two swim bladder patterns of *S. sihama* in the FAO Catalogue based on a Red Sea specimen and a Queensland specimen, with markedly different shapes and concomitant geographical divergence. The swim bladder of *S. nigrofasciata* sp. nov. was very similar to that of *S. sihama* and *S. shaoi*, but there were still some differences: the roots of two posterior extensions in *S. shaoi* were non-adjacent, the two posterior extensions were not well-knit in its natural state, and there was a lacuna between the two posterior extensions; the origin of the duct-like process was at the terminus of the swim bladder and between the roots of two posterior extensions. However, on the swim bladder of *S. nigrofasciata* sp. nov. and *S. sihama*, the roots of two posterior extensions were adjacent and two posterior extensions were in close proximity; and the difference between them was the origin of the duct-like process of *S. nigrofasciata* sp. nov. at the terminus of the swim bladder and starting at the joint of the roots of two posterior extensions, but the origin of the duct-like process of *S. sihama* was anterior to the terminus of the swim bladder and anterior to the joint of the roots of two posterior extensions. Moreover, the swim bladder of *S. indica* had the same framework as that of *S. nigrofasciata* sp. nov. excepting the thin simple anterolateral extensions (vs. *S. nigrofasciata* sp. nov., anterolateral extensions were twisted, long, and complicated). *Sillago nigrofasciata* sp. nov. could also be easily distinguished from *S. intermedius* and *S. caudicula* by those swim bladders with simple anterolateral extensions; *S. parvisquamis* stood out as having the strongest anterolateral extensions in comparison with the others (Fig. 4).

Discussion

Species-level taxonomy for Sillaginidae species was mainly based on the external morphological characteristics and the shape of the swim bladder (McKay 1992; Kaga 2013). Differences between sibling species are generally small and restricted to only a few characters, most of which may be also subject to intraspecific variation. Furthermore, within several newly discovered species, morphological characters did not provide clear taxonomic resolution (Golani et al. 2014). This study described a new species, *Sillago nigrofasciata* sp. nov. As the name implies, the new species is characterized by the black mid-lateral band below the lateral line. However, in fact, there are a few *Sillago* species that have a black band along the sides, including *S. indica* and *S. parvisquamis*. These morphological similarities make identification difficult, especially in the complex *S. sihama* cryptic species group. The new research suggested that the *S. sihama* complex exhibited the highest level of genetic diversity, indicating that a series of *S. sihama* lineages were genetically represented at species level (Cheng et al. 2020). This study presented a thorough molecular phylogeny analysis of all species of *Sillago*, which were monophyletic with 100% bootstrap values. Specimens of *S. nigrofasciata* sp. nov. were grouped together, and shared significant genetic distances with *S. sihama* and other species in the COI genetic analysis. Genetic distances between *S. nigrofasciata* sp. nov. and other species ranged from 0.181 to 0.216, and the interspecific genetic distances were much greater than the intraspecific distances (0.000–0.004), which indicated that the COI gene used as a barcode is an effective tool to identify *Sillago* species.

According to the conventional classification of *Sillago* species, this species could be confused with *S. sihama* based on the countable characters and the shape of the swim bladder. In fact, as one clade of *S. sihama* complex (*S. sihama* ⑧ in Cheng et al. 2020), *S. nigrofasciata* sp. nov. were morphologically similar to *S. sihama* with little difference in swim bladder (Fig. 4), but with significant genetic difference (18.1%, Table 2). *S. nigrofasciata* sp. nov. clearly differs from the true *S. sihama* by its distinct color pattern (with a wide faint stripe composed of tiny black dots on the skin from the opercular to caudal peduncle, and dark spots on the anal fin) and the swim bladder (the origin of the duct-like process of *S. nigrofasciata* sp. nov. is at the terminus of the swim bladder and starting at the joint of the roots of two posterior extensions). *Sillago sihama* lacks the mid-lateral stripe and dark spots on anal fin, and its origin of the duct-like process is anterior to the terminus of the swim bladder and anterior to the joint of the roots of both posterior extensions.

At present, the distribution of *Sillago nigrofasciata* sp. nov. overlaps with that of *S. sihama* in China: the coastal waters of the South China Sea and the Taiwan Strait. Actually, *S. sihama* across its Indo-West Pacific range exhibits by far the highest levels of genetic diversity. A few new species have been described in this range across the IWP: *S. caudicula* (from Oman and Madagascar), *S. sinica* (from China), *S. suezensis* (from the northern Red Sea and Mediterranean), *S. shaoi* (from Taiwan Strait), and *S. panhwari* (from the northern Arabian Sea), and they have been always regarded as junior synonyms of *S. sihama* (Kaga et al. 2010; Kaga and Heemstra 2013; Gao et al. 2011;

Golani et al. 2014; Xiao et al. 2016; Panhwar et al. 2018). However, our DNA barcoding results indicate that there are more genetic lineages across the *S. sihama* range that probably represent species-level taxa. These findings indicate a thorough taxonomic review of *S. sihama* (and its junior synonyms) is necessary (Cheng et al. 2020).

Acknowledgments

We deeply thank Shih-Chieh Shen, Jin-Chywan Gwo, Yuan Li, Bin-Bin Shan, Xiong-Bo He, Jian-Wei Zou, Dong-Ping Ji and Qiang Xu for sample collection. We are also grateful to Ms. Nan Zhang for her valuable suggestions for the manuscript. This work is supported by National Natural Science Foundation of China (Nos. 41776171, 41976083). All authors declare that they have no conflict of interest.

References

- Bae S, Kwun H, Kim J, Kweon SM, Kang CB (2013) New record of *Sillago sinica* (Pisces: Sillaginidae) in Korean waters, and re-identification of *Sillago parvisquamis* previously reported from Korea as *S. sinica*. *Animal Systematics, Evolution and Diversity* 29: 288–293. <https://doi.org/10.5635/ASED.2013.29.4.288>
- Burns JM, Janzen DH, Hajibabaei M, Hallwachs W, Hebert PD (2008) DNA barcodes and cryptic species of skipper butterflies in the genus *Perichares* in Area de Conservacion Guanacaste, Costa Rica. *Proceedings of the National Academy of Sciences of the United States of America* 105: 6350–6355. <https://doi.org/10.1073/pnas.0712181105>
- Cheng J, Xiao JG, Song N, Saha S, Qin JG, Nomura H, Panhwar SK, Farooq N, Shao KT, Gao TX (2020) Molecular phylogeny reveals cryptic diversity and swim bladder evolution of Sillaginidae fishes (Perciformes) across the Indo-West Pacific Ocean. *Diversity and Distributions* 27: 82–94. <https://doi.org/10.1111/ddi.13171>
- Cheng QT, Zheng BS (1987) *Systematic Synopsis of Fishes in China*. Science, Beijing, 303–304.
- Gao TX, Ji DP, Xiao YS, Xue TQ, Yanagimoto T, Setoguma T (2011) Description and DNA barcoding of a new *Sillago* species, *Sillago sinica* (Perciformes: Sillaginidae), from coastal waters of China. *Zoological Studies* 50: 254–263. <https://doi.org/10.1080/03014223.2010.541468>
- Golani D, Fricke R, Tikochinski Y (2014) *Sillago suzezensis*, a new whiting from the northern Red Sea, and status of *Sillago erythraea* Cuvier (Teleostei: Sillaginidae). *Journal of Natural History* 48: 413–428. <https://doi.org/10.1080/00222933.2013.800609>
- Hebert PDN, Ratnasingham S, deWaard JR (2003a) Barcoding animal life: cytochrome c oxidase subunit I divergences among closely related species. *Proceedings of the Royal Society B: Biological Sciences* 270: 96–99. <https://doi.org/10.1098/rsbl.2003.0025>
- Hebert PDN, Cywinska A, Ball SL, Dewaard JR (2003b) Biological identifications through DNA barcodes. *Proceedings of the Royal Society B: Biological Sciences* 270: 313–321. <https://doi.org/10.1098/rspb.2002.2218>

- Kaga T (2013) Phylogenetic systematics of the family Sillaginidae (Percomorpha: order Perciformes). *Zootaxa* 3642: 1–105. <https://doi.org/10.11646/zootaxa.3642.1.1>
- Kaga T, Heemstra E (2013) First record of a rare sand whiting, *Sillago caudicula* (Perciformes: Sillaginidae), from Madagascar. *Marine Biology Research* 9: 332–336. <https://doi.org/10.1080/17451000.2012.742547>
- Kaga T, Ho HC (2012) Redescription of *Sillago* (*Parasillago*) *indica* McKay, Dutt & Sujatha, 1985 (Perciformes: Sillaginidae), with a reassignment to the subgenus *Sillago*. *Zootaxa* 3513: 61–67. <https://doi.org/10.11646/zootaxa.3513.1.3>
- Kaga T, Imamura H, Nakaya K (2010) A new sand whiting, *Sillago* (*Sillago*) *caudicula*, from Oman, the Indian Ocean (Perciformes: Sillaginidae). *Ichthyological Research* 57: 367–372. <https://doi.org/10.1007/s10228-010-0169-z>
- Kwon H, Kim J (2010) A taxonomic review of four Sillaginid fishes (Perciformes) from the adjacent waters of Korea. *Korean Journal of Ichthyology* 22: 105–114.
- Lin S (1933) A new genus and three new species of marine fish from Hainan Island. *Lingnan Science Journal* 12: 93–96.
- Locke SA, Daniel McLaughlin J, Marcogliese DJ (2010) DNA barcodes show cryptic diversity and a potential physiological basis for host specificity among Diplostomoidea (Platyhelminthes: Digenea) parasitizing freshwater fishes in the St. Lawrence River, Canada. *Molecular Ecology* 19: 2813–2827. <https://doi.org/10.1111/j.1365-294X.2010.04713.x>
- McKay RJ (1985) A revision of the fishes of the family Sillaginidae. *Memoirs of the Queensland Museum* 23: 1–73.
- McKay RJ (1992) An annotated and illustrated catalogue of the *Sillago*, smelt or Indo-Pacific whiting species known to date. In: McKay RJ (Ed.) *FAO species catalogue* (Vol. 14). Sillaginid fishes of the world (family Sillaginidae). Food and Agriculture Organisation of the United Nations, Rome, 87 pp.
- Nelson JS, Grande T, Wilson MVH (2016) *Fishes of the world* (5th edn). Wiley, New York, 707 pp. <https://doi.org/10.1002/9781119174844>
- Panhwar SK, Farooq N, Qamar N, Shaikh W, Mairaj M (2018) A new *Sillago* species (family Sillaginidae) with descriptions of six sillaginids from the northern Arabian Sea. *Marine Biodiversity* 48: 1–7. <https://doi.org/10.1007/s12526-017-0710-7>
- Sano M, Mochizuki K (1984) A revision of the Japanese Sillaginid fishes. *Japanese Journal of Ichthyology* 31: 136–149.
- Shao KT, Shen SC, Chen LW (1986) A newly recorded sandborer, *Sillago* (*Sillaginopodys*) *chondropus* Bleeker, with a synopsis of the fishes of family Sillaginidae of Taiwan. *Bulletin of the Institute of Zoology Academia Sinica* 252: 141–150.
- Tamura K, Peterson D, Peterson N, Stecher G, Nei M, Kumar S (2011) MEGA 5: molecular evolutionary genetics analysis using maximum likelihood, evolutionary distance, and maximum parsimony methods. *Molecular Biology and Evolution* 28: 2731–2739. <https://doi.org/10.1093/molbev/msr121>
- Tikochinski Y, Shainin I, Hyams Y, Motro U, Golani D (2013) Genetic evidence for an undescribed species previously considered as *Sillago sibama* from the northern Red Sea. *Marine Biology Research* 9: 309–315. <https://doi.org/10.1080/17451000.2012.731692>

- Ward RD, Zemlak TS, Innes BH, Last P, Hebert PDN (2005) DNA barcoding Australia's fish species. *Philosophical Transactions of the Royal Society of London. Series B, Biological Sciences* 360: 1847–1857. <https://doi.org/10.1098/rstb.2005.1716>
- Xiao JG, Song N, Han ZQ, Gao TX (2016) Description and DNA barcoding of a new *Sillago* species, *Sillago shaoi* (Perciformes: Sillaginidae), in the Taiwan Strait. *Zoological Studies* 55: 1–47. <https://doi.org/10.6620/ZS.2016.55-47>

New records of Demospongiae (Porifera) from Reserva Marina El Pelado (Santa Elena, Ecuador), with description of *Tedania* (*Tedania*) *ecuadoriensis* sp. nov.

Karla B. Jaramillo^{1,2}, Báslavi Córdor-Luján³, Belinda Longakit², Jenny Rodriguez¹, Olivier P. Thomas⁴, Grace McCormack², Eduardo Hajdu⁵

1 ESPOL Polytechnic University, Escuela Superior Politécnica del Litoral, ESPOL. Centro Nacional de Acuicultura e Investigaciones Marinas, CENAIM. Campus Gustavo Galindo Km. 30.5 Vía Perimetral, P.O. Box 09-01-5863, Guayaquil, Ecuador **2** Zoology, School of Natural Sciences and Ryan Institute, National University of Ireland Galway, University Road, H91 TK33 Galway, Ireland **3** Universidad Científica del Sur, Facultad de Ciencias Veterinarias y Biológicas, Carrera de Biología Marina, Antigua Panamericana Sur Km. 19, Villa El Salvador, Lima, Perú **4** Marine Biodiscovery, School of Chemistry and Ryan Institute, National University of Ireland Galway, University Road, H91 TK33 Galway, Ireland **5** Museu Nacional, Universidade Federal do Rio de Janeiro, Depto. Invertebrados, Quinta da Boa Vista, s/n, 20940-040, Rio de Janeiro, RJ, Brazil

Corresponding author: Karla B. Jaramillo (kbjarami@espol.edu.ec)

Academic editor: Ya. Mutafchiev | Received 20 May 2020 | Accepted 23 October 2020 | Published 19 January 2021

<http://zoobank.org/2D67157E-B9B3-4601-8212-3633DD3EBD87>

Citation: Jaramillo KB, Córdor-Luján B, Longakit B, Rodriguez J, Thomas OP, McCormack G, Hajdu E (2021) New records of Demospongiae (Porifera) from Reserva Marina El Pelado (Santa Elena, Ecuador), with description of *Tedania* (*Tedania*) *ecuadoriensis* sp. nov.. ZooKeys 1011: 101–120. <https://doi.org/10.3897/zookeys.1011.54485>

Abstract

The first taxonomic descriptions of the sponge diversity at El Pelado Marine Protected Area in the province of Santa Elena, Ecuador is reported. *Tedania* (*Tedania*) *ecuadoriensis* Jaramillo & Hajdu, **sp. nov.** is described from its shallow waters. In addition, *Callyspongia* (*Callyspongia*) aff. *californica* (*sensu* Cruz-Barraza and Carballo 2008; *non sensu* Dickinson 1945) and *Cliona* aff. *euryphyllae* are reported for the first time. The former species is likely distributed over 4,000 km along the Tropical Eastern Pacific, whereas the latter might be an example of a trans-isthmian lineage. An amended diagnosis for *Callyspongia* (*Callyspongia*) and an updated identification key for the subgenera of *Callyspongia* are provided.

Keywords

Callyspongia, *Cliona*, sponge taxonomy, Tropical Eastern Pacific

Introduction

Sponges represent a key component of marine ecosystems and exhibit high diversity and abundance in some oceans, including tropical, temperate and polar regions (Bell and Barnes 2003; Bell and Smith 2004; Carballo et al. 2008; Hajdu et al. 2013; Hajdu et al. 2015; Pacheco et al. 2018). Due to the broad substrate cover and filtration capacity of sponges, marine ecosystems in general will likely be affected by changes in the geographic distribution of these organisms (Bell and Smith 2004; Bell 2007; Carballo et al. 2008; Cruz-Barraza and Carballo 2008). These reasons, together with sponges' known biomedical potential, have attracted the interest of researchers to explore the distribution and diversity of sponges in maritime ecoregions around the planet.

Despite published reports on sponge distribution in the Pacific Ocean, knowledge gaps still exist in the eastern Pacific, and especially along the coast of Ecuador, where descriptive studies have rarely been conducted (Miloslavich et al. 2011). A recent increase in taxonomic effort in this large area started in Chile (Hajdu et al. 2006; Azevedo et al. 2009; Willenz et al. 2009; Hajdu et al. 2013; Fernandez et al. 2016; Costa et al. 2020), and more recently expanded to the Peruvian coast (Aguirre et al. 2011; Azevedo et al. 2015; Hajdu et al. 2015; Córdor-Luján et al. 2019; Recinos et al. 2020). This collective effort has unveiled a high diversity and abundance of sponges in shallow south-eastern Pacific waters. Since 2003 in Chile, and 2007 in Peru, nearly 3,000 specimens have been collected, with new species reported. Taxonomic identifications of this large collection are still in progress and will certainly lead to many more discoveries.

In this regard, and despite its shorter coastline when compared to Chile and Peru, mainland Ecuador is likely to house a significant diversity of marine sponges. In part, this will be a consequence of being situated in a convergence zone of two different oceanic currents, the northern warm Panama or El Niño Current, and the southern cold Humboldt or Peru Current (Chavez and Brusca 1991; Fiedler et al. 1992; Glynn 2003). In addition, the presence of varied marine coastal ecosystems, such as mangroves, bays, estuaries, and rocky coasts in this area, also supports this hypothesis. So far, knowledge of the sponge biodiversity of Ecuador is entirely restricted to descriptions of species from the Galapagos Islands (Desqueyroux-Faúndez and van Soest 1997; Bustamante et al. 2002). According to the World Porifera Database (WPD), 87 species have been recorded from these islands (van Soest et al. 2020), both from the shallow waters (Topsent 1895; Wilson 1904; Lendenfeld 1910; de Laubenfels 1939; Lee 1987; Hajdu and Desqueyroux-Faúndez 1994; Desqueyroux-Faúndez and van Soest 1996, 1997; Sarà et al. 2000) and deeper waters (Schuster et al. 2018). Surprisingly, no taxonomic study focused on the sponge diversity of coastal mainland Ecuador, a gap due to a historical lack of baseline scientific initiatives and sponge taxonomists in this region. In order to start reverting this scenario, a national project was funded by the Ecuadorian government aiming at the description of the marine invertebrate biodiversity, and their associated chemical and microbial diversity, in a small marine protected area of the peninsula of Santa Elena, named El Pelado Marine Reserve (REMAPE). The first results of this biodiversity assessment

have recently been published with a focus on zoantharians (Jaramillo et al. 2018), and sponges come next, also selected for their known content of metabolites with potential pharmacological use (Carroll et al. 2019). The goal of the present study was therefore to describe the most abundant species of sponges occurring in the El Pelado MPA. Herein, we present three new records of Demospongiae for this area, including one new species.

Materials and methods

Biological material

Specimens were collected using SCUBA diving in different sites of the El Pelado Marine Reserve (REMAPE – Santa Elena, Ecuador, -80.8221, -1.9228) and photographed in situ (Fig. 1). Samples were preserved in 95% EtOH and a voucher sample of each species is deposited at the scientific reference collection of Centro Nacional de Acuicultura e Investigaciones Marinas (**CENAIM**), with some fragments shared with the sponge collections at Museu Nacional do Rio de Janeiro (**MNRJ**) /Universidade Federal do Rio de Janeiro (**UFRJ**, Rio de Janeiro, Brazil).

Morphological examination

Species identification and morphological descriptions were achieved from ethanol samples and in situ observations. Descriptions were based on dissociated spicules and thick anatomical sections obtained for each specimen following standard protocols outlined in

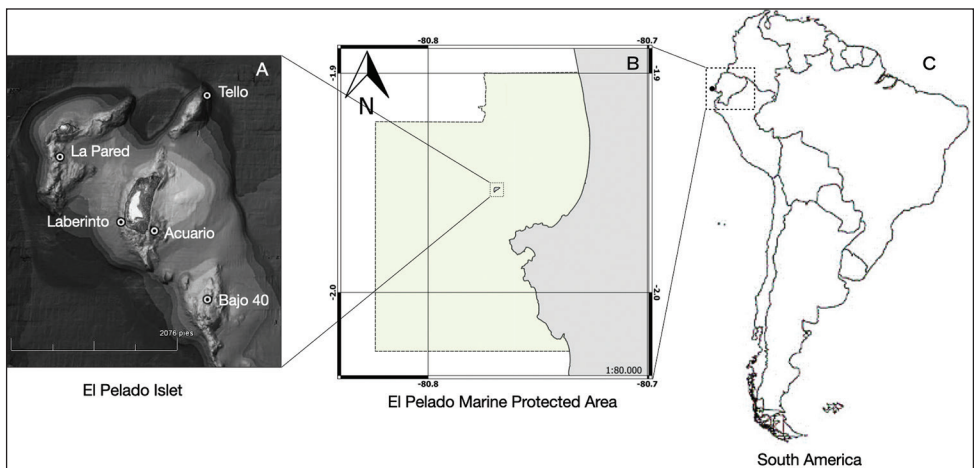


Figure 1. Map of the Marine Protected Area El Pelado **A** The Pelado islet and its submarine platform with five sampling locations of the sponges **B** map of the whole Marine Protected Area El Pelado at the Ecuadorian coast **C** map of South America highlighting Ecuador (map created using QGIS software Version 3.2).

Hajdu et al. (2011). Dissociated spicules and thick sections slides were examined under an EVOS Digital Colour Fluorescence Microscope. For each spicule category, at least 20 measurements were made. Metrical data are given in micrometres, unless otherwise indicated, as the range, with the mean and the number of measurements taken (n) in parentheses. The Scanning Electron Microscopes (SEMs) used to obtain the spicule electron micrographs were a JEOL 6390LV at Museu Nacional (UFRJ), and a Hitachi S-4700 SEM at National University of Ireland, Galway. The classification adopted here is that of the ‘Systema Porifera’ (Hooper and van Soest 2002), as modified by Morrow and Cárdenas (2015), and implemented in the World Porifera Database (van Soest et al. 2020).

Results

Systematics

Phylum Porifera Grant, 1835

Class Demospongiae Sollas, 1885

Subclass Heteroscleromorpha Cárdenas, Pérez & Boury-Esnault, 2012

Order Poecilosclerida Topsent, 1928

Family Tedaniidae Ridley & Dendy, 1886

Genus *Tedania* Gray, 1867

Subgenus *Tedania* Gray, 1867 *sensu* Aguilar-Camacho et al. (2018)

***Tedania (Tedania) ecuadoriensis* Jaramillo & Hajdu, sp. nov.**

<http://zoobank.org/05C00AF3-E75C-402E-AAA1-2D511771ADEF>

Figure 2A–I

Diagnosis. *Tedania (Tedania)* with rather small ectosomal tylotes (139–185 μm), and choanosomal styles (127–183 μm), as well as possessing two size categories of onychaetes (71–133 and 29–69 μm).

Etymology. Named after the country where its type locality is situated.

Type material. *Holotype*: CENAIM 150813EP01-05 with fragment as MNRJ 19918, El Pelado Islet (‘La Pared’, -1.932847; -80.792453), REMAPE, Santa Elena, Ecuador, 13 m deep, collected by O. Thomas, 13 Aug. 2015. *Paratype*: CENAIM 150825EP04-05 with fragment as MNRJ 19923, El Pelado Islet (‘Laberinto’, -1.9355; -80.7896), REMAPE, Santa Elena, Ecuador, 5 m deep, collected by K. Jaramillo, 25 Aug. 2015.

Habit (Fig. 2A). Thickly encrusting to massive (thickness: 0.3 cm). The holotype is fragmented, and the largest piece measures 0.8 \times 0.4 cm. Oscula located at the top of short elevations. Consistency soft and compressible. Texture smooth. Colour in life is orange, and in ethanol it turns to violet with some red spots on the surface.

Skeleton (Fig. 2B). Ectosomal architecture with brushes of tylotes, some of which pierce the surface, not easily detachable from the choanosome. Choanosomal architecture a dense, confused reticulation of styles and scattered onychaetes.

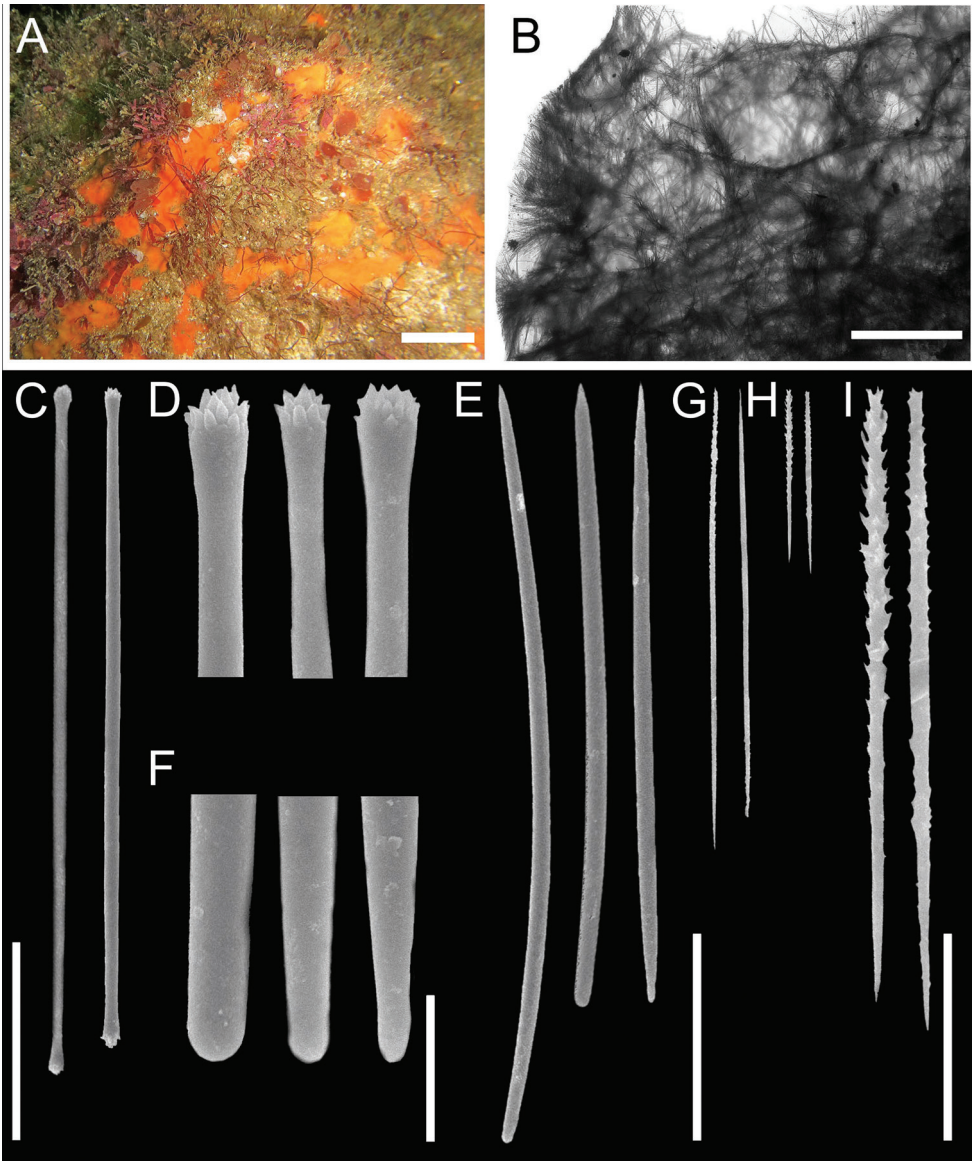


Figure 2. *Tedania (Tedania) ecuadoriensis* sp. nov. **A** holotype in situ (CENAIM 150813EP01-05) **B** transverse section of ectosomal and choanosomal skeletal architecture **C** ectosomal tylores **D** detail of terminally microspined terminations of ectosomal tylores **E** choanosomal styles **F** detail of the bases of choanosomal styles **G** large onychaetes **H–I** small onychaetes. Scale-bars: 2 cm (**A**); 500 µm (**B**); 50 µm (**C, E, G–H**); 10 µm (**D, F, I**).

Spicules. Megascleres (Fig. 2C–F, Table 1): Ectosomal tylores, 139–85 (168; n = 30); choanosomal styles, 127–183 (155; n = 35). Microscleres (Fig. 2G–I): larger onychaetes, 71–133 (92; n = 41); smaller onychaetes, 29–69 (41; n = 25).

Table 1. Morphology of spicules, locality and depth, for East Pacific *Tedania* spp. seemingly closer to *T. (T.) ecuadoriensis* sp. nov., and *T. ignis*. Spicule morphometrics are in micrometres as range with the mean in parentheses, n.r. is not reported.

Species	Tylotes	Styles	Onychaetes	Locality / depth
<i>T. ecuadoriensis</i> sp. nov.	139–185 (168) × 1.9–3.6 (2.4)	127–183 (155) × 2.1–5.5 (3.8)	I, 71–133 (92) II, 29–69 (41)	El Pelado Islet / 5–13 m
<i>T. fulvum</i> (Aguilar-Camacho et al., 2018) (orig. descr.)	130–150 (142.5) × 2.5–5 (2.7)	135–185 (171.5) × 2.5–5 (3.4)	30–120 (60.5) × 0.5–1	Mexican Pacific / 8 m
<i>T. galapagensis</i> (Desqueyroux-Faúndez & van Soest, 1996) (orig. descr.)	179–234 (198) × 3	192–246 (226) × 6	I, 173–205 (188) × 2 II, 61–93 (78) × 0.5–1	Galapagos / 78 m
<i>T. obscurata</i> (de Laubenfels, 1930) (orig. descr.)	200–300 × 6–12	present, but rare	I, n.r. II, 80 × 2	California / intertidal
<i>T. tepitootehenuaensis</i> (Desqueyroux-Faúndez, 1990) (orig. descr.)	192–250 (227) × 3–7 (5)	204–272 (241) × 4–9 (7)	I, 160–285 (188) × 2–3 (2) II, 48–76 (59) × 0.5–0.9 (0.6)	Easter Isl. / 3 m
<i>T. topsenti</i> (de Laubenfels, 1930) (orig. descr.)	200 × 8	250 × 11	I (?), 180 × 2 reported as “? raphides”, and suggested must be young megascleres instead	California / intertidal
<i>T. toxicalis</i> (de Laubenfels, 1930) (orig. descr.)	200 × 8–14	100–200 × 2–7	I, 150 II, “not observed”	California / intertidal
<i>T. tropicalis</i> (Aguilar-Camacho et al., 2018) (orig. descr.)	150–210 × 2.5–5	150–215 × 2.5–7.5	I, 90–180 × 0.5–1.8	Mexican Pacific / 1–5 m
<i>T. ignis</i> (Duchassaing & Michelotti, 1864) sensu Zea (1987)	181–242 (220.4) × 3–6 (4.3)	228–313 (259.8) × 3–8 (4.3)	I, 142–280 (230.7) × 1–3 (1.9) II, 52–138 (83.3) × 0.5–2 (1.2)	Tropical W Atlantic / 0–3 m

Ecology and distribution. The species was found between 5–13 m depth, close to red algae, and slightly covered with sediment. No dermatitis reaction was observed after contact with bare skin.

Remarks. Six species of *Tedania* were described from the Tropical Eastern Pacific (de Laubenfels 1930; Desqueyroux-Faúndez 1990; Desqueyroux-Faúndez and van Soest 1996; Desqueyroux-Faúndez and van Soest 1997; Aguilar-Camacho et al. 2018), namely *T. fulvum* Aguilar-Camacho, Carballo & Cruz-Barraza, 2018; *T. galapagensis* Desqueyroux-Faúndez & van Soest, 1996; *T. obscurata* (de Laubenfels, 1930); *T. tepitootehenuaensis* Desqueyroux-Faúndez, 1990; *T. topsenti* de Laubenfels, 1930; *T. toxicalis* de Laubenfels, 1930 and *T. tropicalis* Aguilar-Camacho, Carballo & Cruz-Barraza, 2018. *Tedania galapagensis* was an obvious first hypothesis for the identification of the El Pelado *Tedania*, for its occurrence in the relatively nearby Galapagos Archipelago, but we found it to be distinct from the new species by its tylotes, styles and onychaetes, with much larger dimensions than observed in our new species. When variation of this sort occurs intraspecifically, it is the continental specimen to harbour the largest spicules, as a consequence of likely increased levels of dissolved silica in comparison to oceanic locations (for a discussion in the context of the Caribbean, see Zea (1987)). Furthermore, *T. galapagensis* was reported from deeper waters (78 m) than those where *T. ecuadoriensis* sp. nov. was found (5–13 m). The species appearing closest to our material, as far as spicule micrometrics go, is the Mexican *T. fulvum*, that also

has a set of relatively small spicules. The onychaetes, reported in a single, variable size-category, match nearly perfectly the full range observed in both categories combined of the new species. On the other hand, the coelosphaerid/hymedesmiid-kind of ectosomal tylote, with smooth, pronounced, elliptical heads, finds no match in the new species, and is seen here as decisive evidence of the non-conspecificity of both species.

Tedania ecuadoriensis sp. nov. with its short tylotes (168 μm , mean length) and styles (155 μm , mean length) is distinct from all known (sub)Tropical Eastern Pacific *Tedania* spp. which have these around 200 μm or bigger. *Tedania ignis*, a Tropical Western Atlantic species with considerable overall similarity to the new species proposed, also bears much larger megascleres and microscleres, which contradicts any hypothesis of possible conspecificity.

Order Clionaida Morrow & Cárdenas, 2015

Family Clionaidae d'Orbigny, 1851

Genus *Cliona* Grant, 1826

Cliona aff. *euryphylle* Topsent, 1888

Figure 3A–E

Material examined. CENAIM: 160510EP07-01, El Pelado Islet ('Bajo 40', -1.938217; -80.786669), REMAPE, Santa Elena, Ecuador, 12 m deep, collected by K. Jaramillo, 10 May 2016.

Habit (Fig. 3A, B). Encrusting alpha stage over 15 \times 15 cm in area. Extended papillae with slightly elevated (up to 5 mm) oscula, up to 2 mm in diameter. Sponges form small patches, with a firm texture, even after removal from substrate. The colour in life is orange, turning to pale yellow in ethanol.

Skeleton. Typical *Cliona* arrangement, with an ectosomal palisade of tylostyles, and the same spicules in a confused arrangement in the choanosome. Small spirasters are scarce in the papillae, but they occur abundantly dispersed in the choanosome.

Spicules. Megascleres (Fig. 3C–E, Table 2). Tylostyles, 221–336 (267; $n = 34$) \times 5–11 (7, $n = 30$), with pronounced rounded to oval heads. Microscleres (Fig. 3F). Small and robust spirasters 8–35 (19; $n = 32$) \times 3–8 (5; $n = 27$), with several large conical spines spiralling around the shaft, in helical and S-shaped forms; occasionally approaching amphiasters morphology.

Ecology and distribution. Occurs from 5 to 10 m depth, over rocks, excavating shells, near red and brown algae, and slightly surrounded with sediment. *Cliona euryphylle* Topsent, 1888 was originally described from the Atlantic Ocean (Gulf of Mexico) by Topsent (1888), followed by a series of records from the Pacific: de Laubenfels (1954) in the Central Pacific, Bergquist (1968) in New Zealand; Carballo et al. (2004); Carballo et al. (2008); Vega (2012) in the Mexican Pacific; and Pacheco et al. (2018) in the Costa Rican Pacific.

Remarks. Our preliminary results are inconclusive with regard to the identification of this Ecuadorian *Cliona* material, as no DNA sequence has been published for *C. eu-*

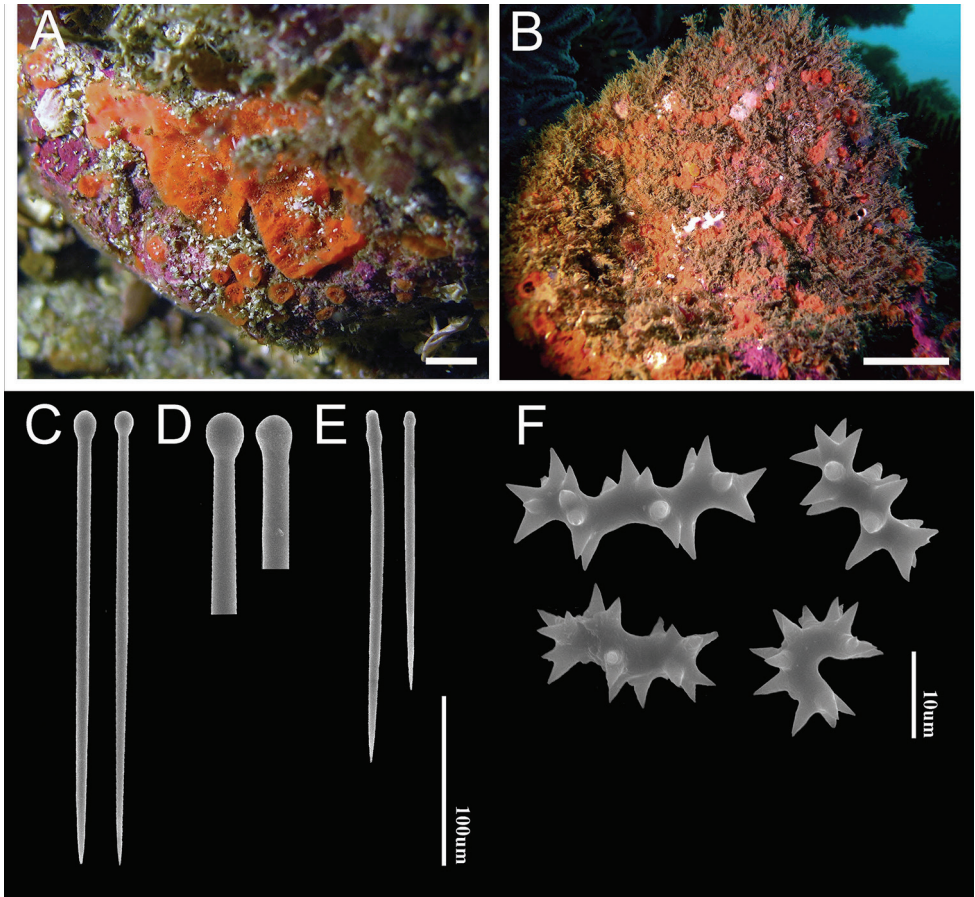


Figure 3. *Cliona* aff. *euryphylla* Topsent, 1888 **A, B** specimen alive in situ (CENAIM 160510EP07-01) collected at El Pelado Marine Reserve **C** large tylostyles **D** heads of tylostyles **E** small tylostyles **F** different sizes of spirasters with large spines. Scale-bars: 1 cm (**A**); 5 cm (**B**); 100 μ m (**C–E**); 10 μ m (**F**).

ryphylla, let alone for an Atlantic record of the species. It is also possible that the Ecuadorian species might belong to a distinct species, rather than suppose its crossing of the isthmus through the Panama Canal, as explicitly suggested by Pacheco et al. (2018). Previous records of *C. euryphylla* need to be revised in an integrative approach with more extensive sampling and molecular analyses with higher resolution capabilities.

Meanwhile, we can highlight what these populations share and what distinguishes them from one another in morphological terms. The first, but unlikely, biogeographical record of *C. euryphylla* is that by de Laubenfels (1954) from Micronesia, perhaps misled by his mistaken interpretation of Topsent's type locality, assumed to be in the Eastern Pacific (Topsent 1888). Even though the proposed transpacific track is unlikely, de Laubenfels' brief description hampers further discussion without re-examining this material. Likely misguided by de Laubenfels' pioneering transpacific range extension, Bergquist (1968) registered the species from New Zealand shallow waters. This is another

Table 2. *Cliona euryphyllae* Topsent 1888 and *Cliona* aff. *euryphyllae*: Morphology of spicules, locality and depth for specimens studied here, and from the literature. Species deemed more closely related are included for comparison. Spicule morphometrics are in micrometres as range with the mean in parentheses, n.r. is not reported.

Species	Tyloles	Spirasters	Locality / depth
<i>C. aff. euryphyllae</i>	I, 221–336 (267) × 5–11 (7); II, 115–264 (211) × 5–9 (7)	8–35 (19) × 3–8 (5)	El Pelado Islet / 5–10 m
<i>C. euryphyllae</i> (Topsent, 1888) (orig. descr.)	300 × 5	35 × 5	Southern Gulf of Mexico
sensu de Laubenfels (1954)	300 × 7	n.r. × 4–8	Micronesia / 5 m
sensu Bergquist (1968)	290–392 (344) × 9.5–17.5 (12.5)	7–28 (24) × 0.9–9.2 (6.3)	New Zealand / 25 m
sensu Carballo et al. (2004)	180–367.5 (277) × 2.5–10 (5.5)	10–30 (18.1)	Mexican Pacific / 4–20 m
sensu Vega (2012)	111–365 × 1.3–11	30–6	Mexican Pacific / 0–3 m
sensu Pacheco et al. (2018)	120–300 (201) × 5–8 (6.7)	9–24 (18) × 2–7 (4.7)	Costa Rica Pacific / 4–20 m
<i>C. aethiopicus</i> (Burton, 1932) (orig. descr.)	260 × 7	28	Gulf of Guinea / 18–30 m
<i>C. burtoni</i> (Topsent, 1932) (orig. descr.)	225–330 (175) × 7–12 (2.5)	15–28 (40) × 5–6 (1.5)	Mediterranean / N/A
sensu Bertolino et al. (2013)	132–287 (225) × 5–7.5 (6)	10–45 (26.5) × 1.3–17.5 (10)	Mediterranean / 30 m
<i>C. caledoniae</i> (van Soest & Beglinger, 2009) (orig. descr.)	246–426 (360.9) × 8–12 (9.8)	19–31 (24.3) × 5–9 (6.8)	NE Atlantic / 82–131 m
<i>C. dioryssa</i> (de Laubenfels, 1950); sensu Rützler (1974)	107–392 (244.4) × 3.7–7.4 (5.4)	I, 11–42 (27.4) × 1.4–4.8 (3.2) (shaft); II, 19–43 (33.9) × 0.6–2.2 (1.5) (shaft)	Bermuda / 0–12 m
sensu Muricy and Hajdu (2006)	200–440	I, 25–40; II, 10–20	SE and NE Brazil / 5–25 m

unlikely record simply from its distance from previous localities. Furthermore, Bergquist offered some observations that might be interpreted to be suggestive of non-conspicuity, such as the larger dimensions of megascleres (up to 392 µm), and the abundance of microscleres. The tylostyles in the specimens described by Bergquist (1968) were reported to reach 17.5 µm in thickness, while Topsent’s original data indicates 5 µm. The same applies to the thickness of the spirasters in Bergquist’s specimens (≤ 9 µm thick, or ≤ 14 µm, if spines are included), while Topsent mentioned a thickness of 5 µm. These differences indicate that these populations do not belong to the same species.

However, a series of records exists that have been considered indicative of the species’ transisthmian distribution (Carballo et al. 2004; Vega 2012; Pacheco et al. 2018). These report on sponges bearing tylostyles up to 368 µm long, and 11 µm thick (Carballo et al. 2004; Vega 2012) respectively, but also, in the case of Pacific Costa Rican specimens, only up to 300 × 8 µm (Pacheco et al. 2018), which considerably approach values originally reported by Topsent. On the other hand, spirasters appear to fall short from those of Topsent, up to nearly 50% longer. While the possibility cannot be discarded that these amphi-American populations belong to the same species, this should be verified by an alternative dataset, as suggested above.

Cliona aff. *euryphyllae* shares the same spicules (thick and short spirasters) with four other *Cliona* spp., namely *C. aethiopicus* Burton, 1932, *C. burtoni* Topsent, 1932, *C. caledoniae* van Soest & Beglinger, 2009 and *C. dioryssa* (de Laubenfels, 1950). However, these species have unusual aspects of their spirasters, both in dimensions as well as outline, which suggest closer proximity between the Ecuadorian species and *C. euryphyllae*. *Cliona aethiopicus* was considered closely allied to *C. chilensis* by Burton (1932),

irrespective of Thiele's (1905) hesitation regarding the origin of a few spirasters found in the encrusting Chilean specimen he studied. The presence of these spirasters in the type material of *C. chilensis* was not confirmed by Desqueyroux-Faúndez and van Soest (1997), which establishes both species' spicule sets as markedly divergent. The former, with abundant microscleres. The latter, devoid of those. Contrastingly to what we have observed in the Ecuadorian *C. aff. euryphyllae*, with varied microsclere morphologies, Burton (1932) did not mention any variation in the spirasters of *C. aethiopicus*.

Cliona burtoni has spirasters with proportionately much shorter spines, and much straighter axes when compared to the pattern seen in *C. aff. euryphyllae*. Furthermore, the tylostyles with predominantly subterminal heads present in *C. burtoni*, are only occasionally present in the latter species. *Cliona caledoniae* has spirasters bearing extremely stout and somewhat obtuse spines that differ considerably from the pointier spines seen in *C. aff. euryphyllae*. Finally, *C. dioryssa*'s tylostyles approach 400 µm, and the species has two categories of spirasters of rather varied morphology, reaching over 40 µm in length, also appearing distinct from those in *C. aff. euryphyllae*.

Order Haplosclerida Topsent, 1928

Family Callyspongiidae de Laubenfels, 1936

Genus *Callyspongia* Duchassaing & Michelotti, 1864

Subgenus *Callyspongia* Duchassaing & Michelotti, 1864

Diagnosis. *Callyspongia* with smooth surface, ectosomal skeleton not echinated, spongin sheath conspicuous, no fibrofascicles. Modified from (Desqueyroux-Faúndez and Valentine 2002).

Remarks. The emphasis by Desqueyroux-Faúndez and Valentine (2002) on a single size of ectosomal mesh of “regular size of single, rounded to polygonal mesh”, in their own words was misleading, as a hierarchical pattern of smaller meshes within larger meshes is apparent in several morphological descriptions of the type species, *C. fallax* (Duchassaing & Michelotti, 1864), such as those by van Soest (1980) and Zea (1987).

Identification key to the subgenera of *Callyspongia*

- 1 Ectosomal skeleton echinated **2**
- Ectosomal skeleton not echinated **3**
- 2 Ectosomal echination by a strong palisade of spicule brushes; narrow spongin sheath on primary multi-spicular choanosomal fibres..... ***Cavochoalina***
- Ectosomal echination by free spicules; large spongin sheath on primary paucispicular choanosomal fibres ***Euplacella***
- 3 Surface smooth; spongin sheath conspicuous ***Callyspongia***
- Surface conulose to spiny; spongin sheath only seldom conspicuous, mostly meagre or absent **4**
- 4 Spongin always visible; toxas absent ***Cladochoalina***
- Spongin scarce; toxas always present ***Toxochalina***

Callyspongia (Callyspongia) aff. californica* Dickinson, 1945sensu* Cruz-Barraza and Carballo (2008)

Figure 4A–H

Callyspongia cf. californica – Calabro et al. 2018: supp. inf., P3.

Material examined. CENAIM 150820EP02–01 with fragment as MNRJ 19920, ‘Acuario’, El Pelado Islet, REMAPE, Santa Elena, Ecuador (-1.936167; -80.788922), 6 m deep, collected by K. Jaramillo, 20 Aug. 2015. CENAIM 150813EP07–07 or MNRJ 19924, ‘Bajo 40’, El Pelado Islet, REMAPE, Santa Elena, Ecuador (-1.938217; -80.786669), 15 m deep, collected by O. Thomas, 13 Aug. 2015. CENAIM 150825EP04–04 or MNRJ 19925, ‘Laberinto’, El Pelado Islet, REMAPE, Santa Elena, Ecuador (-1.9355; -80.7896), 5 m deep, collected by K. Jaramillo, 25 Aug. 2015 [voucher from Calabro et al. 2018]. CENAIM 160213EP04–01 or MNRJ 19949 and CENAIM 160213EP04–02 or MNRJ 19951, ‘Laberinto’, El Pelado Islet, REMAPE, Santa Elena, Ecuador (-1.9355; -80.7896), 5–7 m deep, collected by O. Thomas, 13 Feb. 2016.

Material studied for comparison. *C. californica*, voucher number: IRCSET364 from Parque de la Reina Acapulco, Acapulco, México (16.8491314; -99.9015755), 4–15 m deep, collected by J.L. Carballo, 01 Jul. 2012. Molecular Evolution and Systematics (MEAS) collection at National University of Ireland, Galway (NUIG).

Habit (Fig. 4A–C). Cushion-shaped, usually up to 2–3 cm thick only, frequently bearing short irregularly cylindrical or volcano-shaped projections topped by roundish oscula, 1–5 mm in diameter. Occasionally, larger coalescent tubes with apical oscula (over 1 cm in diameter) can also be seen. Consistency soft, easily torn, yielding moderate amounts of mucus upon collection and handling. Texture smooth. Colour in life ranging from white to blueish/purplish, becoming beige in ethanol.

Skeleton (Fig. 4D–F). Ectosomal architecture a neat reticulation of polygonal primary and secondary meshes, the former outlined by pauci- to multi-spicular fibres, the latter by thin very slender fibres, mostly one or two spicules across, and a single spicule long. Choanosomal architecture an irregular polygonal reticulation of pauci- to multi-spicular fibres, frequently sinuous.

Spicules (Fig. 4G–H, Table 3). Oxeas in a single size category, slender, slightly irregular, mostly slightly curved or bent in the middle, mostly with slightly roundish, irregular ends, 46–83 (57, $n = 31$) \times 1.2–5.0 μm (2.5, $n = 28$).

Ecology and distribution. The sponge is quite abundant in the shallow waters at El Pelado and in the nearby continental shore, where it occurs in areas of considerable water flush, frequently in close association with *Pocillopora* (Lamarck, 1816) corals and many species of octocorals. Red algal turfs are frequently seen as epibionts. *Callyspongia aff. californica* also presents a complete family of bioactive amphiphilic compounds named callyspongic acids that have inhibitory properties against the melanoma cell line A2058, metabolites that could be important for further chemotaxonomy studies (Calabro et al. 2018). Its recorded depth at El Pelado is 5–20 m, but its frequent finding beached after storms suggests its occurrence in even shallower waters. This might be the southernmost record of *C. californica* (*sensu* Cruz-Barraza

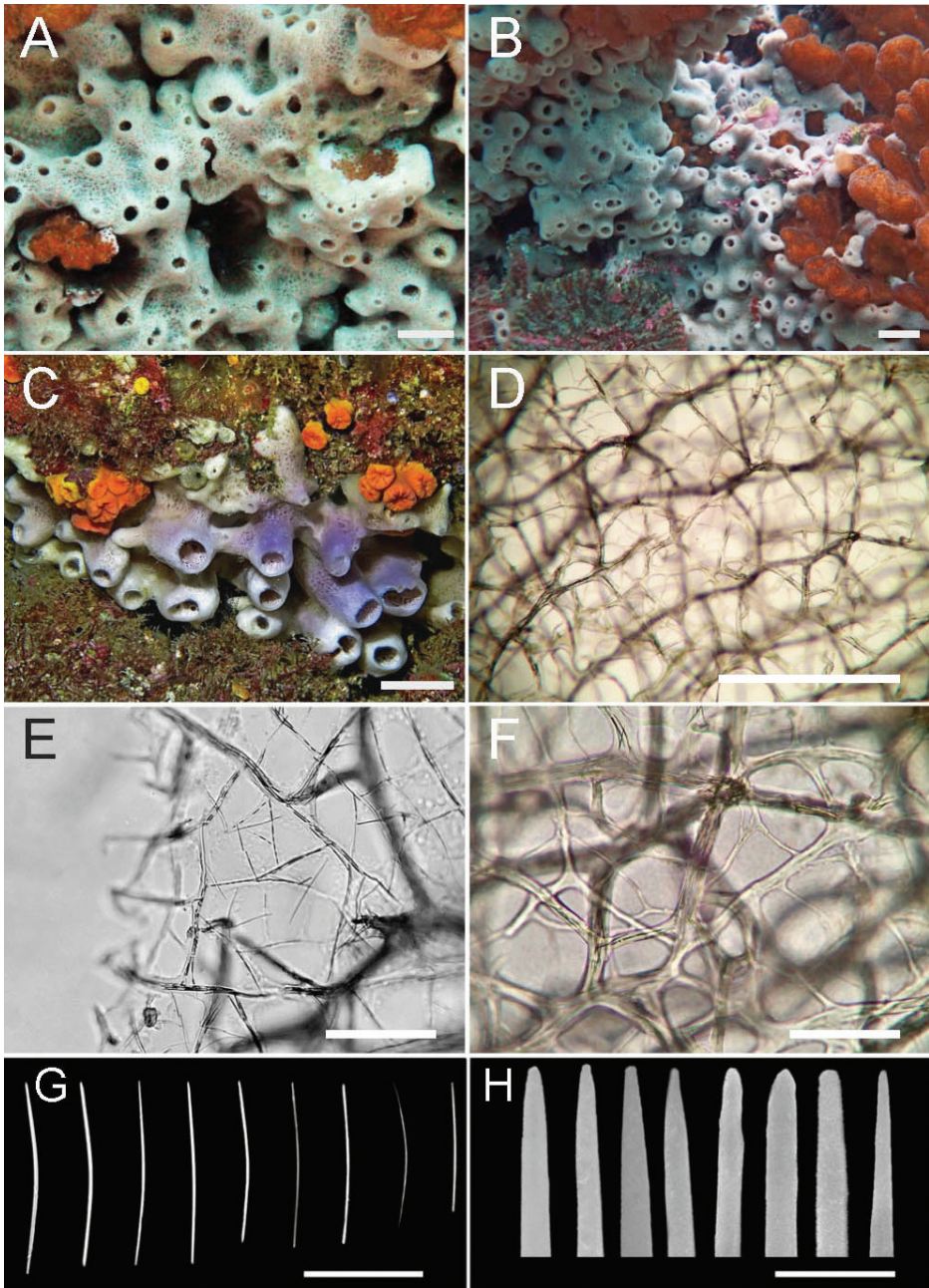


Figure 4. *Callyspongia (Callyspongia) aff. californica* Dickinson, 1945 (*sensu* Cruz-Barraza and Carballo 2008) **A–C** specimens alive in situ: **A** CENAIM 150820EP02-01 **B** CENAIM 150813EP07-07 **C** specimen collected for chemical studies CENAIM 150825EP04-04, of the rarer tubular morphotype **D** delicate ectosomal reticulation seen through stouter subectosomal polygonal meshes **E** detail of ectosomal reticulation with primary and secondary meshes **F** detail of subectosomal reticulation showing stouter, multi-spicular tracts **G** oxeas **H** details of the terminations of the oxeas. Scale bars: 1.5 cm (**A–C**); 1000 μm (**D**); 400 μm (**E–F**); 50 μm (**G**); 50 μm (**H**).

Table 3. *Callyspongia* (*C.*) *californica* Dickinson, 1945 and *C.* (*C.*) aff. *californica*: Morphology of spicules spicule (in micrometres), locality and depth for specimens studied here, and from the literature. Spicule morphometrics are in micrometres as range with the mean in parentheses.

Species	Oxeas	Locality / depth
<i>C.</i> aff. <i>californica</i> 150820EP02–01 (MNRJ 19920)	46–71 (57.5) (N = 30)	El Pelado Islet / 6 m
150813EP07–07 (MNRJ 19924)	48–69 (61.2) (N = 30)	El Pelado Islet / 15 m
150825EP04–04 (MNRJ 19925)	50–81 (67.3) (N = 13)	El Pelado Islet / 5 m
160213EP04–01 (MNRJ 19949)	61–74 (65.9) (N = 16)	El Pelado Islet / 7 m
160213EP04–02 (MNRJ 19951)	50–83 (63.9) (N = 06)	El Pelado Islet / 5 m
IRCSET364	56–105 (67) × 1.5–5.0 (2.4)	Mexican Pacific / 8 m
<i>C. californica</i> Dickinson, 1945 (orig. descr.)	80–150 × 3–5	Mexican Pacific / beached (“shore”)
sensu Sim and Bakus (1986)	84–132 (105) × 2.4–7 (5.3)	California / 3.6 m
sensu Cruz–Barraza and Carballo (2008)	52–117 (73) × 1.3–5.0 (2.4)	Mexican Pacific / 0–15 m

and Carballo 2008; *non sensu* Dickinson, 1945), formerly known only from Mexico (Cruz-Barraza and Carballo 2008) and possibly California (Sim and Bakus 1986), and first time citation to the Tropical South-eastern Pacific (but see the Remarks section). Interestingly, *C. californica* has also been observed in close association with *Pocillopora* corals in the Mexican Pacific coast.

Remarks. *Callyspongia californica*, originally reported from Mexico (Dickinson 1945), has subsequent records from California (Sim and Bakus 1986) and several Mexican locations (Cruz-Barraza and Carballo 2008). Dickinson (1945) highlighted the 150 µm long oxeas in his *C. californica* material as the most striking feature separating this species from any other. Sim and Bakus (1986) found oxeas only up to about 130 µm in California. Then, Cruz-Barraza and Carballo (2008), in spite of studying nearly topotypical specimens (those from Oaxaca), could not find oxeas larger than 117 µm. We had access to a comparative sample kindly sent on loan by JL Carballo, obtained from Acapulco (Guerrero), only about 400 km distant from the type locality at Tangola Island (Oaxaca). While spicule dimensions in the Ecuadorian specimens are even smaller, being ≤ 100 µm in the specimens sampled, the ability of *C. californica* to build oxeas of different sizes even in the same locality (JL Carballo pers. comm. 2019) suggests that spicule size is not a useful trait to distinguish the Ecuadorian specimens as a separate species. Despite the observed difference in spicule dimensions, overall morphological and ecological similarity strongly indicate that our specimen from Ecuador is most likely conspecific to the Mexican sample studied.

Calabro et al. (2018) provided a brief description of the Ecuadorian species in their Supporting Information, but the rationale for this name choice is only given here. Had we revised the species' type specimen, and generated sequences for faster evolving markers, we might have been confident of Ecuadorian specimens being best assigned to *C. californica*, despite a Meridional occurrence about 4,000 km distant from the species' previously known geographic range. Unfortunately, the type specimen could not be located and may have been lost/misplaced in the transfer of the Dickinson material

from the University of Southern California to the Natural History Museum of Los Angeles (K. Omura, pers. comm. May 31st, 2019), so we could not attempt to extract DNA from it for comparison. As such, we opted to identify the Ecuadorian species as *C. aff. californica* instead, for the time being. Whether subsequent Mexican records of *C. californica* (e.g., Carballo et al. 2004, 2008; Vega 2012) are indeed conspecific with the type specimen of this species, we cannot say. Conservatively, we suggest them being provisionally best referred to as *C. aff. californica* too.

Discussion

This work represents the first morphological study of sponges off the coast of mainland Ecuador. As a result, we revealed two new records for the Ecuadorian mainland coast, and the South-eastern Pacific, and one new species *Tedania ecuadoriensis* sp. nov., provisionally endemic of the MPA El Pelado, at the Guayaquil Marine Ecoregion, Tropical Eastern Pacific Realm.

Information and interest in Ecuadorian sponges have increased in recent years as a consequence of the growing body of evidence on the marked underestimation of sponge biodiversity in the whole SE Pacific (e.g., Azevedo et al. 2009, 2015; Hajdu et al. 2013). Increasingly, this renewed interest in the biodiversity inventory of this broad area has been conducted via an integrative approach, by combining classical morphological techniques with an assessment of several molecular markers (De Paula et al. 2012; Azevedo et al. 2015). This will be the way to progress if a sound increase in knowledge on Ecuadorian marine sponges is sought. This is made clear by the partial identifications put forward here for *Callyspongia aff. californica* and *Cliona aff. euryphylle*. The final conclusive identification of these species depends on the integration of alternative data sources, which has not been possible here for several reasons: missing type materials, lack of well-preserved topotypical specimens, failure to obtain sequences from the ideal molecular markers, and time constraints.

The hesitant species determination provided here for *C. aff. euryphylle* and *C. aff. californica* derive in the first place from the insufficient data available for the type specimens of both species. The lack of type data meant that despite how similar Ecuadorian data was to more recent comprehensive records of both species, we could not conclusively identify both. Only molecular evidence can confirm these possibly discontinuous distributions, as verified for *C. celata* Grant, 1826 in the Western Atlantic (De Paula et al. 2012; Gastaldi et al. 2018), or the calcareous sponge *Clathrina aurea* Solé-Cava, Klautau, Boury-Esnault, Borojevic & Thorpe, 1991, formerly endemic to Brazil, but recently recorded from Peru (Azevedo et al. 2015) and the Caribbean (Fontana et al. 2018). Whether subsequent Mexican records of *C. californica* (e.g., Carballo et al. 2004, 2008; Vega 2012) are indeed conspecific with the type specimen of this species, we cannot say. We feel confident though, that the Ecuadorian specimens are conspecific to these subsequent Mexican records of *C. californica*, all of which we suggest being provisionally best referred to as *C. aff. californica*.

Despite the value of the integrative approach to systematics to correctly delimit species (e.g., Schlick-Steiner et al. 2010), a conclusive application of characters other than morphological is often impossible for the type materials. Integrative approaches are also hindered by lack of any alternative data for the type species in a genus, or for any other more closely related species, whatsoever. Our efforts to integratively describe the species presented here were unsuccessful. Nevertheless, we argue this is the way to move forward in the taxonomic study of Ecuadorian sponges, and beyond this, we recommend sponge taxonomists to turn integrative taxonomy into routine work, so, as a community, we can build a reference dataset to help determine the true extent of relatedness among sponge lineages.

Ecuador is a rare, if not unique, example of nation where 97% (87 of 90 recorded species) of the knowledge of the poriferan biological resource, mainly composed of Demospongiae, is derived from an offshore location (Schuster et al. 2018, van Soest et al. 2020). Irrespective of the biological importance of the Galapagos Archipelago, this fact needs a major reversal. It is doubtful that there will ever be a proliferation of research institutes in the archipelago that might deepen the study of several aspects of these holobionts, whose transfer to mainland Ecuador is unlikely, at the least. Getting to know more the easily accessible sponges from the coast of mainland Ecuador is essential to develop this scientific field in the country, as highlighted from pioneering bioprospecting conducted at Reserva Marina El Pelado (Calabro et al. 2018).

The rather localized distributional data generated in this study does not permit to establish biogeographic boundaries for marine sponges along the Ecuadorian mainland. These will ultimately depend on expanding the taxonomic inventory to additional localities to the S and N of MPA El Pelado. Nevertheless, present data help filling in an important knowledge gap on the distribution of Tropical Eastern Pacific sponges, by expanding the notoriously underestimated sponge biodiversity inventory into the Guayaquil Ecoregion. It is expected that sponges will produce patterns similar to those recently reported for Ecuadorian zoantharians (Jaramillo et al. 2018), where Panamanian and Humboldtian affinities are clearly evident, indicating species coming from the north, and from the south, respectively. The first of these patterns is apparent for *C. aff. californica*, known all the way up to Mexico, at least. However, species illustrating affinities to the colder South American Pacific, as well as to the Galapagos Islands remain to be spotted on coastal mainland Ecuador marine sponges.

Acknowledgements

This work was funded by the Secretaría de Educación, Ciencia y Tecnología e Innovación of Ecuador (SENESCYT) in the framework of the PIC-14-CENAIM-001 Project “Caracterización de la Biodiversidad Microbiológica y de Invertebrados de la Reserva Marina “El Pelado” a escalas taxonómica, metabolómica y metagenómica para su uso en Salud Humana y Animal”. K.J. acknowledges NUI Galway for supporting part of her Ph.D. scholarship, but also the Project National Marine Biodiscovery Labo-

ratory through a grant from the Marine Institute PBA/MB/16/01. E.H. is funded by the Brazilian National Council for Scientific and Technological Development (CNPQ), by Coordination of Superior Level Staff Improvement (CAPES), and Carlos Chagas Filho Research Support Foundation (FAPERJ). Authors would like also to thank J.L. Carballo (Universidad Nacional Autónoma de México) for kindly sending the Mexican voucher of *C. californica*; Pierce Lalor (senior technician at NUI-Galway), and Camila Messias and Beatriz C.A. Cordeiro (technicians at Dept. of Invertebrates), who assisted us with the acquisition of SEM images, respectively at the Center for Microscopy and Imaging (CMI) – NUI Galway and the Center for Scanning Electron Microscopy of Museu Nacional/UFRJ; and Kathy Omura (Natural History Museum of Los Angeles) for her efforts in trying to locate the type material of *Callyspongia californica*.

References

- Aguilar-Camacho JM, Carballo JL, Cruz-Barraza JA (2018) *Tedania* (Porifera: Demospongiae: Poecilosclerida) from the Mexican Pacific with the description of two new species. *Journal of Natural History* 52(19–20): 1311–1332. <https://doi.org/10.1080/00222933.2018.1462893>
- Aguirre LK, Hooker Y, Willenz Ph, Hajdu E (2011) A new *Clathria* (Demospongiae, Microcionidae) from Peru occurring on rocky substrates as well as epibiontic on *Euclidaris thouarsii* sea urchins. *Zootaxa* 3085(1): 41–54. <https://doi.org/10.11646/zootaxa.3085.1.3>
- Azevedo F, Condor-Lujan B, Willenz Ph, Hajdu E, Hooker Y, Klautau M (2015) Integrative taxonomy of calcareous sponges (subclass Calcinea) from the Peruvian coast: morphology, molecules, and biogeography. *Zoological Journal of the Linnean Society* 173(4): 787–817. <https://doi.org/10.1111/zoj.12213>
- Azevedo F, Hajdu E, Willenz Ph, Klautau M (2009) New records of Calcareous sponges (Porifera, Calcarea) from the Chilean coast. *Zootaxa* 2072(1): 1–30. <https://doi.org/10.11646/zootaxa.2072.1.1>
- Bell JJ (2007) Contrasting patterns of species and functional composition of coral reef sponge assemblages. *Marine Ecology Progress Series* 339: 73–81. <https://doi.org/10.3354/meps339073>
- Bell JJ, Barnes DKA (2003) The importance of competitor identity, morphology and ranking methodology to outcomes in interference competition between sponges. *Marine Biology* 143: 415–426. <https://doi.org/10.1007/s00227-003-1081-0>
- Bell JJ, Smith D (2004) Ecology of sponge assemblages (Porifera) in the Wakatobi region, south-east Sulawesi, Indonesia: richness and abundance. *Journal of the Marine Biological Association of the United Kingdom* 84(3): 581–591. <https://doi.org/10.1017/S0025315404009580h>
- Bergquist PR (1968) The Marine Fauna of New Zealand: Porifera, Demospongiae, Part 1 (Tetractinomorpha and Lithistida). *New Zealand Department of Scientific and Industrial Research Bulletin* 188 – *New Zealand Oceanographic Institute Memoir* 37: 1–105.
- Burton M (1932) Sponges. *Discovery Reports* 6: 237–392. [pls 48–57] <https://doi.org/10.5962/bhl.part.24379>

- Bustamante RH, Vinueza LR, Smith F, Banks S, Calvopiña M, Francisco V, Chiriboga A, Harris J (2002) Comunidades submareales rocosas I: Organismos sésiles y mesoinvertebrados móviles. In: Danulat E, Edgar GJ (Eds) Reserva Marina de Galápagos. Línea Base de Biodiversidad. Fundación Charles Darwin/Servicio Parque Nacional Galápagos, Santa Cruz, Galápagos, 38–67.
- Calabro K, Chalen BE, Genta-Jouve G, Jaramillo KB, Dominguez C, de la Cruz M, Cautain B, Reyes F, Thomas OP, Rodriguez J (2018) Callyspongidic acids: Amphiphilic diacids from the tropical Eastern Pacific sponge *Callyspongia* cf. *californica*. *Journal of Natural Products* 81(10): 2301–2305. <https://doi.org/10.1021/acs.jnatprod.8b00683>
- Carballo JL, Bautista-Guerrero E, Leyte-Morales GE (2008) Boring sponges and the modeling of coral reefs in the East Pacific Ocean. *Marine Ecology Progress Series* 356: 113–122. <https://doi.org/10.3354/meps07276>
- Carballo JL, Cruz-Barraza JA, Gómez P (2004) Taxonomy and description of clionaid sponges (Hadromerida, Clionaidae) from the Pacific Ocean of Mexico. *Zoological Journal of the Linnean Society* 141(3): 353–397. <https://doi.org/10.1111/j.1096-3642.2004.00126.x>
- Carroll AR, Copp BR, Davis RA, Keyzers RA, Prinsep MR (2019) Marine natural products. *Natural Product Reports* 36: 122–173. <https://doi.org/10.1039/C8NP00092A>
- Chavez FP, Brusca RC (1991) The Galápagos Islands and their relation to oceanographic processes in the Tropical Pacific. In: James MJ (Ed.) *Galápagos Marine Invertebrates: Taxonomy, Biogeography, and Evolution in Darwin's Islands*. Springer, Boston, 9–33. https://doi.org/10.1007/978-1-4899-0646-5_2
- Cóndor-Luján B, Azevedo F, Hajdu E, Hooker Y, Willenz Ph, Klautau M (2019) Tropical Eastern Pacific Amphoriscidae Dendy, 1892 (Porifera: Calcarea: Calcaronea: Leucosolenida) from the Peruvian coast. *Marine Biodiversity* 49: 1813–1830. <https://doi.org/10.1007/s12526-019-00946-y>
- Costa G, Bavestrello G, Pansini M, Bertolino M (2020) *Acanthbella danerii* sp. nov. (Demospongiae, Bubarida, Dictyonellidae) from Chilean fjords (South Pacific Ocean). *Zootaxa*, 4790(2): 393–396. <https://doi.org/10.11646/zootaxa.4790.2.13>
- Cruz-Barraza JA, Carballo JL (2008) Taxonomy of sponges (Porifera) associated with corals from the Mexican Pacific Ocean. *Zoological Studies* 47(6): 741–758. <http://zoolstud.sinica.edu.tw/Journals/47.6/741.pdf>
- de Laubenfels MW (1930) The sponges of California. PhD Thesis, Stanford University, USA.
- de Laubenfels MW (1939) Sponges collected on the presidential cruise of 1938. *Smithsonian Miscellaneous Collections* 98(15): 1–7. <https://doi.org/10.5962/bhl.part.4785>
- de Laubenfels MW (1954) *The Sponges of the West-Central Pacific*. College Press Monographs, Oregon State, 218 pp. <https://doi.org/10.5962/bhl.title.6516>
- De Paula TS, Zilberberg C, Hajdu E, Lôbo-Hajdu G (2012) Morphology and molecules on opposite sides of the diversity gradient: four cryptic species of the *Cliona celata* (Porifera, Demospongiae) complex in South America revealed by mitochondrial and nuclear markers. *Molecular Phylogenetics and Evolution* 62: 529–541. <https://doi.org/10.1016/j.ympev.2011.11.001>
- de Voogd NJ, Becking LE, Hoeksema BW, Noor A, van Soest RWM (2004) Sponge interactions with spatial competitors in the Spermonde Archipelago. In: Pansini M, Pronzato R,

- Bavestrello G, Manconi R, Sarà M (Eds) *Sponge Science in the New Millenium*. Bolletino dei Musei e degli Istituti Biologici dell'Università di Genova 68: 253–261.
- Desqueyroux-Faúndez R (1990) Spongiaires (Demospongiae) de l'Île de Pâques (Isla de Pascua). *Revue Suisse de Zoologie* 97: 373–409. <https://doi.org/10.5962/bhl.part.79743>
- Desqueyroux-Faúndez R, Valentine C (2002) Family Callyspongiidae de Laubenfels, 1936. In: Hopper JNA, van Soest RWM, Willenz Ph (Eds) *Systema Porifera*. Springer, Boston, 835–851. https://doi.org/10.1007/978-1-4615-0747-5_90
- Desqueyroux-Faúndez R, van Soest RWM (1996) A review of Iophonidae, Myxillidae and Tedaniidae occurring in the south east Pacific (Porifera: Poecilosclerida). *Revue suisse de Zoologie* 103: 3–80. <https://doi.org/10.5962/bhl.part.79938>
- Desqueyroux-Faúndez R, van Soest RWM (1997) Shallow-water Demosponges of the Galapagos Islands. *Revue Suisse de Zoologie* 104: 379–467. <https://doi.org/10.5962/bhl.part.80003>
- Dickinson MG (1945) Sponges of the Gulf of California. In: Reports on the collections obtained by Alan Hancock Pacific Expeditions of Velero III off the coast of Mexico, Central America, South America, and Galapagos Islands in 1932, in 1933, in 1934, in 1935, in 1936, in 1937, in 1939, and 1940. The University of Southern California Press, Los Angeles, 55 pp. [pls 1–97]
- Fernandez JCC, Cárdenas CA, Bravo A, Lôbo-Hajdu G, Willenz Ph, Hajdu E (2016) *Lissodendoryx* (*Ectyodoryx*) Lundbeck, 1909 (Coelosphaeridae, Poecilosclerida, Demospongiae) from Southern Chile: new species and a discussion of morphologic characters in the subgenus. *Zootaxa* 4092(1): 69–89. <https://doi.org/10.11646/zootaxa.4092.1.4>
- Fiedler PC, Chavez FP, Behringer DW, Reilly SB (1992) Physical and biological effects of Los Niños in the eastern tropical Pacific, 1986–1989. *Deep Sea Research Part A. Oceanographic Research Papers* 39(2): 199–219. [https://doi.org/10.1016/0198-0149\(92\)90105-3](https://doi.org/10.1016/0198-0149(92)90105-3)
- Fontana T, Córdor-Luján B, Azevedo F, Pérez T, Klautau M (2018) Diversity and distribution patterns of Calcareous sponges (subclass Calcinea) from Martinique. *Zootaxa* 4410(2): 331–369. <https://doi.org/10.11646/zootaxa.4410.2.5>
- Gastaldi M, De Paula TS, Narvarte MA, Lôbo-Hajdu G, Hajdu E (2018) Marine sponges (Porifera) from the Bahía San Antonio (North Patagonian Gulfs, Argentina), with additions to the phylogeography of the widely distributed *Cliona* aff. *celata* and *Hymeniacion* *perlevis*, and the description of two new species. *Marine Biology Research* 14(7): 682–716. <https://doi.org/10.1080/17451000.2018.1506136>
- Glynn PW (2003) Coral communities and coral reefs of Ecuador. In: Cortés J (Ed.) *Latin American Coral Reefs*. Elsevier Science B.V., Amsterdam, 449–472. <https://doi.org/10.1016/B978-044451388-5/50020-5>
- Hajdu E, Desqueyroux-Faúndez R (1994) A synopsis of South American *Mycale* (*Mycale*) (Poecilosclerida, Demospongiae), with description of three new species and a cladistic analysis of Mycalidae. *Revue Suisse de Zoologie* 101: 563–600. <https://doi.org/10.5962/bhl.part.79918>
- Hajdu E, Desqueyroux-Faúndez R, Carvalho MD, Lôbo-Hajdu G, Willenz Ph (2013) Twelve new Demospongiae (Porifera) from Chilean fjords, with remarks upon sponge-derived biogeographic compartments in the SE Pacific. *Zootaxa* 3744(1): 1–64. <https://doi.org/10.11646/zootaxa.3744.1.1>

- Hajdu E, Desqueyroux-Faúndez R, Willenz Ph (2006) *Clathria (Cornulotrocha) rosetafjordica* sp. nov. from a south-east Pacific fjord (Chilean Patagonia) (Microcionidae: Poecilosclerida: Demospongiae: Porifera). *Journal of the Marine Biological Association of the United Kingdom* 86(5): 957–961. <https://doi.org/10.1017/S0025315406013920>
- Hajdu E, Hooker Y, Willenz Ph (2015) New *Hamacantha* from Peru and resurrection of *Zygherpe* as subgenus (Demospongiae, Poecilosclerida, Hamacanthidae). *Zootaxa* 3926(1): 87–99. <https://doi.org/10.11646/zootaxa.3926.1.3>
- Hajdu E, Peixinho S, Fernandez JCC (2011) Esponjas Marinhas da Bahia. Guia de Campo e Laboratório. Museu Nacional, Rio de Janeiro, 276 pp.
- Hooper JNA, van Soest RWM (2002) Systema Porifera. A Guide to the Classification of Sponges. In: Hooper JNA, van Soest RWM, Willenz Ph (Eds) Systema Porifera. Springer Boston, 7 pp. https://doi.org/10.1007/978-1-4615-0747-5_1
- Jaramillo KB, Reverter M, Guillen PO, McCormack G, Rodriguez J, Sinniger F, Thomas OP (2018) Assessing the Zoantharian diversity of the tropical Eastern Pacific through an integrative approach. *Scientific Reports* 8: e7138. <https://doi.org/10.1038/s41598-018-25086-4>
- Lee WL (1987) *Guitarra abbotti* and *G. isabellae*, new sponges from the Eastern Pacific. *Proceedings of the Biological Society of Washington* 100(3): 465–479.
- Lendenfeld R von (1910) The Sponges. 2. The Erylidae. In: Reports on the Scientific Results of the Expedition to the Eastern Tropical Pacific, in charge of Alexander Agassiz, by the U.S. Fish Commission Steamer 'Albatross', from October, 1904, to March, 1905, Lieut. Commander L.M. Garrett, U.S.N., Commanding, and of other Expeditions of the Albatross, 1888–1904. (21). *Memoirs of the Museum of Comparative Zoology at Harvard College* 41(2): 261–324.
- Miloslavich P, Klein E, Diaz JM, Hernández CE, Bigatti G, Campos L, Artigas F, Castillo J, Penchaszadeh PE, Neill PE, Carranza A, Retana MV, Diaz de Astarloa JM, Lewis M, Yorio P, Piriz ML, Rodriguez D, Yoneshigue-Valentin Y, Gamboa L, Martin A (2011) Marine biodiversity in the Atlantic and Pacific coasts of South America: Knowledge and gaps. *PLoS ONE* 6(1): e14631. <https://doi.org/10.1371/journal.pone.0014631>
- Morrow CC, Cárdenas P (2015) Proposal for a revised classification of the Demospongiae (Porifera). *Frontiers in Zoology* 12: 1–7. <https://doi.org/10.1186/s12983-015-0099-8>
- Pacheco C, Carballo JL, Cortés J, Segovia J, Trejo A (2018) Excavating sponges from the Pacific of Central America, descriptions and a faunistic record. *Zootaxa* 4370(5): 451–491. <https://doi.org/10.11646/zootaxa.4370.5.1>
- Patil AD, Freyer AJ, Carte B, Taylor PB, Johnson RK, Faulkner DJ (2002) Haploscleridamine, a novel tryptamine-derived alkaloid from a sponge of the order Haplosclerida: An inhibitor of cathepsin K. *Journal of Natural Products* 65(4): 628–629. <https://doi.org/10.1021/np010500l>
- Recinos R, Pinheiro US, Willenz Ph, Hajdu E (2020) Three new Raspailiidae Hentschel, 1923 (Axinellida, Demospongiae) from Peru. *Zootaxa* 4778(3): 521–545. <https://doi.org/10.11646/zootaxa.4778.3.5>
- Sarà M, Bavestrello G, Calcinai B (2000) New *Tethya* species (Porifera, Demospongiae) from the Pacific area. *Zoosystema* 22(2): 345–354.

- Schlick-Steiner BC, Steiner FM, Seifert B, Stauffer C, Christian E, Crozier RH (2010) Integrative Taxonomy: A Multisource Approach to Exploring Biodiversity. *Annual Review of Entomology* 55(1): 421–438. <https://doi.org/10.1146/annurev-ento-112408-085432>
- Schuster A, Cardenas P, Pisera A, Pomponi SA, Kelly M, Wörheide G, Erpenbeck D (2018) Seven new deep-water Tetractinellida (Porifera: Demospongiae) from the Galápagos Islands – morphological descriptions and DNA barcodes. *Zoological Journal of the Linnean Society* 184(2): 273–303. <https://doi.org/10.1093/zoolinlean/zlx110>
- Sim C-J, Bakus GJ (1986) Marine sponges of Santa Catalina Island, California. *Occasional Papers of the Allan Hancock Foundation. Allan Hancock Foundation (New Series)* 5: 1–23.
- Spalding MD, Fox HE, Allen GR, Davidson N, Ferdaña ZA, Finlayson M, Halpern BS, Jorge MA, Lombana A, Lourie SA, Martin KD, McManus E, Molnar J, Recchia CA, Robertson J (2007) Marine ecoregions of the world: A bioregionalization of coastal and shelf areas. *BioScience* 57(7): 573–583. <https://doi.org/10.1641/B570707>
- Thiele J (1905) Die Kiesel- und Hornschwämme der Sammlung Plate. *Zoologische Jahrbücher Supplement 6 (Fauna Chilensis III)*: 407–496. <http://www.marinespecies.org/porifera/porifera.php?p=sourcedetails&cid=8300>
- Topsent E (1888) Contribution à l'étude des Clionides. *Archives de Zoologie Expérimentale et Générale*, 2(5 bis): 1–165.
- Topsent E (1891) Deuxième contribution à l'étude des Clionides. *Archives de Zoologie Expérimentale et Générale* 9: 555–592.
- Topsent E (1895) Étude monographique des spongiaires de France. II. Carnosa. *Archives de Zoologie Experimentale et Générale* 3: 493–590.
- van Soest RWM (1980) Marine sponges from Curaçao and other Caribbean localities. Part II. Haplosclerida. *Studies on the Fauna of Curaçao and other Caribbean Islands* 62(191): 1–173.
- van Soest RWM, Boury-Esnault N, Hooper JNA, Rützler K, de Voogd NJ, Alvarez B, Hajdu E, Pisera AB, Manconi R, Schönberg C, Klautau M, Kelly M, Vacelet J, Dohrmann M, Díaz MC, Cárdenas P, Carballo JL, Ríos P, Downey R, Morrow CC (2020) World Porifera Database. <https://doi.org/10.14284/359> [on 2020-04-03]
- Vega C (2012) Composición y afinidades biogeográficas de esponjas (Demospongiae) asociadas a comunidades coralinas del Pacífico Mexicano. PhD Thesis, Instituto Politécnico Nacional, Mexico.
- Willenz Ph, Hajdu E, Desqueyroux-Faúdez R, Lôbo-Hajdu G, Carvalho M (2009) Porifera. In: Häussermann V, Försterra G (Eds) *Marine Benthic Fauna of Chilean Patagonia. Nature in Focus*, Puerto Montt, 93–170.
- Wilson HV (1904) The Sponges. Reports on an exploration off the west coasts of Mexico, Central and South America, and off the Galapagos Islands, in charge of Alexander Agassiz, by the US Fish Commission steamer "Albatross" during 1891, Lieut. Commander Z.L. Tanner, U.S.N., Commanding. *Memoirs of the Museum of Comparative Zoology at Harvard College* 30(1): 1–164. [pls 1–26]
- Zea S (1987) Esponjas del Caribe colombiano. *Catálogo Científico*, Bogotá, 286 pp.

A new species of the genus *Pareas* (Squamata, Pareidae) from Yunnan, China

Shuo Liu¹, Dingqi Rao²

1 Kunming Natural History Museum of Zoology, Kunming Institute of Zoology, Chinese Academy of Sciences, 32 Jiaochang Donglu, Kunming, Yunnan 650223, China **2** Kunming Institute of Zoology, Chinese Academy of Sciences, 32 Jiaochang Donglu, Kunming, Yunnan 650223, China

Corresponding author: Dingqi Rao (raodq@mail.kiz.ac.cn)

Academic editor: T. Ziegler | Received 28 September 2020 | Accepted 4 January 2021 | Published 21 January 2021

<http://zoobank.org/336122EE-57C0-407A-A680-B00B86DC6C7D>

Citation: Liu S, Rao D (2021) A new species of the genus *Pareas* (Squamata, Pareidae) from Yunnan, China. ZooKeys 1011: 121–138. <https://doi.org/10.3897/zookeys.1011.59029>

Abstract

A new species of *Pareas* is described from Yunnan Province, China, based on morphological comparisons and molecular data. Genetically, the new species is most closely related to the recently-described *Pareas geminatus*, for which we present new topotypic findings. The genetic divergence (uncorrected p-distance) of the cytb gene between the new species and congeners ranged from 6.14% to 24.68%. Morphologically, the new species can be distinguished from *P. geminatus* and all other congeners. Our work brings the total number of species within the genus *Pareas* to 22.

Keywords

Molecular, morphological, snail-eating snake, taxonomy

Introduction

The family Pareidae Romer encompasses two subfamilies and four genera (Deepak et al. 2018; Uetz et al. 2020) and was once considered as a subfamily (called Pareatinae) of Colubridae (Smith 1943; Zhao et al. 1998; Zhao 2006). The taxonomy of the genus *Pareas* Wagler remains in a state of flux and species complexes with wide distributions and several lineages with an unclear taxonomic status remain especially

challenging (Guo et al. 2011; Vogel 2015; You et al. 2015; Vogel et al. 2020; Wang et al. 2020). You et al. (2015) re-evaluated the taxonomic status of the *P. hamptoni-formosensis* complex from Taiwan, China, Ryukyus and adjacent regions, but the taxonomic status of the complex from mainland China was not involved. Wang et al. (2020) described *P. menglaensis* Wang, Che, Liu, Li, Jin, Jiang, Shi and Guo in the *P. carinatus-nuchalis* complex from Yunnan, China, but without any comments on the distribution of *P. carinatus* (Wagler) and described *P. mengziensis* Wang, Che, Liu, Li, Jin, Jiang, Shi and Guo without first resolving the historically taxonomic confusions of *P. yunnanensis* (Vogt) and *P. niger* (Pope). Vogel et al. (2020) re-assessed the taxonomy of the *P. margaritophorus-macularius* complex, re-validated two species and further re-confirmed the full species status of *P. macularius* Theobald in the complex. Vogel et al. (2020) underlined that the taxonomy of the genus *Pareas* has not yet been fully assessed, especially in widely-distributed taxa often representing complexes of cryptic or morphologically-similar species.

During our field research in Yunnan Province, China, from 2019 to 2020, some small and slender arboreal nocturnal snakes with blunt snouts and no mental groove and no teeth on the anterior part of maxillary, which could be assigned to the genus *Pareas*, were collected from Lancang County, Jiangcheng County and Kunming City. Morphological comparison and molecular analyses indicated that the specimens from Lancang County are distinct from all named species of the genus *Pareas* and we consequently described them as a new species.

Materials and methods

Specimens were collected in the field. Photographs were taken to document the colour pattern in life prior to euthanasia. Liver tissues were stored in 99% ethanol and snakes were preserved in 75% ethanol. Specimens were deposited at Kunming Natural History Museum of Zoology, Kunming Institute of Zoology, Chinese Academy of Sciences (KIZ).

Morphometrics

Measurements were taken to the nearest 1 mm with digital calipers. Paired meristic characters are given as left/right. The methodology of measurements and meristic counts followed Wang et al. (2020). The abbreviations of measurements and meristic counts are given below:

- DS** dorsal scale rows (counted at one head length behind head, at mid-body and at one head length before vent, respectively);
- InfL** infralabials;
- LoBO** loreal bordering orbit;
- Max** maxillary teeth;
- NED** number of enlarged dorsal scale rows at mid-body;

NKD	number of keeled dorsal scale rows at anterior/middle/posterior of body;
PosO	postoculars;
PreO	preoculars;
PrFBO	prefrontal bordering orbit;
Sc	subcaudals;
SPOF	subocular-postocular fused or not;
SubO	suboculars;
SupL	supralabials;
SVL	snout-vent length (from tip of snout to posterior margin of cloacal plate);
Tem	temporals;
TL	tail length (from posterior margin of cloacal plate to tip of tail);
Vs	ventrals.

For comparison, data for other species were taken from related publications (Boulenger 1900, 1905; Pope 1935; Zhao et al. 1998; Grossmann and Tillack 2003; Guo and Deng 2009; Guo et al. 2011; Loredo et al. 2013; Vogel 2015; You et al. 2015; Hauser 2017; Bhosale et al. 2020; Ding et al. 2020; Vogel et al. 2020; Wang et al. 2020). In addition, we examined the topotypic specimens of *Pareas niger* preserved in KIZ.

Phylogenetic analyses

Molecular data were generated for two specimens from Lancang County, two specimens from Jiangcheng County and one specimen from Kunming City. Homologous sequences were obtained from GenBank. All new sequences have been deposited in GenBank. *Aplopeltura boa* (Boie), *Asthenodipsas laevis* (Boie) and *Xylophis captaini* Gower and Winkler were selected as outgroups, based on Wang et al. (2020). All the GenBank accession numbers for taxa used in this study are listed in Table 1.

Total genomic DNA was extracted from liver tissues using the OMEGA DNA Kit (Omega Bio-Tek, Inc., Norcross, GA, USA). The sequences of the mitochondrial gene fragment, cytochrome b (cytb), were amplified by polymerase chain reaction (PCR) using primers L14910/H16064 (Burbrink et al. 2000). The double-stranded products were purified and sequenced at Genewiz Co. (Suzhou, China). Sequences were edited and manually managed using SeqMan in Lasergene 7.1 (DNASTAR Inc., Madison, WI, USA) and MEGA 7 (Kumar et al. 2016).

Sequences were aligned using ClustalW (Thompson et al. 1994) integrated in MEGA 7 with default parameters (Kumar et al. 2016). The genetic divergence (uncorrected p-distance) between species was calculated in MEGA 7 with the parameters Transitions + Transversions, Uniform rates and Pairwise deletion (Kumar et al. 2016). The substitution model GTR+I was selected in MODELTEST 3.7 (Posada and Crandall 1998). Bayesian Inference was performed in MrBayes 3.2.6 (Ronquist et al. 2012), based on the selected substitution model. Two runs were performed simultaneously with four Markov chains starting from a random tree. The chains were run for 1,000,000 generations and sampled every 100 generations. The first 25% of the sampled trees was discarded as burn-in after the standard deviation of

Table 1. Sequences (cytb) used in phylogenetic analysis of this study.

Species	Locality	Voucher no.	GenBank no.
<i>Pareas andersonii</i>	Longchuan, Yunnan, China	CHS 015	MK201238
<i>Pareas atayal</i>	N. Cross-Is. Highway, Taiwan, China	HC 000618	JF827685
<i>Pareas boulengeri</i>	Jiangkou, Guizhou, China	GP 2923	MK135090
<i>Pareas carinatus</i>	Malaysia	KIZ 011972	MK135111
<i>Pareas chinensis</i>	Junlian, Sichuan, China	GP 2196	MK135088
<i>Pareas formosensis</i>	N. Cross-Is. Highway, Taiwan, China	NMNS 05632	MK135088
<i>Pareas formosensis</i>	Hainan, China	YBU 12015	MK135068
<i>Pareas formosensis</i>	Leishan, Guizhou, China	YBU 12090	MK135074
<i>Pareas formosensis</i>	Guangxi, China	YBU 14508	MK135076
<i>Pareas formosensis</i>	Jingning, Zhejiang, China	GP 4581	MK135072
<i>Pareas geminatus</i>	Jiangcheng, Yunnan, China	CIB 118021	MW287068
<i>Pareas geminatus</i>	Jiangcheng, Yunnan, China	KIZ L2020020	MW436707
<i>Pareas geminatus</i>	Jiangcheng, Yunnan, China	KIZ L2020024	MW436708
<i>Pareas hamptoni</i>	Myanmar	YPX 18219	MK135077
<i>Pareas hamptoni</i>	Myanmar	YPX 18604	MK135078
<i>Pareas iwasakii</i>	Ishigaki Is., S. Ryukyu, Japan	I03-ISG1	KJ642158
<i>Pareas kaduri</i>	Lohit, Arunachal, India	BNHS 3574	MT188734
<i>Pareas komaii</i>	Lijia, Taidong, Taiwan, China	HC 000669	JF827687
<i>Pareas macularius</i>	Hainan, China	GP815	MK135101
<i>Pareas margaritophorus</i>	Cangwu, Guangxi, China	YBU 16061	MK135097
<i>Pareas menglaensis</i>	Mengla, Yunnan, China	YBU 14124	MK135114
<i>Pareas mengziensis</i>	Mengzi, Yunnan, China	GP 1294	MK135079
<i>Pareas mengziensis</i>	Mengzi, Yunnan, China	YBU 14251	MK135080
<i>Pareas mengziensis</i>	Mengzi, Yunnan, China	YBU 14252	MK135081
<i>Pareas mengziensis</i>	Mengzi, Yunnan, China	YBU 14253	MK135082
<i>Pareas mengziensis</i>	Mengzi, Yunnan, China	YBU 14288	MK135083
<i>Pareas mengziensis</i>	Kaiyuan, Yunnan, China	YBU 15100	MK135084
<i>Pareas mengziensis</i>	Kaiyuan, Yunnan, China	YBU 15114	MK135085
<i>Pareas modestus</i>	Tanhril, Aizawl, Mizoram, India	MZMU 1293	MT968773
<i>Pareas monticola</i>	Motuo, Xizang, China	KIZ 014167	MK135109
<i>Pareas niger</i>	Kunming, Yunnan, China	KIZ 059339	MW436706
<i>Pareas nigriceps</i>	Gaoligongshan, Yunnan, China	CHS 656	MK201455
<i>Pareas stanleyi</i>	Guangxi, China	GP 229	MK135086
<i>Pareas vindumi</i>	Lukpwi, Chipwi, Kachin, Myanmar	CAS 248147	MT968776
<i>Pareas xuelinensis</i> sp. nov.	Lancang, Yunnan, China	KIZ XL1	MW436709
<i>Pareas xuelinensis</i> sp. nov.	Lancang, Yunnan, China	KIZ XL2	MW436710
<i>Aplopeltura boa</i>	Malaysia	LSUHC 7248	KC916746
<i>Asthenodipsas laevis</i>	Peninsular Malaysia	LSUHC 10346	KC916749
<i>Xylophis captaini</i>	Kottayam, Kerala, India	BNHS 3376	MK340914

split frequencies of the two runs was less than a value of 0.01 and then the remaining trees were used to create a 50% majority-rule consensus tree and to estimate Bayesian posterior probabilities. Maximum Likelihood analysis was performed in RaxmlGUI 2.0 (Silvestro and Michalak 2012) and nodal support was estimated by 1,000 rapid bootstrap replicates.

Results

Meristic and mensural characters were noted for all examined specimens (Tables 2, 3). The three specimens collected from Lancang County could be distinguished from all other congeners. Morphological characters of the two specimens from Jiangcheng

Table 2. Measurements (in mm) and scalation data of *Pareas xuelinensis* sp. nov. and *P. geminatus*. For abbreviations, see Materials and methods section. Paired meristic characters are given as left/right.

	<i>Pareas xuelinensis</i> sp. nov.			<i>Pareas geminatus</i>	
	KIZ XL1	KIZ XL2	KIZ XL3	KIZ L2020020	KIZ L2020024
	Holotype	Paratype	Paratype	Topotype	Topotype
SEX	♂	♂	♀	♂	♂
SVL	403	431	287	344	316
TL	132	145	94	96	87
PrFBO	Yes	Yes	Yes	Yes	Yes
PreO	1	1	1	1	1
PosO	Fused	Fused	Fused	Fused	Fused
SubO	Fused	Fused	Fused	Fused	Fused
SPOF	Yes	Yes	Yes	Yes	Yes
Tem	2+2+2/2+2+2	2+3+2/2+2+3	2+2+2/2+2+2	1+2+1/1+2+1	1+1+1/1+2+1
SupL	7/7	7/7	7/7	7/7	7/7
InfL	7/7	7/7	8/8	8/8	7/7
LoBO	No	No	No	No	No
Vs	188	182	183	184	183
Sc	89	87	93	73	74
Ds	15-15-15	15-15-15	15-15-15	15-15-15	15-15-15
NED	0	0	0	1	1
NKD	0-3-5	0-3-5	0-3-5	0-5-5	0-5-5
Max	7/6	6/7	8/8	6/5	5/5

Table 3. Measurements (in mm) and scalation data of *Pareas niger*. For abbreviations, see Materials and methods section. Paired meristic characters are given left/right.

	KIZ 059339	KIZ 76003	KIZ 790009	KIZ 82001	KIZ 9010004
	Topotype	Topotype	Topotype	Topotype	Topotype
SEX	♂	♂	♂	♂	♂
SVL	192	364	396	384	383
TL	53	103	incomplete	99	92
PrFBO	Yes	Yes	Yes	Yes	Yes
PreO	1	1	1	1	1
PosO	Fused	Fused	Fused	Fused	Fused
SubO	Fused	Fused	Fused	Fused	Fused
SPOF	Yes	Yes	Yes	Yes	Yes
Tem	2+3+3/2+3+3	2+2+2/2+1+3	2+3+2/1+3+3	1+3+3/1+3+1	2+3+2/2+3+3
SupL	7/7	7/7	7/8	7/7	7/7
InfL	9/9	9/8	7/7	7/7	8/9
LoBO	No	No	No	No	No
Vs	154	169	172	163	161
Sc	55	66	incomplete	59	65
Ds	15-15-15	15-15-15	15-15-15	15-15-15	15-15-15
NED	0	0	0	1	3
NKD	0-0-0	0-5-5	0-5-5	0-0-3	0-5-5
Max	6/6	8/7	6/6	6/6	6/7

County agreed with *Pareas geminatus* Ding, Chen, Suwannapoom, Nguyen, Poyarkov and Vogel and morphological characters of the specimen collected from Kunming City agreed with the topotypic specimens of *P. niger*.

Maximum Likelihood analyses and Bayesian Inference showed similar results, the specimen from Kunming City clustered with *Pareas mengziensis*, the specimens from Jiangcheng County clustered with *P. geminatus* and the specimens from Lancang Coun-

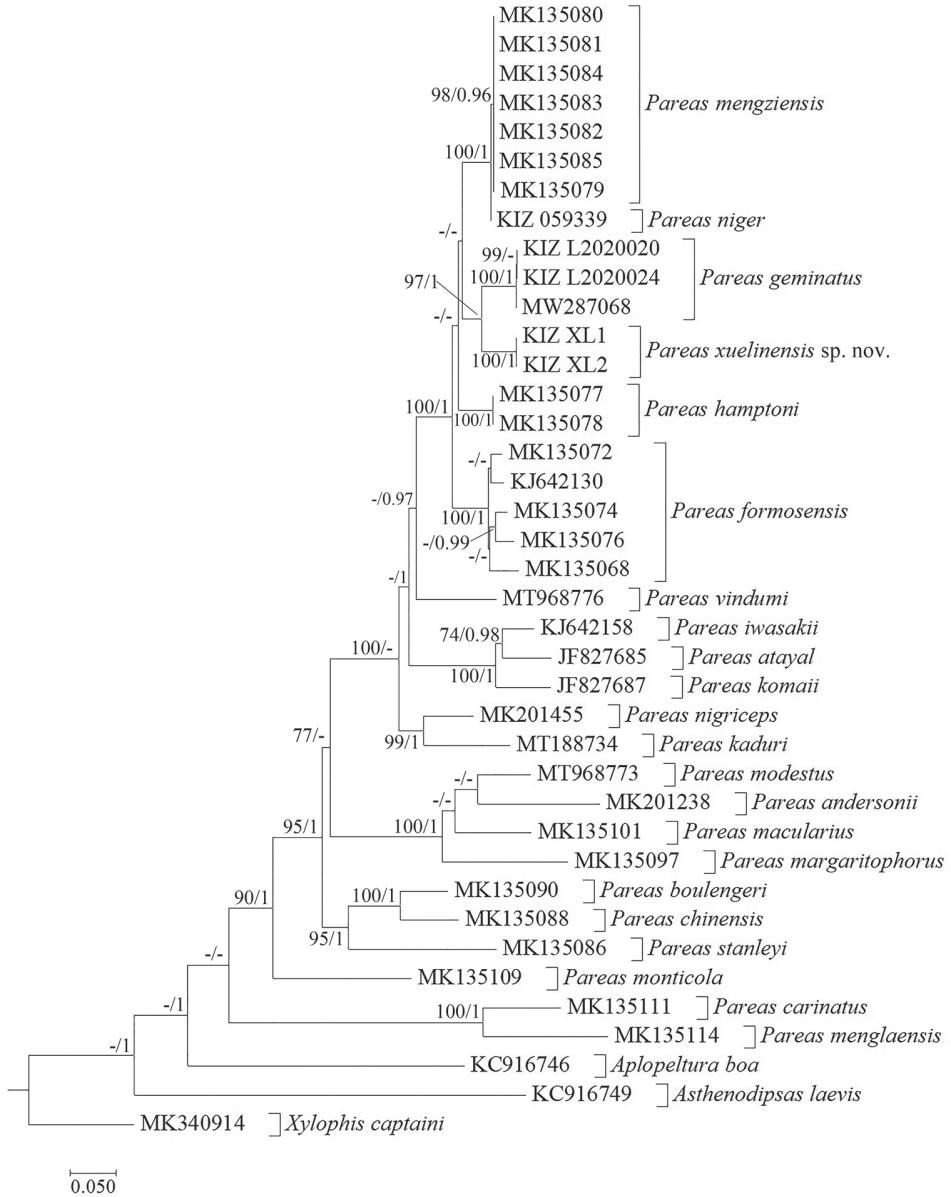


Figure 1. Maximum Likelihood phylogram of investigated members of *Pareas* and outgroups inferred from *cytb* gene. Numbers before slashes indicate bootstrap support for Maximum Likelihood analyses (only values above 70 are shown) and numbers after slashes indicate Bayesian posterior probabilities (only values above 0.9 are shown).

ty formed a distinct lineage which is sister to *P. geminatus* with strong support (Fig. 1). The genetic divergence (uncorrected p-distance) between the lineage from Lancang County and *P. geminatus* was 6.14% (Table 4).

Table 4. Uncorrected p-distances (%) amongst the members of Pareidae, calculated from cytb gene sequences.

	1	2	3	4	5	6	7	8	9	10	11	12	13	14	15	16	17	18	19	20	21	22	23	24	
1 <i>Pareus anderssonii</i>																									
2 <i>Pareus atajal</i>	20.68																								
3 <i>Pareus boukengeri</i>	17.61	18.51																							
4 <i>Pareus carinatus</i>	23.93	23.20	22.56																						
5 <i>Pareus chinensis</i>	17.61	18.42	9.04	23.01																					
6 <i>Pareus formosensis</i>	18.84	15.10	16.60	24.02	16.88																				
7 <i>Pareus germinatus</i>	20.91	14.62	17.45	23.57	18.61	9.11																			
8 <i>Pareus hamptoni</i>	20.00	14.27	17.17	23.74	18.08	7.53	7.42																		
9 <i>Pareus ivasakii</i>	19.83	7.18	16.84	23.73	17.22	13.86	14.59	13.49																	
10 <i>Pareus kaduri</i>	20.85	16.26	20.17	22.49	19.01	13.96	14.22	13.41	15.63																
11 <i>Pareus komati</i>	18.97	8.66	18.14	23.94	18.23	14.40	15.09	14.46	7.94	16.58															
12 <i>Pareus macularius</i>	16.07	19.24	18.17	23.56	18.08	19.34	20.56	19.27	19.81	20.38	18.69														
13 <i>Pareus margaritophorus</i>	17.44	19.24	19.18	24.02	18.72	20.35	22.19	20.46	18.76	21.01	19.52	14.16													
14 <i>Pareus meglaiensis</i>	22.91	23.39	23.56	14.06	25.02	24.24	23.04	23.56	23.44	24.82	23.94	24.29	24.93												
15 <i>Pareus mengziensis</i>	19.32	14.47	17.64	23.30	17.27	7.85	7.02	5.86	13.79	13.21	14.75	19.10	20.20	23.57											
16 <i>Pareus modestus</i>	12.82	18.42	19.18	24.11	19.09	19.98	20.34	19.63	19.33	19.54	17.77	10.87	13.88	24.02	19.01										
17 <i>Pareus monticola</i>	19.66	17.50	18.72	23.11	18.63	18.85	19.90	19.00	17.80	19.22	17.86	17.53	19.73	22.83	18.73	18.17									
18 <i>Pareus niger</i>	19.32	14.26	17.50	23.15	17.13	7.67	7.01	5.56	13.72	13.09	14.91	18.98	20.09	23.33	0.29	18.89	18.52								
19 <i>Pareus nigripes</i>	17.61	16.07	16.92	22.91	16.07	12.92	13.39	12.65	16.07	10.43	16.24	20.00	17.95	23.08	12.65	16.41	19.15	12.48							
20 <i>Pareus stanleyi</i>	18.46	19.24	15.80	24.84	15.80	19.27	19.80	18.72	18.18	20.80	17.40	19.18	19.54	25.66	19.74	19.54	19.18	19.54	18.97						
21 <i>Pareus vindami</i>	22.39	15.01	18.45	24.20	17.53	12.14	12.45	11.42	14.74	13.52	15.19	18.54	20.46	24.57	11.06	19.93	18.26	10.83	12.31	19.45					
22 <i>Pareus xuclimensis</i> sp. nov.	19.66	14.03	16.90	24.31	18.19	8.19	6.14	8.10	13.72	14.15	14.86	19.68	21.30	24.68	7.36	20.19	19.81	7.27	12.48	19.49	12.64				
23 <i>Aplopeltura boa</i>	23.25	23.16	21.43	23.78	21.43	23.37	24.56	23.78	23.27	24.39	23.67	23.98	24.49	23.16	23.38	22.45	21.12	23.37	23.25	22.65	23.78	25.00			
24 <i>Ashendonaspas laevis</i>	25.81	26.56	26.00	27.40	25.54	26.26	27.56	26.75	26.74	26.72	25.82	26.37	26.37	27.03	25.92	26.19	23.49	25.98	27.35	24.60	26.37	27.01	25.31		
25 <i>Xylophis captani</i>	22.39	21.66	19.68	22.72	20.87	22.91	23.87	24.17	21.32	24.29	21.66	22.32	21.93	21.80	23.51	20.87	20.08	23.47	23.08	22.85	22.72	23.34	20.34	22.72	

Systematics

Pareas xuelinensis sp. nov.

<http://zoobank.org/98E4DB90-251B-4C93-9B38-3A4C09001AD9>

Figs 2, 3, 6A

Type material. *Holotype*. KIZ XL1, adult male, Xuelin Township, Lancang County, Pu'er City, Yunnan Province, China, 23°2'38"N, 99°32'35"E; 1840 m elevation, collected on 13 July 2019 by Shuo Liu.

Paratypes. KIZ XL2, adult male and KIZ XL3, adult female, the same collection data as the holotype.

Diagnosis. Single preocular; postocular fused with subocular; loreal not bordering orbit; prefrontal bordering orbit; fourth or fifth infralabial fused with second chin-shield; three chin-shield pairs; dorsal scales in 15 rows throughout; vertebral scales not enlarged; scales not keeled at the anterior part of the body, three rows of mid-dorsal scales keeled at the middle of the body, five rows of mid-dorsal scales keeled at the posterior of body; seven supralabials; seven or eight infralabials; cloaca undivided; ventral scales 182–188; subcaudals 87–93, paired.

Description of holotype. Male, SVL 403 mm, TL 132 mm, TL/total length 0.25; body elongated; head distinct from neck; snout wide and blunt, projecting beyond lower jaw; body laterally compressed, vertebral ridge poorly developed. Rostral approximately as wide as high, almost invisible from above; nasals undivided; internasals elongated, much wider than long; prefrontals triangular, wider than long, bordering orbits; frontal shield-shaped, longer than wide; parietals large, longer than wide, median suture longer than frontal; single loreal, separated from eyes; single preocular; one relatively small supraocular, longer than wide; subocular and postocular fused into one thin elongated crescent-shaped scale; temporals 2+2+2 on both sides; seven supralabials on both sides, separating from eyes; seven infralabials on both sides, anterior-most in contact with its opposite between mental and anterior chin-shields, first four in contact with anterior chin-shields; fourth fused with second chin-shield; three chin-shields pairs, the first pair and the third pair triangle and almost equal size, the second pair elongate; ventral scales 188; cloaca undivided; subcaudals 89, paired; dorsal scales in 15 rows throughout, vertebral scales not enlarged, scales not keeled at anterior of body, three rows of mid-dorsal scales keeled at middle of body, five rows of mid-dorsal scales keeled at posterior of body; seven maxillary teeth on left side and six maxillary teeth on right side; hemi-penis in situ extending to the 19th subcaudal.

Colouration in life. Dorsal surface of head and body reddish-yellow with many black tiny spots on each scale; a thin black discontinuous postorbital stripe extending from postocular to neck, which is connected with its fellow on the opposite side by a thick black line which curves forward so as to almost touch the parietals; two thick black discontinuous stripes on neck followed the black curves forward line; many irregular longitudinal black stripes on the sides of body and tail, the stripes on different

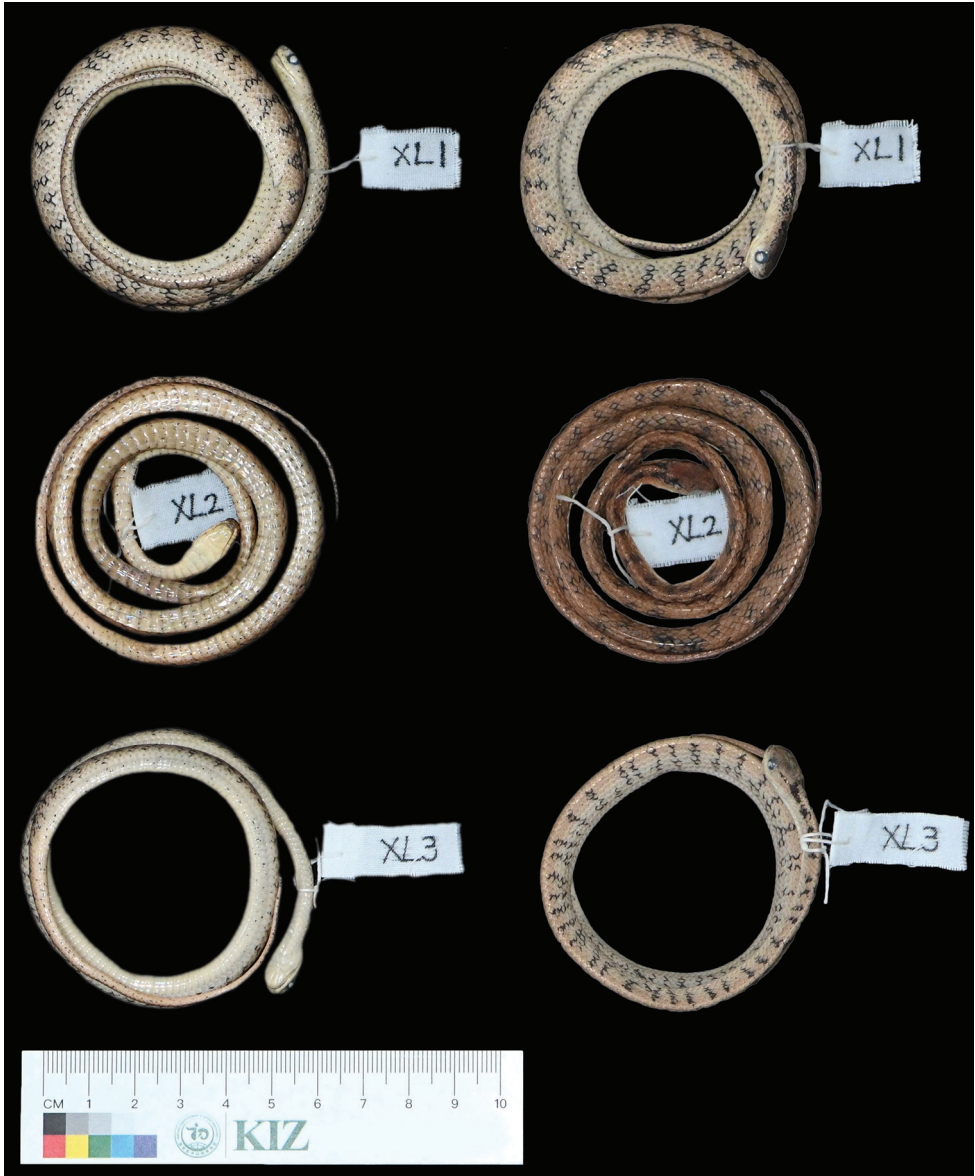


Figure 2. The type specimens of *Pareas xuelinensis* sp. nov. in preservative.

sides not connected to each other on the vertebrals; belly and ventral surface of head and tail yellow with sparse small black spots; iris reddish-yellow, pupil black.

Colouration in preservative. The reddish-yellow dorsal surface of the head and body faded to yellowish-white; the yellow belly and ventral surface of head and tail faded to pale white; the iris changed to greyish-black from reddish-yellow and the pupil changed from black to white.

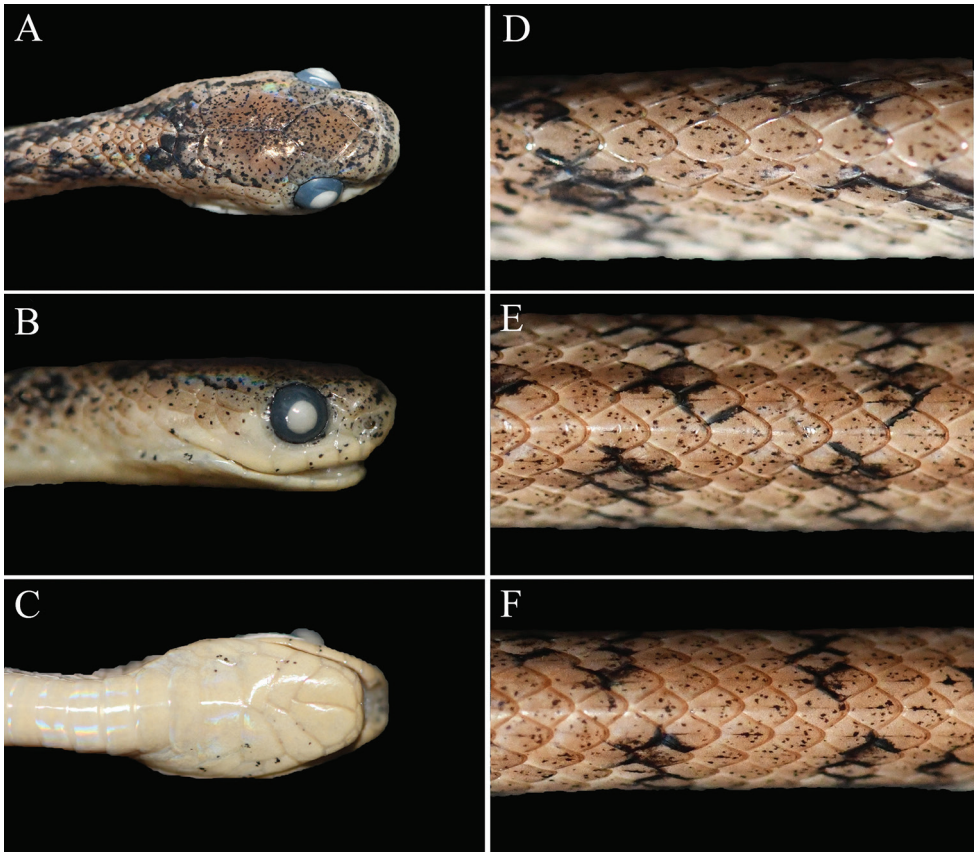


Figure 3. Holotype (KIZ XL1) of *Pareas xuelinensis* sp. nov. **A** dorsal view of the head **B** lateral view of the head **C** ventral view of the head **D** dorsal view of the anterior of body **E** dorsal view of the middle of body **F** dorsal view of the posterior of body.

Variations. Morphometric and meristic data for the type series are provided in Table 3. The paratype KIZ XL2 has 2+3+2 temporals on the left side and 2+2+3 temporals on the right side. The paratype KIZ XL3 has eight infralabials on both sides, first five being in contact with anterior chin-shields, fifth fused with second chin-shield.

Etymology. The specific epithet *xuelinensis* refers to Xuelin Township, the type locality of the new species.

Distribution. This species is currently known only from the type locality Xuelin Township, Lancang County, Pu'er City, Yunnan Province, China. It is expected to be found in Myanmar.

Habitat. Both the holotype and paratypes were found on the bushes beside a small road at night, surrounded by forest and farmland, with no river or stream nearby.

Comparison. *Pareas xuelinensis* sp. nov. can be distinguished from *P. andersonii* Boulenger, *P. atayal* You, Poyarkov & Lin *P. iwasakii* (Maki), *P. komaii* (Maki),

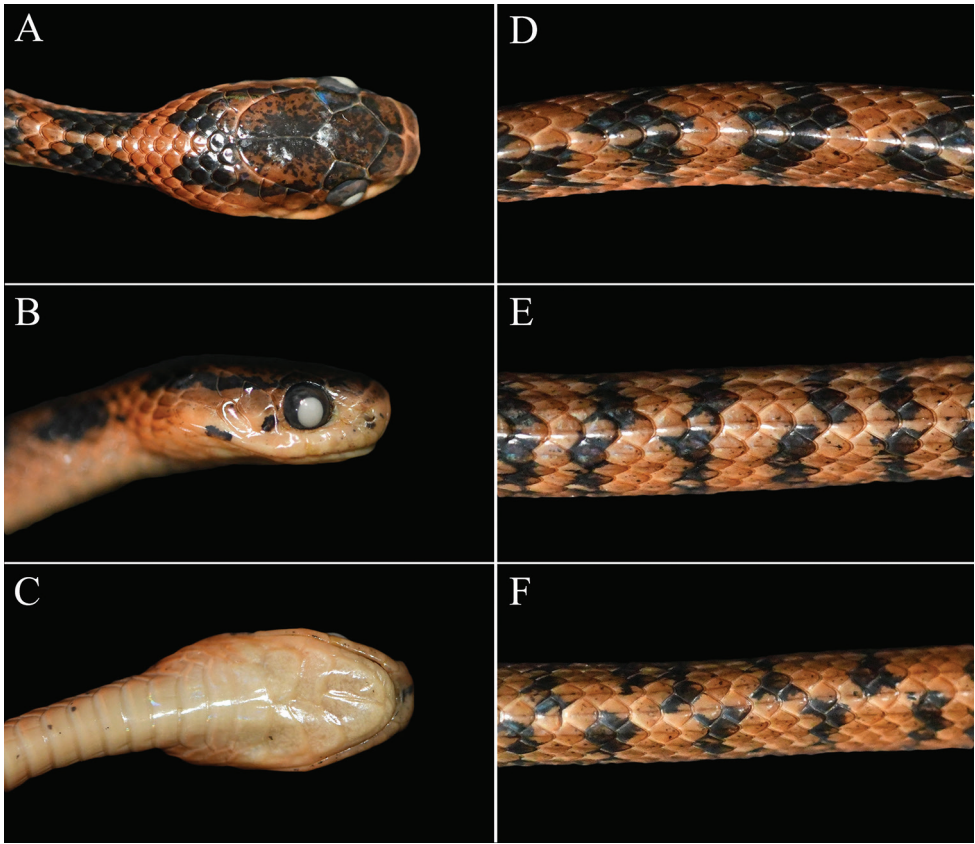


Figure 4. The specimen (KIZ L2020020) of *Pareas geminatus* collected from Jiangcheng County, Pu'er City, Yunnan Province, China **A** dorsal view of the head **B** lateral view of the head **C** ventral view of the head **D** dorsal view of the anterior of body **E** dorsal view of the middle of body **F** dorsal view of the posterior of body.

P. macularius Theobald, *P. nigriceps* Guo & Deng and *P. stanleyi* (Boulenger) by 0–5 rows of mid-dorsal scales keeled (vs. 5–13 rows of mid-dorsal scales keeled); from *P. boulengeri* (Angel), *P. margaritophorus* (Jan), *P. monticola* (Cantor) and *P. vindumi* Vogel by three rows of mid-dorsal scales keeled at middle of body, five rows of mid-dorsal scales keeled at posterior of body (vs. all dorsal scales smooth); from *P. carinatus*, *P. menglaensis* and *P. nuchalis* (Boulenger) by subocular and postocular fused into one thin elongated crescent-shaped scale (vs. two or three distinct narrow suboculars); from *P. chinensis* (Barbour) and *P. modestus* Theobald by more ventral scales (182–188 vs. 136–176); and from *P. formosensis* (Van Denburgh) and *P. kaduri* Bhosale, Phansalkar, Sawant, Gowande, Patel and Mirza by vertebral scales not enlarged (vs. vertebral scales enlarged).

Pareas xuelinensis sp. nov. can be distinguished from *P. geminatus* by vertebral scales not enlarged (vs. vertebral scales enlarged), three rows of mid-dorsal scales keeled at

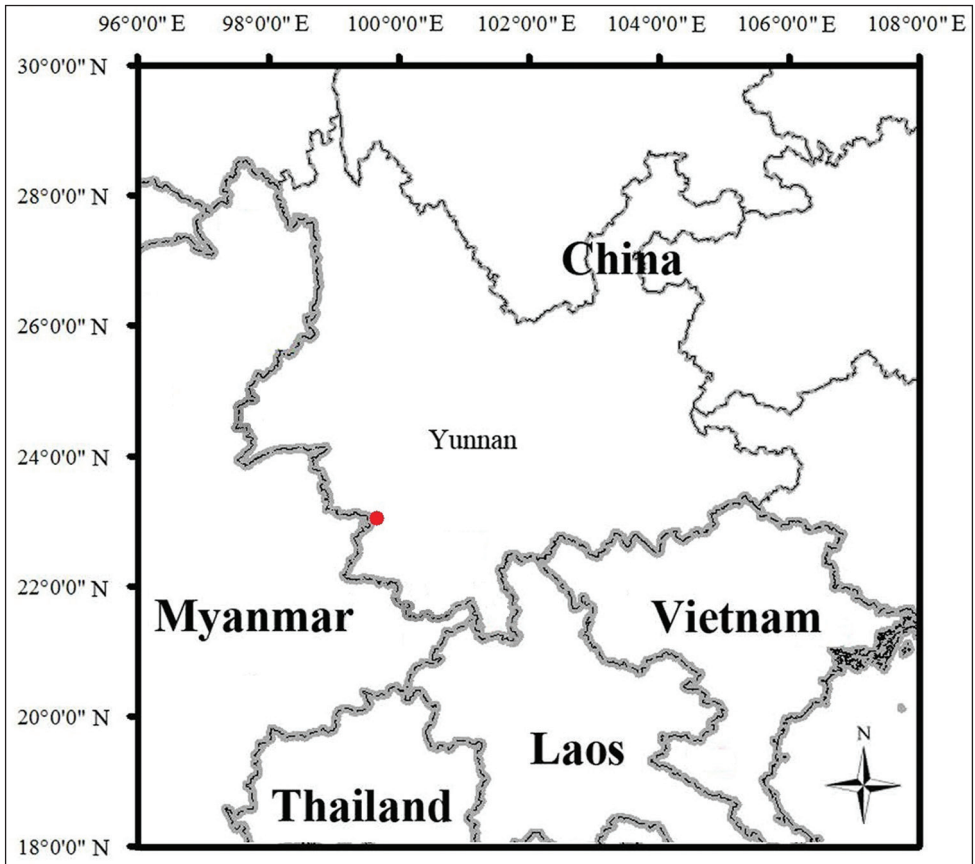


Figure 5. The type locality of *Pareas xuelinensis* sp. nov. (red dot) in Xuelin Township, Lancang County, Pu'er City, Yunnan Province, China.

middle of body (vs. five rows of mid-dorsal scales keeled at middle of body), fourth or fifth infralabial fused with the second chin-shield (vs. infralabials not fused with chin-shield), temporals 2+2+2 or 2+3+3 (vs. 1+2+1 or 1+1+1) and no black spot on each side of head (vs. having two black spots on each side of head).

Pareas xuelinensis sp. nov. can be distinguished from *P. hamptoni* (Boulenger) by vertebral scales not enlarged (vs. vertebral scales enlarged), temporals 2+2 or 2+3 (vs. 1+2) and less ventral scales (182–188 vs. 202).

Pareas xuelinensis sp. nov. can be distinguished from *P. mengziensis* by vertebral scales not enlarged (vs. vertebral scales enlarged), 0–5 rows of mid-dorsal scales keeled (vs. 3–9 rows of mid-dorsal scales keeled), having more ventral scales (182–188 vs. 167–173), more subcaudals (87–93 vs. 54–61) and the dorsal surface of head and body reddish-yellow (vs. the dorsal surface of head and body solid black).

Pareas xuelinensis sp. nov. can be distinguished from *P. niger* by having more ventral scales (182–188 vs. 154–172), more subcaudals (87–93 vs. 55–66) and the dorsal surface of head and body reddish-yellow (vs. the dorsal surface of head and body solid black).



Figure 6. *Pareas xuelinensis* sp. nov. in life (A) and the habitat of *Pareas xuelinensis* sp. nov. at the type locality (B).

Pareas xuelinensis sp. nov. can be distinguished from *P. yunnanensis* by the loreal separating from the eye (vs. the point of the large loreal touching the eye), vertebral scales not enlarged (vs. vertebral scales enlarged), and 0–5 rows of mid-dorsal scales keeled (vs. six rows of dorsal scales keeled).

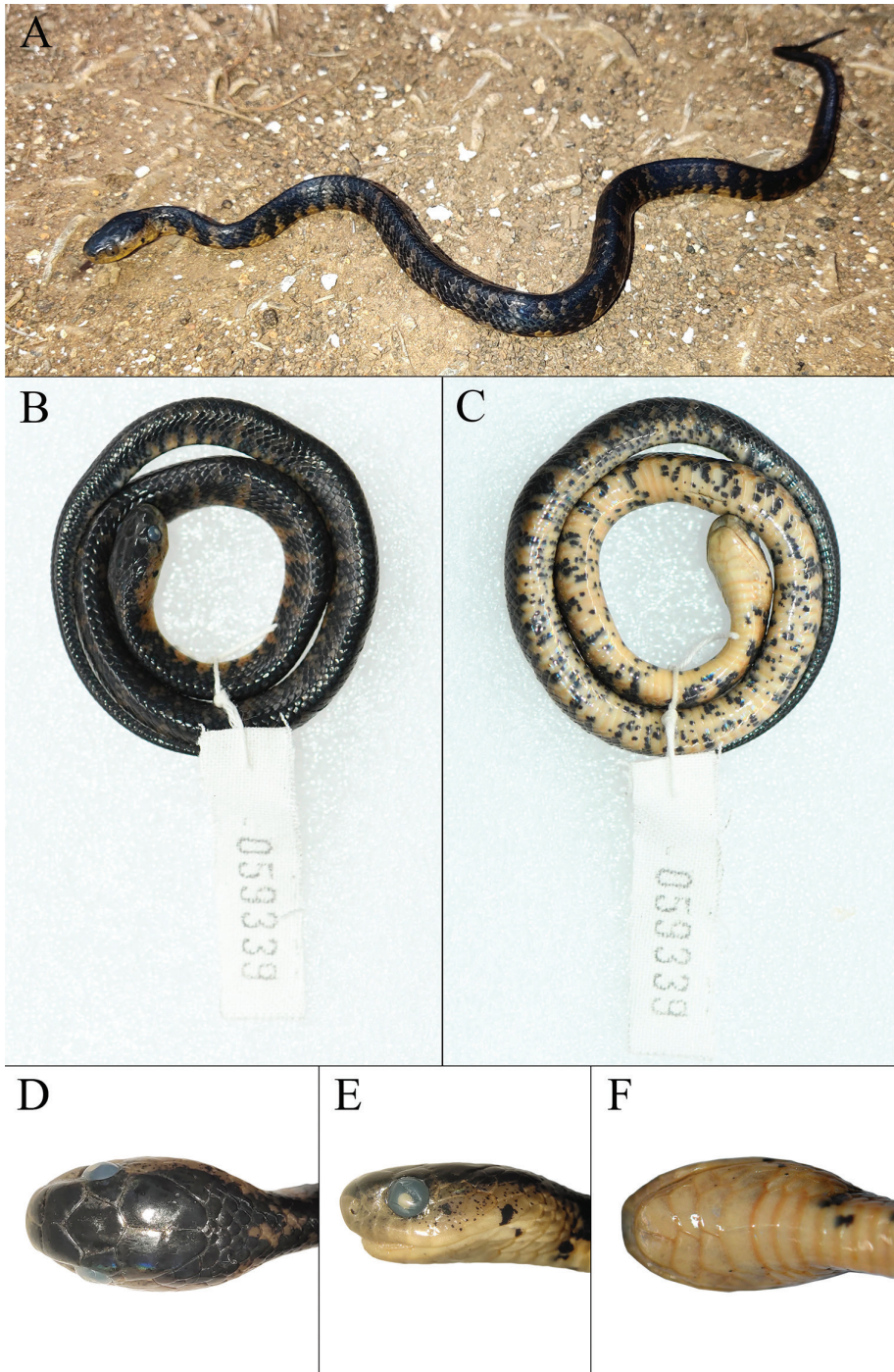


Figure 7. The specimen (KIZ 059339) of *Pareas niger* collected from Kunming, Yunnan, China **A** in life **B** dorsal view in preservative **C** ventral view in preservative **D** dorsal view of the head **E** lateral view of the head **F** ventral view of the head.

Table 5. Comparisons of morphometric and meristic data for *Pareas niger*, *P. chinensis*, *P. komaii* and *P. yunnanensis*. The data for *P. chinensis*, *P. komaii* and *P. yunnanensis* were obtained from the original descriptions and the subsequent descriptions of the type specimens (Barbour 1912; Vogt 1922; Maki 1931; Pope 1935). “?” = data not available.

	<i>Pareas niger</i>	<i>Pareas chinensis</i>	<i>Pareas komaii</i>	<i>Pareas yunnanensis</i>
SVL	192–396	?	430–470	385–410
TL	53–103	?	130	95–100
TL/Total length	0.19–0.22	?	0.20–0.25	0.20
PrFBO	Yes	Yes	Yes	Yes
PreO	1	2	1	2
PosO	Fused	1–2	1	1–2
SubO	Fused	0	1	1
SPOF	Yes	No	No	No
Anterior temporals	1–2	2	2	2
Posterior temporals	1–3	3	3	2–3
SupL	7–8	7	7	6–7
Infl	7–9	?	7	?
LoBO	No	No	No	Yes
Vs	154–172	180	175–179	171–176
Sc	55–66	60	72–75	64–65
Ds	15-15-15	15-15-15	15-15-15	15-15-15
NED	0–3	3	1	1
NKD	0–5	0	3–13	6
Max	6–8	5–6	?	?

Discussion

Amblycephalus niger (now *Pareas niger*) was described by Pope (1928) from Yunnanfu (now Kunming). *Pareas niger* was considered as synonyms of *P. chinensis*, *P. yunnanensis* and *P. komaii*, successively (Sichuan Institute of Biology 1977; Rao and Yang 1992; Uetz et al. 2020). We compared the morphometric and meristic data of *P. niger*, *P. chinensis*, *P. komaii* and *P. yunnanensis* (Table 5) and found that *P. niger* can be distinguished from *P. chinensis*, *P. komaii* and *P. yunnanensis*, so we consider *P. niger* to represent a valid species. During August 2019, we collected one specimen (voucher: KIZ 059339; Fig. 7) of *Pareas* with a solid black dorsal surface on the head and body and no enlarged mid-dorsal scales from Changchong Mountain in Kunming City, its morphological characters agreeing with the original description of *P. niger*, except that it has nine infralabials, which agreed with the original description of *P. mengziensis*. Molecularly, the specimen from Kunming was clustered together with *P. mengziensis* and the genetic divergence (uncorrected p-distance) between the specimen from Kunming and *P. mengziensis* was only 0.29%. After checking the topotypic specimens of *P. niger* preserved in KIZ, we found that the infralabials of *P. niger* range from seven to nine and one or three rows of mid-dorsal scales of several individuals are slightly enlarged. This means that the specimen (KIZ 059339) from Kunming should belong to *P. niger* and it is not appropriate to distinguish *P. mengziensis* and *P. niger* either morphologically or molecularly; therefore, we consider *P. mengziensis* and *P. niger* as the same species, *P. mengziensis* being a synonym of *P. niger*.

Acknowledgements

We would like to thank Decai Ouyang, Lei Ouyang and Zhongqiang Yang for assistance in the field. Thanks also to our workmates for their help and advice. This work was supported by Science-Technology Basic Condition Platform from the Ministry of Science and Technology of the People's Republic of China (Grant No. 2005DKA21402).

References

- Barbour T (1912) Some Chinese Vertebrates: Amphibia and Reptilia. *Memoirs of the Museum of Comparative Zoölogy* 40(4): 125–136.
- Bhosale H, Phansalkar P, Sawant M, Gowande G, Patel H, Mirza ZA (2020) A new species of snail-eating snakes of the genus *Pareas* Wagler, 1830 (Reptilia: Serpentes) from eastern Himalayas, India. *European Journal of Taxonomy* 729(1): 54–73. <https://doi.org/10.5852/ejt.2020.729.1191>
- Boulenger GA (1900) Descriptions of new reptiles and batrachians from Borneo. *Proceedings of the Zoological Society of London*, Blackwell Publishing Ltd, Oxford 69(2): 182–187. <https://doi.org/10.1111/j.1096-3642.1890.tb01716.x>
- Boulenger GA (1905) Descriptions of two new snakes from Upper Burma. *Bombay Natural History Society* 16: 235–236. <https://doi.org/10.1080/03745480509443665>
- Burbrink FT, Lawson R, Slowinski JB (2000) Mitochondrial DNA phylogeography of the polytypic North American rat snake (*Elaphe obsoleta*): a critique of the subspecies concept. *Evolution* 54(6): 2107–2118. <https://doi.org/10.1111/j.0014-3820.2000.tb01253.x>
- Ding L, Chen ZN, Suwannapoom C, Nguyen TV, Poyarkov NA, Vogel G (2020) A new species of the *Pareas hamptoni* complex (Squamata: Serpentes: Pareidae) from the Golden Triangle. *TAPROBANICA* 9(2): 174–193. <https://doi.org/10.47605/tapro.v9i2.230>
- Deepak V, Ruane S, Gower DJ (2018) A new subfamily of fossorial colubroid snakes from the Western Ghats of peninsular India. *Journal of Natural History* 52(45–46): 2919–2934. <https://doi.org/10.1080/00222933.2018.1557756>
- Grossmann W, Tillack F (2003) On the taxonomic status of *Asthenodipsas tropidonotus* (Van Lidth de Jeude, 1923) and *Pareas vertebralis* (Boulenger, 1900) (Serpentes: Colubridae: Pareatinae). *Russian Journal of Herpetology* 10(3): 175–190. <http://rjh.folium.ru/index.php/rjh/article/view/636>
- Guo KJ, Deng XJ (2009) A new species of *Pareas* (Serpentes: Colubridae: Pareatinae) from the Gaoligong Mountains, southwestern China. *Zootaxa* 2008: 53–60. <https://www.biotaxa.org/Zootaxa/article/view/zootaxa.2008.1.5>
- Guo YH, Wu YK, He SP, Shi HT, Zhao EM (2011) Systematics and molecular phylogenetics of Asian snail-eating snakes (Pareatidae). *Zootaxa* 3001(1): 57–64. <https://doi.org/10.11646/zootaxa.3001.1.4>
- Hauser S (2017) On the validity of *Pareas macularius* Theobald, 1868 (Squamata: Pareidae) as a species distinct from *Pareas margaritophorus* (Jan in Bocourt, 1866). *Tropical Natural History* 17(1): 25–52.

- Kumar S, Stecher G, Tamura K (2016) MEGA7: Molecular Evolutionary Genetics Analysis version 7.0 for bigger datasets. *Molecular Biology and Evolution* 33(7): 1870–1874. <https://doi.org/10.1093/molbev/msw054>
- Loredo AI, Wood PL, Quah ES, Anuar S, Greer L, Norhayati A, Grismer LL (2013) Cryptic speciation within *Asthenodipsas vertebralis* (Boulenger, 1900) (Squamata: Pareatidae), the description of a new species from Peninsular Malaysia and the resurrection of *A. tropidonotus* (Lidth de Jude, 1923) from Sumatra: an integrative taxonomic analysis. *Zootaxa* 3664(4): 505–524. <https://doi.org/10.11646/zootaxa.3664.4.5>
- Maki M (1931) A monograph of the snakes of Japan. Dai-Ichi Shobo, Tokyo, 240 pp.
- Pope CH (1928) Four new snakes and a new lizard from South China. *American Museum Novitates* 325: 1–4.
- Pope CH (1935) The reptiles of China. Turtles, Crocodilians, Snakes, Lizards. *Natural History of Central Asia* (Vol. X). The American Museum of Natural History, New York, 604 pp.
- Posada D, Crandall KA (1998) Modeltest: testing the model of DNA substitution. *Bioinformatics* 14(9): 817–818. <https://doi.org/10.1093/bioinformatics/14.9.817>
- Rao DQ, Yang DT (1992) Phylogenetic systematics of Pareatinae (Serpentes) of Southeastern Asia and adjacent islands with relationship between it and the geology changes. *Acta Zoologica Sinica* 38: 139–150.
- Ronquist F, Teslenko M, Van Der Mark P, Ayres DL, Darling A, Höhna S, Larget B, Liu L, Suchard MA, Huelsenbeck JP (2012) MrBayes 3.2: efficient Bayesian phylogenetic inference and model choice across a large model space. *Systematic Biology* 61(3): 539–542. <https://doi.org/10.1093/sysbio/sys029>
- Sichuan Institute of Biology (1977) The reference reptiles in China. Science Press, Beijing, 111 pp.
- Silvestro D, Michalak I (2012) raxmlGUI: a graphical front-end for RAxML. *Organisms Diversity and Evolution* 12(4): 335–337. <https://doi.org/10.1007/s13127-011-0056-0>
- Smith MA (1943) The fauna of British India, Ceylon and Burma, including the whole of the Indo-Chinese sub-region, Vol. III Serpentes. Taylor and Francis, London, 583 pp.
- Thompson JD, Higgins DG, Gibson TJ (1994) CLUSTAL W: improving the sensitivity of progressive multiple sequence alignment through sequence weighting, position-specific gap penalties and weight matrix choice. *Nucleic Acids Research* 22: 4673–4680. <https://doi.org/10.1093/nar/22.22.4673>
- Uetz P, Freed P, Hošek J (2020) The Reptile Database. <http://www.reptile-database.org> [Accessed on 25 Sep 2020]
- Vogel G (2015) A new montane species of the genus *Pareas* Wagler, 1830 (Squamata: Pareatidae) from northern Myanmar. *TAPROBANICA* 7(1): 1–7. <https://doi.org/10.4038/tapro.v7i1.7501>
- Vogel G, Nguyen TV, Lalremsanga HT, Biakzuala L, Hrima V, Poyarkov NA (2020) Taxonomic reassessment of the *Pareas margaritophorus-macularius* species complex (Squamata, Pareidae). *Vertebrate Zoology* 70(4): 547–569. <https://doi.org/10.26049/VZ70-4-2020-02>
- Vogt T (1922) Zur Reptilien-und Amphibienfauna Südchinas. *Archiv für Naturgeschichte* 88(10): 135–146.
- Wang P, Che J, Liu Q, Li K, Jin JQ, Jiang K, Shi L, Guo P (2020) A revised taxonomy of Asian snail-eating snakes *Pareas* (Squamata, Pareidae): evidence from morphological com-

- parison and molecular phylogeny. *ZooKeys* 939: 45–64. <https://doi.org/10.3897/zookeys.939.49309>
- You CW, Poyarkov NA, Lin SM (2015) Diversity of the snail-eating snakes *Pareas* (Serpentes, Pareatidae) from Taiwan. *Zoologica Scripta* 44(4): 349–361. <https://doi.org/10.1111/zsc.12111>
- Zhao EM (2006) *Snakes of China* (Vol. 1). Anhui Science Technology Publishing House, Hefei, 372 pp.
- Zhao EM, Huang MH, Zong Y (1998) *Fauna Sinica Reptilia* (Vol. 3). Squamata: Serpentes. Science Press, Beijing, 522 pp.

A new species of *Polypedilum* (*Cerobregma*) (Diptera, Chironomidae) from Oriental China

Wen-Bin Liu¹, Yuan Yao¹, Chun-Cai Yan¹, Xin-Hua Wang², Xiao-Long Lin²

1 Tianjin Key Laboratory of Conservation and Utilization of Animal Diversity, Tianjin Normal University, Tianjin, 300387, China **2** College of Life Sciences, Nankai University, Tianjin, 300071, China

Corresponding author: Xiao-Long Lin (lin880224@gmail.com)

Academic editor: F.L. da Silva | Received 11 October 2020 | Accepted 15 December 2020 | Published 22 January 2021

<http://zoobank.org/B350C4DE-6597-499C-B209-D9A363A6F88D>

Citation: Liu W-B, Yao Y, Yan C-C, Wang X-H, Lin X-L (2021) A new species of *Polypedilum* (*Cerobregma*) (Diptera, Chironomidae) from Oriental China.. ZooKeys 1011: 139–148. <https://doi.org/10.3897/zookeys.1011.59554>

Abstract

Polypedilum (*Cerobregma*) *huapingensis* Liu & Lin, **sp. nov.** is described and illustrated based on an adult male from Huaping National Nature Reserve, Guangxi, China. A DNA barcode analysis, including the known partial COI sequences of species in the *Cerobregma* subgenus, was conducted. An updated key to adult males of the subgenus *Cerobregma* is provided.

Keywords

COI, Chironomini, integrative taxonomy, new species

Introduction

The genus *Polypedilum* Kieffer is one of the largest chironomid genera, containing eight subgenera and more than 520 described species (Sæther et al. 2010; Cranston et al. 2016; Yamamoto et al. 2016; P. Ashe, pers. comm.). The larvae mostly occur in sediments, but some species are associated with mines of aquatic plants or co-inhabit pupal retreats of caddisflies (Cranston et al. 1989). Adult males of the subgenus *Cerobregma* Sæther & Sundal, 1999 are characterized by having extremely long and strong, split setae along the inner margin of the gonostylus and gonocoxite, with an apicolateral

bulb-like extension with deep lateral incision between the bulb and the gonostylus. The subgenus *Cerobregma* includes 15 valid species recorded in the Afrotropical, Holarctic and Oriental regions (Tokunaga 1940; Sæther and Sundal 1999; Kobayashi et al. 2003; Zhang and Wang 2005; Zhang et al. 2006; Moubayed-Breil 2007; Tang and Niitsuma 2017; Lin et al. 2019).

The DNA barcode corresponding to the 658-bp fragment of the mitochondrial gene cytochrome c oxidase I (COI) has been identified as the core of a global bio-identification system at the species level (Hebert et al. 2003a, b) and has proved to be useful in non-biting midge species delimitation (Anderson et al. 2013; Silva et al. 2014; Lin et al. 2015; Montagna et al. 2016; Gilka et al. 2018; Lin et al. 2018; Qi et al. 2017). COI barcodes have provided important evidence to confirm new species descriptions within *Polypedilum* species (Song et al. 2016, 2018; Lin et al. 2019).

The Nanling-Mountain region, located in the middle subtropical zone of China, rich in biological resources and with a warm and moist climate, is a typical natural ecosystem and one of the most biologically diverse areas in the world. Recently, during investigations of insect diversity in the Nanling Mountains, we discovered an unknown species of the subgenus *Cerobregma* from Huaping National Nature Reserve. In the present study, *Polypedilum (Cerobregma) huapingensis* Liu & Lin sp. nov. is described and delimited by its morphology and DNA barcode. An updated key to adult males of the subgenus is provided.

Materials and methods

The single specimen of the new species, collected by a Malaise trap, was preserved in 85% ethanol and stored in the dark at 4 °C before morphological and molecular analyses. Genomic DNA was extracted from the thorax and head using a Qia-gen DNA Blood and Tissue Kit at Nankai University, Tianjin, China, following the standard protocol except for the final elution volume of 100 µl. After DNA extraction, the exoskeleton of each specimen was mounted in Euparal on a microscope slide together with the corresponding wings, legs, antennae and abdomen, following the procedures outlined by Sæther (1969). Morphological terminology follows Sæther (1980).

The color pattern of new species is described based on the specimen preserved in ethanol. Digital photographs of slide-mounted specimens were taken with a 300-dpi resolution using a Nikon Digital Sight DS-Fil camera mounted on Nikon Eclipse 80i compound microscope using the software NIS-Elements F v.4.60.00. at the College of Life Sciences, Nankai University, Tianjin, China.

The universal primers LCO1490 and HCO2198 (Folmer et al. 1994) were used to amplify the standard 658-bp mitochondrial COI barcode region. Polymerase chain reaction (PCR) amplifications followed Song et al. (2018) and were conducted in a 25 µl volume including 12.5 µl 2× Es Taq MasterMix (CoWin Biotech Co., Beijing, China), 0.625 µl of each primer, 2 µl of template DNA and 9.25 µl of deionized H₂O.

PCR products were electrophoresed in 1.0% agarose gel, and purified and sequenced in both directions at Beijing Genomics Institute Co. Ltd., Beijing, China.

Raw sequences were assembled and edited in Geneious Prime 2020 (Biomatters Ltd., Auckland, New Zealand). Alignment of the sequences was carried out using the MUSCLE algorithm (Edgar 2004) on amino acids in MEGA 6 (Tamura et al. 2013). The pairwise distances using the Kimura 2-Parameter (K2P) substitution model of six species within the subgenus *Cerobregma* were calculated in MEGA. The neighbor-joining tree was constructed using the K2P substitution model, 1000 bootstrap replicates and the “pairwise deletion” option for missing data in MEGA. Novel sequences, trace-files, and metadata of the new species were uploaded to the Barcode of Life Data Systems (BOLD) (Ratnasingham and Hebert 2013). The GenBank accession number for the new species is MW472357.

The holotype of the new species is deposited at the College of Life Sciences, Nankai University, Tianjin, China (NKU).

Results

DNA barcode analysis

The neighbor joining tree based on COI DNA barcodes of the six sequenced species within the subgenus *Cerobregma* revealed six distinct genetic clusters, suggesting one species new to science (Fig. 1). In some barcode studies in Chironomidae, the average threshold intraspecific divergence is 4–5% in *Tanytarsus* van der Wulp (Lin et al. 2015) and 5%–8% in *Polypedilum* Kieffer (Song et al. 2016, 2018). *Polypedilum (Cerobregma) huapingensis* sp. nov. can be differentiated from the other sequenced species by a more than 13% divergence in the COI barcode sequence (Tab. 1; Fig. 1).

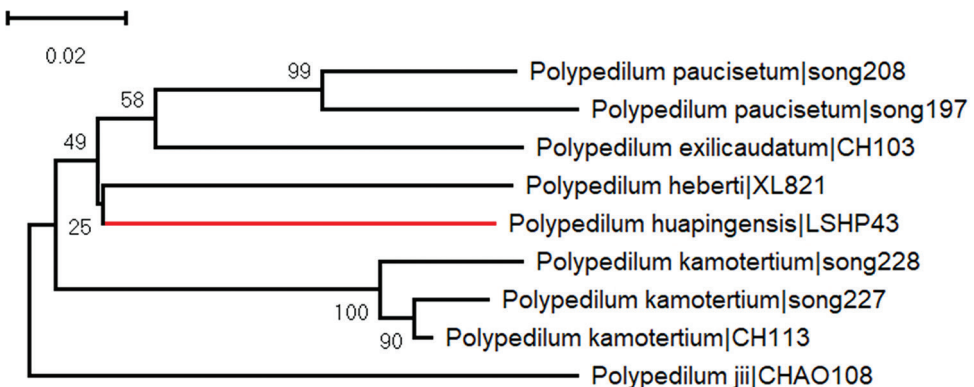


Figure 1. Neighbor-joining tree for six species of the subgenus *Cerobregma* based on K2P distance in DNA barcodes. Numbers on branches represent bootstrap support (>70%) based on 1000 replicates; scale equals K2P genetic distance.

Table 1. Kimura 2-parameter pairwise genetic distances based on COI barcodes of the *Polypedilum* (*Cerobregma*).

Species	Specimen reference number	Pairwise genetic distances								GenBank accessions
<i>P. exilicaudatum</i>	CH103									MG950021
<i>P. yamasinense</i>	song227	0.155								MG949754
<i>P. yamasinense</i>	CH113	0.147	0.015							MG949955
<i>P. jii</i>	CHAO108	0.185	0.168	0.156						MG950056
<i>P. yamasinense</i>	song228	0.155	0.041	0.034	0.179					MG950029
<i>P. paucisetum</i>	song208	0.117	0.161	0.147	0.171	0.157				MG950008
<i>P. paucisetum</i>	song197	0.138	0.163	0.153	0.162	0.170	0.075			MG949790
<i>P. heberti</i>	XL821	0.140	0.146	0.137	0.174	0.157	0.142	0.155		MK505566
<i>P. huapingensis</i>	LSHP43	0.130	0.145	0.136	0.173	0.153	0.140	0.159	0.135	MW472357

Taxonomy

Polypedilum (*Cerobregma*) *huapingensis* Liu & Lin, sp. nov.

<http://zoobank.org/79EB5D46-B309-4459-8D2C-903589EC65F3>

Figures 2–4

Type material. *Holotype*: male (NKU & BOLD sample ID: LSHP43), China, Guangxi Zhuang Autonomous Region, Guilin City, Lingui County, Huaping National Nature Reserve, 25.563°N, 109.942°E, 1271 m a.s.l., 10–20.VI.2020, Malaise trap, S.G. Zhao.

Etymology. The specific name refers to the Huaping National Nature Reserve, where the holotype was collected.

Diagnostic characters. According to the morphological characters of the adult male, the new *Polypedilum* species keys to the subgenus *Cerobregma*, and can be distinguished from other known species of the subgenus by the following combination of characters: tergites III–VI brown with dark brown spots at middle; wing pale brown with a large black spot on entire basal area of wing; superior volsella with basal microtrichia and two inner setae; anal point strong, contracted in middle, a large inflated globe apically with candle-like spine.

Adult male (n = 1). Total length 4.29 mm. Wing length 2.71 mm. Total length/wing length 1.58. Wing length/length of profemur 1.57.

Coloration (Fig. 2). Head brown. Antenna yellow. Thorax ground color brown with dark brown stripes on scutum, laterally under parapsidal suture, postnotum and on preepisternum. Tergites III–VI brown with dark brown spots at middle; tergites I, II, VII, and VIII and hypopygium largely dark brown. Most of femora and tibiae dark brown, all tarsomeres yellow. Wing pale brown with a large black spot on entire basal area.

Head (Fig. 3A). Antenna with 13 flagellomeres; ultimate flagellomere 425 µm long; AR 0.44. Temporal setae 27, including 7 inner verticals and 20 outer verticals. Clypeus with 79 setae. Tentorium 132 µm long; 45 µm wide. Stipes 112 µm long, 24 µm wide. Lengths of palpomeres 1–5 (in µm): 52.5, 97.5, 192, 170, 232. Palpomere ratio (5th/3rd) 1.21.

Thorax (Fig. 3B). Acrostichals 31; humerals 38; dorsocentrals 104; prealars 16. Scutellum with 86 setae.



Figure 2. *Polypedilum (Cerobregma) huapingensis* Liu & Lin, sp. nov., holotype male.

Wing (Fig. 3C). VR 1.15. Brachiolum with 13 setae; R with 36 setae; R₁ with 32 setae; R₄₊₅ with 36 setae; M with 22 setae; remaining veins bare. R₂₊₃ distinct. Squama with 16 setae. Anal lobe moderately developed.

Legs. Spur of mid tibia 28 µm long, mid tibia including 55 µm long comb, un-spurs comb 35 µm long; spur of hind tibia 36 µm long including 78 µm long comb, un-spurs comb 40 µm long. Apical width of fore tibia 60 µm; of mid tibia 76 µm; of hind tibia 80 µm. Lengths (in µm) and proportions of legs as in Table 2.

Hypopygium (Fig. 4). Anal tergite with 46 median setae. Laterosternite IX with seven setae. Anal point as in Fig. 4D, strong, contracted in middle, as a large inflated globe apically with a single candle-like spine, tapering, 143 µm long. Transverse sternapodeme 93 µm long; phallapodeme 168 µm long. Gonocoxite 320 µm long. Superior volsella 143 µm long, with basal microtrichia and two inner setae (Fig. 4E). Inferior

Table 2. Lengths (in µm) and proportions of legs of *Polypedilum (Cerobregma) huapingensis* sp. nov., male holotype (n = 1).

	fe	ti	ta ₁	ta ₂	ta ₃	ta ₄	ta ₅	LR	BV	SV	BR
P ₁	1725	1108	2405	1025	725	625	275	2.17	2.11	1.98	3.14
P ₂	1702	1225	655	475	355	175	148	0.53	2.67	3.11	4.50
P ₃	1850	1208	1075	925	503	362	154	0.89	2.34	2.13	4.90

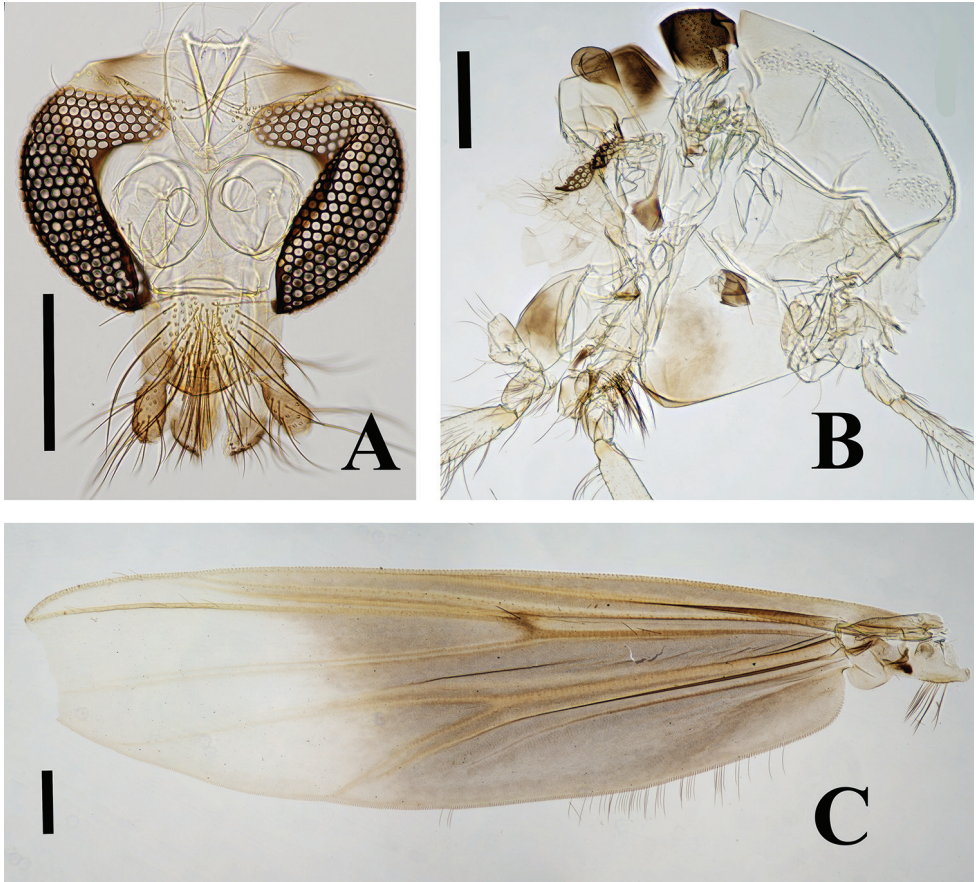


Figure 3. *Polypedilum (Cerobregma) huapingensis* Liu & Lin, sp. nov., holotype male **A** head **B** thorax **C** wing. Scale bars: 200 μm .

volsella 164 μm long, finger-shaped, divided into two lobes apically, with 24 long setae. Gonostylus 310 μm long. HR 1.03; HV 1.38.

Female and immatures unknown.

Discussion. The characters of the anal point and superior volsella of the new species place it within the subgenus *Cerobregma*. The morphology of the new species resembles that of *Polypedilum heberti* Lin & Wang, 2019, but it can be separated from it on the basis of the following: 1) tergites III–VI brown with dark brown spots at middle in the new species, versus tergites III–VI with dark brown bands at middle in *P. heberti*; 2) thorax of the new species (acrostichals 31; humerals 38; dorsocentrals 104) with much more setae than in *P. heberti* (acrostichals 8; humerals 5; dorsocentrals 20); 3) anal point strong and tapering in *P. heberti*, versus constricted in middle, with a large inflated globe apically with candle-like spine in the new species.

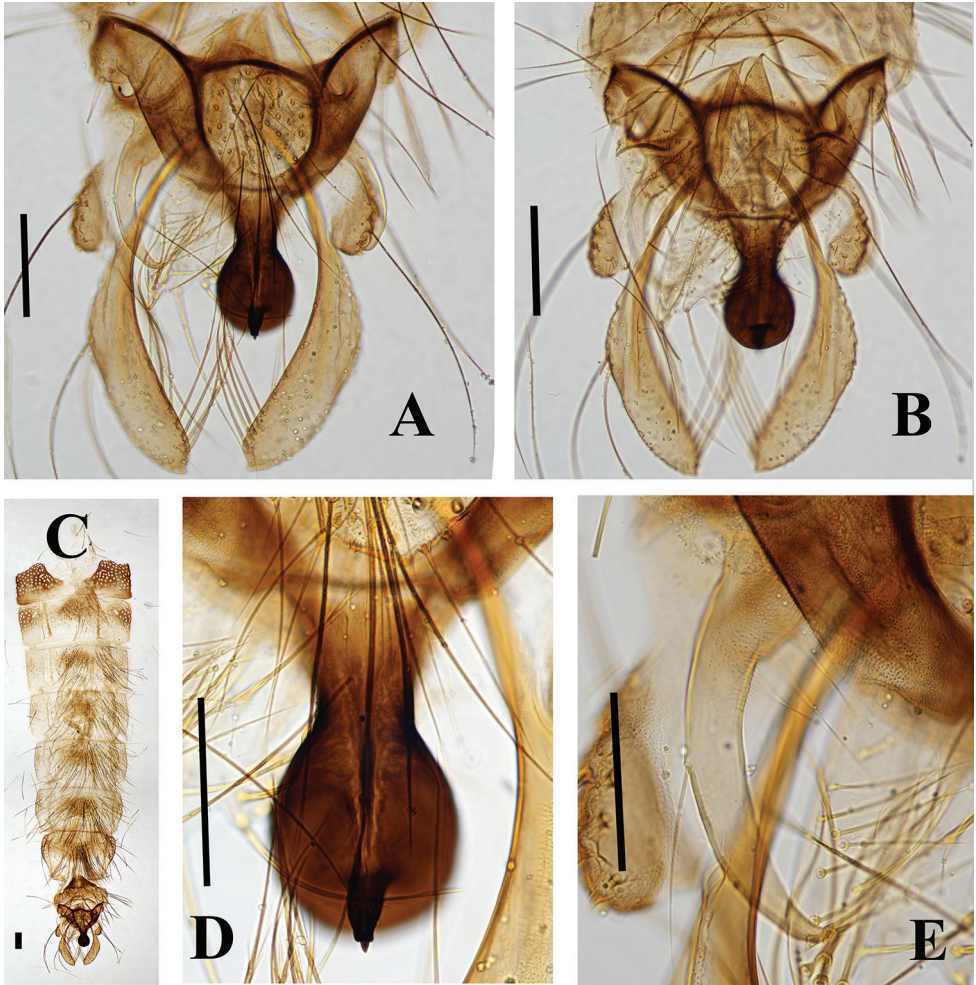


Figure 4. *Polypedilum (Cerobregma) huapingensis* Liu & Lin, sp. nov., holotype male **A** hypopygium, dorsal view **B** hypopygium, ventral view **C** abdomen **D** superior volsella **E** anal point. Scale bars: 100 μ m.

Updated key to known adult males of *Polypedilum (Cerobregma)*

The following key replaces couplet 5 in Lin et al. (2019) and adds a couplet 5a to include the male of the newly described species.

- 5 Wing with several spots; setae along inner margin of gonostylus strongly split *P. ramiferum* Kieffer, 1921
- Wing with a large black spot on entire basal area; setae along inner margin of gonostylus not split..... **5a**

- 5a Acrostichals 8; humerals 5; dorsocentrals 20; anal point strong and tapering...
 *P. heberti* Lin & Wang, 2019
- Acrostichals 31; humerals 38; dorsocentrals 104; anal point strong, contract-
 ed in middle, as a large inflated globe apically with candle-like spine
 *P. huapingensis* Liu & Lin, sp. nov.

Acknowledgements

Financial support from the National Natural Science Foundation of China (31672264, 31672324, 31801994, 31900344), the China Postdoctoral Science Foundation Grant (2018M640227), GDAS Special Project of Science and Technology Development (No. 2020GDASYL-20200102021, 2020GDASYL-20200301003) and the Natural Science Foundation of Tianjin (18JCQNJC14700, 18JCYBJC96100, S20QNS624) is acknowledged with thanks.

References

- Anderson AM, Stur E, Ekrem T (2013) Molecular and morphological methods reveal cryptic diversity and three new species of Nearctic *Micropsectra* (Diptera: Chironomidae). *Freshwater Science* 32: 892–921. <https://doi.org/10.1899/12-026.1>
- Cranston PS, Dillon ME, Pinder LCV, Reiss F (1989) The adult males of Chironominae (Diptera: Chironomidae) of the Holarctic region – Keys and diagnoses. In: Wiederholm T (Ed.) *Chironomidae of the Holarctic region. Keys and diagnoses. Part 3 – Adult males.* *Entomologica Scandinavica Supplement* 34: 353–502.
- Cranston PS, Martin J, Spies M (2016) Cryptic species in the nuisance midge *Polypedilum nubifer* (Skuse (Diptera: Chironomidae) and the status of *Tripedilum* Kieffer. *Zootaxa* 4079: 429–447. <https://doi.org/10.11646/zootaxa.4079.4.3>
- Edgar RC (2004) MUSCLE: multiple sequence alignment with high accuracy and high throughput. *Nucleic Acids Research* 32: 1792–1797. <https://doi.org/10.1093/nar/gkh340>
- Folmer O, Black M, Hoeh W, Lutz R, Vrijenhoek R (1994) DNA primers for amplification of mitochondrial cytochrome *c* oxidase subunit I from diverse metazoan invertebrates. *Molecular Marine Biology and Biotechnology* 3: 294–299.
- Giřka W, Paasivirta L, Gadawski P, Grabowski M (2018) Morphology and molecules say: *Tanytarsus latens*, sp. nov. from Finland (Diptera: Chironomidae). *Zootaxa* 4471: 569–579. <https://doi.org/10.11646/zootaxa.4471.3.8>
- Hebert PDN, Cywinska A, Ball SL (2003a) Biological identifications through DNA barcodes. *Proceedings of the Royal Society of London B: Biological Sciences* 270: 313–321. <https://doi.org/10.1098/rspb.2002.2218>
- Hebert PDN, Ratnasingham S, de Waard JR (2003b) Barcoding animal life: cytochrome *c* oxidase subunit I divergences among closely related species. *Proceedings of the Royal Society of London B: Biological Sciences* 270: S96–S99. <https://doi.org/10.1098/rsbl.2003.0025>

- Kobayashi T, Ohtaka A, Takahashi T (2003) The second record of ectoparasitic Chironomidae on Trichoptera from Japan, *Polypedilum (Cerobregma) kamotertium* Sasa, 1989 (Insecta, Diptera, Chironomidae, Chironomini). *Spixiana* 26: 83–91.
- Lin XL, Stur E, Ekrem T (2015) Exploring genetic divergence in a species-rich insect genus using 2790 DNA Barcodes. *PLoS ONE* 10: e0138993. <https://doi.org/10.1371/journal.pone.0138993>
- Lin XL, Stur E, Ekrem T (2018) DNA barcodes and morphology reveal unrecognized species of Chironomidae (Diptera). *Insect Systematics & Evolution* 49: 329–398. <https://doi.org/10.1163/1876312X-00002172>
- Lin XL, Yu HJ, Zhang RL, Wang XH (2019) *Polypedilum (Cerobregma) heberti* sp. n. (Diptera: Chironomidae) from Gaoligong Mountains, Yunnan, China. *Zootaxa* 4571(2): 255–262. <https://doi.org/10.11646/zootaxa.4571.2.5>
- Montagna M, Mereghetti V, Lencioni V, Rossaro B (2016) Integrated taxonomy and DNA barcoding of alpine midges (Diptera: Chironomidae). *PLoS ONE* 11(3): e0149673. <https://doi.org/10.1371/journal.pone.0149673>
- Moubayed-Breil J (2007) *Polypedilum (Cerobregma) lotensis*, new species, and *P. (C.) saetheri*, new species, from lowland streams and rivers in France (Diptera: Chironomidae). In: Andersen T (Ed.) Contributions to the systematics and ecology of aquatic Diptera—A tribute to Ole A. Sæther. The Caddis Press, Columbus, Ohio, 205–213.
- Qi X, Wang XH, Andersen T, Lin XL (2017) A new species of *Manoa Fittkau* (Diptera: Chironomidae), with DNA barcodes from Xianju National Park, Oriental China. *Zootaxa* 4231: 398–408. <https://doi.org/10.11646/zootaxa.4231.3.6>
- Ratnasingham S, Hebert PDN (2013) A DNA-based registry for all animal species: the barcode index number (BIN) system. *PLoS ONE* 8: e66213. <https://doi.org/10.1371/journal.pone.0066213>
- Sæther OA (1969) Some Nearctic Podonominae, Diamesinae, and Orthocladiinae (Diptera: Chironomidae). *Bulletin of the Fisheries Research Board of Canada* 170: 1–154.
- Sæther OA (1980) Glossary of chironomid morphology terminology (Diptera: Chironomidae). *Entomologica Scandinavica Supplement* 14: 1–51.
- Sæther OA, Andersen T, Pinho LC, Mendes HF (2010) The problems with *Polypedilum* Kieffer (Diptera: Chironomidae), with the description of *Probolum* subgen. n. *Zootaxa* 2497: 1–36. <https://doi.org/10.11646/zootaxa.2497.1.1>
- Sæther OA, Sundal A (1999) *Cerobregma*, a new subgenus of *Polypedilum* Kieffer, with a tentative phylogeny of subgenera and species groups within *Polypedilum* (Diptera: Chironomidae). *Journal of the Kansas Entomological Society* 71: 315–382.
- Silva FL, Fonseca-Gessner AA, Ekrem T (2014) A taxonomic revision of genus *Labrundinia* Fittkau, 1962 (Diptera: Chironomidae: Tanypodinae). *Zootaxa* 3769(1): e185. <https://doi.org/10.11646/zootaxa.3769.1.1>
- Song C, Lin XL, Wang Q, Wang XH (2018) DNA barcodes successfully delimit morphospecies in a superdiverse insect genus. *Zoologica Scripta* 47: 311–324. <https://doi.org/10.1111/zsc.12284>
- Song C, Wang Q, Zhang RL, Sun BJ, Wang XH (2016) Exploring the utility of DNA barcoding in species delimitation of *Polypedilum (Tripodura)* non-biting midges (Diptera: Chironomidae). *Zootaxa* 4079: 534–550. <https://doi.org/10.11646/zootaxa.4079.5.2>

- Tamura K, Stecher G, Peterson D, Filipski A, Kumar S (2013) MEGA6: molecular evolutionary genetics analysis version 6.0. *Molecular Biology and Evolution* 30: 2725–2729. <https://doi.org/10.1093/molbev/mst197>
- Tang HQ, Niitsuma H (2017) Review of the Japanese *Microtendipes* (Diptera: Chironomidae), with description of a new species. *Zootaxa* 4320: 535–553. <https://doi.org/10.11646/zootaxa.4320.3.8>
- Tokunaga M (1940) Chironomidae from Japan (Diptera), XI1. New or little-known Ceratopogonidae and Chironomidae. *The Philippine Journal of Science* 72: 255–311.
- Yamamoto N, Yamamoto M, Hirowatari T (2016) Erection of a new subgenus in the genus *Polypedilum* Kieffer, 1912 (Diptera: Chironomidae) from Japan. *Japanese Journal of Systematic Entomology* 22: 195–197.
- Zhang RL, Wang XH (2005) *Polypedilum* (*Cerobregma*) Sæther & Sundal from China (Diptera: Chironomidae). *Aquatic Insects* 27: 47–55. <https://doi.org/10.1080/01650420400019262>
- Zhang RL, Wang XH, Sæther OA (2006) Two unusual species of *Polypedilum* Kieffer (Diptera: Chironomidae) from Oriental China. *Zootaxa* 1282: 39–48. <https://doi.org/10.11646/zootaxa.1282.1.4>